

NATIONAL LIBRARY
OTTAWA



BIBLIOTHÈQUE NATIONALE
OTTAWA

NAME OF AUTHOR..... P. D. Cradwick
TITLE OF THESIS..... The Crystal structures of
..... some organic and inorganic
..... compounds
UNIVERSITY..... of Alberta (Edmonton)
DEGREE FOR WHICH THESIS WAS PRESENTED..... Ph.D.
YEAR THIS DEGREE GRANTED..... 1969

Permission is hereby granted to THE NATIONAL LIBRARY
OF CANADA to microfilm this thesis and to lend or sell copies
of the film.

The author reserves other publication rights, and
neither the thesis nor extensive extracts from it may be
printed or otherwise reproduced without the author's
written permission.

(Signed)..... P. D. Cradwick

PERMANENT ADDRESS:

..... #201 9936 87 AVE.
..... Edmonton
..... Alberta

DATED..... 6th June 1969

THE UNIVERSITY OF ALBERTA

The Crystal Structures of Some
Organic and Inorganic Compounds

by



Peter Denys Cradwick

A THESIS

SUBMITTED TO THE FACULTY OF GRADUATE STUDIES
IN PARTIAL FULFILMENT OF THE REQUIREMENTS FOR
THE DEGREE OF DOCTOR OF PHILOSOPHY

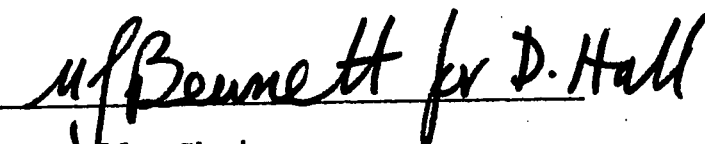
Department of Chemistry

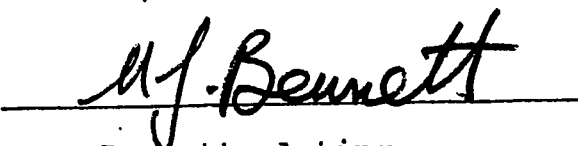
Edmonton, Alberta

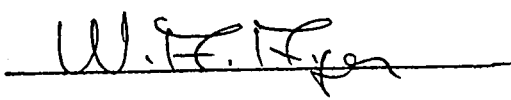
Fall, 1969

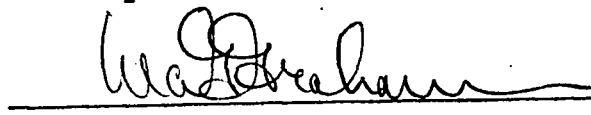
UNIVERSITY OF ALBERTA
FACULTY OF GRADUATE STUDIES

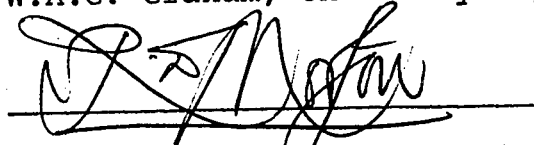
The undersigned certify that they have read, and recommend to the Faculty of Graduate Studies for acceptance, a thesis entitled THE CRYSTAL STRUCTURES OF SOME ORGANIC AND INORGANIC COMPOUNDS submitted by Peter Denys Cradwick in partial fulfilment of the requirements for the degree of Doctor of Philosophy.

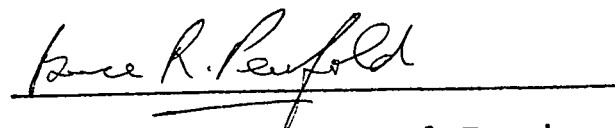

D. Hall, Chairman


M.J. Bennett, Acting
Chairman


W.A. Ayer, Chemistry Dept.


W.A.G. Graham, Chemistry Dept.


R.D. Morton, Geology Dept.


B.R. Penfold, External Examiner

Date: 4th June 1969

ABSTRACT

The crystal structure of 5,8-dihydroxy 1,4-naphthoquinone has been redetermined in order to decide the true molecular formula of the molecule, which can be alternatively described as 4,8-dihydroxy 1,5-naphthoquinone. The bond length pattern shows that the molecular formula in the solid state is best described as a charged structure in which the positions of the non-hydrogen atoms approximate to what would be expected for 5,8-dihydroxy 1,4-naphthoquinone. The symmetry requirements of the space group favour the alternative molecular formula 4,8-dihydroxy 1,4-naphthoquinone which has $2/m$ (C_{2h}) molecular symmetry, thus the crystal structure determinations of related molecules of lower molecular symmetry were also attempted. These were: 5-hydroxy 1,4-naphthoquinone, 2-methyl 5,8-dihydroxy 1,4-naphthoquinone and 2-chloro 5,8-dihydroxy 1,4-naphthoquinone. Work on these compounds was in progress when an n.m.r. spectral study of all the above compounds was published and these results showed that the crystal structure of the related compounds could not be directly related to that of 5,8-dihydroxy 1,4-naphthoquinone. The crystal structure

of 5-hydroxy 1,4-naphthoquinone and the preliminary results of 2-methyl 5,8-dihydroxy 1,4-naphthoquinone are described. In attempting to solve what was thought to be 2-chloro 5,8-dihydroxy 1,4-naphthoquinone it transpired that the product was in fact 2,5-dichloro 3,6-dihydroxy-p-benzoquinone; the crystal structure determination of this compound is also described.

The crystal structure determinations of tribromotriindiumtetracobalt pentadecacarbonyl and tetraethylammonium dibromobis tetracarbonyl cobalt indate(III) are described within. These compounds contain the first observed bond between indium and cobalt atoms.

ACKNOWLEDGEMENTS

I would like to express my sincere appreciation to Professor D. Hall for his advice and continued interest throughout this work.

I wish to acknowledge the assistance of Professor M.J. Bennett and Dr. M. Elder, in the form of many helpful discussions during this work.

Financial assistance provided by the University of Alberta is gratefully acknowledged.

TABLE OF CONTENTS

	<u>Page</u>
Abstract	i
Acknowledgements	iii
List of figures	vi
List of Tables	ix
Preface	xii
 <u>Part I</u>	
(a) Introduction	1
(b) The refinement of 5,8-dihydroxy 1,4-naphthoquinone (Naphthazarin).	19
(c) The crystal and molecular structure of 5-hydroxy 1,4-naphthoquinone (Juglone).	79
 <u>Part II</u>	
(a) Introduction	110
(b) The crystal and molecular structure of Tribromotriindiumtetracobalt Pentadecakiscarbonyl ($\text{In}_3\text{Br}_3\text{Co}_4(\text{CO})_{15}$).	112
(c) The crystal and molecular structure of Tetraethylammonium dibromo bistetracarbonylcobalt indate(III) ($\text{InBr}_2\text{Co}_2(\text{CO})_8$) ⁻ Et_4N^+ .	142

PagePart III

(a) The crystal and molecular structure of 2,5-dichloro 3,6-dihydroxy-p- benzoquinone.	172
(b) The refinement of dipotassium nitro- acetate.	195
(c) The refinement of 2,2',2"-triamino- triethylene Ni(II) dithiocyanate (Ni tren(SCN) ₂).	207
(d) Preliminary investigation of 2-methyl 5,8-dihydroxy 1,4-naphthoquinone (methyl naphthazarin).	220
Appendix A: Programme system	232
Appendix B: Analysis of rigid body thermal motion	243
Appendix C: Patterson superposition	252
References	257

LIST OF FIGURES

<u>Figure</u>		<u>Page</u>
1.	Bond lengths for naphthazarin form "C" published by Pascard-Billy.	14
2.	Molecular dimensions for naphthazarin form "A" and bond lengths after correction for molecular librations.	57
3.	Thermal ellipsoids for naphthazarin form "A".	58
4.	Molecular dimensions for naphthazarin form "C".	59
5.	Thermal ellipsoids for naphthazarin form "C".	60
6.	Molecular packing for naphthazarin form "A". Projection onto [ac] plane.	61
7.	Molecular packing for naphthazarin form "A". Projection onto [bc] plane.	62
8.	Molecular packing for naphthazarin form "C" viewed down [a] axis.	63
9.	Electron density of naphthazarin form "A", without hydrogens.	64
10.	Electron density of naphthazarin form "A", with hydrogens.	65

<u>Figure</u>		<u>Page</u>
11.	Electron density of molecule 1, form "C", without hydrogens.	66
12.	Electron density of molecule 1, form "C" with hydrogens.	67
13.	Electron density of molecule 2, form "C", without hydrogens	68
14.	Electron density of molecule 2, form "C", with hydrogens.	69
15.	Molecular dimensions for juglone.	98
16.	Molecular packing for juglone. Projection onto [ac] plane.	99
17.	Molecular packing for juglone. Projection onto [bc] plane.	100
18.	Residual electron density for juglone, at end of refinement.	101
19.	Numbering scheme for $\text{In}_3\text{Br}_3\text{Co}_4(\text{CO})_{15}$.	133
20.	Thermal ellipsoids of heavy atoms for $\text{In}_3\text{Br}_3\text{Co}_4(\text{CO})_{15}$.	134
21.	Molecular packing for $\text{In}_3\text{Br}_3\text{Co}_4(\text{CO})_{15}$.	135
22.	Numbering scheme for $[\text{InBr}_2\text{Co}_2(\text{CO})_8]^- \text{Et}_4\text{N}^+$.	164
23.	Molecular packing for $[\text{InBr}_2\text{Co}_2(\text{CO})_8]^- \text{Et}_4\text{N}^+$.	165

<u>Figure</u>		<u>Page</u>
24.	Molecular dimensions and thermal ellipsoids for chloranilic acid.	189
25.	Molecular packing for chloranilic acid. Projection onto [ac] plane.	190
26.	Electron density for chloranilic acid before inclusion of the hydrogen atom.	191
27.	Molecular dimensions for dipotassium nitroacetate.	205
28.	Thermal ellipsoids and numbering scheme for Ni tren(SCN) ₂ .	217
29.	Intramolecular vectors for methyl-naphthazarin.	227.

LIST OF TABLES

<u>Table</u>	<u>Page</u>
Tables for Naphthazarin	
1. Summary of previous structural determinations.	8
2. Analysis of weak reflections of form "A".	25
3. Final atomic coordinates of form "A".	42
4. Anisotropic temperature factors of form "A"	43
5. Final atomic coordinates of form "C"	45
6. Temperature factors of form "C"	45
7. Intermolecular contacts of forms "A" and "C"	47
8. Root-mean-square amplitudes of vibration of forms "A" and "C"	48
9. Rigid body vibrations of form "A" (carbon atoms only)	50
10. Rigid body vibrations of form "A" (carbon and oxygen atoms)	52
11. Least squares planes of forms "A" and "C"	54
12. Structure factors of form "A"	55
13. Structure factors of form "C"	56

<u>Table</u>	<u>Page</u>
Tables for Juglone	
14. Final atomic coordinates	93
15. Temperature factors	94
16. Intermolecular contacts	95
17. Least squares planes	96
18. Structure factors	97
19. Bond lengths of some quinonoid compounds	107
Tables for $\text{In}_3\text{Br}_3\text{Co}_4(\text{CO})_{15}$	
20. Final atomic coordinates and isotropic temperature factors	123
21. Anisotropic temperature factors	125
22. Root-mean-square amplitudes of vibration	126
23. Intramolecular distances	127
24. Intramolecular non-bonded contacts	128
25. Intermolecular contacts	129
26. Bond angles	130
27. Structure factors	132
Tables for $[\text{InBr}_2\text{Co}_2(\text{CO})_8]^- \text{Et}_4\text{N}^+$	
28. Final atomic coordinates and temperature factors	154
29. Intramolecular distances	157

<u>Table</u>	<u>Page</u>
30. Bond angles	159
31. Pseudo c glide relationship	161
32. Structure factors	162
Tables for Chloranilic acid	
33. Final atomic coordinates	183
34. Root-mean-square amplitudes of vibration	184
35. Rigid body vibrations	185
36. Intermolecular contacts	187
37. Structure factors	188
Tables for Dipotassium nitroacetate	
38. Final atomic coordinates and temperature factors	202
39. R factors for various models	203
40. Structure factors	204
Tables for Ni tren(SCN) ₂	
41. Final atomic coordinates	211
42. Temperature factors	212
43. Summary of bond lengths	213
44. Bond angles	215
45. Structure factors	216
46. Flow diagram of programme system used	232

PREFACE

The initial project of this thesis was a study in the field of intramolecular hydrogen bonding under Professor D. Hall at the University of Auckland, and was partly completed at the time of transfer to Canada. This work was continued at the University of Alberta and is described in Part I.

There were two side effects resulting from the transfer to Canada which directly affect this thesis:

- (a) Other interests developed within the group, specifically the study of organo-metallic molecules and the crystal structures of two of these are described in Part II.
- (b) During the setting up period of the laboratory, considerable time was spent in setting up X-ray equipment and in the development of a system of programmes for computation. During this time two projects, which are described in Parts IIIB and IIIC were undertaken at least in part as bases for testing computer programmes.

PART I

(A) Introduction

Of the various weaker interatomic forces known in chemistry, one of the most important is the hydrogen bond, which is an interaction of about 5 kcal/mole energy between two electronegative atoms, one of which is formally attached to the hydrogen atom. Two of the most useful techniques for study of the hydrogen bond are:

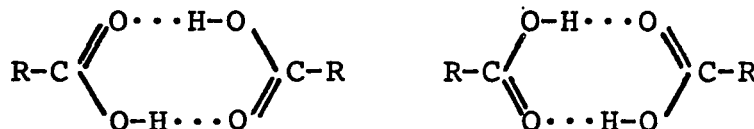
- (a) X-ray and neutron diffraction
- and (b) Infrared spectroscopy.

X-ray diffraction as a technique is notoriously ineffective for locating of hydrogen atom positions although with small light atom molecules it is quite practical to do so if the intensities are accurately measured. Nevertheless the study of large numbers of organic molecules in which hydrogen bonds are possible, demonstrates clearly that hydrogen bonding is the principal intermolecular force, and the geometry of the atoms involved is always such that the hydrogen atom may be supposed to be on or near the line joining the two electronegative atoms. Neutron diffraction studies, from which hydrogen atoms can be located with accuracy comparable to other atoms, have confirmed such deductions (1) and have demonstrated that if a series of intermolecular hydrogen bonds between the same atom types

(e.g., O-O) are considered, then it is reasonable to relate the strengths of the hydrogen bond to the shortness of the O-O approach. Further, it is seen that the stronger the hydrogen bond, the longer is the formal O-H bond i.e. the closer is the hydrogen to the central position between the two oxygens. Simultaneously it is observed that as the hydrogen bond strength increases so does the O-H stretching frequency observed in the infrared decrease due to the weakening of the formal O-H bond. This frequency is normally sharp at approximately 3600 wave numbers. In valence bond terms this requires the existence of the following canonical forms:



The second canonical form is obviously favoured in conditions where formal charge transfer is not necessary, as for example in carboxylic acid dimers:



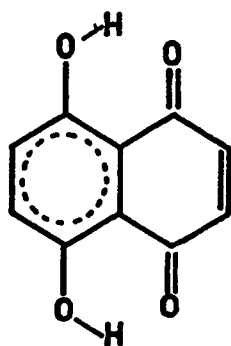
Whether in such a system the hydrogen atom is to be thought of as residing exactly at the mid-point of the two oxygens or in two equally favoured positions either side of the mid-point (i.e. whether the potential energy function has a single or double minimum) is a major

problem in its own right but is not the immediate concern of this discussion. The strongest hydrogen bond known, found in the hydrogen difluoride anion, does have the hydrogen atom at the midpoint of the hydrogen bond (1).

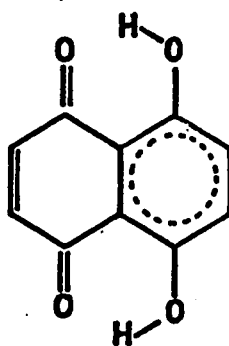
A somewhat less studied phenomenon is the intramolecular hydrogen bond, although it is well known that these do occur and that they can have a marked effect on the physical properties of compounds containing them e.g., the acid dissociation constants of benzoic acid and dihydroxy-benzoic acid are 6.37×10^{-5} (2) and 5×10^{-2} respectively (3).^a



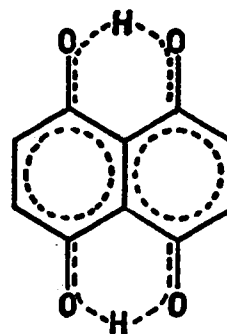
The acid O-H bond in 2,6-dihydroxybenzoic acid is obviously weakened by the participation of the oxygen in an intramolecular hydrogen bond (see ref. (79) for other examples). Of the many molecules in which intramolecular hydrogen bonds can be expected to occur, one of the most widely studied is naphthazarin, which is formally described as 5,8-dihydroxy-1,4-naphthoquinone (I).



IA



IB



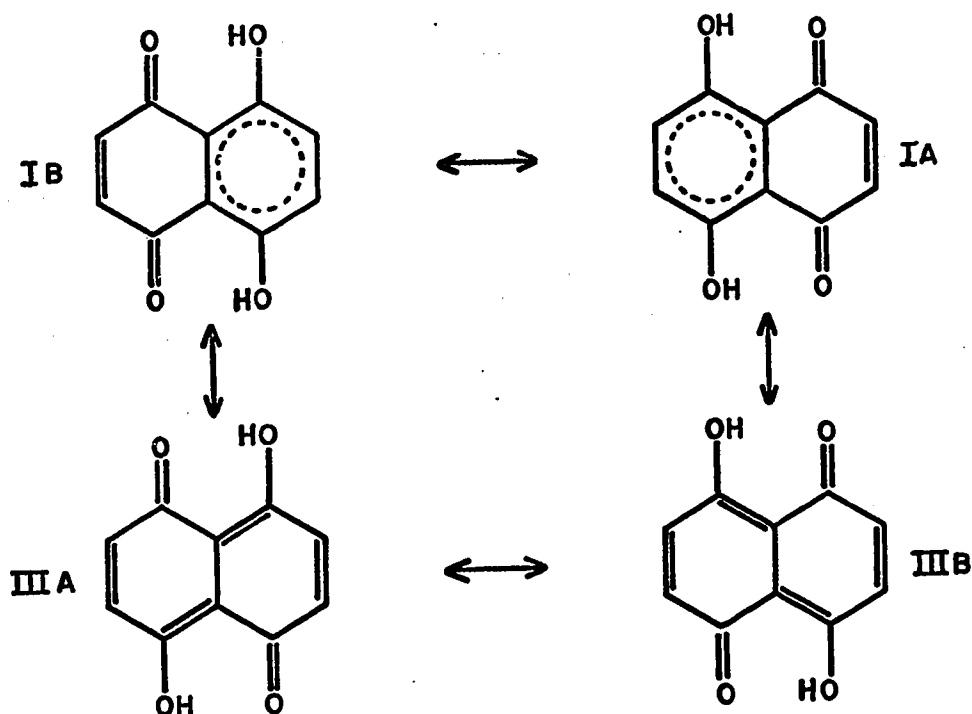
II

There has long been conjecture as to whether this molecule should indeed be thought of as a naphthoquinone i.e. as to whether the six membered rings are benzenoid-quinonoid as in the canonical forms IA and IB, or whether both rings are equivalent and the molecule is to be thought of as "delocalised" (II).

The infrared spectrum of naphthazarin was first studied by Fuson et al. (5) who were unable to locate the O-H stretching frequency and assumed that this was because of a large shift caused by the hydrogen bonding. This large shift led them to conclude that the hydrogen was symmetrically disposed between the two oxygens. The spectrum was subsequently investigated by Hadzi and Sheppard (6) who identified a broad weak band at 2920 cm^{-1} as the O-H stretching vibration (normally observed at $3650\text{--}3590\text{ cm}^{-1}$ (41)). They claimed that this was very much higher than expected for the symmetrical hydrogen

bond (1800 cm^{-1}) and therefore this inferred definite asymmetry in the hydrogen atom location. The assumption of this argument is the well established relationship between O-H frequency shift and O-O separation for near linear hydrogen bonds. The value that the oxygen-hydrogen-oxygen angle might be expected to adopt in II is uncertain but the system is certainly not likely to be linear. Rundle (97) has pointed out that bent hydrogen bonds show large deviations from the above relationship for linear bonds. There is in fact little experimental evidence relevant to bent hydrogen bonds and the correct interpretation of the above observed frequencies is thus uncertain.

The n.m.r. spectra of naphthazarin and related compounds have been studied by Moore and Shueur (34), who have noted that the four benzene protons in naphthazarin give a single resonance peak. This result has been interpreted by these authors as indicating a rapid tautomerism between the canonical forms IA, IB, IIIA and IIIE, as shown below:



It is quite possible, but by no means certain, that by lowering the temperature of the sample, the rate of tautomerism may be reduced to below 10^6 c.p.s. (the frequency of the n.m.r. oscillator) whence it should be possible to resolve the benzene proton peaks in the now dominant tautomeric form. The n.m.r. spectrum was carried out in this department at a temperature of -60°C but the benzene proton peak showed no splitting and in general there was no significant change in the spectrum when compared to that taken at room temperature.

Although the above interpretation is certainly consistent with the observed spectrum, it is not the only possible explanation: the delocalised model II would give the same spectrum and thus the n.m.r. technique would be unable to distinguish these two situations. Thus it was felt that neither of the spectroscopic results has fully resolved the problem and that a crystallographic study should be capable of doing this, e.g., the Moore and Shueur tautomerism and the model II should be distinguishable crystallographically.

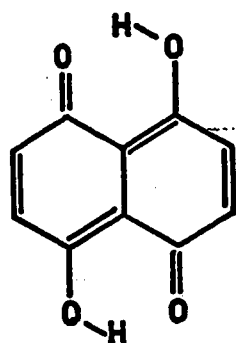
Naphthazarin exists in three crystalline forms and the various crystal structure investigations made to date are summarised in Table 1. All three modifications crystallise in space group $P2_1/c$ and in all cases the symmetry requirements of the structure dictate that the molecule possesses a centre of inversion. (In form "C" there are 4 molecules per cell, but the molecules occupy 2 sets of 2 fold positions rather than the 4 fold general positions). At first sight this would seem to eliminate I and to indicate that the molecule is indeed form II or alternatively that it exists in the form 1,5-dihydroxy 4,8-naphthoquinone, III.

TABLE 1

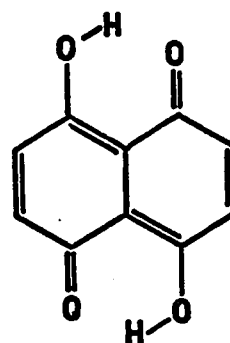
Author	Summary of Results	Crystal form	Ref.
1938 Palacios & Salvia	Structure not solved.	A	19
1955 Billy	Preliminary report (final results not given).	B	12
1956 Borgen	Preliminary report (no results given).	A,B,C	14
1957 Watase et al.	Forbidden $h0l$ reflections reported. Molecular dimensions not given	A	15
1958 Srivastava	Preliminary report (no results given).	C	16
1958 Golder & Zhdanov	Projection data used; final R factor 0.18 no standard deviations given for bond lengths.	A	18
1958 Billy	Molecule stated to be III, but no bond lengths given.	C	13
1959 Srivastava	Analysis of Renninger reflections.	C	17
1961 Pascard-Billy	Three dimensional refinement; final R factor 0.18. Molecule is concluded to be III but bond lengths do not support this.	C	7
1961 Pascard-Billy	Identical content to above paper.	C	8

Table 1 cont'd.

	Author	Summary of Results	Crystal form	Ref.
1961	Srivastava	Preliminary report of low temperature study.	C	21
1962	Pascard-Billy	Structure solved from two projections; final R factors were 0.142, 0.148. Results have been interpreted as indicating model III, although bond length pattern does not support this in view of errors (0.03A).	B	9
1962	Pascard-Billy	Structure solved from two projections; final R factors were 0.169; 0.140. The same conclusions were drawn from the bond length as in (11), and the same criticism applies.	A	11
1962	Pascard-Billy	Results of (10) are viewed in relation to (11) and (13). In these three reports, the assignment of single and double bonds on the basis of the published bond lengths and standard deviations seems unreasonable.	C	10



IIIA



IIIB

It must however be appreciated that crystal diffraction effects are the result of scattering from a large number of molecules, and where non-centrosymmetric molecules are disordered in the sense that they randomly occupy two centrosymmetrically related orientations, the resultant diffraction pattern shows the average situation i.e. an apparently centrosymmetrical molecule. Similarly if tautomerism occurs in the solid state as well as in solution, and there seems little reason to preclude this possibility, the net result seen in a crystal diffraction study will be an apparently centrosymmetrical molecule. This implies that stacking disorder and tautomerism would be indistinguishable crystallographically. The orientation of a molecule within a crystal structure is determined by interactions of the molecule with its neighbours, and the type of situation where such disorder might occur is when the non-centrosymmetric

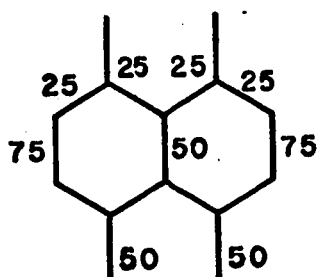
molecule is very nearly centrosymmetric and thus the lattice energy corresponding to the "mistake" is little different to the ordered situation. Naphthazarin, if it existed as I would be just such a molecule, and it is then quite possible that the apparent centre of symmetry is due to stacking disorder involving structures IA and IB, and not to a true molecular centre of symmetry. It is also formally possible that structures IIIA and IIIB could be involved in a stacking disorder whence the "averaged result" would again appear centrosymmetric, but distinct from either contributor.

The bases on which a decision concerning the true structure of naphthazarin might be made from a crystallographic structure determination are as follows:

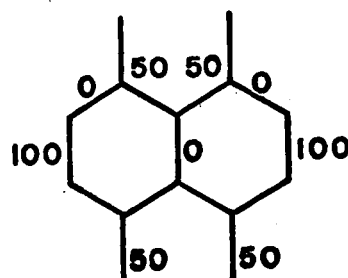
(a) Structure III (either IIIA or IIIB separately) has molecular symmetry $2/m$ (C_{2h}) whereas structure II and the disordered or tautomeric version of I and/or III would have molecular symmetry mmm (D_{2h}).

The molecules corresponding to structure II, to disorder between IA and IB, or to the tautomeric model (assuming equal energy for all forms) would all be expected to show bonds with double bond character as shown in A below, (it being assumed that uncharged Kekule type canonicals will predominate). The molecule corresponding to disorder between IIIA and IIIB

would show bond pattern B. Thus an accurate determination of the heavy atom (non-hydrogen) bond pattern should be capable of establishing or eliminating the ordered or disordered versions of III, but would not distinguish the other possibilities.



A



B

This assumption is undoubtedly a simplification but nonetheless the expected patterns are distinct. The delocalised model (II) on the other hand can be thought of as a resonance structure with presumably these four as major contributors, and thus its expected bond length pattern would be more or less intermediate, and it might in practice be difficult to distinguish.

(b) The hydrogen atom involved in hydrogen bonding would in III be located off centre i.e. bonded to one oxygen, whereas in II it would presumably be at a position equidistant from the two oxygen atoms, and in disordered or tautomeric models, there should appear

two half weight hydrogens each attached to an oxygen.

In principal the above two considerations should resolve the problem, but in practice the distinction between the four possibilities postulated above may well be beyond the capabilities of X-ray methods. It is, however, obvious from these considerations that only a precise structure determination of naphthazarin can be of any value, and equally obvious from Table 1 that none of the numerous studies that have previously been made have been of this calibre. By far the most meaningful of these, is the three dimensional investigation of modification of "C" by Pascard-Billy (7) which yielded the results shown in Fig. 1.

Pascard-Billy herself interpreted these results in favour of structure III mainly on the basis of apparent deviations from mmm molecular symmetry. It must, however, be noted that the bond length pattern as reported could, within the estimated standard deviation (the method used for error estimation is notoriously prone to optimism), be interpreted in favour of any of the possible structures. The two dimensional studies by Pascard-Billy (9, 11) have all yielded hydrogen atom positions which appear to be asymmetrical with respect to the oxygen atoms, and have again been interpreted as supporting III, but the

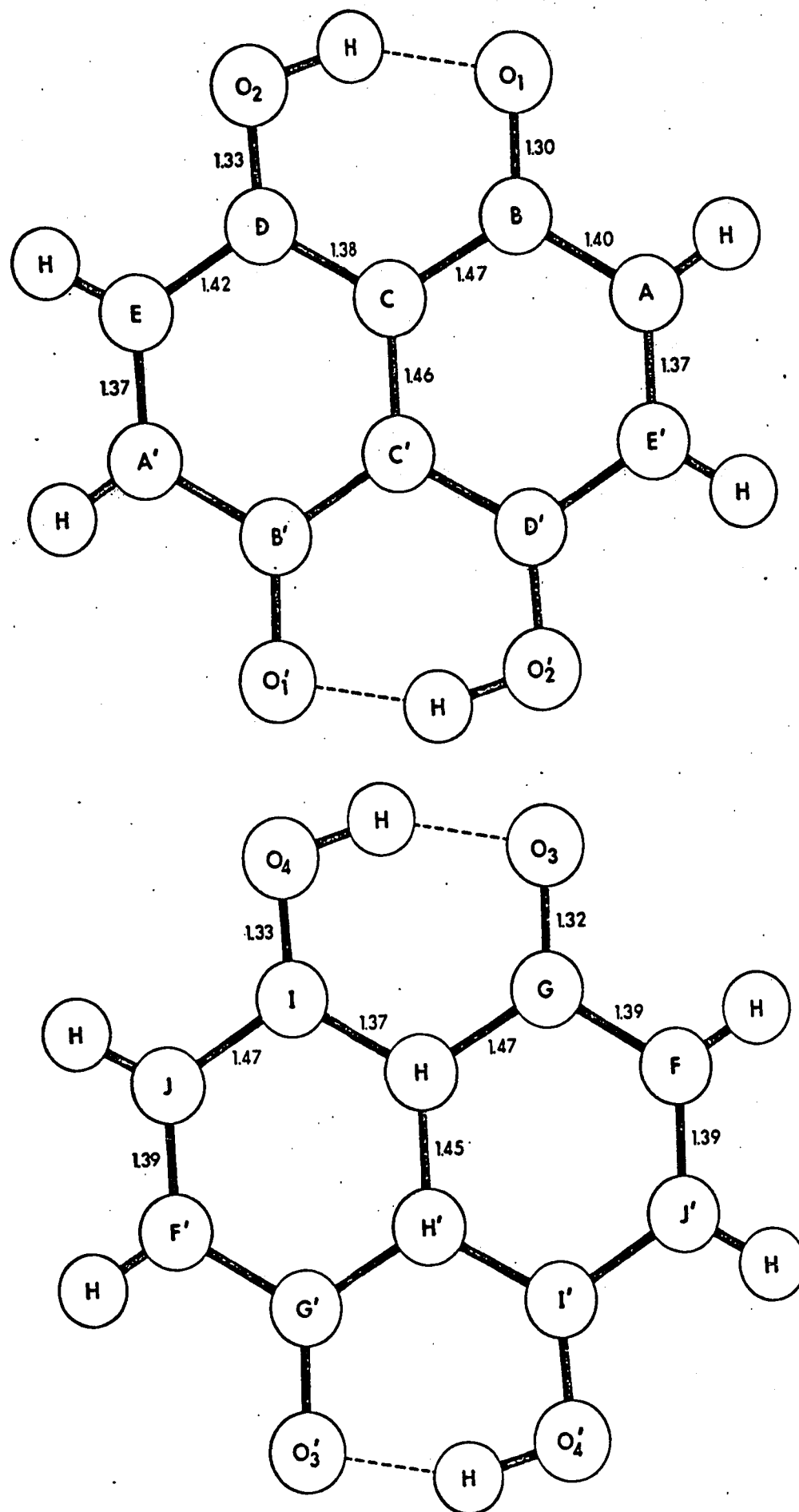


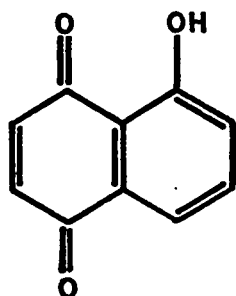
Fig. 1. Bond lengths for form "C".

standard deviations quoted are too large (0.02 \AA) to support such a conclusion.

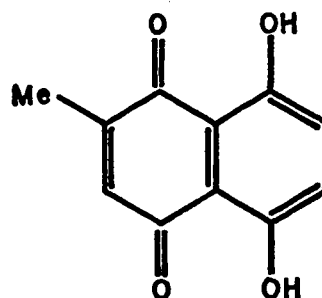
It was observed in the paper by Watase (15) that although the systematic extinctions on normally exposed photographs do indicate space group $P2_1/c$ ($h0\ell$, $\ell = 2n + 1$; $0k0$, $k = 2n + 1$) for modification "A", on very long exposure photographs a small number of very faint reflections of the type $h0\ell$, $\ell = 2n + 1$ were observed. The implication of this is that the structure is a close approximation, but only an approximation to the centrosymmetric structure in space group $P2_1/c$, and it appeared then very possible that the true structure is I and in this modification the stacking is not disordered (the true space group would be $P2_1$). Watase et al. had apparently made no attempt to interpret these weak reflections, but if indeed they are genuine diffraction effects, it seemed that further investigation of this modification was warranted.

In addition, it was decided to refine further the data reported by Pascard-Billy for modification "C"; it appeared from the account of the work that a very complete set of data had been collected for this modification, but the refinement had not been completed and much more reliable bond length information could probably be obtained.

Another approach to this problem could be a study of molecules closely related to naphthazarin but which do not approximate to centrosymmetry. Suitable molecules of this type might be juglone (5-hydroxy-1,4-naphthoquinone), or a substituted naphthazarin such as 2-methyl-5,8-dihydroxy 1,4-naphthoquinone.

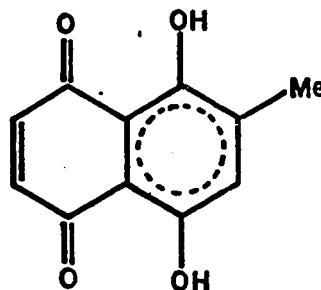
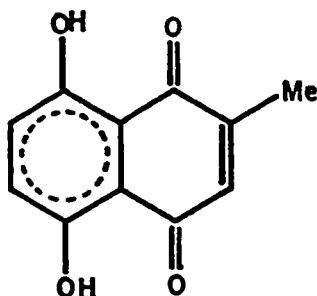


Juglone



Methylnaphthazarin

It is reasonable to suppose that the structures of such compounds would not be disordered, as the molecular packing would presumably be such that a "mistake" would be very different energetically. It must however, also be recognised that the very loss of symmetry which makes disorder unlikely must also make delocalisation less possible. Canonical forms such as:



are not identical (one could well be sufficiently more stable to be dominant), and investigations of such molecules may or may not be relevant to the problem of naphthazarin itself.

In fact the crystal structure of juglone was determined; 2-methyl 5,8-dihydroxy 1,4-naphthoquinone was prepared and the data had been collected when the publication of Moore and Shueur (see p. 5) appeared describing the n.m.r. spectra of juglone, naphthazarin and various substituted naphthazarins. The spectrum of juglone clearly showed that this molecule does not undergo the tautomerism (even though it is still possible) observed in naphthazarin. The quinonoid protons, which have an identical environment give rise to a single peak and the three benzenoid protons show peaks consistent with the ABX spectra normally obtained from three non-equivalent protons. Likewise the spectrum of methyl-naphthazarin showed that this molecule is also "fixed" in a particular quinonoid-benzenoid form. Thus if these molecules exhibit a different behaviour to naphthazarin in solution, it is doubtful that the crystal structures could be compared with any validity, and hence the crystal structure of methyl-naphthazarin was not continued. The preliminary results are given in Part III(d).

Previously, an attempt had been made to prepare a chloro-substituted naphthazarin but it transpired that the product was in fact chloranilic acid. As the results of this particular investigation are not relevant to the naphthazarin problem, they are described in Part III(a).

PART I(B) The refinement of 5,8-dihydroxy 1,4-naphthoquinone
(Naphthazarin)

Naphthazarin was prepared by the Friedel-Crafts reaction between hydroquinone and maleic anhydride (4) Dark green crystals of modification "A" were obtained from glacial acetic acid, along with some red crystals of modification "B".

Crystal Data

The data obtained is compared to that published by Watase et al (15), Borgen (14) and Pascard-Billy (11), after transforming their data to $P2_1/n$.

Watase	Borgen	Pascard-Billy	This work
$a = 3.74 \text{ \AA}$	$a = 3.81 \text{ \AA}$	$a = 3.75 \text{ \AA}$	$a = 3.743 \pm .004 \text{ \AA}$
$b = 7.63 \text{ \AA}$	$b = 7.63 \text{ \AA}$	$b = 7.66 \text{ \AA}$	$b = 7.622 \pm .008 \text{ \AA}$
$c = 14.55 \text{ \AA}$	$c = 14.55 \text{ \AA}$	$c = 14.50 \text{ \AA}$	$c = 14.549 \pm .015 \text{ \AA}$
$\beta = 97.4^\circ$	$\beta = 97.2^\circ$	$\beta = 97.0^\circ$	$\beta = 97.7 \pm 0.1^\circ$

The unit cell dimensions and errors were calculated from precession photograph measurement using the method of Patterson and Love (64). When film shrinkage corrections

were made, the films were found to have expanded by 0.1%. The space group was confirmed as $P2_1/n$ and as there are two molecules in the unit cell, these must occupy special positions of two-fold multiplicity, requiring the molecular centre of each molecule to lie on a centre of symmetry. Intensity data were initially collected by Weissenberg photography using $\text{CuK}\alpha$ radiation and with the crystal rotating about the needle, or $[a]$ axis. Two exposures of the layers $h = 0, 1, 2$ were recorded using exposure times of 14 and 100 hours. Some weak reflections have been reported by Watase et al (15), which should normally be excluded by the glide symmetry element of the space group, and several of these viz: (102) , $(\bar{1}02)$, (106) , $(\bar{2}03)$, were apparently observed on the 100 hour exposures. The fact that these reflections occur on the regular data festoons and appear to be true crystal diffraction effects, requires that they be given special consideration.

It is well known that diffraction anomalies can occur on very long exposure photographs when an old X-ray tube is used, and many of these can safely be attributed to target impurities. The photographs on which the forbidden $(h0l)$ reflections were observed certainly did contain other such weak reflections although

in general they did not fall on the same festoons as the copper data and they always occurred at low θ values where the geometric and thermal conditions are favourable for their observation (those reflections due to iron impurities were readily identified; the ratio between the $\text{FeK}\alpha$ and $\text{CuK}\alpha$ wavelengths is 1.937:1.542 or 5:4, and weak reflections were observed along the (00 l) festoons with a repeat in the ratio 5:4 with the stronger $\text{CuK}\alpha$ reflections). A possible explanation for these weak reflections is that they are Renninger (43) or double reflections, where a strong reflected beam from one set of crystal planes fulfils the conditions for reflection from another set. Fankuchen et al (44) and Zachariasen (45) have shown that this situation is invariably encountered when equi-inclination geometry is used with the crystal rotation axis coincident with a symmetry reciprocal lattice axis, and indeed Srivastava (17) has satisfactorily explained the presence of a weak forbidden reflection in modification "C", when the data was collected in just this situation. The data collection in the present work (and that by Watase) was made with the crystal rotating about a non-unique axis and although Renninger reflections can still occur by chance, the likelihood of their doing so is much more remote.

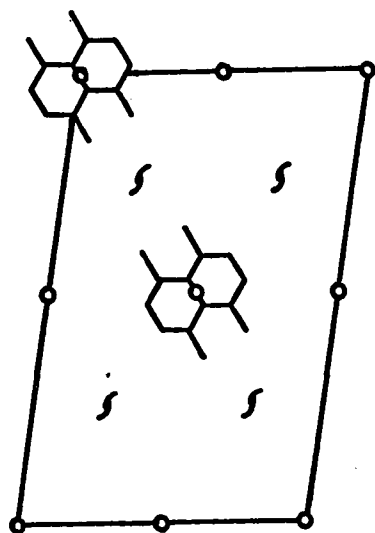
As the geometrical requirements for such a reflection are so exact, they are usually observed as much sharper reflections than singly reflected data, but the weak reflections under consideration did not show any marked difference in spot shape from the bulk of the data. However, in view of the great difference in intensity between these forbidden reflections and their near neighbours and also the fact that they are all low θ reflections and somewhat distorted, it is not possible to state that their shape was identical. Further, in view of the relatively large number of these weak reflections, it does seem unlikely that they are the result of double reflections.

If these weak reflections are genuine diffraction effects from the crystal then the n glide symmetry element must be absent from the space group, and whereas $P2_1/n$ will be a good approximation to the true symmetry, the space group will be more correctly represented as $P2_1$. The implications of this so far as the naphthazarin molecule is concerned are:

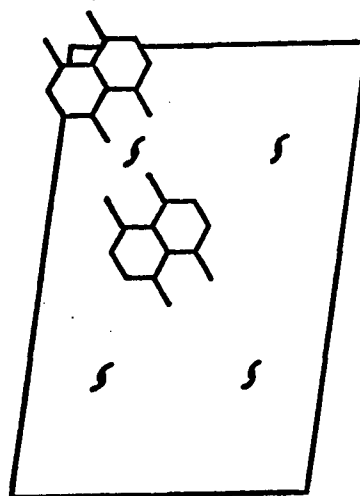
- (a) The molecule can now truly be represented as a non-centrosymmetric structure such as (I)
(see p. 4).

or (b) The molecules can still be centrosymmetric
(III) (see p. 10) but now not truly related
by the n glide symmetry element.

With reference to the Pascard-Billy representation of the molecule i.e. model III in space group $P2_1/n$, (a) implies a slight change in molecular geometry since the molecules will have $mm2$ symmetry as opposed to $2/m$, whereas (b) involves no change in molecular geometry but the molecular centres of the two molecules in the unit cell need only approximate to the special positions of $P2_1/n$ viz: (000) , $(\frac{1}{2}\frac{1}{2}\frac{1}{2})$; the deviations from these positions can only be along the x and z directions.



Molecules in $P2_1/n$



Molecules in $P2_1$

The collection of data on a diffractometer is distinctly advantageous to collection by film techniques,

especially in a problem of this nature where the observation of weak reflections considerably affects the arguments pertaining to the structure. Diffractometer collected data is inherently more accurate than film collected data because of the different recording technique used and in addition, with the Pailred instrument, crystal monochromatised radiation is available which will eliminate anomalous reflections caused by target impurities in the X-ray tube. Finally, the problem of the relative scale between the weak and strong reflections does not arise; films generally have only a limited range over which the optical density is proportional to the intensity of the X-ray beam, whereas this range is considerably greater for a crystal scintillator. Initially, the strong reflections of the three layers $(0k\ell)$, $(1k\ell)$, $(2k\ell)$, were recorded to ensure that the crystal was correctly aligned (these reflections were counted for 1.8 min at a scan speed of $1^\circ/\text{min}$, and background was counted for 1.3 min), and then the weak reflections were considered. All reflections in the above three layers which are normally excluded by the n glide $((h0\ell), h + \ell = 2n + 1)$ were scanned for ten minutes with a scan speed of $0.1^\circ/\text{min}$ and the background was counted for eight minutes to ensure favourable counting statistics; these results are tabulated in Table 2.

TABLE 2

ANALYSIS OF WEAK REFLECTIONS

 $t_T = 10 \text{ mins}$ $t_1 = t_2 = 4 \text{ mins}$ $t = 10/8 = 1.25.$
 $t^2 = 1.563$

h	k	l	B ₁	T	B ₂	B=B ₁ +B ₂	I	σI	$\sigma I/I$
0	0	1	6588	16250	6736	13324	16250-16655	-	-
0	0	3	2609	6550	2577	5186	67.50	121.06	1.79
		5	1131	2935	1229	2360	2935-2950	-	-
		7	713	1756	702	1415	1756-1769	-	-
		9	501	1126	484	985	1126-1231	-	-
		11	489	1178	454	943	1178-1179	-	-
		13	337	876	330	667	32.25	43.8	1.36
		15	305	834	296	601	82.75	42.1	0.51
		17	371	912	392	763	912-954	-	-
		$\overline{1}$	6418	16278	6487	12905	146.75	190.9	1.30
		$\overline{3}$	2636	6466	2655	5291	6466-6614	-	-
		$\overline{5}$	1220	2905	1120	2340	2905-2925	-	-
		$\overline{7}$	707	1824	701	1408	64.00	63.4	0.99
		$\overline{9}$	502	1143	467	969	1143-1211	-	-
		$\overline{11}$	492	1161	457	949	1161-1186	-	-
		$\overline{13}$	343	791	295	638	791-798	-	-
		$\overline{15}$	276	741	296	572	26.00	40.4	1.55
		$\overline{17}$	345	876	356	701	876-877	-	-

Table 2 cont'd.

h k l	B	T	B ₂	B=B ₁ +B ₂	I	σI	$\sigma I/I$
1 0 16	397	798	374	771	798-964	-	-
14	368	779	369	737	779-921	-	-
12	388	949	373	761	949-951	-	-
10	430	1120	438	868	35	44.7	1.2
8	539	1318	514	1053	2	49.8	2.5
6	1149	2829	1091	2240	29	79.6	2.7
4	1054	2766	1117	2171	52	78.5	1.5
2	1948	4869	1946	3894	1	-	-
$\bar{2}$	2553	6467	2602	5155	23	120.5	5.2
$\bar{4}$	1416	3571	1347	2763	117	88.8	0.8
$\bar{6}$	934	2352	963	1897	2352-2371	-	-
$\bar{8}$	848	2179	822	1670	91	69.2	0.8
$\bar{10}$	498	1225	510	1008	1225-1260	-	-
$\bar{12}$	417	1061	433	850	1061-1063	-	-
$\bar{14}$	307	803	293	600	53	41.7	0.8
$\bar{16}$	298	804	314	612	39	42.0	1.1

Table 2 cont'd.

h k l	B ₁	T	B ₂	B=B ₁ +B ₂	I	σI	$\sigma I/I$
2 0 13	404	1105	435	839	56	49.2	0.88
11	355	921	405	760	921-950	-	-
9	396	1085	411	807	76	48.43	0.64
7	510	1322	518	1028	37	54.1	1.46
5	632	1522	569	1201	21	58.3	2.78
3	914	2536	967	1881	185	74.0	0.4
1	888	2080	854	1742	2080-2178	-	-
$\bar{1}$	877	2278	811	1688	168	70.1	0.4
$\bar{3}$	932	2373	954	1886	15	73.0	0.5
$\bar{5}$	624	1682	669	1293	66	60.8	0.92
$\bar{7}$	526	1298	541	1067	1248-1334		
$\bar{9}$	370	1081	384	754	138	47.5	0.34
$\bar{11}$	365	875	378	743	-		
$\bar{13}$	396	910	377	773	-		

In collecting diffractometer data, one normally determines I and $\sigma I(68)$ ($I = T - tB$, $\sigma I = (T + t^2 B)^{1/2}$ where T = total count, B = total background count and t = ratio of reflection counting time over the total background counting time. i.e. $t_T/(t_1 + t_2)$ and a reflection is conventionally considered to be significantly greater than background if the ratio $\sigma I/I$ is less than a pre-chosen constant normally in the range 0.3 to 0.5. Clearly from Table 2, none of the (00 ℓ) or (10 ℓ) reflections meet this requirement and three only of the (20 ℓ) reflections are marginal. Most significantly, not one of the reflections thought to have been observed on the films has been confirmed by this experiment. Although it is not possible to say that the weak reflections do not exist, it does seem most likely that those observed on the photographs are in some way artifacts of the experiment, or at most, are so very weak that they can have little structural significance and from this point they were completely ignored.

The model published by Pascard-Billy (11) was now refined by full matrix least squares (33) using the diffractometer collected data which comprised the 355 observed reflections remaining after the application of

the exclusion limit $\sigma I/I = 0.5$. Throughout all refinements the scattering factors used for oxygen and carbon were those listed in the International Tables (38) and the weighting scheme used was of the form

$$w = a^2 / (a^2 + (F - b)^2) \quad \text{with } a = 3.1, b = 3.6$$

which ensured that mean $w(\Delta F)^2$ was invariant with F . The starting model gave an R factor $(\sum ||F_o| - |F_c|| / \sum |F_o|)$ of 0.189, assuming all atoms to have isotropic temperature factors. This model would not refine further so anisotropic temperature factors were given to all atoms, whence the R factor dropped immediately to 0.073. Eight large low θ reflections were found to be suffering from secondary extinction (attenuation of the primary X-ray beam by the transfer of energy to the reflected beam (101))^a so these were removed and the refinement converged in one further cycle to an R factor of 0.071.

Concurrently with this refinement, the model of form "C" published by Pascard-Billy (7) was refined further in the same manner as above using her published data. This form has four molecules in the unit cell, thus considerably more data is available than for "A" and 1254 reflections were reported in all. The reported model gave an R factor of 0.189 with isotropic

temperature factors for all atoms and refined slowly to an R factor of 0.174. When anisotropic thermal motion was assumed the refinement converged in four cycles to an R factor of 0.134. It was noticed, at this stage, that ten large low θ reflections were showing exceptionally bad agreement and were obviously suffering from secondary extinction, hence these reflections were removed and the R factor dropped to 0.113.

To facilitate the location of the hydrogen atoms, a Fourier synthesis programme was used which calculated electron density in a general plane (55). Difference syntheses, phased by the heavy atoms, were thus calculated for both forms in planes defined by the two oxygen atoms and one of the carbon atoms to which an oxygen was bonded. This particular plane was chosen to ensure that the phenolic hydrogen would lie in or close to it; Table 11 (Least Squares planes) shows that the oxygen atoms do deviate from the mean plane ($O1, 0.009 \text{ \AA}$; $O2, 0.018 \text{ \AA}$ for form "A") and this will inevitably cause some distortion in the carbon atom positions plotted on the maps in Figs. 9 to 14 and also in the position of the residual electron density due to the "ring" hydrogen atoms

(see Figs 9, 11 and 13). The former distortion is insignificant in view of the minor deviation of the oxygen from the molecular plane and the latter was not felt to be important as it was intended to refine the hydrogen atom positions by least squares methods. The contour levels shown on these maps are in intervals of the standard deviation in electron density as calculated by the Cruickshank formula (56) and, at this stage of refinement of the two models, these values were: form "A", $0.07 \text{ e.}\text{\AA}^{-3}$; form "C", $0.145 \text{ e.}\text{\AA}^{-3}$. These values have almost certainly been underestimated as the formula given by Cruickshank assumes that the data set is complete i.e. contains all reflections within the limiting sphere, and with only single axis data for form "A" the data set is clearly far from complete. In all molecules, the hydrogen atoms were placed on the positions of maximum density and were given the equivalent isotropic temperature factor of the atom to which they were bonded (the average of the two oxygen temperature factors was used for the phenolic hydrogen). The positional, and temperature parameters of the hydrogen atom together with the heavy atom parameters, were refined by full matrix least squares. The scattering factor curve used for the hydrogen atoms

was that published by Mason and Robertson (54), who derived the new curve experimentally from the refinement of diphenyl (59). The refinement of model "A" converged in two more cycles at an R factor of 0.051 and model "C" converged at a final R factor of 0.095. Because of the large thermal motion of the molecule in form "A" and the elliptical electron density for the hydrogen atoms (see Fig. 9), the refinement was continued assuming anisotropic temperature factors for the hydrogen atoms in the hope that this would yield better hydrogen atom positions, especially for the phenolic hydrogen. All temperature factor tensors remained positive definite ($|\beta_{ij}| > 0$) and this refinement resulted in a further drop in R factor to 0.048.

Results

Final atomic coordinates and temperature factors are listed in Tables 3 to 6. The latter are expressed as dimensioned U_{ij} values which were calculated from the β_{ij} s used in the refinement by the method given by Cruickshank (67)

$$U_{ij} = \beta_{ij} / 2\pi^2 a_i^* \cdot a_j^*$$

This is the form used for all anisotropic temperature factors in this thesis. The refined β_{ij} s refer to the

temperature factor expression:

$$\beta_{11}h^2a^{*2} + \beta_{22}k^2b^{*2} + \beta_{33}l^2c^{*2} + 2\beta_{12}hka^*b^*\sin\gamma^* \\ + 2\beta_{13}hla^*c^*\sin\beta^* + 2\beta_{23}klb^*c^*\sin\alpha^*.$$

Figs 2 to 5 show the dimensions of the molecules and the 50% probability vibrational ellipsoids (66) which are also used for all other thermal ellipsoid diagrams in this thesis. Structure factors[†](for form "A" these correspond to the model with isotropic hydrogen atoms), least squares planes and the results for the rigid body vibration analysis are shown in Tables 8 to 13 . The molecule packing can be seen in the projections onto the [ac] and [bc] planes in Figs. 6 and 7 , and the shorter intermolecular approaches are shown in Table 7.

Hydrogen atom anisotropy

In any least square process, an increase in the number of variable parameters will almost certainly result in a better correlation between the observed and calculated quantities, thus the decrease in R factor of 0.003, on the assumption of anisotropic temperature factors for the hydrogen atoms, must be tested to ascertain whether it is statistically significant or simply the expected result of increasing the number of variable parameters. This test can be made by a method

[†] All structure factors in this thesis are on the absolute scale $\times 10$.

devised by Hamilton (20). The ratio of the weighted R factors R_w ($=[\sum_w ||F_o| - |F_c||^2 / \sum_w |F_o|^2]^{1/2}$) is checked against a table of significant points pertinent to the situation, and when this ratio exceeds a value in this table, the hypothesis under test can be rejected at the specific significance level. The hypothesis in the present context would be: "The anisotropic motion of the hydrogen atoms is not significant".

The R factors in the two situations are:

	<u>R</u>	<u>R_w</u>
model with isotropic hydrogen atoms	0.051	0.048
" " anisotropic " "	0.048	0.046

The ratio of the weighted R factors is 1.046

The dimension of the hypothesis = 15

The number of degrees of freedom = 347 - 91 = 256

Pertinent significance points obtained from the Table in (20) are:

1.048 at the 5% significance level

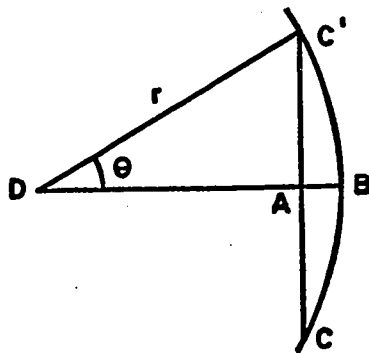
1.043 " " 10% " "

i.e. the above hypothesis can be rejected at a significance level between 5% and 10%.

The criterion for rejection of hypotheses has been stated by Hamilton (65) as: "Rejection at a significance level greater than 5% is not significant". Thus this test shows that the refinement of the hydrogen atoms with anisotropic temperature factors does not yield a significantly improved model. Hydrogen atoms contribute to a very small fraction of the total diffraction pattern from a crystal and so if this type of refinement is to be attempted, the utmost care must be taken at the data collection stage in order to minimise experimental errors. This can best be done by collecting data from more than one crystal (see acridene (58) and diphenyl (59)); a technique which was not employed in the present case.

Rigid body vibrations

When molecular librations constitute the major mode of vibration of a group of atoms, the bond lengths determined from the final atomic coordinates can be subject to error because of the approximation of atomic vibrations to ellipsoids.



Let B be the position of an atom at rest; if the molecule makes rotational oscillations about the point D, the motion of B (in 2 dimensions) will describe an arc CBC' with centre at D. This motion will be described crystallographically by an ellipse with CC' as one axis, and thus the time average electron density will have its maximum at A which will be the atomic position of atom B as given by the refined coordinates. If θ is the angle of oscillation of the molecule, then atom B will appear closer to D by $r.(1 - \cos\theta)$. The amplitude of the oscillation θ can be determined from the vibrational ellipsoids of the atoms by the method given by Cruickshank (63) which is outlined briefly below (the mathematics of the method are given in Appendix B).

The mean-square amplitudes of vibration (\bar{u}^2) can be expressed in terms of the refined parameters (U_{ij}^o) which describe the vibrational ellipsoids of the atoms; \bar{u}^2 can also be expressed in terms of the mean-square amplitudes of the rigid body translational (T_{ij}) and librational (ω_{ij}) components from which it is possible to calculate the U_{ij}^c parameters that will now describe the atomic vibrations purely in terms of rigid body motions. Assuming that the atomic motion is totally due to rigid body vibrations, then the relation given

below will hold

$$\bar{u}^2 = f(U_{ij}^O) = f(U_{ij}^C) = f(T_{ij}, \omega_{ij})$$

from which it is possible to calculate the terms T_{ij} and ω_{ij} by a linear least squares procedure, where the residuals $\sum (U_{ij}^O - U_{ij}^C)^2$ are minimised with respect to these parameters.

The amplitudes of the molecular librations (ω_{ij}) can now be used to correct the bond lengths of the molecule by the expression given above, or more precisely, by the method given by Cruickshank in (60). In the latter correction, Cruickshank seeks to establish the point of maximum scattering density of an individual atom, which requires knowledge of the peak-shape of the electron density for the atom at rest. These peak-shape parameters are not always known with certainty, thus rather than introduce further approximations at this stage, an expression derived more recently by Busing and Levy (61) was used. This expression corrects the mean separation of a pair of atoms rather than the individual positions and thus probably yields results closer to physical reality, although the two methods do give essentially the same bond length corrections when applied to benzene (61, 62)

The Busing and Levy correction which gives the corrected bond length, \bar{S} , in terms of the refined bond lengths, S_o , is: $\bar{S} = S_o + (\omega_{ii} \cdot S_o \cdot \sin^2 \psi) / 2$, where ω_{ii} is the mean-square amplitude of libration about the principal axis, i , and ψ is the angle between this axis and the bond, S_o . For oscillations about more than one principal axis, the correction terms are additive.

Table 8 shows the root-mean-square vibrational amplitudes along the minor, medium and major axes for the heavy atoms of both forms and, from inspection of this Table and Figs 3 and 5, it can be seen that the major atomic vibration for the carbon skeleton is a molecular libration about the molecular normal, with little out-of-plane deformation. The oxygen atoms confirmed this observation although the vibrational amplitudes along the medium axes (which are approximately normal to the molecular plane (see Fig 3)) show that they do vibrate considerably in the out-of-plane bending mode. Clearly the correction for molecular libration was warranted in both forms. In view of the oxygen out-of-plane vibrations, the first analysis was done by considering the carbon atoms only in order to obtain the corrections due to true rigid body

vibrations. A second calculation was done including the oxygen contributions. The results of these analyses are tabulated in Tables 9 and 10. The good agreement between the calculated and observed U_{ij} values shows that the major vibration is indeed due to rigid body librations. The largest amplitude of oscillation is 6° about the molecular normal, which is slightly lower than that found in benzene (7.9° (62)) as expected because of the greater mass of the naphthazarin molecule. The oscillations about axes in the molecular plane ($\omega_{11} = 3.1^\circ$, $\omega_{22} = 2.4^\circ$) are smaller than those found in benzene (6.2° , 3.8°). The influence of the oxygen out-of-plane bending vibration can be seen by comparing the oscillation amplitudes in the two separate calculations; when the oxygens are included the oscillation amplitude about the y axis (ω_{22}) becomes comparable to that about the molecular normal (ω_{33}) but the agreement between observed and calculated U_{ij} values is worse. The agreement indices ($(\Sigma(|U_o| - |U_c|))/\Sigma|U_o|$) for the two calculations were 5% and 6.2%. The corrected bond lengths are shown in Fig. 2. The thermal motion analysis results for form "C" are shown below for the "carbon only" case:

<u>Molecule (1)</u>	<u>Molecule (2)</u>
$\omega_{11} = 2.8(3)^\circ$	$\omega_{11} = 2.7(2)^\circ$
$\omega_{22} = 1(2)^\circ$	$\omega_{22} = 2(1)^\circ$
$\omega_{33} = 2.96(7)^\circ$	$\omega_{33} = 4.04(3)^\circ$

When the oxygen atoms were included in the calculations, ω_{11} , ω_{33} remained constant, and ω_{22} increased to approximately 4.3° . The agreement indices for U_{ij} (observed) and U_{ij} (calculated) were: molecule (1), 6.9%, 7.5%; molecule (2), 5.4%, 7.2%. The behaviour of molecule (2) is rather similar to that of the molecule in form "A" but the above results indicate that the oxygens of molecule (1) have large out-of-plane bending vibrations. In addition, the relatively bad agreement obtained for the calculated U_{ij} values indicates that the assumption that this molecule vibrates as a rigid body has not been very well approximated. Although molecule (2) does appear to vibrate as a rigid body, the small oscillation angles (particularly that about ω_{33}) are rather surprising when compared to the molecule in form "A". This analysis seems to suggest that anisotropic parameters in form "C" have not only accounted for thermal motion, but also random errors in the data and thus the refinement of the hydrogen atoms in form "C" is likely to

do the same thing. The rather "messy" electron density observed on the difference Fourier maps (Figs 11, 13), especially that associated with H_{13} and H_{21} , is most likely due to data errors.

For above reasons the discussion of molecular geometry is restricted to the molecule in form "A".

Least Squares planes

The equations of the least squares planes for both forms and the deviations from planarity are listed in Table 11; only the carbon atoms were used to define the planes so that the deviations from planarity of the other atoms might be more readily seen. The carbon atoms in form "A" are clearly exactly planar, their deviations from planarity are all less than 1σ . The oxygen atoms show deviations of 2σ from the plane for O_1 and 6σ for O_2 ; the latter deviation is probably significant and will be discussed in the next section. All hydrogen atoms lie fairly well in the plane although the phenolic hydrogen has a deviation of 2.5σ in the same direction as O_2 , to which it is bonded. Molecule (2) of form "C" is clearly planar as the biggest deviations from the plane are 2σ (for O_{21} and H_{21}), while molecule (1) shows deviations of 2σ for C_{12} and an apparently significant deviation of 7σ for O_{11} .

TABLE 3FINAL ATOMIC COORDINATES FOR FORM "A"

	x	y	z
C ₁	-0.1549(13)	0.1564(6)	0.1450(4)
C ₂	-0.0153(11)	-0.0134(6)	0.1286(2)
C ₃	0.0421(9)	-0.0609(5)	0.0365(2)
C ₄	0.1820(11)	-0.2294(5)	0.0176(3)
C ₅	0.2348(13)	-0.2725(7)	-0.0758(3)
O ₁	0.0609(10)	-0.1216(5)	0.1975(2)
O ₂	0.2667(10)	-0.3441(5)	0.0823(3)
H ₁	0.169(13)	0.806(8)	0.789(3)
H ₅	0.325(13)	0.612(7)	0.913(3)
H ₃	-0.228(18)	0.271(6)	0.857(3)

TABLE 4
ANISOTROPIC TEMPERATURE FACTORS FOR FORM "A" (\AA^2)

Atom	U_{11}	U_{22}	U_{33}	U_{12}	U_{13}	U_{23}	equivalent isotropic B
C ₁	0.053(4)	0.088(3)	0.067(3)	-0.007(3)	0.013(2)	-0.035(3)	5.5
C ₂	0.045(3)	0.084(3)	0.044(2)	-0.006(2)	0.007(2)	0.003(2)	4.6
C ₃	0.039(3)	0.037(2)	0.050(2)	-0.002(2)	0.009(1)	0.002(1)	3.3
C ₄	0.046(3)	0.044(2)	0.087(3)	-0.002(2)	0.011(2)	0.009(2)	4.6
C ₅	0.056(4)	0.053(2)	0.097(3)	-0.004(2)	0.020(3)	-0.029(3)	5.3
O ₁	0.094(3)	0.141(4)	0.055(2)	0.002(2)	0.014(2)	0.032(2)	7.6
O ₂	0.095(3)	0.060(2)	0.122(3)	0.020(2)	0.016(2)	0.034(2)	7.3
H ₁	0.10(4)	0.24(6)	0.06(3)	-0.02(4)	0.03(2)	-0.06(3)	10.2
H ₅	0.09(4)	0.10(4)	0.10(3)	0.02(3)	0.02(2)	-0.03(3)	7.4
H ₃	0.22(6)	0.05(3)	0.07(3)	0.04(3)	0.03(3)	0.02(3)	9.0

TABLE 5
NAPHTHAZARIN FORM "C"

Final Atomic Coordinates (fractional)

Atom	x	y	z
C ₁₁	-0.0537(7)	0.1664(7)	-0.1601(4)
C ₁₂	0.0430(6)	0.2119(6)	-0.0705(3)
C ₁₃	0.0452(6)	0.0862(6)	0.0072(3)
C ₁₄	0.1379(6)	0.1250(7)	0.0985(3)
C ₁₅	0.1381(7)	-0.0084(7)	0.1737(3)
O ₁₁	0.1246(5)	0.3668(5)	-0.0627(3)
O ₁₂	0.2231(5)	0.2762(5)	0.1154(3)
C ₂₁	0.6845(7)	0.2358(7)	0.0989(4)
C ₂₂	0.6068(6)	0.2311(7)	0.0013(4)
C ₂₃	0.5093(6)	0.0746(6)	-0.0324(3)
C ₂₄	0.4310(6)	0.0641(7)	-0.1280(3)
C ₂₅	0.3326(6)	-0.0943(8)	-0.1593(3)
O ₂₁	0.6288(6)	0.3681(5)	-0.0553(3)
O ₂₂	0.4450(5)	0.1962(6)	-0.1898(3)
H ₁₁	-0.056(9)	0.248(10)	-0.215(5)
H ₁₅	0.210(8)	0.021(8)	0.237(4)
H ₁₃	0.211(12)	0.370(14)	0.039(7)
H ₂₅	0.271(9)	-0.127(9)	-0.223(5)
H ₂₁	0.761(8)	0.327(9)	0.117(4)
H ₂₃	0.541(9)	0.297(9)	-0.137(5)

TABLE 6

NAPHTHAZARIN FORM "C"

(a) Anisotropic temperature factors (\AA^2)							
Atom	U_{11}	U_{22}	U_{33}	U_{12}	U_{13}	U_{23}	equivalent isotropic B
C ₁₁	0.045(3)	0.041(3)	0.040(3)	0.003(2)	0.008(2)	0.013(2)	3.3
C ₁₂	0.035(3)	0.032(2)	0.037(2)	-0.001(2)	0.003(2)	0.004(2)	2.8
C ₁₃	0.033(2)	0.031(2)	0.028(2)	0.001(2)	0.002(2)	0.001(2)	2.4
C ₁₄	0.036(3)	0.036(3)	0.034(2)	-0.004(2)	0.006(2)	-0.005(2)	2.8
C ₁₅	0.046(3)	0.048(3)	0.031(2)	-0.002(2)	0.000(2)	0.003(2)	3.3
O ₁₁	0.058(3)	0.039(2)	0.058(2)	-0.010(2)	0.002(2)	0.013(2)	4.1
O ₁₂	0.052(2)	0.041(2)	0.051(2)	-0.015(2)	-0.007(2)	-0.006(2)	3.9
C ₂₁	0.037(3)	0.043(3)	0.048(3)	-0.013(2)	0.005(2)	-0.021(2)	3.4
C ₂₂	0.036(3)	0.031(2)	0.043(2)	-0.002(2)	0.006(2)	-0.004(2)	2.9
C ₂₃	0.029(2)	0.026(2)	0.031(2)	0.001(2)	0.001(2)	-0.001(2)	2.3
C ₂₄	0.033(2)	0.042(3)	0.027(2)	0.004(2)	0.001(2)	0.001(2)	2.7
C ₂₅	0.034(3)	0.055(3)	0.035(2)	-0.002(2)	-0.004(2)	-0.010(2)	3.3
O ₂₁	0.070(3)	0.030(2)	0.064(2)	-0.013(2)	0.011(2)	0.010(2)	4.3
O ₂₂	0.055(2)	0.061(3)	0.040(2)	0.002(2)	-0.005(2)	0.021(2)	4.2

Table cont'd over

Table 6 cont'd.

(b) Isotropic Temperature Factors (\AA^2)

<u>Atom</u>	<u>B</u>
H ₁₁	7(2)
H ₁₅	5(1)
H ₁₃	10(2)
H ₂₅	6(1)
H ₂₁	5(1)
H ₂₃	6(1)

TABLE 7
INTERMOLECULAR CONTACTS

Atom 1	Atom 2	Vector to be applied to atom 2	Distance (Å)
<u>Form "A"</u>			
H ₁	O ₁	$\frac{1}{2}-x-1, \frac{1}{2}+y, \frac{1}{2}+z$	2.58
H ₅	O ₂	$x-1, y+1, z$	2.54
O ₁	H ₁	$\frac{1}{2}-x-1, \frac{1}{2}+y-1, \frac{1}{2}+z$	2.58
H ₁	H ₃	$\frac{1}{2}-x, \frac{1}{2}+y, \frac{1}{2}-z$	2.55
H ₅	O ₂	$x, y+1, z$	3.01
H ₃	H ₁	$\frac{1}{2}-x, \frac{1}{2}+y-1, \frac{1}{2}+z$	2.55
<u>Form "C"</u>			
O ₁₁	H ₂₁	$\bar{x}+1, \bar{y}+1, \bar{z}$	2.582
H ₁₁	O ₁₂	$\frac{1}{2}+x-1, \frac{1}{2}-y, \frac{1}{2}+z-1$	2.761
H ₁₁	H ₂₅	$\frac{1}{2}-x, \frac{1}{2}+y, \frac{1}{2}-z-1$	2.705
H ₁₁	H ₁₅	$\frac{1}{2}-x-1, \frac{1}{2}+y, \frac{1}{2}-z-1$	2.510
H ₁₅	O ₁₂	$\frac{1}{2}+x-1, \frac{1}{2}-y, \frac{1}{2}+z-1$	2.757
H ₁₅	H ₂₃	$\frac{1}{2}-x, \frac{1}{2}+y-1, \frac{1}{2}-z-1$	2.705
O ₁₂	H ₁₅	$\frac{1}{2}-x-1, \frac{1}{2}+y, \frac{1}{2}-z-1$	2.534

Mean error for O-H contacts is $\pm 0.05 \text{ Å}$
and for H-H contacts is $\pm 0.07 \text{ Å}$

TABLE 8
ROOT-MEAN-SQUARE AMPLITUDES OF VIBRATION

	minor axis	medium axis	major axis
<u>(a) Form "A"</u>			
C ₁	.2023	.2279	.3377
C ₂	.2054	.2129	.2925
C ₃	.1874	.2003	.2238
C ₄	.2005	.2176	.2977
C ₅	.1929	.2305	.3344
O ₁	.2080	.3057	.3899
O ₂	.2030	.3120	.3712
<u>(b) Form "C"</u> <u>(molecule 1)</u>			
C ₁₁	.1651	.2098	.2318
C ₁₂	.1732	.1854	.2005
C ₁₃	.1662	.1750	.1836
C ₁₄	.1729	.1822	.2039
C ₁₅	.1712	.2138	.2221
O ₁₁	.1732	.2310	.2693
O ₁₂	.1620	.2294	.2594

Table 8 cont'd.

	minor axis	medium axis	major axis
<u>(c) Form "C"</u> <u>(molecule 2)</u>			
C ₂₁	.1414	.2005	.2618
C ₂₂	.1719	.1887	.2115
C ₂₃	.1589	.1657	.1840
C ₂₄	.1621	.1796	.2088
C ₂₅	.1577	.2031	.2418
O ₂₁	.1503	.2585	.2730
O ₂₂	.1591	.2375	.2743

TABLE 9
RIGID BODY VIBRATIONS FOR FORM "A"
 (Carbon atoms only)

(a) Translational tensor			\AA
T_{11}	0.041(2)		0.203(5)
T_{22}	0.047(2)		0.217(4)
T_{33}	0.035(4)		0.186(11)
T_{12}	0.004(2)		
T_{13}	0.001(2)		
T_{23}	0.007(2)		
(b) Librational tensor			\AA
ω_{11}	0.0028(7)		3.1(4)
ω_{22}	0.0018(23)		2.4(15)
ω_{33}	0.0110(5)		6.02(2)
ω_{12}	-0.0002(5)		
ω_{13}	-0.0012(5)		
ω_{23}	0.001(9)		
(c) Direction cosines of molecular axes (see fig) referred to abc*			
x	0.1230	-0.6566	0.7441
y	-0.3728	0.6643	0.6478
z	-0.9209	-0.3502	-0.1709
The z axis is normal to the least square plane through these atoms			

Table 9 cont'd.

Observed and rigid body U_{ij} s referred to
molecular axes (OBS/CALC)

	U_{11}	U_{22}	U_{33}	U_{12}	U_{13}	U_{23}
C_1	0.111	0.050	0.053	-0.014	0.012	0.006
	0.108	0.052	0.053	-0.014	0.013	0.003
C_2	0.060	0.069	0.044	-0.018	0.009	-0.005
	0.058	0.069	0.044	-0.016	0.008	-0.002
C_3	0.042	0.047	0.036	0.007	-0.001	0.002
	0.041	0.052	0.036	0.004	0.001	0.005
C_4	0.057	0.077	0.042	0.022	-0.001	0.003
	0.058	0.069	0.042	0.023	-0.003	0.002
C_5	0.103	0.051	0.053	0.022	0.003	0.010
	0.108	0.052	0.052	0.022	0.003	0.007

TABLE 10
RIGID BODY VIBRATIONS FOR FORM "A"
 (Carbon and Oxygen atoms)

(a) Translational Tensor		\AA	
T_{11}	0.041(2)	0.203(4)	
T_{22}	0.047(2)	0.216(4)	
T_{33}	0.024(3)	0.153(10)	
T_{12}	0.003(2)		
T_{13}	0.001(2)		
T_{23}	0.005(2)		
(b) Librational Tensor		($^{\circ}$)	
ω_{11}	0.0039(7)	3.6(3)	
ω_{22}	0.0098(6)	5.7(2)	
ω_{33}	0.0107(3)	5.93(2)	
ω_{12}	0.0001(3)		
ω_{13}	-0.0013(5)		
ω_{23}	0.0020(4)		
(c) <u>Direction cosines of molecular axes</u> (see Fig.) referred to abc*			
x	0.1230	-0.6566	0.7441
y	-0.3738	0.6639	0.6477
z	-0.9201	-0.3533	-0.1688

The z axis is normal to the least squares plane through these atoms.

Table 10 cont'd.

Observed and rigid body U_{ij} s referred to molecular axes (OBS/CALC)

	U_{11}	U_{22}	U_{33}	U_{12}	U_{13}	U_{23}
C_1	0.112	0.050	0.053	-0.014	0.012	0.006
	0.106	0.051	0.051	-0.015	0.013	0.002
C_2	0.060	0.069	0.044	-0.018	0.009	-0.005
	0.059	0.068	0.049	-0.016	0.007	-0.001
C_3	0.042	0.047	0.036	0.007	0.000	0.002
	0.041	0.052	0.028	0.003	0.001	0.004
C_4	0.057	0.077	0.042	0.022	-0.001	0.003
	0.058	0.068	0.049	0.022	-0.000	0.003
C_5	0.103	0.052	0.053	0.022	0.003	0.010
	0.107	0.052	0.052	0.021	0.006	0.006
O_1	0.061	0.127	0.101	-0.038	0.009	-0.016
	0.059	0.125	0.101	-0.035	0.011	-0.014
O_2	0.054	0.119	0.104	0.039	-0.002	-0.005
	0.059	0.125	0.102	0.040	-0.003	-0.005

TABLE 11
LEAST SQUARES PLANES*

(a) Form "A" $-0.9162x - 0.3620y - 0.1719z = 0$

Deviations from plane (\AA)

C_1	0.002(5)	O_1	-0.009(4)
C_2	0.000(4)	O_2	-0.018(3)
C_3	0.001(3)	H_1	-0.06(5)
C_4	0.001(4)	H_5	-0.03(5)
C_5	0.001(4)	H_3	-0.12(5)

(b) Form "C" (molecule 1)

$$0.8532x - 0.4301y - 0.2951z = 0$$

Deviations from plane (\AA)

C_{11}	-0.007(5)	O_{11}	0.030(4)
C_{12}	0.010(5)	O_{12}	0.000(4)
C_{13}	-0.007(4)	H_{11}	0.021(8)
C_{14}	-0.005(5)	H_{15}	-0.052(6)
C_{15}	0.003(5)	H_{13}	0.048(10)

(c) Form "C" (molecule 2)

$$0.8598x - 0.4305y - 0.2746z - 3.3933 = 0$$

Deviations from plane (\AA)

C_{21}	0.000(5)	O_{21}	0.009(4)
C_{22}	-0.003(5)	O_{22}	0.004(4)
C_{23}	0.003(4)	H_{21}	0.02(7)
C_{24}	0.003(5)	H_{25}	0.14(6)
C_{25}	-0.004(5)	H_{13}	0.06(7)

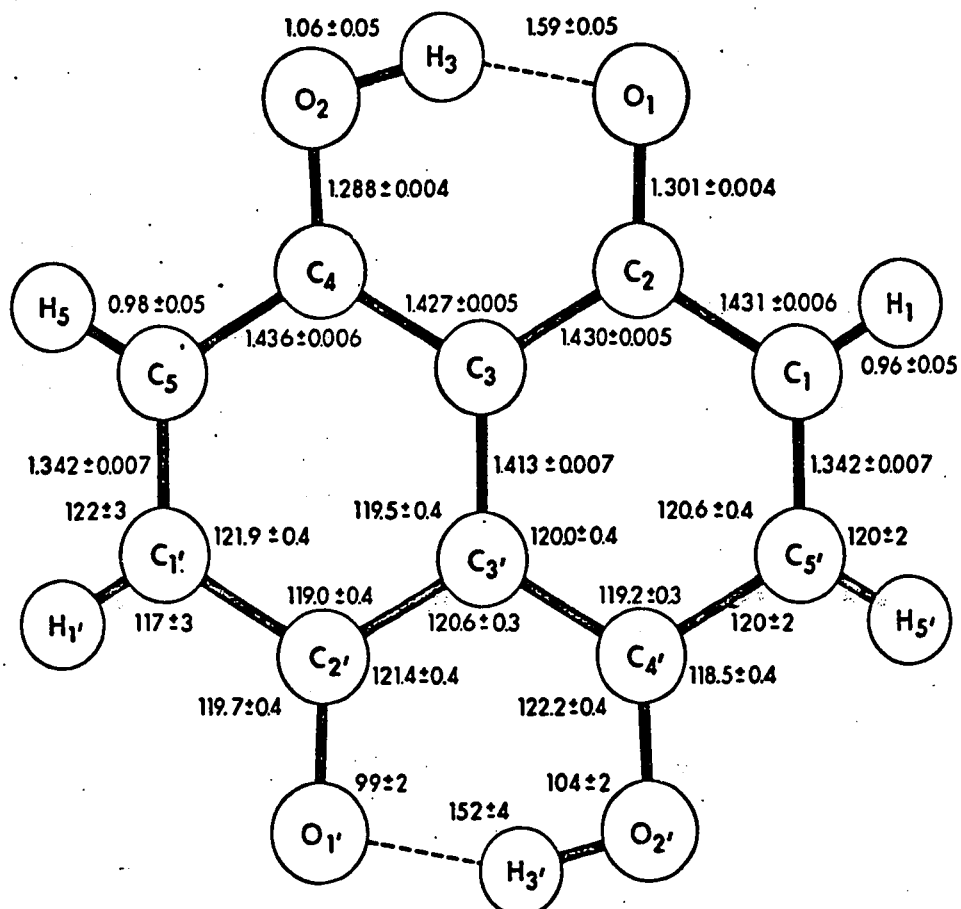
All planes are referred to the orthogonal axes abc

TABLE 12

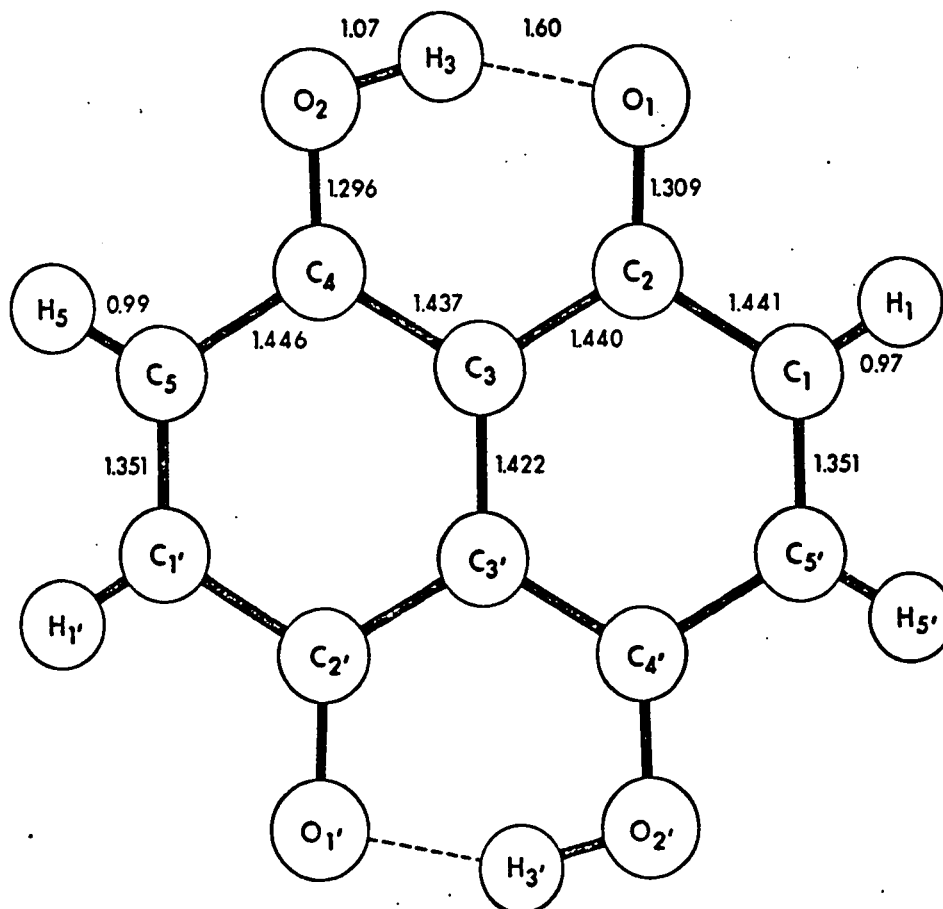
H	L	FD	FC	H	L	FD	FC	H	L	FD	FC	H	L	FD	FC
K = 0				K = 2				K = 4				K = 6			
0	4	87	-91	0	1	23	21	0	1	61	62	0	1	15	14
0	6	11	10	0	2	76	-79	0	2	67	66	0	2	25	-25
0	8	31	-31	0	3	91	-92	0	3	56	53	0	3	49	50
0	10	16	16	0	4	5	-7	0	4	13	-12	0	4	50	-50
0	12	36	-35	0	5	58	54	0	5	20	19	0	5	36	35
0	14	15	12	0	6	22	23	0	6	20	20	0	6	10	-9
1	3	97	-98	0	7	89	91	0	7	27	25	0	7	22	23
-1	3	83	-82	0	8	21	20	0	8	16	15	0	8	10	8
1	5	7	6	0	9	14	-13	0	9	11	-10	0	9	19	19
1	7	9	-10	0	10	24	-24	0	10	31	31	0	10	7	-4
-1	7	64	63	0	11	52	52	0	11	46	45	0	11	10	-9
1	9	24	22	0	12	42	-42	0	12	47	47	0	12	13	-18
1	13	40	-41	0	14	10	-9	0	13	64	63	0	13	9	-6
-1	13	17	-17	0	15	14	-13	0	14	9	-11	0	14	16	-17
1	15	12	13	1	1	77	36	0	15	27	-27	0	15	12	13
-1	15	11	13	-1	1	72	71	0	16	26	-26	0	16	14	16
-1	17	10	-9	1	2	21	-21	0	17	23	23	0	17	12	16
2	0	21	-22	-1	2	122	125	0	18	21	21	0	18	15	12
2	2	42	-43	1	3	27	-27	0	19	19	-16	0	19	13	13
-2	2	90	-86	-1	3	6	-8	0	20	17	17	0	20	7	-5
2	4	7	7	1	4	18	13	0	21	16	15	0	21	11	-11
-2	4	20	20	-1	4	41	-41	0	22	15	14	0	22	14	16
-2	6	18	-19	1	5	26	-27	0	23	14	13	0	23	12	16
-2	6	144	141	-1	5	17	-18	0	24	13	-14	0	24	10	12
-2	8	18	16	1	6	148	152	0	25	12	-11	0	25	8	3
2	10	11	-11	1	7	16	13	0	26	11	-10	0	26	7	-7
2	12	52	-52	1	8	13	13	0	27	10	-9	0	27	6	6
-2	12	17	-19	-1	8	30	-31	0	28	9	-8	0	28	5	5
2	14	8	-7	1	9	20	17	0	29	8	-7	0	29	4	4
-2	14	20	-20	-1	10	15	18	0	30	7	-6	0	30	3	3
-2	16	7	6	1	11	13	-12	0	31	6	-5	0	31	2	2
K = 1				-1	11	44	-47	0	32	5	-4	0	32	1	1
0	2	45	45	-1	12	44	46	0	33	4	-3	0	33	0	0
0	3	119	-121	-1	13	30	-32	0	34	3	-2	0	34	0	0
0	4	12	11	1	14	10	-11	0	35	2	-1	0	35	0	0
0	5	114	111	-1	14	16	-16	0	36	1	0	0	36	0	0
0	6	112	108	2	1	103	109	0	37	0	0	0	37	0	0
0	7	56	56	2	2	9	8	0	38	0	0	0	38	0	0
0	9	17	15	2	2	39	40	0	39	0	0	0	39	0	0
0	10	11	13	-2	3	83	80	0	40	0	0	0	40	0	0
0	11	43	-42	-2	3	64	64	0	41	0	0	0	41	0	0
0	12	44	44	2	4	21	-23	0	42	0	0	0	42	0	0
0	13	35	-34	-2	4	13	-14	0	43	0	0	0	43	0	0
0	15	10	10	2	5	26	28	0	44	0	0	0	44	0	0
0	17	9	-8	2	5	17	-17	0	45	0	0	0	45	0	0
1	2	47	48	-2	6	8	-5	0	46	0	0	0	46	0	0
-1	2	46	-48	2	6	12	-11	0	47	0	0	0	47	0	0
1	3	26	-27	2	7	15	15	0	48	0	0	0	48	0	0
-1	3	21	-22	-2	7	12	15	0	49	0	0	0	49	0	0
-1	4	42	-43	2	8	18	20	0	50	0	0	0	50	0	0
1	5	10	5	-2	11	17	19	0	51	0	0	0	51	0	0
-1	5	69	69	-2	12	23	-24	0	52	0	0	0	52	0	0
1	6	7	-6	K = 3				0	53	0	0	0	53	0	0
-1	6	93	91	0	1	92	95	0	54	0	0	0	54	0	0
1	7	24	23	0	2	92	92	0	55	0	0	0	55	0	0
-1	7	86	85	0	3	53	53	0	56	0	0	0	56	0	0
1	8	8	2	0	4	33	38	0	57	0	0	0	57	0	0
-1	9	10	-10	0	5	120	-120	0	58	0	0	0	58	0	0
1	10	10	-10	0	6	66	64	0	59	0	0	0	59	0	0
1	11	34	33	0	7	37	-37	0	60	0	0	0	60	0	0
-1	11	19	21	0	8	30	-29	0	61	0	0	0	61	0	0
1	12	46	-48	0	11	10	-9	0	62	0	0	0	62	0	0
-1	12	29	-30	0	14	18	-19	0	63	0	0	0	63	0	0
1	13	13	13	1	0	8	-12	0	64	0	0	0	64	0	0
-1	13	8	-8	1	1	8	8	0	65	0	0	0	65	0	0
-1	15	15	-14	-1	1	100	103	0	66	0	0	0	66	0	0
-1	17	13	12	1	2	25	-25	0	67	0	0	0	67	0	0
2	1	78	83	-1	2	101	103	0	68	0	0	0	68	0	0
2	2	31	30	1	3	19	-20	0	69	0	0	0	69	0	0
-2	2	20	20	-1	3	54	54	0	70	0	0	0	70	0	0
2	3	6	-5	1	4	33	-33	0	71	0	0	0	71	0	0
-2	3	26	-25	1	5	36	36	0	72	0	0	0	72	0	0
2	4	10	-7	-1	5	17	18	0	73	0	0	0	73	0	0
-2	4	39	-38	1	6	14	14	0	74	0	0	0	74	0	0
2	5	38	-38	-1	6	50	-51	0	75	0	0	0	75	0	0
-2	5	32	32	1	7	12	7	-1	76	0	0	0	76	0	0
2	6	45	43	-1	7	37	36	1	77	0	0	0	77	0	0
-2	6	27	-27	1	8	34	34	1	78	0	0	0	78	0	0
2	7	27	-26	-1	8	21	24	1	79	0	0	0	79	0	0
-2	7	14	11	1	9	16	-14	1	80	0	0	0	80	0	0
2	9	11	12	1	10	9	-10	1	81	0	0	0	81	0	0
-2	9	12	-10	-1	10	18	-20	-1	82	0	0	0	82	0	0
-2	10	8	-6	1	11	10	11	1	83	0	0	0	83	0	0
2	11	26	-25	-1	11	36	37	1	84	0	0	0	84	0	0
2	12	8	-7	-1	12	28	-27	-1	85	0	0	0	85	0	0
2	13	15	-16	1	13	12	-13	1	86	0	0	0	86	0	0
-2	13	19	-18	-1	13	9	-3	-1	87	0	0	0	87	0	0
-2	14	16	-16	1	14	9	-6	-1	88	0	0	0	88	0	0
				2	0	11	10	1	89	0	0	0	89	0	0

TABLE 13

[illegible]



Molecular dimensions for form "A".



Bond lengths after correction for molecular librations.
Fig. 2.

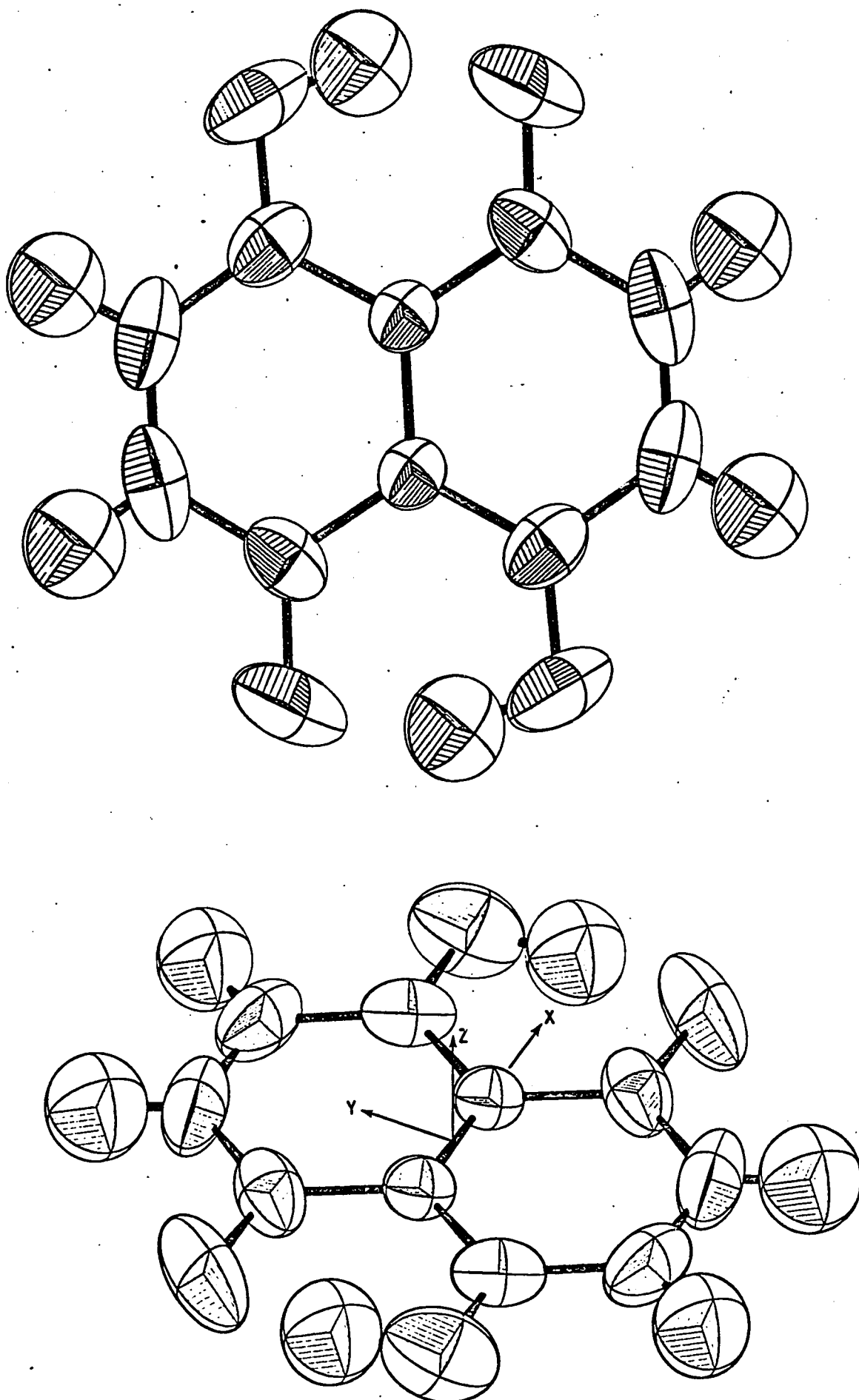


Fig. 3. Thermal ellipsoids for form "A".

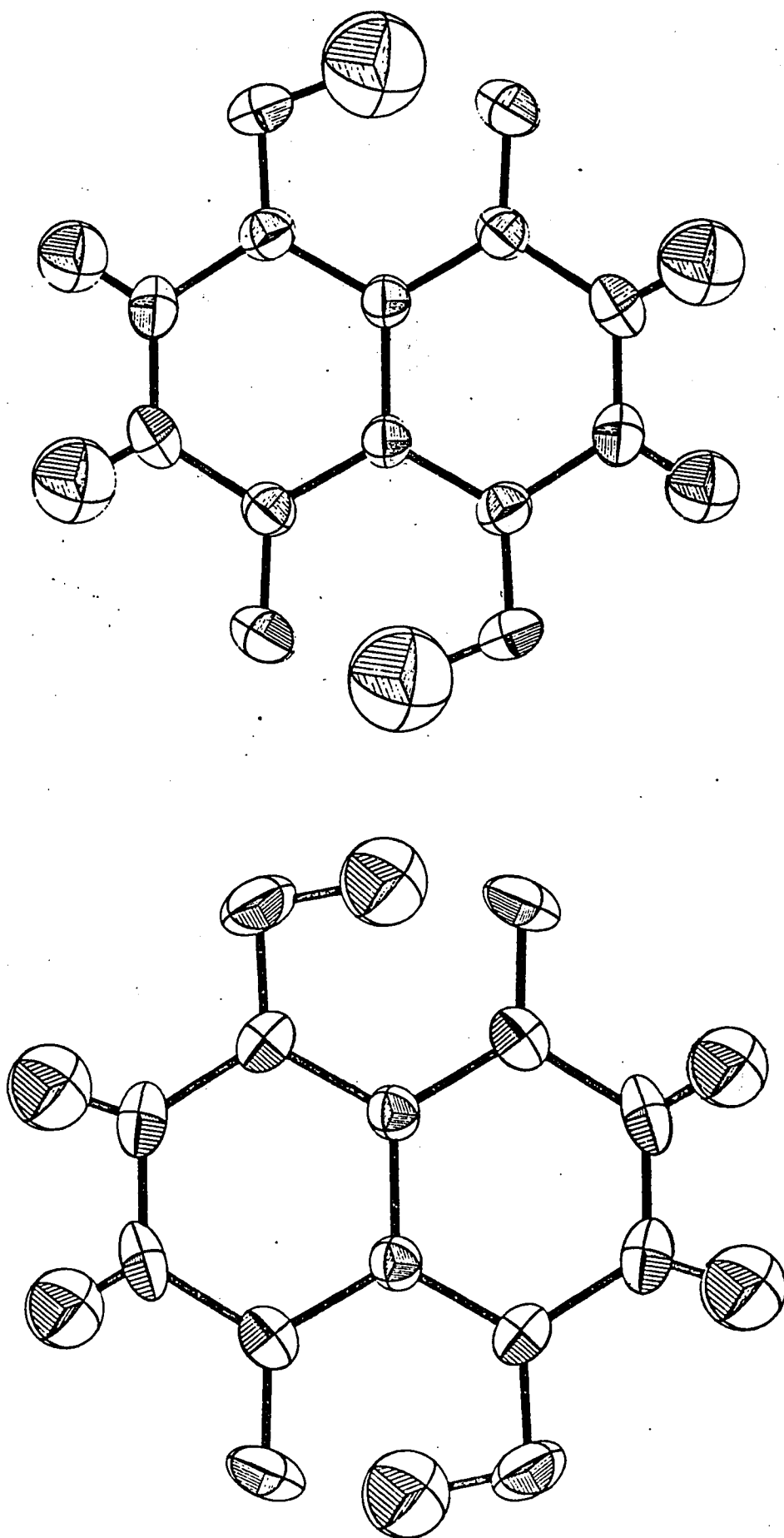


Fig. 5. Thermal ellipsoids for form "C".

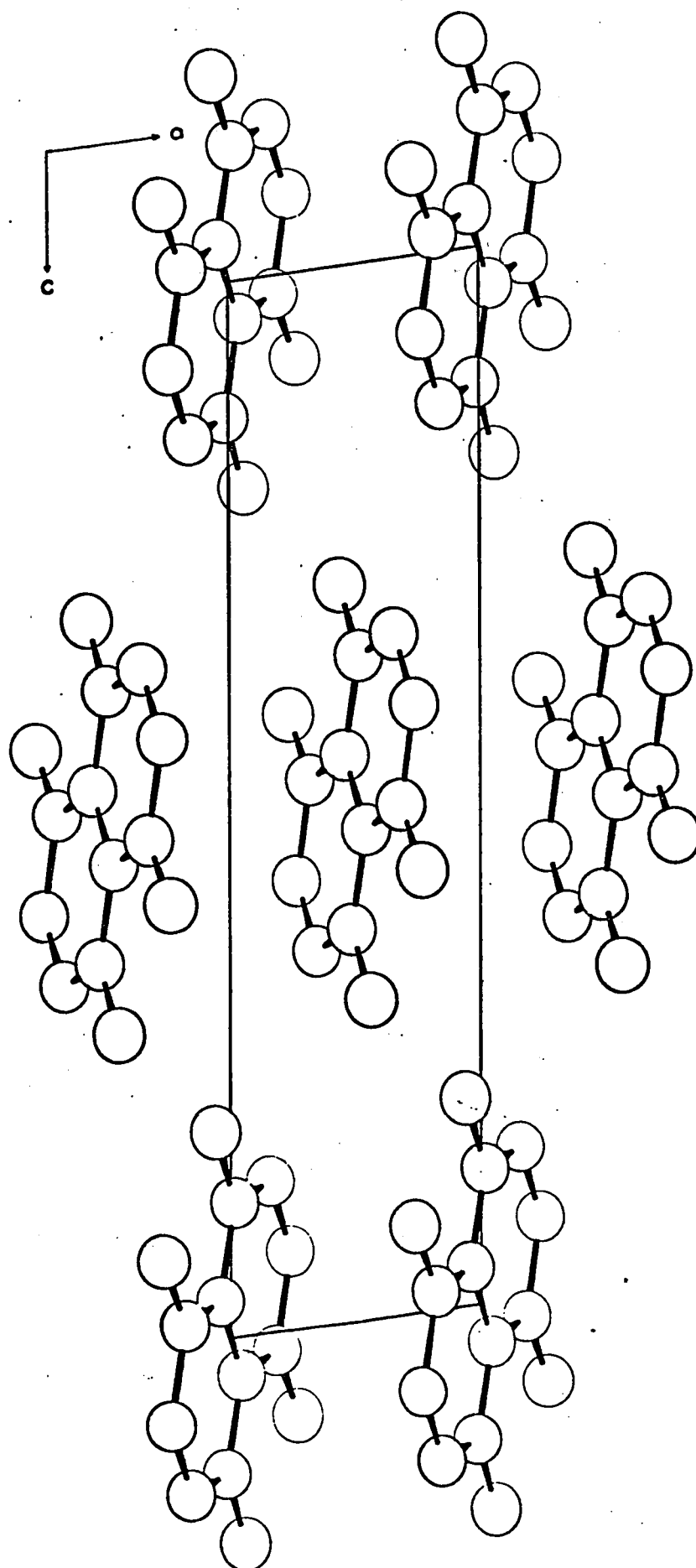


Fig. 6. Molecular packing. Projection onto [ac] plane.

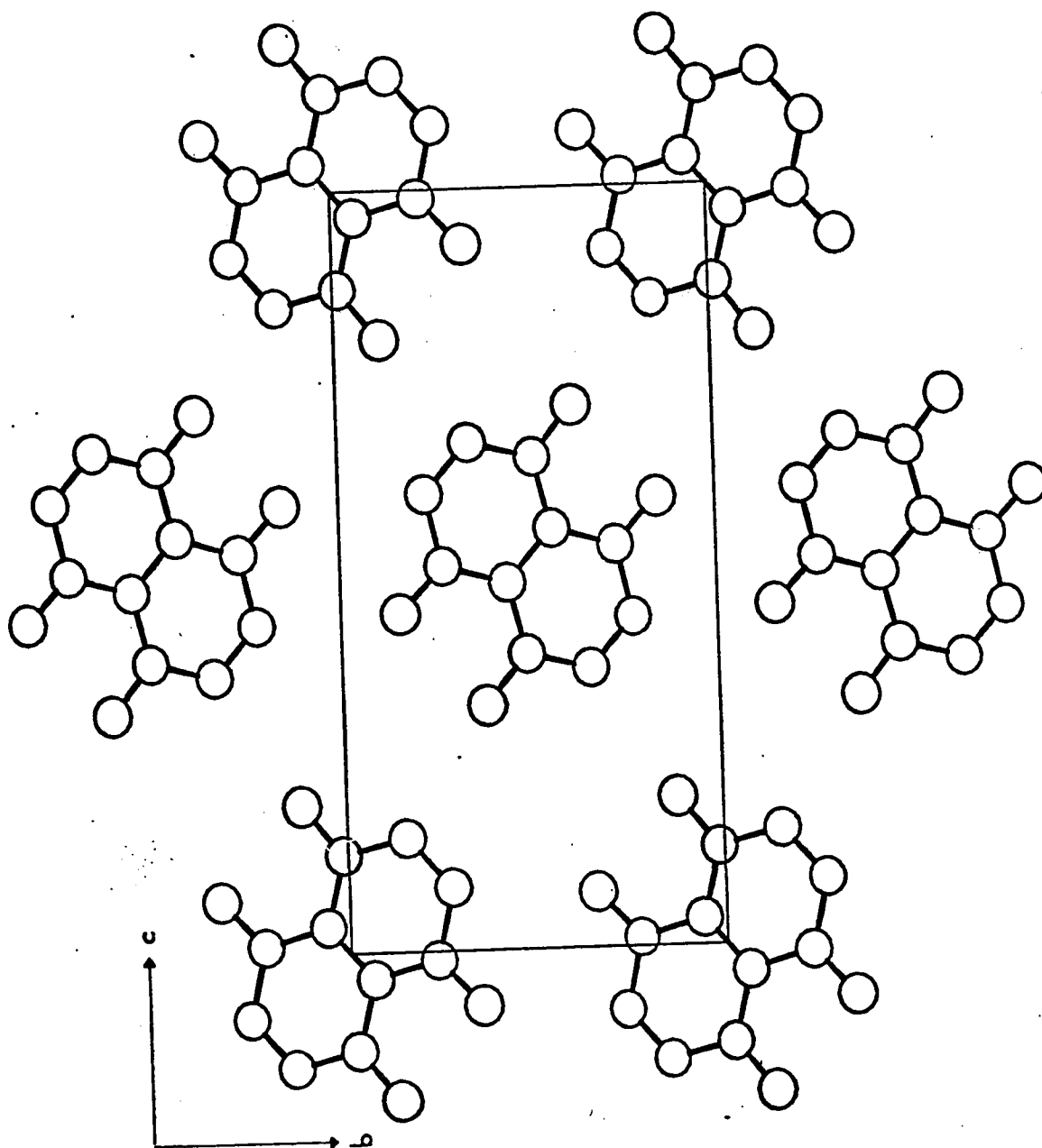


Fig. 7. Molecular packing.
Projection onto $[bc]$ plane.

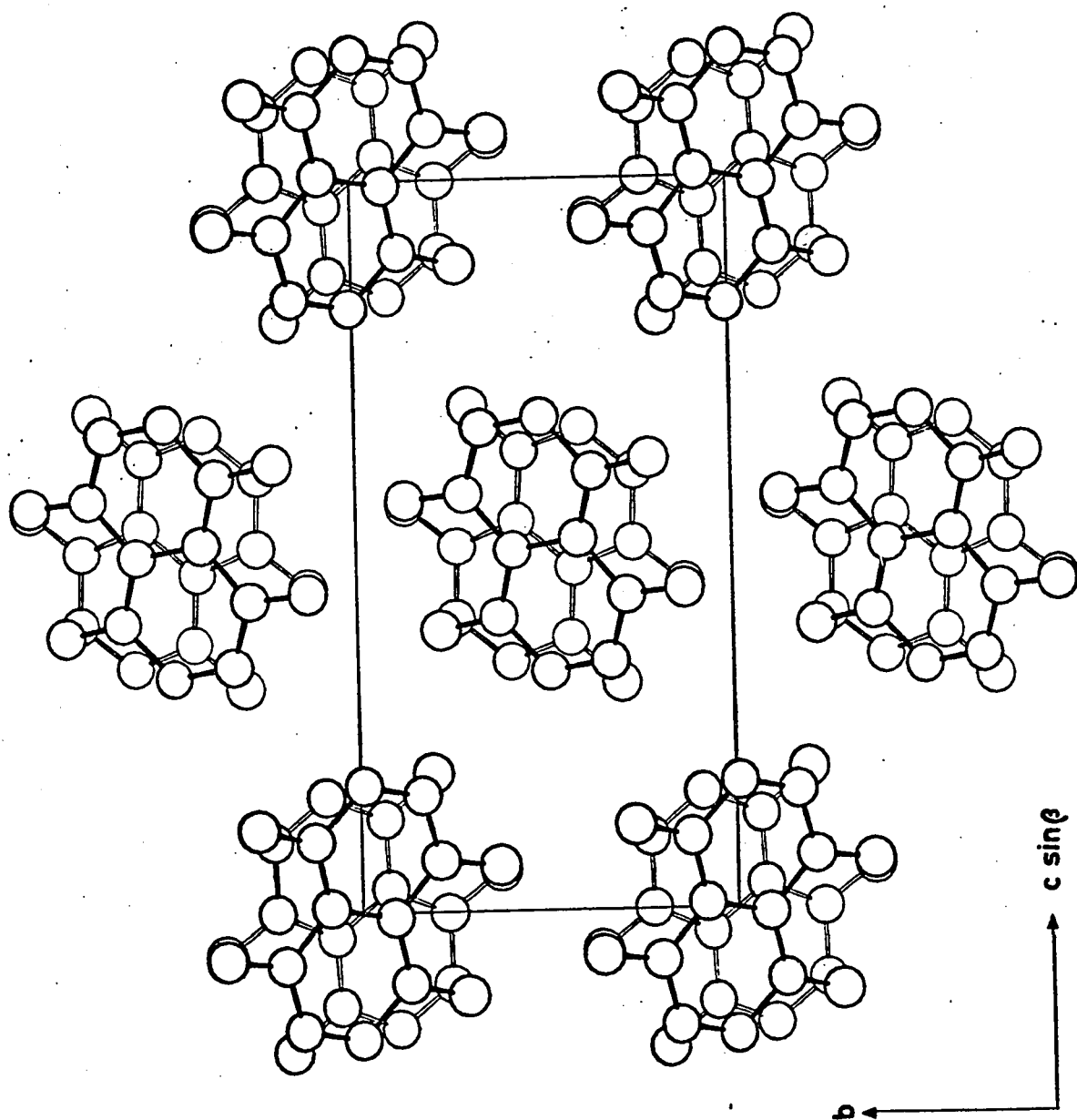


Fig. 8. Molecular packing of form "C" viewed down [a] axis.

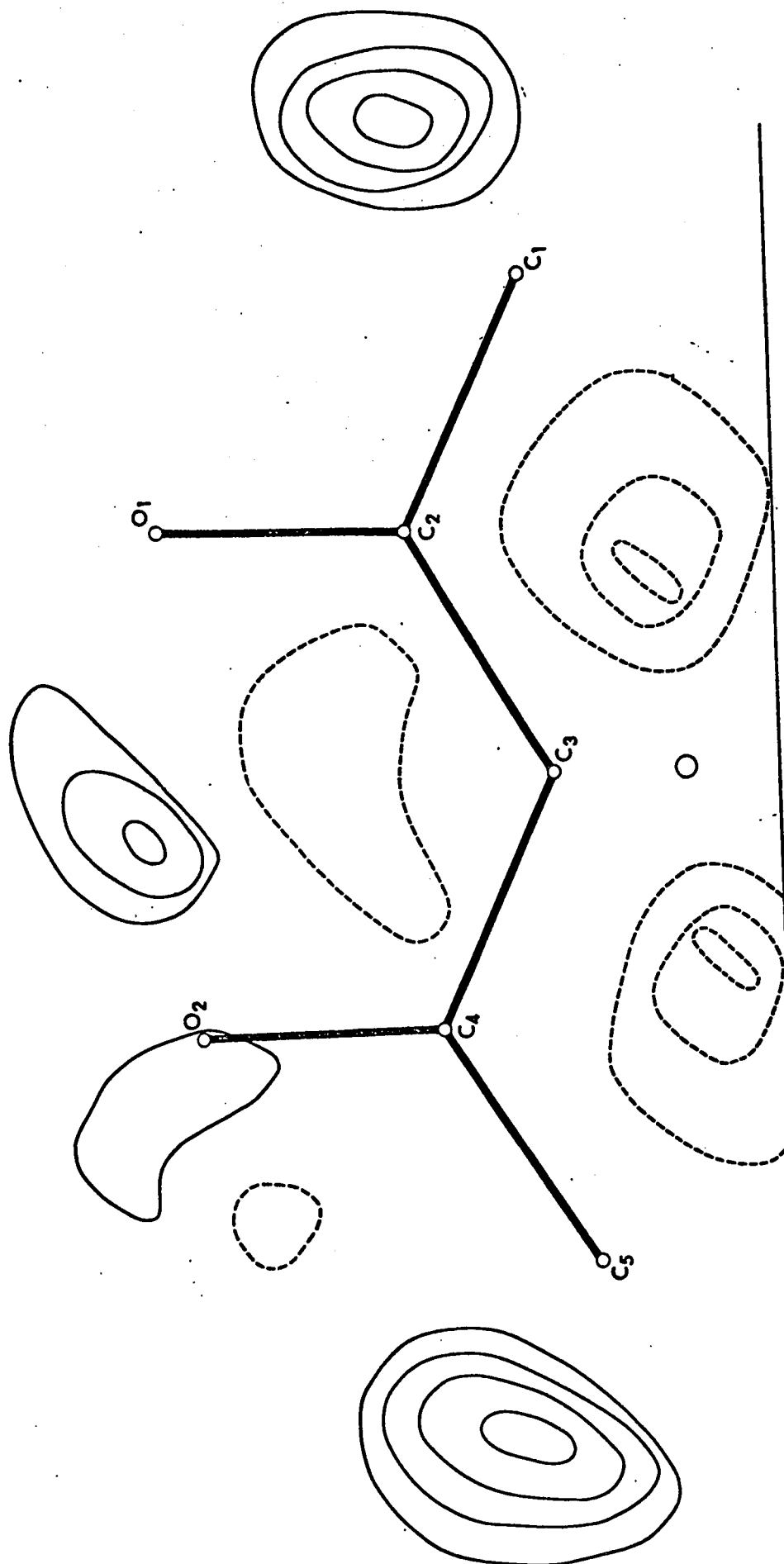


Fig. 9. Electron density of form "A" without hydrogens.

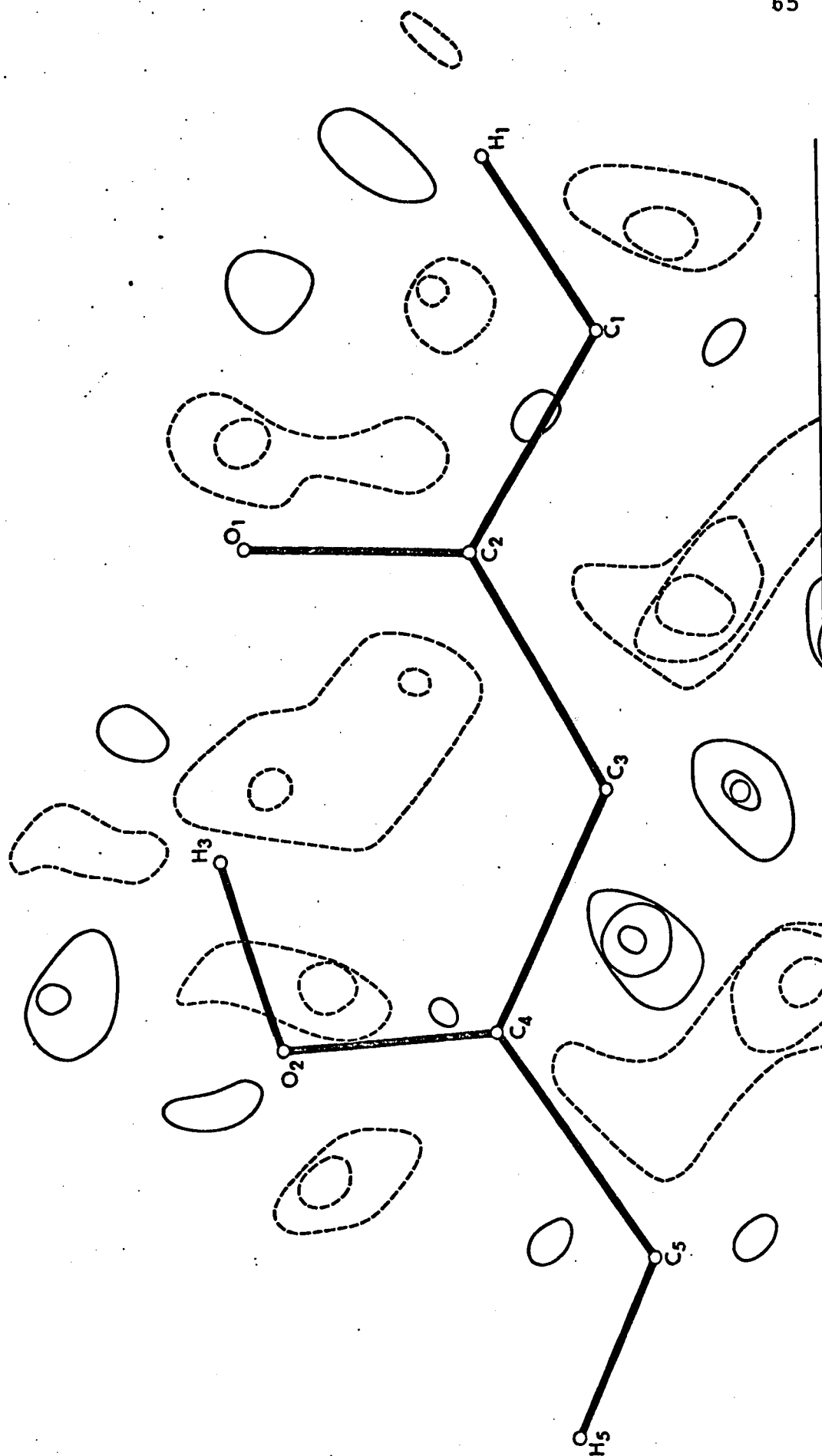


Fig. 10. Electron density of form "A" with hydrogens.

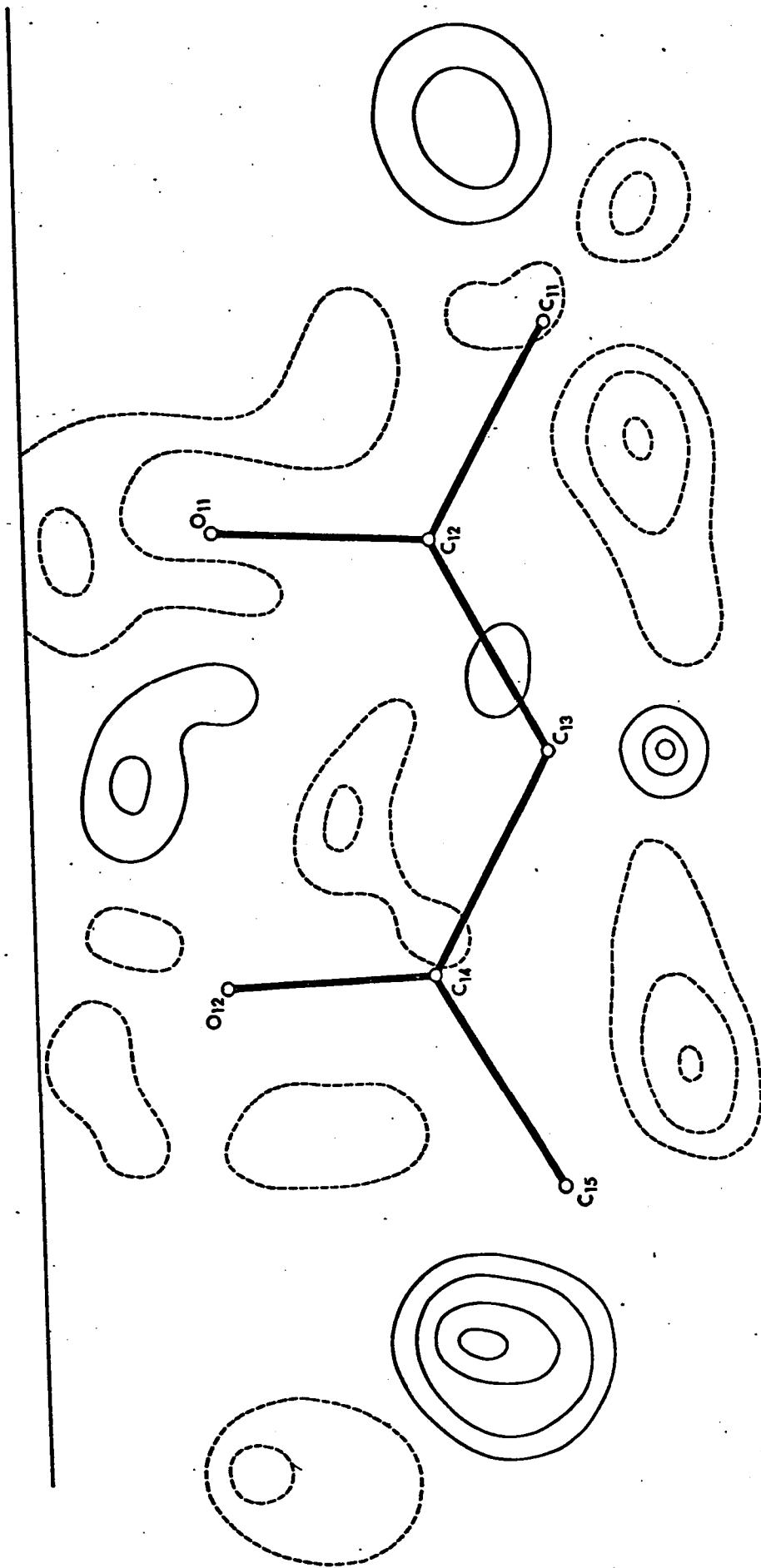


Fig. 11. Electron density of molecule 1, form "C" without hydrogens.

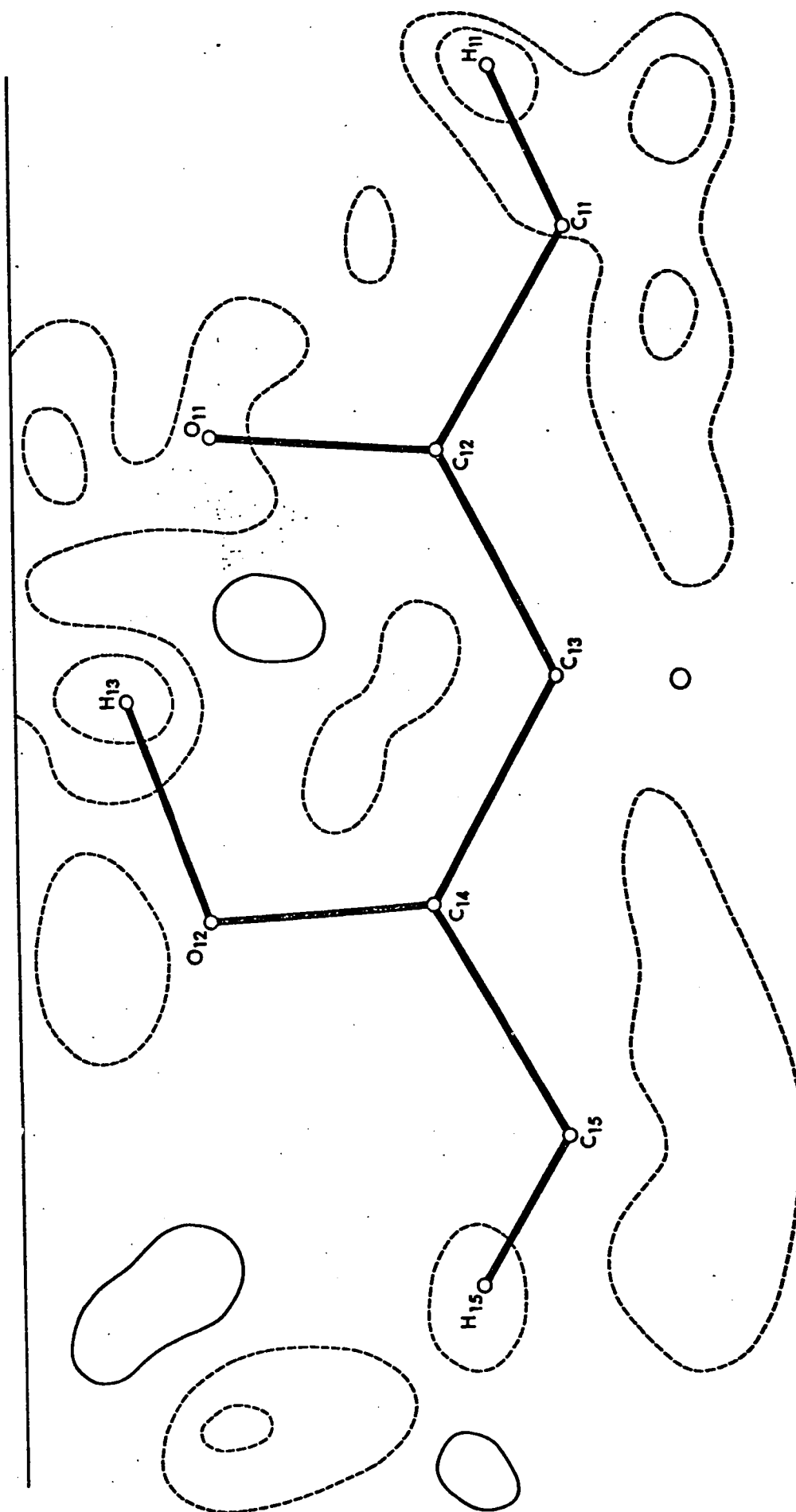


Fig. 12. Electron density of molecule 1, form "C" with hydrogens.

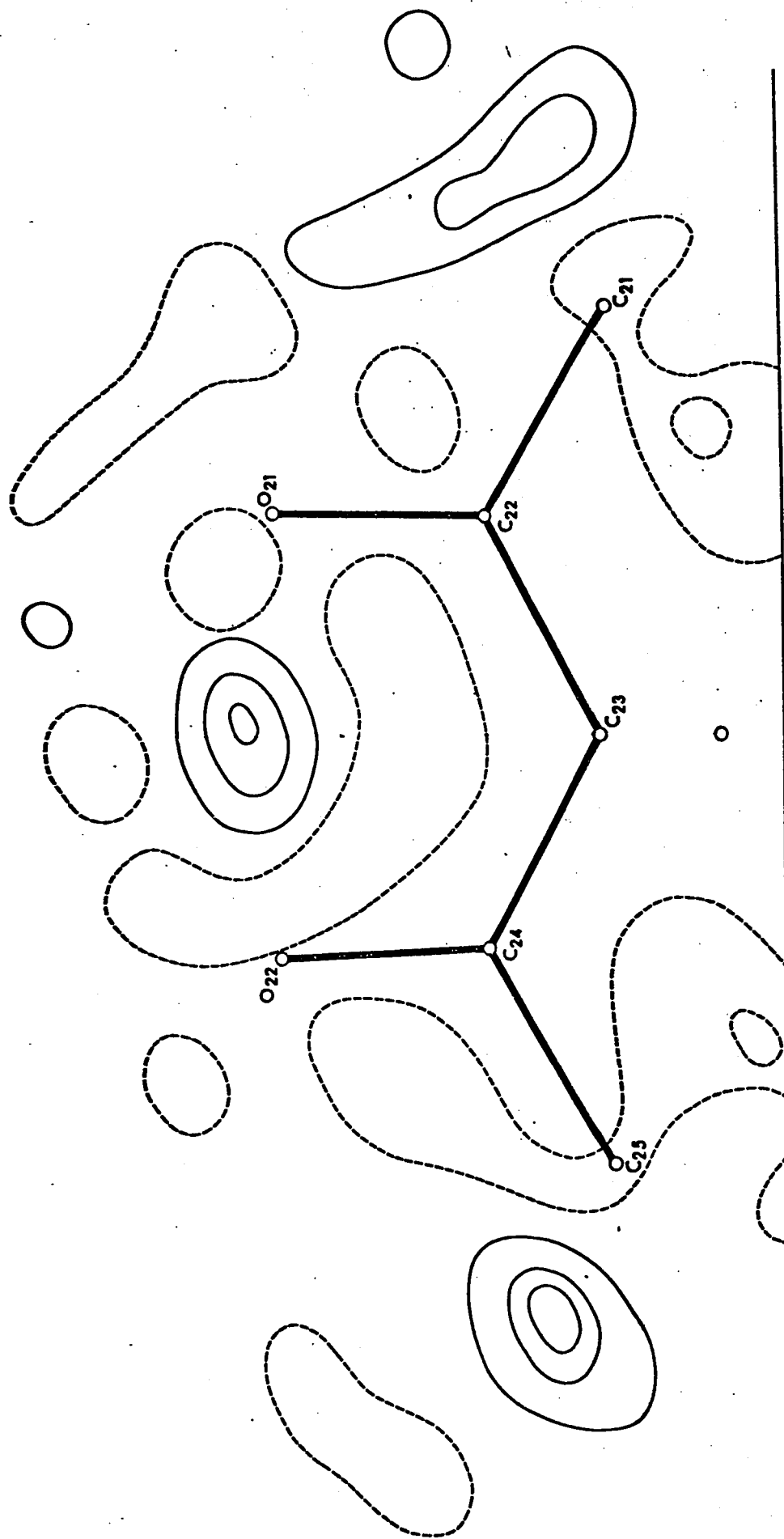


Fig. 13. Electron density of molecule 2, form "C" without hydrogens.

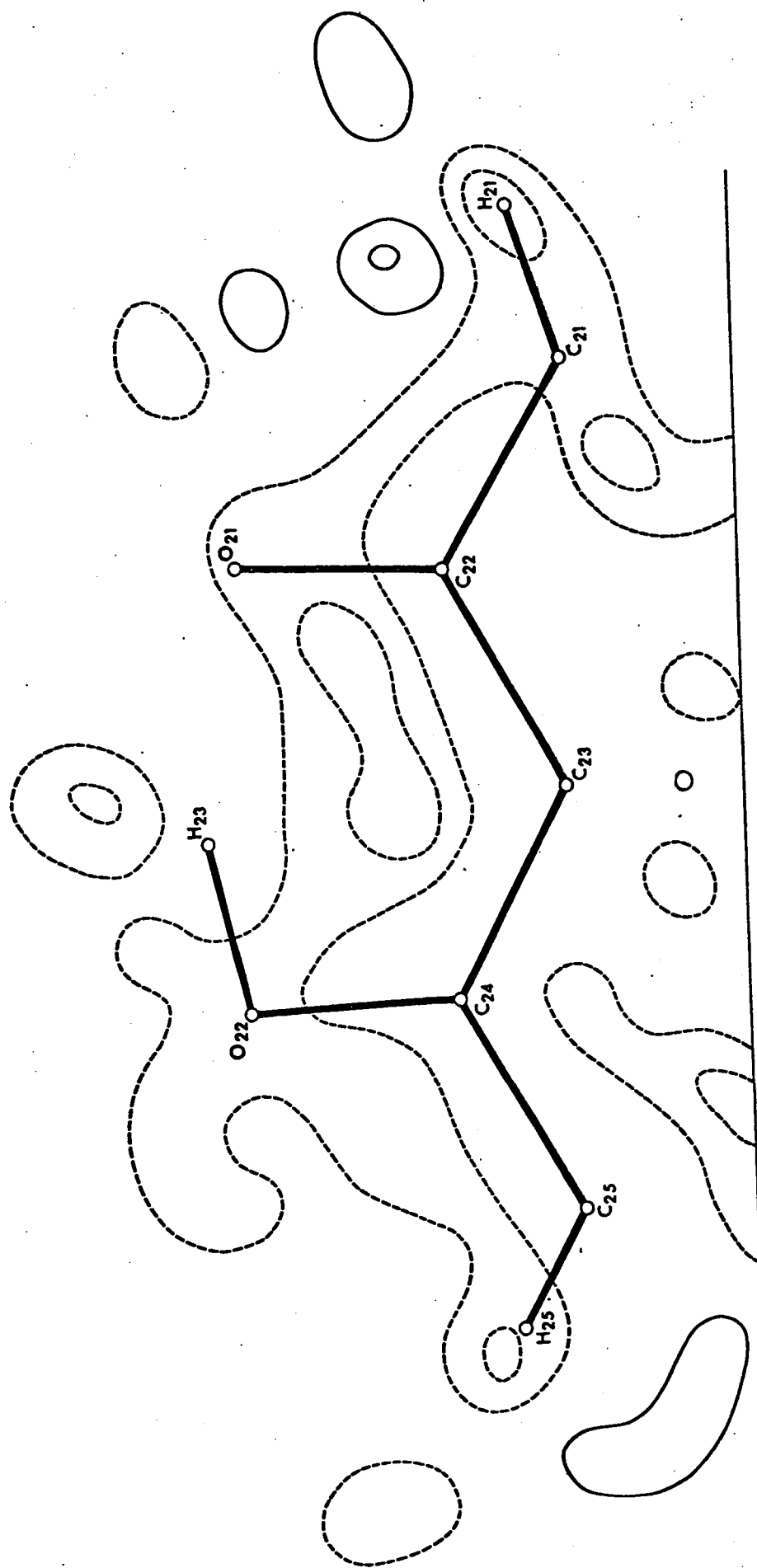


Fig. 14. Electron density of molecule 2, form "C" with hydrogens.

These deviations from planarity (for molecule (1)) can probably be attributed to errors in the data (the quality of which is unknown) as there seems to be no reason as to why molecules (1) and (2) should be different.

Discussion

Molecular Packing

The molecules in both forms pack in the "herring bone" mode found in aromatic hydrocarbons (69) with parallel stacking along [a]; in form "A", the angle between the molecular normal and the [a] axis is 23.6° , while in form "C", the two molecules are closely parallel (1.1° between molecular normals) and the average angle between molecular normals and the [a] axis is 31° . The values of the closer intermolecular contacts that will be responsible for stable molecular packing in the crystal, are listed in Table 7. On the basis of the Pauling, Van der Waals radii ($O = 1.4 \text{ \AA}$, $H = 1.2 \text{ \AA}$ (3)), these contacts are all within error of the expected values assuming that all intermolecular forces are of Van der Waals type. Intermolecular contacts between parallel molecules stacked along the [a] axis are normal: the perpendicular distances between molecules of both forms are 3.42 \AA (form "A") and 3.39 \AA (form "C").

These values agree closely with that given by Pauling (3)^b for the thickness of an aromatic molecule (3.40 Å) and the small differences from this value are probably not significant. Prout and Wallwork (70) have suggested the existence of molecular interaction in form "C" between the C=O of one molecule and the benzene ring of the next, parallel to it along [a]; the orientation of molecules when viewed in projection onto the [bc] plane (see Fig. 8) does suggest this, but the normal perpendicular distance between molecules indicates that this type of interaction is rather weak (c.f. quinol, (71) perpendicular separation between molecules is 3.16 Å).

The unusually short O...H-C distances given by Pascard-Billy (11) of 2.04 Å and 1.85 Å are clearly erroneous; these values are actually 3.01 Å and 2.58 Å. The closer intermolecular contacts for form "C" are shown in Table 7. These are generally slightly larger than those observed for form "A" although still sufficiently close to the normal O-H non-bonded contact to provide stable packing.

Molecular geometry

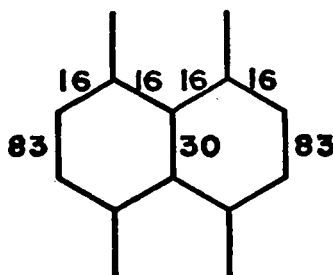
O₂ shows a deviation of 0.018 Å from the mean plane through the carbon atoms which is highly significant in view of the estimated error in this measurement of 0.003 Å. In the structures of (i) 1,5-dihydroxyanthraquinone (72) (ii) chloranilic acid (81) and (iii) chloranilic acid dihydrate (80) in which a similar intramolecular hydrogen

bond occurs, the phenolic oxygen shows deviations of the same magnitude from the plane defined by the carbon atoms i.e. 0.023 \AA in (i), 0.02 \AA and 0.038 \AA in (ii) and 0.018 \AA and 0.008 \AA in (iii). This suggests that the intramolecular hydrogen bonded ring system (involving $H_3, O_2, C_4, C_9, C_2, O_1$) would be strained if it were coplanar with the aromatic system, and that this strain is relieved by a small distortion of the O-H group out of the plane.

The $O \cdots O$ separation is 2.571 \AA and therefore the hydrogen bond should be stronger than salicyclic acid where this separation is 2.62 \AA (98). The O-H stretching frequencies confirm this (3225 cm^{-1} in the latter (97) and 2920 cm^{-1} in naphthazarin (6)) but in bissalicylaldehyde nickel, the $O \cdots O$ separation is 2.45 \AA (99) and the O-H stretching frequency is 3270 cm^{-1} (97). This suggests that the hydrogen is made more labile in naphthazarin by some other means (probably intramolecular) in addition to hydrogen bond formation. However, in 1,5-dihydroxyanthraquinone the O-H stretching frequency also occurs at 2950 cm^{-1} (6) and the crystal structure shows that the phenolic hydrogen is definitely asymmetric and the carbon-oxygen bonds are distinctly $C=O$ and $C-O$ in character. The O-H stretching frequency in the latter case may have been lowered as a result of recording the spectrum

in the solid state when intermolecular hydrogen bonding can occur (a close intermolecular contact has been observed between a quinonoid oxygen and a phenolic oxygen of 2.79 Å) although at the present stage of formulation of hydrogen bonding theories it is probably safer to regard naphthazarin and 1,5-dihydroxyanthraquinone as two further points on the plots of O-H bond length versus stretching frequency for bent hydrogen bonds. It must be borne in mind that these plots in the case of bent intramolecular hydrogen bonds, now contain a further variable viz: the C-O-H bond angle.

The final bond length pattern clearly shows that the structure of naphthazarin in the solid state does not correspond to that of non-disordered III (see p. 10) and the location of the hydrogen atom in a definately asymmetric position would seem to eliminate model II. It is therefore necessary to postulate the existence of tautomerism in the solid state (which will be crystallographically equivalent to stacking disorder) in order to explain the observed bond length pattern. The percentage double bond character for each of the naphthazarin bond lengths has been derived from the bond-order versus bond-length curve given by Mason (54) and these figures are shown below:

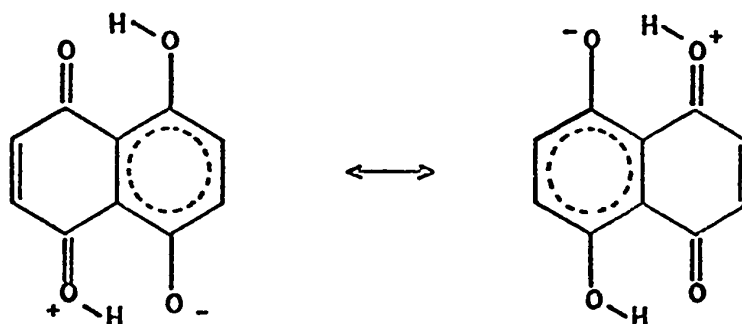


Comparison of this figure with those shown on p. 12 (Part I(a)), on which are depicted the percentage double bond character expected as a result of tautomerism (or disorder) involving models I and III separately, indicates that form III tautomerism does not fit the experimental pattern, whereas form I tautomerism does approximate to the observed bond lengths. The only models which predict equality for the top carbon-carbon bond lengths are (i) the form I tautomerism and (ii) model II, although the expected bond length pattern for this model will depend on the degree of contribution from the various canonicals. To ensure that the asymmetric location of this atom was the best situation, a structure factor calculation was done with the phenolic hydrogen located exactly mid-way between the oxygen atoms. Accurate positioning of the hydrogen atom was readily accomplished with the aid of coordinates referred to the molecular axes (obtained from the rigid body analysis), and the new location, was 0.3 \AA from the asymmetric position making the two hydrogen to oxygen distances 1.33 \AA .

The structure factor calculation gave a normal R factor ($\sum ||F_o| - |F_c|| / \sum |F_o|$) of 0.0555 and a weighted R factor ($[\sum w ||F_o| - |F_c||^2 / \sum w |F_o|^2]^{1/2}$) of 0.0535, significantly worse than the corresponding values for the asymmetric model viz: 0.0514, 0.0481. On refining the symmetrical model, using full matrix least squares (allowing all positional and temperature parameters to vary), two cycles were necessary to reach convergence at which point the hydrogen had moved to the asymmetric position and all parameters were identical to those obtained at the termination of the normal refinement; the phenolic hydrogen atom is clearly better located in the asymmetric position.

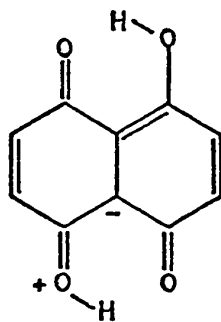
The Moore and Shueur tautomerism involves the four structures IA, IB, IIIA, IIIB, but as the relative stability of these structures is unknown (e.g., are the structures IIIA and IIIB, transition states between IA and IB?) it is difficult to predict an expected bond length pattern, although this should lie somewhere between the patterns for the tautomeric IA, IB, and IIIA, IIIB. Partial "mixing" of these schemes, however, cannot give rise to the observed pattern. Thus the only reasonable scheme which satisfactorily accounts for the observed bond length pattern is the tautomerism (or disordered stacking) involving model I. The acceptance

of this model, however, introduces a further problem: the phenolic proton should appear on the Fourier map as two half-weight protons each attached to one of the oxygen atoms. The difference Fourier maps (Figs. 9, 11 and 13) however, clearly show a single proton; in view of the electron density smears close to O_1 (also O_{11} and O_{21} in form "C") two half-weight protons at the expected positions were included in a structure factor calculation but subsequent least squares refinement showed that this model was unreal. The "half" hydrogen close to O_1 was effectively removed and that attached to O_2 was reinforced back to full weight (the temperature factor for the "half" proton on O_2 refined to 2.0 and that of the "extra" proton refined to 16.0 in 1 cycle). The single asymmetric proton then effectively excludes any model involving disorder or tautomerism but such a model is the only one which can account for the heavy atom bond length pattern! The dilemma can only be resolved by the introduction of charged canonicals such as those shown below:



This scheme can no longer be called tautomerism as no proton shift occurs but it is actually a resonance in the aromatic system for which the cannonicals shown above are contributors.

This resonance is probably best thought of as stemming from the uncharged form, 1,5-dihydroxy 4,8-naphthoquinone (III), which in itself does not have resonance forms. If charged contributors are allowed, however, a large number of cannonicals can be drawn including those shown above and also those in which charges can reside on the carbon atoms themselves:



Contribution from this type of structure and also from the neutral molecule would account for the observed lengthening of the C_9-C_{10} bond and the shortening of the C_2-C_3 , C_6-C_7 bonds (see bond order diagram on p. 74). The conventional structure, 1,4-dihydroxy 5,8-naphthoquinone, is presumably less favoured because of the fewer stable cannonicals that can be drawn for this molecule, and also its lower molecular symmetry.

PART I

- (C) The crystal structure of 5,-hydroxy 1,4-naphthoquinone
(Juglone)

Experimental

Crude juglone is available commercially and is readily recrystallised from acetone yielding orange needle crystals elongated along the [a] axis, with approximately hexagonal cross-section. The unit cell and space group were determined from precession photographs and errors were estimated by the method of Patterson and Love (64) The density was measured by flotation in an aqueous solution of zinc bromide.

Crystal data:

$$\begin{aligned}a &= 7.335 \pm 0.006 \text{ \AA} \\b &= 7.692 \pm 0.006 \text{ \AA} \\c &= 13.908 \pm 0.010 \text{ \AA} \\\beta &= 99.2 \pm 0.5^\circ\end{aligned}$$

$$\begin{aligned}d_{\text{calc}} &= 1.47 \text{ gm/cm}^3 \text{ for 4 molecules/unit cell} \\d_{\text{obs}} &= 1.47 \text{ gm/cm}^3\end{aligned}$$

Intensity data were collected by equi-inclination Weissenberg photographs with $\text{CuK}\alpha$ radiation and with the crystal rotating about the [a] axis. A striking feature of the intensity set was that alternate layers about the [a] axis were found to consist of weak

intensity reflections and Weissenberg photographs of these odd order layers showed these reflections to be also very diffuse. The exposure time required to record measurable data for these layers was 120 hrs, compared to 14 hrs for the even order layers. Data were collected only for the layers $h = 0, 1, 2, 4$; the $(3k\ell)$ layer was so diffuse as to be unmeasurable. The crystal shape was unsuitable for data collection about the other axes and although the $(h0\ell)$ layer was collected it was used only for initial scaling of the $[a]$ axis data.

Space Group

The point group symmetry was found to be $2/m$ and the observed systematic absences were:

$(h0\ell)$ $h + \ell = 2n + 1$ implying an n glide perpendicular to $[b]$

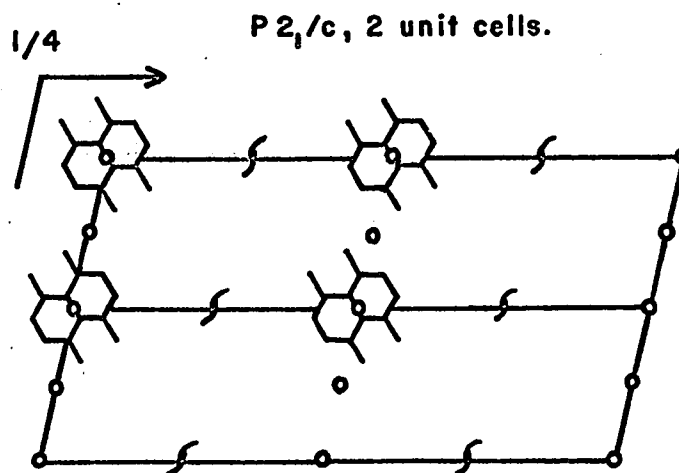
$(0k0)$ $k = 2n + 1$ implying a 2_1 screw axis parallel to $[b]$,

hence the space group is $P2_1/n$. If however the weak odd order layers are ignored and the reflections are reindexed so that $[a] = 3.7 \text{ \AA}$, then the systematic absences become:

$(h0\ell)$ $\ell = 2n + 1$ implying a c glide perpendicular to $[b]$

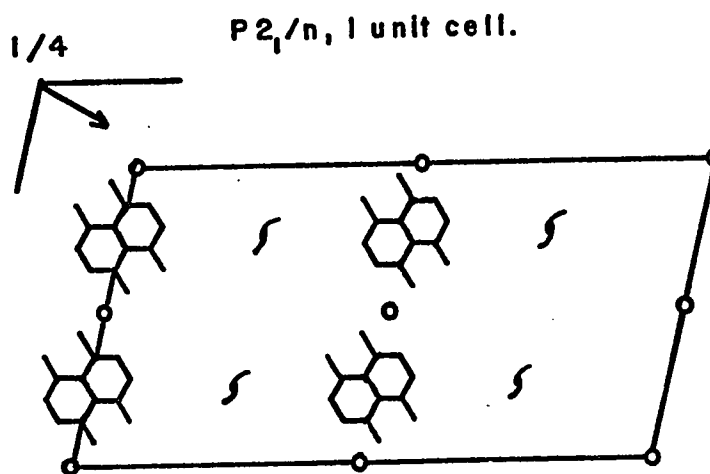
$(0k0)$ $k = 2n + 1$ implying a 2_1 screw axis parallel to $[b]$ and the space group changes to $P2_1/c$.

Because the odd layers are weak it may be assumed that the structure approximates to the latter space group. There would be only two molecules per unit cell and the symmetry would require that they be situated on centres of inversion. In relation to the symmetry elements then, the requirements of space group $P2_1/c$ mean that the molecular centre of the molecule will be displaced from the screw axes by $x = 0$, $z = 0.25$ and from the c glide plane by $y = 0.25$.



The structure in the true space group, $P2_1/n$, has four molecules per unit cell which may then occupy general positions and are no longer required to be centrosymmetric. Further the two molecules which are separated by 3.7 \AA along the $[a]$ axis are no longer

identical, and it is their non-identity which requires [a] to be doubled and which gives rise to the h odd reflections. The relative positioning of the four molecules in the $P2_1/n$ cell must however be very similar to that deduced for $P2_1/c$ (which was an approximation to the true situation) i.e. the relationship to the symmetry elements will be the same.



From the above diagram it can be seen that the two molecules separated by 3.7 \AA are now centrically related.

The fact that the h odd reflections are all diffuse indicates disorder in the crystal packing along the [a] axis i.e. in the packing of the centrosymmetrically related molecules. If the orientation of the molecules with respect to the centres of inversion was completely

random (the term random is here applied to the oxygen atoms and not the carbon skeleton) these h odd reflections would not appear at all, as the apparent molecule derived from a crystal structure analysis would be the average of the disordered ones and therefore would appear centrosymmetric. If the orientation of the molecules with respect to the centres was retained throughout, these reflections would be sharp although weak. It can be readily shown that atoms related by a centre of inversion at $x = 0.25$ do not contribute to the structure factors for h odd reflections.

For centrosymmetric space groups, the trigonometric part of the structure factor expression is:

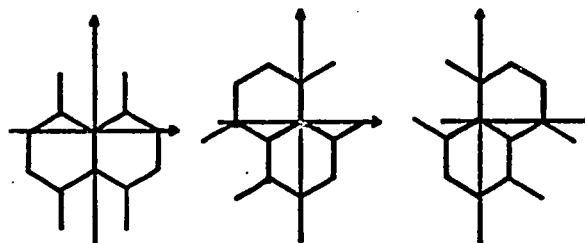
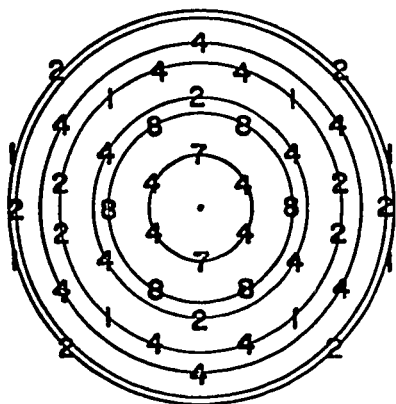
$$F_{hkl} = 2 \cdot \cos 2\pi (hx + ky + lz)$$

and for two atoms at $(\frac{1}{4} + x, y, z)$ and $(\frac{1}{4} - x, \bar{y}, \bar{z})$:

$$\begin{aligned} F_{hkl} &= 2 \cdot \cos 2\pi (h(\frac{1}{4} + x) + ky + lz) \\ &\quad + \cos 2\pi (h(\frac{1}{4} - x) + k\bar{y} + l\bar{z}) \\ &= 2 \cdot \cos 2\pi (h/4 + (hx + ky + lz)) \\ &\quad + \cos 2\pi (h/4 - (hx + ky + lz)) \\ &= 2 [\cos 2\pi (h/4) \cdot \cos 2\pi (hx + ky + lz) \\ &\quad - \sin 2\pi (h/4) \cdot \sin 2\pi (hx + ky + lz) \\ &\quad + \cos 2\pi (h/4) \cdot \cos 2\pi (hx + ky + lz) \\ &\quad + \sin 2\pi (h/4) \cdot \sin 2\pi (hx + ky + lz)] \\ &= 4 \cdot \cos \pi/2(h) \cdot \cos 2\pi (hx + ky + lz) \\ &= 0 \text{ when } h \text{ is odd.} \end{aligned}$$

Any deviation from centrosymmetry which is now possible in $P2_1/n$ and which of necessity must occur because the molecule is not centrosymmetric, would account for these weak reflections. The fact that the reflections are observed but diffuse indicates that order is maintained for short distances along $[a]$ but that mistakes do occur.

The structure solution was carried out in the sub-cell with the molecules occupying the centrosymmetric special positions. The molecule will appear to contain four "oxygen" atoms although in fact there are only three. The molecular centres are established by the above arguments and thus the problem to be solved is only one of orientation. As the $[a]$ axis is very short this was first attempted in projection down this axis. The expected intramolecular vector set for an idealised naphthazarin molecule in which both rings are assumed to be regular hexagons, all bonds are assumed to be of length 1.4 \AA , and all atoms are assumed to be of equal weight, is shown below:



This has pseudo-hexagonal symmetry which implies a three-fold ambiguity in the orientation of the two fused rings as illustrated above. In principle the choice could be made, as the symmetry is not true, but in practice this may not be possible. Such a pattern of peaks could readily be discerned on the Patterson projection and thus the orientation problem was solved apart from the ambiguity. In view of the small amount of data involved (82 (0k ℓ) reflections), it was thought that the most expedient way to resolve the ambiguity was to refine all three possible models by least squares methods. The block diagonal approximation was used, and isotropic temperature factors assumed for each atom. Only one of the three models refined satisfactorily, and the R factor ($R = \Sigma ||F_o| - |F_c|| / \Sigma |F_o|$) for this model changed from 0.49 to 0.33. At this stage the collection of the other layers of data was complete and before the refinement was continued, it was decided to calculate the three dimensional Patterson map to confirm that the refined projection model was in fact the true solution. As the intensities had been collected about one axis only, (h0 ℓ) data was used for scaling purposes, although during all subsequent refinements, the scale factors were adjusted after each cycle to make ΣF_o equal to ΣF_c for

the individual layers. The three dimensional Patterson maxima were sharpened to improve definition and especially to reduce the possibility of origin ripples obscuring the near origin peaks. This can be accomplished by assuming the unit cell to contain point atoms at rest, in which case the scattering from the crystal would be invariant with $\sin\theta$. In practice the sharpening is affected by modifying the F^2 values to give "sharpened" coefficients by the following expression:

$$F_{\text{sharp}}^2 = F^2 \cdot \frac{\sum_{i=1}^N Z_i^2}{\sum_{i=1}^N f_i^2} \cdot \exp(2B \cdot \sin^2\theta/\lambda^2)$$

where z = atomic number, N = number of atoms in the unit cell, f = scattering factor for the appropriate value of $\sin\theta$, B = overall temperature factor as obtained from a Wilson plot (57).

The pattern of near origin peaks in the three dimensional Patterson map confirmed the orientation deduced from the projection although the ambiguity was still not resolvable with certainty. Consideration of the Harker section did, however, confirm that the model refined in projection was in fact correct. The Harker section contains all vectors between atoms related by the screw axis of the

space group symmetry i.e. atoms at (x, y, z) and $(\frac{1}{2} - x, \frac{1}{2} + y, \frac{1}{2} - z)$, thus these vectors will have the general form: $(\frac{1}{2} + 2x, \frac{1}{2}, \frac{1}{2} + 2z)$. This pattern of vectors will clearly form a double scale projection of the molecule onto the section $y = \frac{1}{2}$ (translated by $\frac{1}{2}$ in the x and z directions). When the molecular shape is known the location and orientation of the molecules within the space group can be readily obtained by projecting a double scale model of the molecule onto the Harker section and adjusting the orientation and position of the model until a satisfactory correlation is obtained between the projected image and the calculated Harker section. In applying this method in the present instance, it was found that the only orientation of the model that correlated satisfactorily did indeed correspond to the orientation refined with the projection data. The required x coordinates for each atom were then read off the Harker section and combined with the projection coordinates to provide the model for the three dimensional refinement. The initial R factor for the three dimensional data was 0.49, and the coordinates and isotropic temperature factors were refined by the same method as the projection data, to an R factor of 0.26. It was noted at this point that

the temperature factors for two symmetrically related oxygen atoms were larger (7 \AA^2) than the other pair (4 \AA^2) whereas little difference would normally be expected. A Fourier synthesis calculated at this stage again showed the apparent disparity in the weights of these atoms, and thus confirmed the fact that one pair would have to be half-weighted while the other pair would have to be given full weight. This behaviour was anticipated during the refinement as one of the centrosymmetric pairs of oxygen atoms in the model is indeed a genuine pair of atoms, while the other pair is a result of the disorder, and should be represented in the model as $\frac{1}{2}$ weighted oxygens. Previously both pairs had been described identically as $\frac{3}{4}$ weight oxygens and in an attempt to describe the electron density correctly, the least squares procedure has given low temperature factors for the genuine pair and high temperature factors for the other. Thus the scattering factors were weighted accordingly and the refinement proceeded to an R factor of 0.23. The model would refine no further in the sub-cell and at this stage the (1k $\bar{2}$) layer was introduced. The true space group, $P2_1/n$, was now assumed and as explained above, the molecular centre must be moved to $x = 0.25$, and only one of the previously $\frac{1}{2}$ weighted oxygen atoms must now be specified (with full weight)

i.e. the molecule is now described in its correct, non-averaged way.

As the (1k ℓ) reflections were both weak and diffuse the measurement of their intensities proved difficult. A new intensity scale should have been made using one of these reflections, but their low intensity made this impractical, and the same intensity scale was used as for the other layers. The diffuse nature of these reflections does mean that a significant fraction of the intensity will have merged into the background; thus quite apart from the experimental difficulty of relating strong and weak intensities, the scale factor necessary to convert experimental measurements of diffuse reflections to absolute values will likely be quite different to that for sharp reflections. Furthermore, until some knowledge of the deviation of the molecule from centrosymmetry was available, the scale factor could not be accurately estimated from the comparison of ΣF_o and ΣF_c . This was the only means available, however, and the initial structure factor calculation for the (1k ℓ) data (to which the only contributing atom was the unique oxygen atom) was scaled in this manner giving an R factor of 0.80. Several cautious least squares cycles then followed in which only the positional

parameters of the atoms and the scale factor of the (1kℓ) data (but not those of the other layers) were permitted to vary. When the R factor for the (1kℓ) layer had fallen to 0.66 (and that for all data had fallen from 0.61 to 0.27), the temperature factors for all atoms and the other scale factors were permitted to vary, the latter being adjusted to make $\Sigma F_o = \Sigma F_c$ when it became apparent that adjustment was necessary. After six cycles of refinement the R factor of the (1kℓ) layer had decreased to a level comparable with the other layers, and that of all the data had fallen slowly to 0.211; the individual R factors were:

0kℓ	1kℓ	2kℓ	4kℓ
0.229	0.226	0.206	0.246

At this stage it became possible to continue the refinement using full matrix least squares procedures (33) in which the individual scale factors could be included as variable parameters. This is highly desirable as it must lead to a much more realistic estimate of these quantities. Continuing the refinement in this manner, convergence for this model was reached at an overall R factor of 0.171; the R factors of the individual layers being:

0kℓ	1kℓ	2kℓ	4kℓ
0.173	0.162	0.156	0.200

It was then decided to continue the refinement assuming anisotropic temperature factors, even though the meaning of doing so was uncertain, as it was not known how effective the inclusion of the (1kl) data had been. The model which resulted from the refinement of the h even layers would presumably be the average of the true molecule and its centrosymmetrically related image. Such an average would have ellipsoidal "atoms" and would most certainly be better approximated by an assumption of anisotropic rather than isotropic thermal motion. If the final refinement had included all of the h odd data then one could expect the resulting model to be the correct molecule (separated from its image) and a significant improvement in agreement on the assumption of anisotropy could then be interpreted as a true reflection of the actual thermal motion of the molecule. Whether in practice the inclusion of one layer of possibly low accuracy data would have this effect could not be predicted and thus this stage of the refinement was undertaken in the hope that a significant improvement in the agreement, and therefore the model, would provide the justification.

A further complication arose on the assumption of anisotropic thermal motion: as the data comprised several non-overlapping layers whose relative scale

factors were being determined internally, a strong degree of interaction will exist in the calculations between the scale factors and the β_{11} term of the thermal motion tensor. The strong correlation between these parameters was prevented by not permitting the scale factors to vary. This means that any adjustment to the scale factors will be taken up by the β_{11} terms and hence it is certainly not possible to interpret the anisotropic temperature factors as being due to any one effect but rather a combination of thermal motion, uncertainty in atomic positions due to the disordering and also in the case of the β_{11} term, any required scale factor adjustment.

In practice the refinement proceeded satisfactorily apart from the fact that the anisotropic thermal parameters for C_8 became physically meaningless, hence the isotropic temperature factor was retained for this atom. At the conclusion of this refinement the overall R factor was 0.111 and those for the individual layers are listed below:

0k ℓ	1k ℓ	2k ℓ	4k ℓ
0.097	0.103	0.108	0.154

It was felt that the 6% improvement in the agreement index and the consequent decrease in the errors of the positional parameters did indeed justify the assumption of anisotropy.

TABLE 14FINAL ATOMIC COORDINATES (FRACTIONAL)

Atom	x	y	z
C ₁	0.317(4)	0.218(2)	-0.006(1)
C ₂	0.393(5)	0.268(2)	0.090(1)
C ₃	0.392(4)	0.149(3)	0.165(1)
C ₄	0.310(4)	-0.016(2)	0.145(1)
C ₅	0.172(4)	-0.239(2)	0.034(1)
C ₆	0.098(4)	-0.291(2)	-0.067(1)
C ₇	0.110(4)	-0.178(2)	-0.140(1)
C ₈	0.184(4)	-0.005(2)	-0.127(1)
C ₉	0.253(3)	0.050(2)	-0.026(1)
C ₁₀	0.254(3)	-0.061(2)	0.052(1)
O ₄	0.185(2)	0.096(1)	-0.198(1)
O ₁	0.336(3)	0.335(2)	-0.074(1)
O ₃	0.166(3)	-0.337(2)	0.101(1)

TABLE 15
TEMPERATURE FACTORS (\AA^2)

(a)	<u>Anisotropic</u>			<u>equivalent isotropic B</u>			
Atom	U_{11}	U_{12}	U_{33}	U_{12}	U_{13}	U_{23}	
C ₁	0.04(2)	0.038(9)	0.067(12)	0.01(1)	-0.01(1)	0.022(7)	3.89
C ₂	0.15(4)	0.017(7)	0.078(12)	0.00(1)	-0.01(2)	-0.001(8)	6.53
C ₃	0.07(4)	0.082(11)	0.057(10)	0.03(2)	0.00(1)	-0.011(10)	5.64
C ₄	0.04(2)	0.086(12)	0.039(8)	0.02(1)	-0.02(1)	0.010(8)	4.44
C ₅	0.09(3)	0.032(8)	0.052(9)	0.00(1)	0.03(2)	0.010(7)	4.48
C ₆	0.06(3)	0.046(9)	0.067(11)	0.00(1)	0.02(1)	-0.018(8)	4.34
C ₇	0.09(3)	0.051(10)	0.044(9)	-0.02(1)	-0.01(1)	-0.033(7)	4.97
C ₉	0.07(3)	0.036(9)	0.029(7)	0.02(1)	0.00(1)	0.003(5)	3.60
C ₁₀	0.08(3)	0.021(7)	0.035(8)	-0.01(1)	-0.01(1)	0.004(6)	3.76
O ₄	0.10(2)	0.103(8)	0.029(5)	0.021(9)	-0.012(8)	0.034(5)	6.38
O ₁	0.14(3)	0.061(8)	0.095(9)	-0.01(1)	0.00(1)	0.040(7)	7.79
O ₃	0.17(3)	0.050(7)	0.080(9)	0.01(1)	0.05(1)	0.025(6)	7.70

(b) Isotropic

<u>Atom</u>	<u>B</u>
C8	4.2(4)

TABLE 16
INTERMOLECULAR CONTACTS

Atom 1	Atom 2	Vector to be applied to atom 2	Distance (Å) ^o
C ₂	O ₃	x, y+1, z	3.479
C ₂	O ₄	$\frac{1}{2}+x, \frac{1}{2}-y, \frac{1}{2}+z$	3.512
C ₃	O ₄	$\frac{1}{2}+x, \frac{1}{2}-y, \frac{1}{2}+z$	3.303
C ₃	O ₃	$\frac{1}{2}-x, \frac{1}{2}+y, \frac{1}{2}-z$	3.270
C ₇	O ₄	$\frac{1}{2}-x, \frac{1}{2}+y-1, \frac{1}{2}-z-1$	3.319
O ₁	C ₆	x, y+1, z	3.377

Mean error is $\pm 0.02 \text{ Å}^{\circ}$

TABLE 17LEAST SQUARES PLANE*

Equation of plane: $0.9283x - 0.3379y - 0.1553z$
 $- 1.6964 = 0$

Deviations of atoms from plane (Å)

C ₁	-0.06 (3)
C ₂	0.00 (3)
C ₃	0.04 (3)
C ₄	-0.03 (3)
C ₅	-0.02 (3)
C ₆	-0.03 (3)
C ₇	0.01 (3)
C ₈	0.03 (3)
C ₉	0.01 (2)
C ₁₀	0.03 (2)
O ₁	-0.03 (2)
O ₃	0.02 (2)
O ₄	0.01 (2)

*The plane is defined by the carbon atoms

TABLE 1.8

H	L	FJ	FC	H	L	FJ	FC	H	L	FJ	FC	H	L	FJ	FC	H	L	FJ	FC
K = 0				K = 2				K = 5				K = 7				K = 8			
0	4	179	-200	0	0	185	-164	0	2	18	29	0	2	18	29	0	1	33	-35
0	6	23	17	0	1	46	-58	0	3	194	-176	0	3	194	-176	0	2	32	31
0	8	38	-42	0	2	162	-196	0	4	111	125	0	4	111	125	0	3	69	-72
0	12	30	-31	0	3	106	-126	0	5	181	182	0	5	181	182	0	4	53	50
0	14	17	17	0	4	18	17	0	6	136	139	0	6	136	139	0	5	29	-35
1	3	119	-119	0	5	140	122	0	7	104	106	0	7	104	106	0	6	16	14
-1	3	50	96	0	6	90	67	0	8	11	-20	0	8	11	-20	0	7	32	-27
-1	5	37	-47	0	7	112	116	0	9	36	36	0	9	36	36	0	8	11	-6
-1	7	64	-96	0	8	104	-40	0	10	55	-59	0	10	55	-59	0	9	25	-12
-1	9	54	51	0	10	44	-40	0	11	101	96	0	11	101	96	0	10	26	25
1	11	29	32	0	11	54	57	0	12	58	-52	0	12	58	-52	0	11	69	-69
-1	11	84	-81	0	12	46	-55	0	13	47	47	0	13	47	47	0	12	39	39
1	13	29	-34	1	1	117	-105	0	14	79	76	0	14	79	76	0	13	92	91
2	6	108	-106	-1	0	97	106	0	15	54	-50	0	15	54	-50	0	14	34	-36
2	8	35	35	-1	1	33	32	0	16	32	30	0	16	32	30	0	15	93	95
2	10	23	-7	-1	1	33	-38	0	17	61	57	0	17	61	57	0	16	45	-47
-4	4	52	-48	1	2	89	94	0	18	2	18	0	18	2	18	0	17	34	27
4	6	42	37	-1	2	50	-54	0	19	1	1	0	19	1	1	0	18	29	28
4	10	26	-24	1	4	66	-66	0	20	75	75	0	20	75	75	0	19	31	29
-4	12	42	-32	-1	4	23	13	0	21	22	-37	0	21	22	-37	0	20	28	30
-4	14	42	-36	1	5	33	33	0	22	39	37	0	22	39	37	0	21	44	44
K = 1				-1	5	19	-14	0	23	4	4	0	23	4	4	0	22	31	29
0	2	18	29	-1	6	151	150	0	24	59	58	0	24	59	58	0	23	28	30
0	3	194	-176	1	9	39	37	0	25	51	-57	0	25	51	-57	0	24	49	49
0	4	111	125	1	10	107	-112	0	26	2	2	0	26	2	2	0	25	38	38
0	5	181	182	-1	10	40	46	0	27	7	7	0	27	7	7	0	26	30	-24
0	6	136	139	-1	11	99	104	0	28	10	10	0	28	10	10	0	27	26	25
0	7	104	106	-1	11	47	-50	0	29	11	11	0	29	11	11	0	28	69	-69
0	9	11	-20	-1	13	30	33	0	30	12	12	0	30	12	12	0	29	92	91
0	10	32	36	-1	14	25	-25	0	31	13	13	0	31	13	13	0	30	34	-36
0	11	55	-59	2	0	147	-136	0	32	14	14	0	32	14	14	0	31	93	95
0	12	47	58	2	1	165	-144	0	33	15	15	0	33	15	15	0	32	45	-47
0	13	25	-26	-2	1	35	34	0	34	16	16	0	34	16	16	0	33	34	27
1	1	32	30	2	2	61	53	0	35	17	17	0	35	17	17	0	34	37	-27
-1	1	61	57	-2	2	38	-36	0	36	18	18	0	36	18	18	0	35	29	28
1	2	18	9	2	3	40	9	0	37	19	19	0	37	19	19	0	36	44	44
-1	2	64	-59	2	4	78	65	0	38	20	20	0	38	20	20	0	37	31	29
-1	3	76	-24	2	5	27	30	0	39	21	21	0	39	21	21	0	38	28	30
1	4	75	-71	2	6	63	70	0	40	22	22	0	40	22	22	0	39	44	44
-1	4	86	84	2	7	49	45	0	41	23	23	0	41	23	23	0	40	29	28
1	5	135	-139	-2	7	99	-86	0	42	24	24	0	42	24	24	0	41	44	44
-1	5	101	96	2	8	36	37	0	43	25	25	0	43	25	25	0	42	31	29
1	8	58	-52	-2	8	214	-216	0	44	26	26	0	44	26	26	0	43	28	30
-1	8	53	47	2	9	32	29	0	45	27	27	0	45	27	27	0	44	44	44
1	9	34	-41	2	10	46	-34	0	46	28	28	0	46	28	28	0	45	29	28
1	10	79	76	2	11	79	80	0	47	29	29	0	47	29	29	0	46	44	44
-1	10	54	-50	2	12	48	-47	0	48	30	30	0	48	30	30	0	47	31	29
1	11	34	-43	2	13	43	42	0	49	31	31	0	49	31	31	0	48	28	30
-1	11	102	89	4	0	124	138	0	50	32	32	0	50	32	32	0	49	44	44
1	12	42	51	4	1	130	138	0	51	33	33	0	51	33	33	0	50	31	29
-1	12	95	-91	4	2	99	91	0	52	34	34	0	52	34	34	0	51	44	44
-1	13	48	46	4	3	30	20	0	53	35	35	0	53	35	35	0	52	29	28
2	1	24	40	4	4	44	-50	0	54	36	36	0	54	36	36	0	53	44	44
2	3	67	77	4	5	22	-28	0	55	37	37	0	55	37	37	0	54	31	29
-2	3	77	-81	4	6	103	115	0	56	38	38	0	56	38	38	0	55	28	30
2	4	166	-164	4	7	20	-16	0	57	39	39	0	57	39	39	0	56	44	44
-2	4	34	17	4	8	34	26	0	58	40	40	0	58	40	40	0	57	31	29
2	5	164	-165	4	9	36	-27	0	59	41	41	0	59	41	41	0	58	28	30
-2	5	39	24	4	10	47	44	0	60	42	42	0	60	42	42	0	59	44	44
2	6	107	-104	4	11	8	-25	0	61	43	43	0	61	43	43	0	60	31	29
2	7	20	-8	4	12	23	-25	0	62	44	44	0	62	44	44	0	61	44	44
-2	8	27	-12	4	13	15	15	0	63	45	45	0	63	45	45	0	62	29	28
2	11	44	41	4	14	37	-41	0	64	46	46	0	64	46	46	0	63	44	44
-2	11	40	32	4	15	24	11	0	65	47	47	0	65	47	47	0	64	31	29
-2	12	13	-39	4	16	11	11	0	66	48	48	0	66	48	48	0	65	28	30
-2	13	44	37	4	17	30	23	0	67	49	49	0	67	49	49	0	66	44	44
4	0	24	-35	0	1	221	234	0	68	50	50	0	68	50	50	0	67	44	44
-4	0	29	36	0	2	160	167	0	69	51	51	0	69	51	51	0	68	31	29
4	1	32	-33	0	3	43	32	0	70	52	52	0	70	52	52	0	69	44	44
4	2	31	-25	0	4	63	65	0	71	53	53	0	71	53	53	0	70	29	28
4	3	47	35	0	5	96	78	0	72	54	54	0	72	54	54	0	71	44	44
4	4	46	-48	0	6	89	-87	0	73	55	55	0	73	55	55	0	72	31	29
-4	4	39	36	0	7	42	-40	0	74	56	56	0	74	56	56	0	73	44	44
4	5	31	33	0	8	16	22	0	75	57	57	0	75	57	57	0	74	29	28
-4	5	34	-37	0	9	11	-10	0	76	58	58	0	76	58	58	0	75	44	44
4	7	19	-21	0	10	11	-17	0	77	59	59	0	77	59	59	0	76	31	29
-4	7	53	-43	0	11	30	23	0	78	60	60	0	78	60	60	0	77	44	44
-4	8	57	60	-1	0	26	23	0	79	61	61	0	79	61	61	0	78	29	28
-4	9	23	-5	-1	1	26	16	0	80	62	62	0	80	62	62	0	79	44	44
-4	13	36	-27	-1	2	46	41	0	81	63	63	0	81	63	63	0	80	31	29
				1	2	16	-15	0	82	64	64	0	82	64	64	0	81	44	44
								0	83	65	65	0	83	65	65	0	82	29	28
								0	84	66	66	0	84	66	66	0	83	44	44
								0	85	67	67	0	85	67	67	0	84	31	29
								0	86	68	68	0	86	68	68	0	85	44	44
								0	87	69	69	0	87	69	69	0	86	29	28

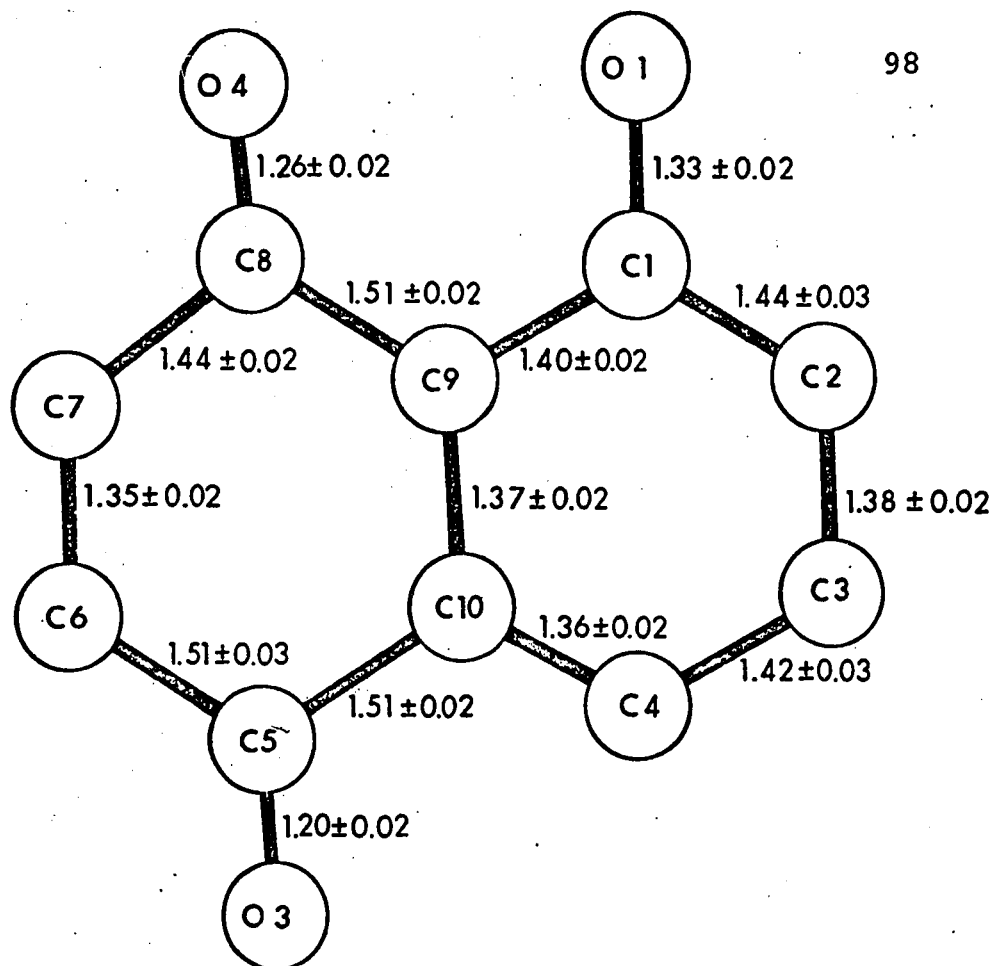
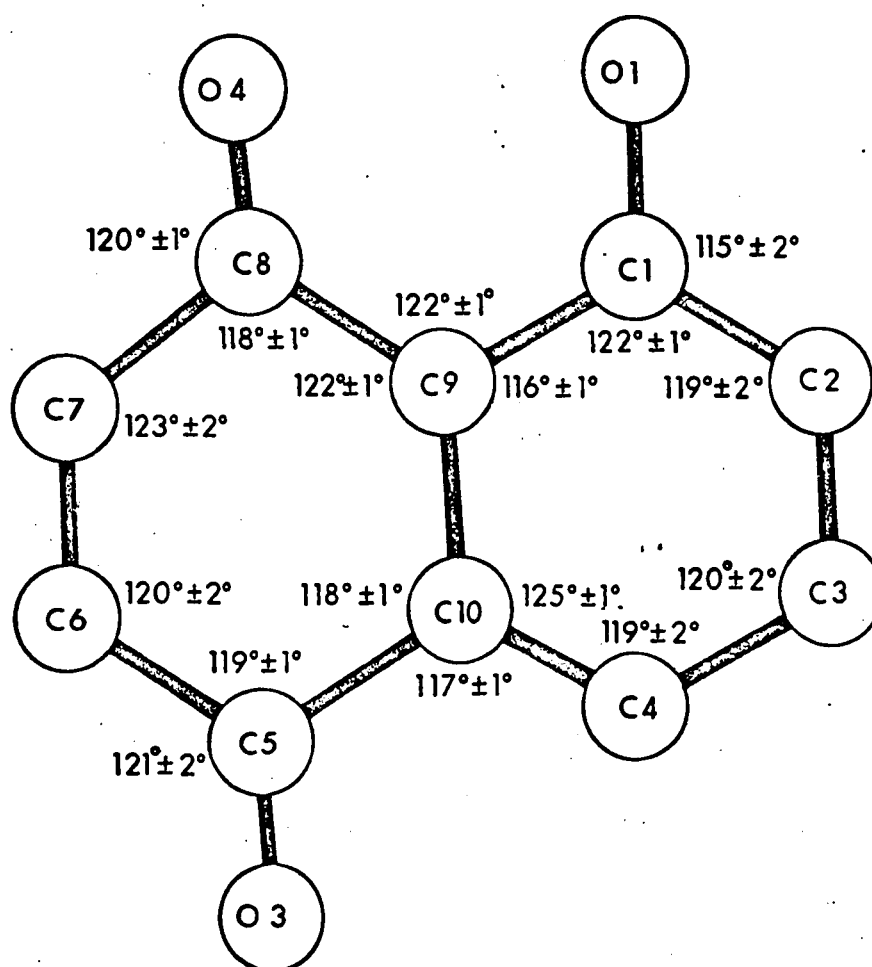


Fig. 15. Molecular dimensions.



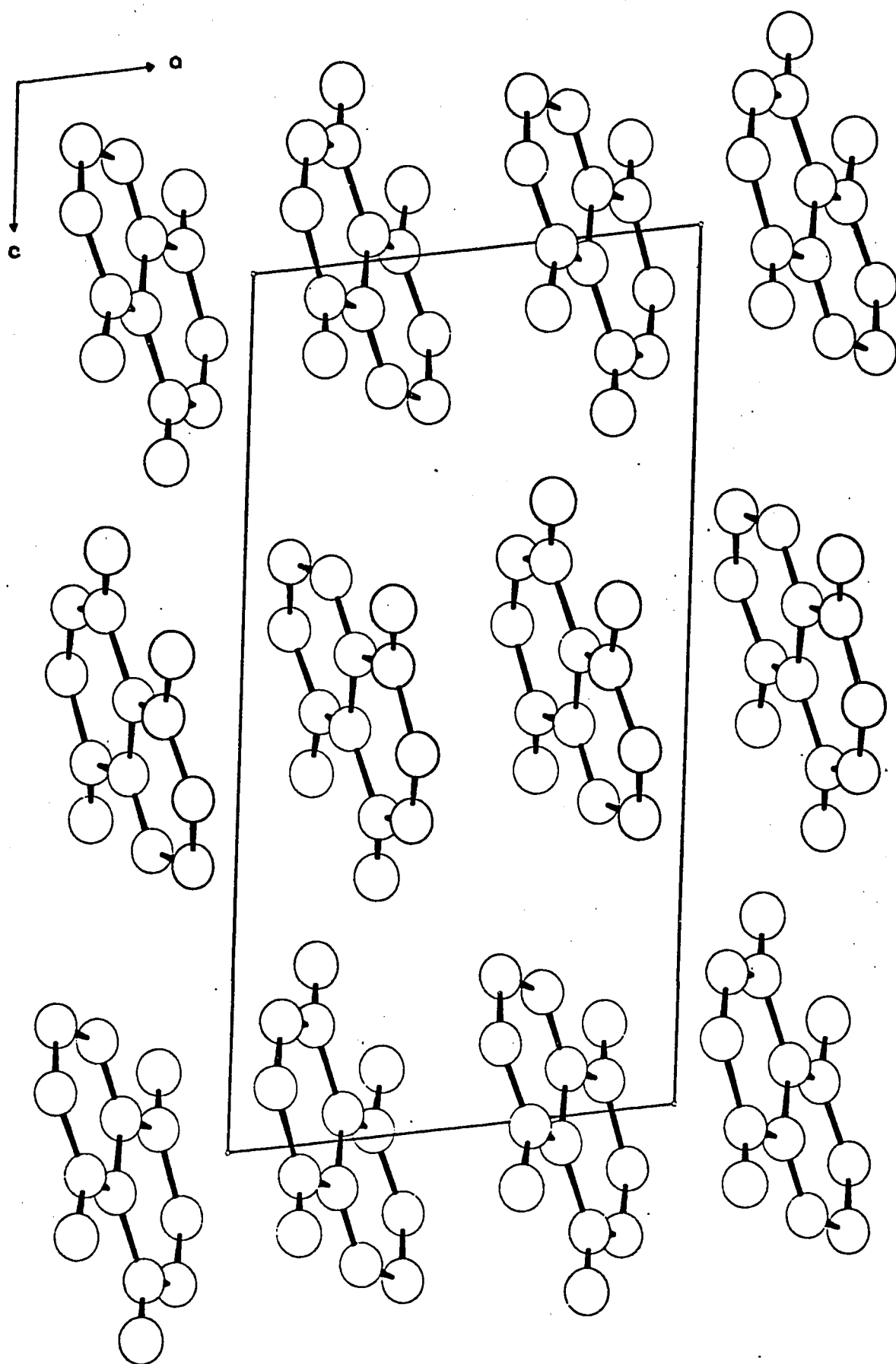


Fig. 16. Molecular packing. Projection onto $[ac]$ plane.

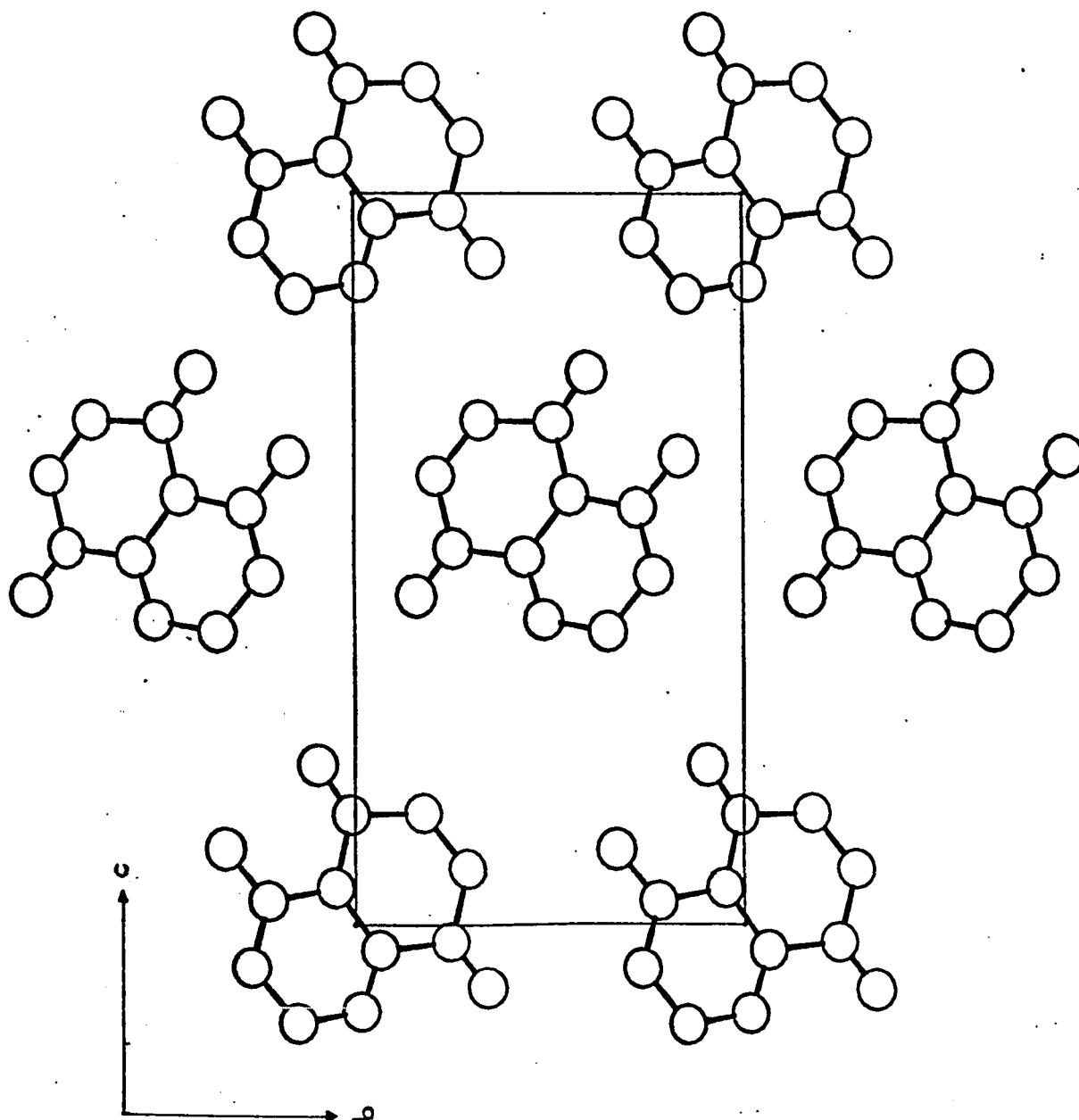


Fig. 17. Molecular packing. Projection onto $[bc]$ plane.

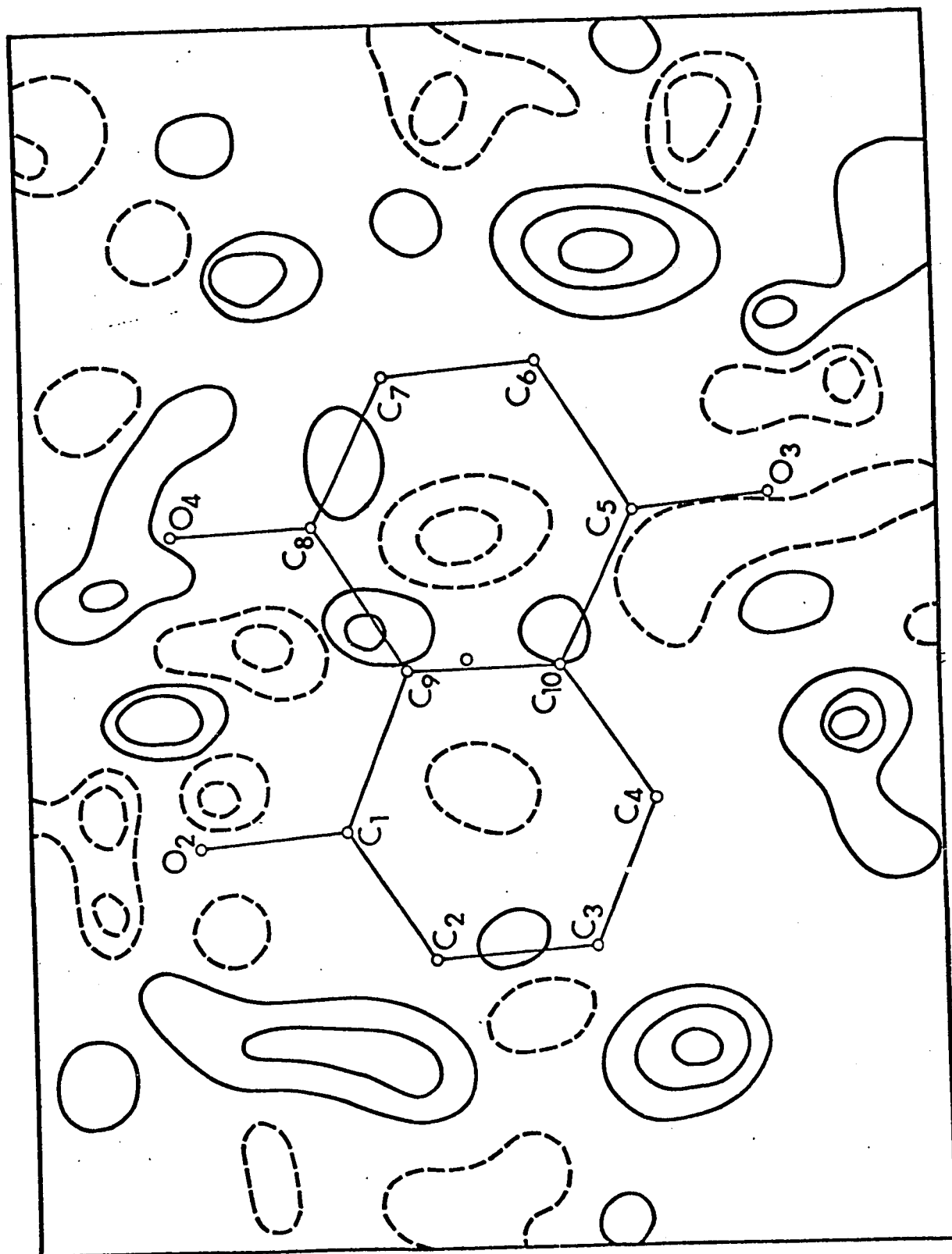


Fig. 18. Residual electron density at end of refinement.
Contour level is 1σ .

Results

The final atomic coordinates and temperature factors are listed in Tables 14, 15. The latter are expressed in U_{ij} values as defined on p.32. The true thermal vibration of this molecule would probably be similar to that of naphthazarin, thus the rather large value for U_{11} observed for atom C_2 can be safely attributed to scale factor corrections required during the anisotropic refinement. This is also partially true for the U_{11} term of the oxygen atoms although electron density smearing due to disorder will be more pronounced for these atoms and this will tend to falsify the anisotropic parameters. The molecular geometry is shown in Fig 15 which also shows the numbering scheme for the atoms. The equation of the least squares plane through the carbon atoms is shown with the deviations of each atom from the plane in Table 17. The packing of the molecules in the unit cell can be seen from the two projections onto the [ac] and [bc] planes shown in Figs. 16, 17 and the shorter intermolecular contacts are listed in Table 16.

Hamilton's test (20)

This test was applied to determine whether the 6% drop in R factor was due to a significant improvement in the

model or merely a result of increasing the number of variable parameters in the least squares refinement.

The ratio of the weighted R factors

$(R_w = [\sum_w (|F_o| - |F_c|)^2 / \sum_w |F_o|^2])$ obtained before and after the assumption of anisotropic motion is compared with a table of significance points $(R_{b,N,\alpha})$ and when the ratio exceeds the tabulated value, the hypothesis under test can be rejected at the $100.\alpha\%$ significance level.

	R	R_w
R factors before anisotropic refinement	0.1710	0.1982
R factors after anisotropic refinement	0.1110	0.1105

Ratio of weighted R factors is 1.794

The hypothesis under test is: "the anisotropic refinement is not physically significant".

The dimension of the hypothesis is the difference in the number of variables refined i.e.

$$b = 112 - 56 = 56$$

and the number of degrees of freedom is

$$N = 389 - 112 = 277$$

A relevant significance point, obtained by interpolation of the table given in (20) is:

$$R_{56,277,0.05} = 1.127$$

The criterion for rejection of hypotheses has been given by Hamilton (65) as: "Rejection at a significance level less than 5% is significant". Rejection in the present situation will occur at a significance level greater than 0.05 and thus the test shows that the improvement in the model which resulted from the assumption of anisotropic temperature factors is physically meaningful.

Discussion

Molecular Packing

As in the case of naphthazarin (see p 61), juglone exhibits the 'herring bone' packing characteristic of aromatic hydrocarbons (69). The angle between the molecular normal and the [a] axis is 21.8° which is very similar to the same angle in naphthazarin form "A". Comparison of the packing diagrams of juglone (p91) and naphthazarin (p 61) clearly shows the close similarity between these two structures, and in view of this the stacking disorder responsible for the diffuse reflections in juglone becomes obvious, as the energy differences between molecular orientations where C_3 was at the positions occupied by C_1 , C_5 , C_8 must be very small.

A final difference Fourier map was calculated in the plane of the molecule (using the Fourier programme written by Zalkin (55)) in order to observe the residual electron

density which should be present at the "missing OH" position off C_4 as a result of the stacking disorder. There is of course a genuine hydrogen atom at this position which should be observable on this Fourier map, but this peak should be elongated along C_4 -H bond because of the presence of an oxygen atom when disordered stacking occurs. This Fourier map is shown in Fig 18 and all the hydrogen atoms can be clearly seen at 2 or 3 σ (the standard deviation in electron density as calculated by the Cruickshank formula (56) is $0.097 \text{ e}^{-\text{\AA}^{-3}}$). The positions of these protons are in some cases quite badly distorted (e.g., those attached to C_7 and C_2) which could be a result of disorder or more realistically, errors in the data. In addition, the refinement with anisotropic temperature factors could give rise to distortion of the hydrogen positions, particularly in view of the electron density observed in the region of O_3 which shows the classic distribution observed when anisotropic motion has not been correctly accounted for (i.e. the appearance of two positive regions either side of the atom and at 90° to these, two negative regions (106)^a. The hydrogen atom attached to C_4 does indeed show marked distortion when compared to the other protons, although not in the direction expected; in view of the other distortions present on this Fourier map it is likely that any result

other than that obtained is beyond the capabilities of the data set, and for this reason it was not felt that inclusion of the hydrogen atoms in the structure factor calculations would lead to an improvement of the model.

The closer intermolecular contacts are listed in Table 16, and all are clearly weak Van der Waals interactions. This is to be expected, for if stronger intermolecular forces existed these would certainly stabilise the packing of the molecules and disordered stacking would not occur. The perpendicular distance between molecules stacked along the [a] axis is 3.44 \AA which agrees well (in view of the accuracy of the final model) with the Pauling value $(3)^b$ for the thickness of aromatic molecules viz. 3.4 \AA . Clearly there is no evidence for intermolecular interactions of the type suggested by Prout and Wallwork (70), involving overlap of molecular orbitals of parallel molecules.

Molecular geometry

The bond lengths of the final model indicate that within the limits of the errors, the structure does indeed have the quinonoid-benzenoid form observed by Moore and Shueur (34) viz:

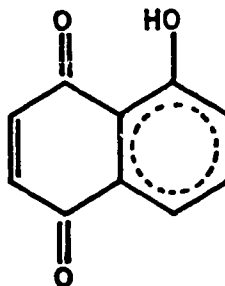
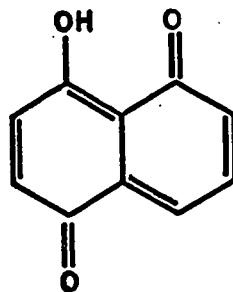


TABLE 19
BOND LENGTHS OF SOME QUINONOID COMPOUNDS

	C=O	C-O	C ₆ -C ₇	Mean C ₇ -C ₈	Mean benzene	ref.
1,5-dihydroxy anthraquinone	1.214 (5)	1.343 (6)		1.482 (6)	1.394 (7)	(72)
1,5-dinitro 4,8-dihydroxy anthraquinone	1.219 (5)	1.336 (5)		1.463 (5)	1.383 (5)	(73)
10,10-dianthranyl	1.240 (5)			1.495 (5)	1.391 (5)	(74)
2-methyl, 3-amino naphthoquinone	1.24 (1)		1.35 (1)	1.48 (1)	1.40 (1)	(75)
2,3-dibromo 1,4-naphthoquinone	1.19		1.34	1.49	1.40	(76)
2,3-dimethyl 1,4-naphthoquinone	1.23 (5)		1.34 (3)	1.47 (3)	1.39 (3)	(77)
tetrahydroxy-p- benzoquinone	1.229 (5)	1.344 (5)	1.342 (5)	1.478 (5)		(78)
juglone	1.23 (1)	1.33 (2)	1.35 (2)	1.49 (1)	1.39 (1)	this work

The bond lengths in the two rings are similar to those observed in comparable compounds, some of which are listed in Table 19. For all compounds listed, averages were taken of the like bonds and in view of the large discrepancies in some of the juglone "like" bonds, these are quoted as weighted means ($r_w = \sum w_i r_i / \sum w_i$). The fact that the observed bond lengths agree so well with other structures indicates that the molecules must pack predominantly in the one orientation and that "mistakes" occur only with relatively small numbers of molecules.

The initial purpose of this structural investigation was to determine whether this molecule existed as 5,-hydroxy 1,4-naphthoquinone (see above) or as 4,-hydroxy 1,5-naphthoquinone shown below:



It is significant that even this relatively inaccurate structural determination indicates that the structure of juglone is actually the former. This result agrees with those obtained from the crystal structure determinations of other polynuclear hydroxy-quinones e.g. 1,5-dihydroxyanthraquinone (72),

see also Table 19, which can exist in the di-quinonoid state. In general these compounds have only one quinonoid ring, which suggests that this form is of slightly lower energy; a result which is not too surprising in view of the known resonance stabilisation of the benzene ring.

PART II

(A) Introduction

One of the current fields of research being carried out in the inorganic section of this department, under the supervision of Professor W.A.G. Graham, is the synthesis of compounds involving metal-metal bonds between transition metals and metals of the main groups III and IV (30, 42, 50). The preparative route to these compounds has frequently been the "insertion reaction" in which halides of main group metals undergo insertion into the metal-metal bond of a transition metal carbonyl e.g. SnCl_2 can be "inserted" into the iron-iron bond of π -cyclopentadienyliron dicarbonyl dimer (116). It appears that the criteria for the "insertion reaction" to occur are (i) the main group metal must be capable of increasing its oxidation state by two units, and (ii) it must be capable of forming covalent bonds with transition metals. The indium(I) halides fulfil these criteria, thus the insertion reactions involving InBr and $\text{Co}_2(\text{CO})_8$ were studied by Dr. D. Patmore (30, 50).

The reaction in tetrahydrofuran produced the compound $\text{THFBrIn}(\text{Co}(\text{CO})_4)_2$ in which the indium atom is tetrahedral by the coordination of a solvent molecule.

However, when the reaction was carried out in benzene, a solvent that does not have the electron donor properties of tetrahydrofuran, a different product resulted which was assigned the formula $\text{In}_3\text{Br}_3\text{Co}_4(\text{CO})_{16}$ on the basis of the elemental analysis. As no rational structures could be postulated for this molecule, on the basis of the above formula, the crystal structure analysis was undertaken. This work is described in Part II(B).

Further study of the reactions between InBr and $\text{Co}_2(\text{CO})_8$ in the presence of tetraethylammonium chloride, produced the molecule $[\text{Br}_2\text{InCo}_2(\text{CO})_8]^- \text{Et}_4\text{N}^+$ (50). The crystal structure of this compound was studied in the hope of comparing the geometry of the heavy metals in the two molecules, and in particular to observe the effect (if any) of the negative charge on the geometry. The results of this work are described in Part II(C).

PART II

(B) The Crystal and Molecular Structure of
 Tribromotriindiumtetracobalt Pentadecakiscarbonyl,
 $(\text{In}_3\text{Br}_3\text{Co}_4(\text{CO})_{15})$.

Experimental

Orange crystals were provided by Dr. D. Patmore who had described the preparation (30). The crystals were needle shaped with approximately hexagonal cross-section. Unit cell and space group data were obtained from precession and Weissenberg photographs using Mo K α radiation; the errors in axial lengths were estimated by the method of Patterson and Love (64). The density was estimated by flotation in a solution of tetrabromoethane and n-hexane.

Crystal data

Space Group $P2_1/c$
 $a = 14.25 \pm 0.01 \text{ \AA}$
 $b = 17.62 \pm 0.02 \text{ \AA}$
 $c = 16.87 \pm 0.02 \text{ \AA}$
 $\beta = 133.2 \pm 0.5^\circ$

$$d_{\text{calc}} = 2.64 \text{ gm/cm}^3$$

$$d_{\text{obs}} = 2.69 \text{ gm/cm}^3$$

A β angle which is not close to 90° will give rise to high correlation between x and z parameters in the least squares refinement, and if these correlations are not taken into account, as in the case of the block diagonal approximation, incorrect refinement of these parameters could result. As a full matrix least squares programme was not available at the data collection stage it was decided to transform the data to a unit cell for which β was approximately 90° . A reciprocal lattice plot of the a^*c^* plane was made in order to find a more suitable cell. The B centred cell that had a common [c] axis with the primitive cell had a β value of 99° , thus the data was transformed to this cell by the following transformation matrix:

$$\begin{pmatrix} h \\ k \\ l \end{pmatrix}_B = \begin{pmatrix} 2 & 0 & 1 \\ 0 & 1 & 0 \\ 0 & 0 & 1 \end{pmatrix} \begin{pmatrix} h \\ k \\ l \end{pmatrix}_P$$

The new unit cell data are:

Space group $B2_1/c$

$$a = 21.26 \text{ \AA}$$

$$b = 17.62 \text{ \AA}$$

$$c = 16.87 \text{ \AA}$$

$$\beta = 99.3^\circ$$

This cell was used throughout the determination.

Intensity data were collected on the Pailred linear diffractometer using crystal-monochromatised (Si, (111) plane) Mo $K\alpha$ radiation, with the crystal rotating about the needle or [c] axis; the layers $l = 0$ to $l = 11$ were collected. As this compound provided the first set of data to be collected on the diffractometer in this laboratory, data of the four forms hkl , $\bar{h}kl$, $h\bar{k}l$, $hk\bar{l}$ were collected to provide the symmetry equivalent reflections as a check on the operation of the machine. There were no significant differences between the symmetry equivalent reflections (hkl , $\bar{h}kl$) and ($\bar{h}kl$, $h\bar{k}l$), and furthermore as the crystal was slowly decomposing, only the layers $l = 0$ to $l = 3$ were collected in this manner, since two automatic runs must be done for each layer in order to collect all four forms. For subsequent layers only the unique data hkl , $\bar{h}kl$ were collected. Each reflection was scanned for 60 sec. at a rate of $1^\circ/\text{min}$ and the background was counted with the crystal stationary at each side of the peak, for a total of 80 sec. Reflections were rejected on the basis of two tests: (1) $I \leq 0$ and (2) $\sigma I/I > 0.5$ (see p. 28) leaving a total of 1920 reflections of 4374 reflections scanned.

Fourteen $hk0$ reflections were checked after the recording of each layer and as the intensities of these reflections decreased steadily a correction for decomposition was made. Collection of one layer of data took approximately 24 hrs and as the crystal was continuously irradiated during the data collection, the time scale for plots of $\log I$ versus time for each standard reflection was taken as the number of days the layer was recorded after the $hk0$ layer. These plots were linear and the average slope of the lines (-0.0088) was used to derive the correction factor k for each layer, (ℓ) from the expression: $k = I_0/I_\ell = 10^{0.0088 \cdot t_\ell}$. The individual slopes ranged from -0.0064 to 0.01 and no dependence on $\sin\theta$ or intensity was observed. The correction factors used are shown below:

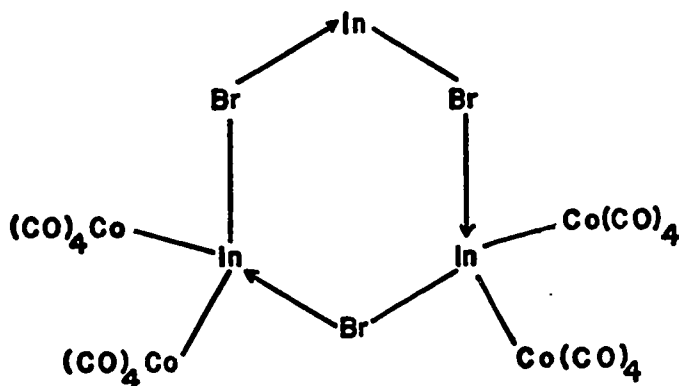
ℓ	0	1	2	3	4	5
k	1.0	1.02/1.04	1.06/1.08	1.11/1.13	1.15	1.20
ℓ	6	7	8	9	10	11
k	1.22	1.25	1.28	1.30	1.33	1.36

Absorption corrections were not applied to the data as the linear absorption coefficient for Mo $K\alpha$ radiation was 84 cm^{-1} and by approximating the crystal to a cylinder, the value for μR was 0.8 . Lorentz and

Polarisation corrections were applied to the data and all equivalent reflections were averaged.

Structure Solution

The analysis figures for this compound gave the empirical formula as $\text{In}_3\text{Br}_3\text{Co}_4(\text{CO})_{16}$ (30) and the only structure that could be postulated using this formula involved a ring of alternating indium and bromine atoms as shown below:



This structure is somewhat unusual in that the indium atoms exist in two different oxidation states, however, it was accepted as an initial model and the three dimensional Patterson synthesis was calculated in order to locate the heavy atom positions. The Patterson synthesis contained two Harker sections: a plane at $y = \frac{1}{2}$ on which are found all vectors between atoms related by the screw axis i.e.

$$(x, y, z) - (\frac{1}{2} - x, \frac{1}{2} + y, \frac{1}{2} - z) = (\frac{1}{2} + 2x, \frac{1}{2}, \frac{1}{2} + 2z)$$

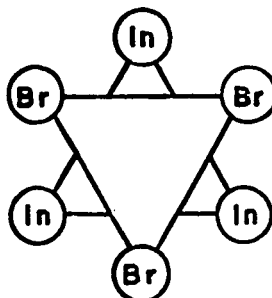
and a line at $x = \frac{1}{2}, z = \frac{1}{2}$, which contains all vectors

between atoms related by the c glide i.e.

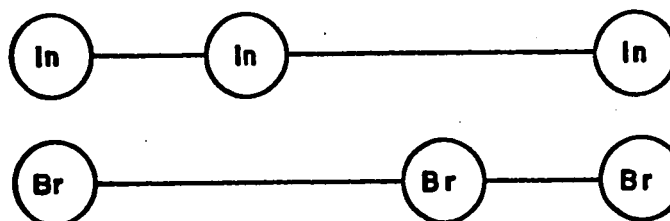
$$(x, y, z) - (\frac{1}{2} + x, \frac{1}{2} - y, \frac{1}{2} + z) = (\frac{1}{2}, \frac{1}{2} + 2y, \frac{1}{2}).$$

The Harker plane contained seven large vectors, one of which was approximately twice as large as the others and was situated very close to a two-fold axis at $x = z = 0.25$. This vector could be either a genuine large vector at the observed position, or the result of superposition of two smaller vectors situated on either side of the two fold axis and because of this uncertainty, it was not given full consideration in the early stages of the structure solution. The Harker line showed only four large vectors which suggests that some of the heavy atoms have similar y coordinates.

The Harker plane, $y = \frac{1}{2}$, effectively represents a double scale projection of the unit cell contents i.e. the vectors on this plane have the form $(\frac{1}{2} + 2x, \frac{1}{2}, \frac{1}{2} + 2z)$ hence, considering only the indium and bromine atoms, the pattern of Harker vectors on this plane should form two triangles of vectors which have the same relative positions as they do in the molecule:



This pattern of Harker vectors will only be observed if the planes of the triangles are normal to the [b] axis (the 2_1 axis is parallel to [b]). Allowing for small deviations from this orientation the pattern of Harker vectors should be easily recognisable, but if the planes of the indium and bromine triangles were actually parallel to the [b] axis then the observed Harker pattern would no longer be clear, as these vectors would then fall on two parallel lines (assuming that the bromine atoms would not be coplanar with the indium atoms) as shown below:



The hexagonal pattern of Harker vectors was not observed on the Harker plane and so Harker vectors were considered in groups of three in the hope of identifying those vectors due to the indium atoms. The through-centre vectors ($2x$, $2y$, $2z$) and cross-vectors were checked for any possible model, and provided these vectors were present at the expected peak heights (the cross-vectors should appear with approximately the same height as the Harker vectors and the ($2x$, $2y$, $2z$) vectors

will be half this value), the three indium atoms were tested in structure factor and Fourier calculations. No prospective model could be lightly discarded without extensive checking, as the molecular structure was unknown, but unfortunately no model was found that refined (by Fourier and least-squares methods) to an R factor of less than 0.40.

A more direct method of checking a proposed model is by the use of Patterson superposition. A computer programme was written for this purpose using the method outlined by Lipscomb et al (31); the general method of Patterson superposition, and the programme used are given in Appendix C. If a superposition is carried out using one of the atoms of a proposed model, then provided that atom is correct, a corresponding peak should remain in the superposition map, and furthermore all other atoms should appear as peaks on this map. On a re-examination of the Harker section it was noticed that the largest Harker peak, which was situated close to a two-fold axis, was actually half-way between two other large Harker peaks. This is the characteristic pattern observed on the Harker section when two atoms have a common y coordinate: two atoms at (x_1, y, z_1) and (x_2, y, z_2) will give rise to Harker vectors at $(2x_1, \frac{1}{2}, \frac{1}{2} + 2z_1)$ and $(2x_2, \frac{1}{2}, \frac{1}{2} + 2z_2)$ and the

coordinates of the mid-point of the line joining these vectors is given by half the sum of the respective coordinates i.e. $(x_1 + x_2, \frac{1}{2}, \frac{1}{2} + z_1 + z_2)$. This is actually a cross-vector between the original atoms, $(x_2, y, z_2) - (\bar{x}_1, \frac{1}{2} + y, \frac{1}{2} - z_1) = (x_2 + x_1, \frac{1}{2}, \frac{1}{2} + z_2 + z_1)$ and should therefore have the same peak height as the Harker vectors, but although the peak height could not be explained at the present time, one of the atom positions derived from the two Harker vectors was used in the superposition procedure. The resulting map showed the positions of the ten heavy atoms, and the reason for the enhanced peak height of the large cross-vector became clear: Harker vectors resulting from the third indium atom and also a cobalt atom (In_1 and Co_2 in Fig. 19) coincided on this peak. The molecule did indeed consist of a puckered ring of bromine and indium atoms and the planes through these atoms were approximately parallel to the [b] axis, thus the second pattern of Harker vectors (see p. 118) should have been observed. This pattern was not recognised as the large vector on the Harker plane that was initially ignored because of its proximity to the two-fold axis, actually contained the third indium Harker vector. Furthermore as several other atoms had similar y coordinates (see Table 20)

there will be other large cross-vectors on the Harker section and in fact three of the seven largest vectors were actually cross-vectors.

The positions of indium atoms were quite clear from the peak heights on the superposition map; the bromine atoms were positioned so that they completed the six membered ring with the indium atoms and the cobalt atoms were assigned to the four remaining large peaks. Structure factors were calculated using this model and these yielded an R factor of 0.24. The ten heavy atoms were now refined by least squares, using the block-diagonal approximation and isotropic temperature factors for all atoms, to an R factor of 0.17, when the F_{obs} Fourier map phased by this model showed the positions of all the carbonyl atoms. With these atoms included in the refinement the R factor dropped to 0.11. All atoms were then refined with anisotropic temperature factors, but some of the light atom temperature parameters became physically meaningless; thus only the ten heavy atoms were given anisotropic temperature factors in the final refinement. All observations had been previously included in the least squares procedure with unit weights. Now, however, weights were calculated as a function of F_{obs} by the formula $w^{\frac{1}{2}} = 1/[1 + [(F_o - b)/a]^2]^{\frac{1}{2}}$ where

a and b were given the values 73 e⁻ and 129 e⁻ respectively, which ensured that the mean $w|F_o - F_c|^2$ was invariant with F_{obs} . Further refinement this time using full-matrix least squares (33), resulted in convergence at an R factor of 0.072. Throughout all refinements the scattering factors given in the International Tables (38) were used and the three heavy atom curves were corrected for the real component of anomalous dispersion.

Results

Final atomic coordinates and isotropic temperature factors are listed in Table 20. The anisotropic temperature factors for the ten heavy atoms are listed in Table 21 as U_{ij} values (see p. 32). The root-mean-square amplitudes of vibration for these atoms are given in Table 22 and the orientations of the ellipsoids are shown in Fig. 20. Bond angles and distances are shown in Tables 26 and 23, and non-bonded inter- and intramolecular contacts are given in Tables 24 and 25. Structure factors are listed in Table 27. The atom numbering scheme is given on Fig. 19 and the molecular packing is shown in the stereoscopic diagram Fig. 21 (stereo viewers are supplied inside the back cover).

TABLE 20
FINAL ATOMIC COORDINATES AND
ISOTROPIC TEMPERATURE FACTORS

Atom	x	y	z	B (Å ²)
In ₁	0.1203(1)	0.1252(1)	0.3838(2)	
In ₂	0.0473(1)	0.2913(1)	0.3997(2)	
In ₃	0.1766(1)	0.2793(1)	0.3120(2)	
Br ₁	0.0796(2)	0.1892(2)	0.5156(3)	
Br ₂	0.1574(2)	0.3716(2)	0.4332(3)	
Br ₃	0.2431(2)	0.1768(2)	0.4099(3)	
Co ₁	0.0666(2)	0.2143(3)	0.2748(3)	
Co ₂	0.1219(2)	-0.0172(3)	0.4041(4)	
Co ₃	-0.0470(2)	0.3788(3)	0.4172(3)	
Co ₄	0.2512(2)	0.3464(3)	0.2296(4)	
C ₁₁	0.038(2)	0.296(3)	0.224(3)	5.8(10)
O ₁₁	0.018(1)	0.349(2)	0.190(2)	6.6(7)
C ₁₂	0.096(2)	0.161(2)	0.203(3)	5.4(9)
O ₁₂	0.116(1)	0.126(2)	0.154(2)	7.5(8)
C ₁₃	-0.006(1)	0.165(2)	0.278(2)	3.7(7)
O ₁₃	-0.052(1)	0.128(2)	0.280(2)	5.9(6)
C ₂₁	0.122(2)	-0.119(3)	0.422(3)	7.4(12)
O ₂₁	0.120(2)	-0.180(2)	0.433(2)	9.2(9)
C ₂₂	0.151(3)	-0.018(3)	0.311(4)	8.1(13)
O ₂₂	0.175(2)	-0.023(3)	0.253(3)	11.2(12)

Table 20 cont'd.

Atom	x	y	z	B (Å ²)
C ₂₃	0.041(2)	-0.007(2)	0.402(3)	5.3(9)
O ₂₃	-0.015(2)	0.001(2)	0.402(2)	6.9(7)
C ₂₄	-0.173(2)	0.005(2)	0.490(3)	5.6(9)
O ₂₄	0.211(2)	0.018(2)	0.544(2)	7.9(8)
C ₃₁	-0.112(2)	0.441(2)	0.435(3)	5.3(9)
O ₃₁	-0.154(1)	0.479(2)	0.442(2)	6.8(7)
C ₃₂	-0.088(2)	0.325(2)	0.342(3)	4.4(8)
O ₃₂	-0.116(1)	0.296(2)	0.285(2)	6.8(7)
C ₃₃	-0.035(2)	0.340(2)	0.517(3)	5.9(10)
O ₃₃	-0.030(2)	0.323(2)	0.578(3)	8.0(8)
C ₃₄	-0.000(2)	0.450(3)	0.384(3)	6.8(11)
O ₃₄	0.028(2)	0.502(2)	0.359(2)	8.8(9)
C ₄₁	0.303(3)	0.389(3)	0.172(4)	8.0(13)
O ₄₁	0.339(2)	0.410(2)	0.130(3)	9.5(10)
C ₄₂	0.301(2)	0.354(3)	0.321(3)	6.4(11)
O ₄₂	0.333(2)	0.359(2)	0.380(2)	7.4(8)
C ₄₃	0.247(2)	0.259(3)	0.176(3)	6.6(11)
O ₄₃	0.248(2)	0.203(3)	0.145(3)	10.7(11)
C ₄₄	0.189(2)	0.413(3)	0.210(3)	6.8(11)
O ₄₄	0.146(2)	0.457(2)	0.201(2)	9.1(9)

TABLE 21.
ANISOTROPIC TEMPERATURE FACTORS (\AA^2)

Atom	U_{11}	U_{22}	U_{33}	U_{12}	U_{13}	U_{23}	equivalent isotropic B
In ₁	0.049(2)	0.034(1)	0.068(3)	0.000(1)	0.006(1)	0.004(1)	4.00
In ₂	0.048(1)	0.036(1)	0.061(2)	-0.001(1)	0.011(1)	-0.006(1)	3.82
In ₃	0.040(2)	0.038(1)	0.074(3)	-0.001(1)	0.009(1)	0.003(1)	3.98
Br ₁	0.096(3)	0.051(3)	0.058(4)	0.014(2)	0.019(3)	0.007(2)	5.34
Br ₂	0.053(2)	0.050(2)	0.096(5)	-0.014(2)	0.015(2)	-0.024(3)	5.66
Br ₃	0.038(2)	0.052(2)	0.119(4)	0.002(2)	-0.007(2)	0.024(3)	5.22
Co ₁	0.037(2)	0.036(2)	0.052(4)	0.002(2)	0.005(2)	-0.004(2)	3.31
Co ₂	0.060(3)	0.037(3)	0.071(5)	-0.004(2)	0.007(3)	-0.006(3)	4.44
Co ₃	0.041(3)	0.038(3)	0.075(5)	0.002(2)	0.009(3)	-0.002(3)	4.06
Co ₄	0.039(3)	0.057(3)	0.084(5)	0.000(2)	0.013(3)	0.016(3)	4.71

TABLE 22ROOT-MEAN-SQUARE AMPLITUDES OF VIBRATION

Atom	Minor axis	Medium axis	Major axis
In ₁	0.182	0.221	0.264
In ₂	0.187	0.218	0.250
In ₃	0.191	0.201	0.272
Br ₁	0.214	0.238	0.316
Br ₂	0.183	0.218	0.366
Br ₃	0.185	0.239	0.326
Co ₁	0.185	0.194	0.232
Co ₂	0.189	0.245	0.271
Co ₃	0.191	0.206	0.274
Co ₄	0.193	0.224	0.302

TABLE 23

INTRAMOLECULAR DISTANCES (Å)

In ₁ -Br ₁	2.800(6)	Co ₂ -C ₂₁	1.82(6)
In ₁ -Br ₃	2.732(4)	Co ₂ -C ₂₂	1.81(7)
In ₁ -Co ₁	2.573(5)	Co ₂ -C ₂₃	1.72(4)
In ₁ -Co ₂	2.532(5)	Co ₂ -C ₂₅	1.73(5)
In ₂ -Br ₁	2.696(5)	C ₂₁ -O ₂₁	1.10(5)
In ₂ -Br ₂	2.716(4)	C ₂₂ -O ₂₂	1.20(6)
In ₂ -Co ₁	2.637(6)	C ₂₃ -O ₂₃	1.20(4)
In ₂ -Co ₃	2.585(5)	C ₂₄ -O ₂₄	1.16(5)
In ₃ -Br ₃	2.710(5)	Co ₃ -C ₃₁	1.83(4)
In ₃ -Br ₂	2.735(5)	Co ₃ -C ₃₂	1.73(4)
In ₃ -Co ₁	2.591(5)	Co ₃ -C ₃₃	1.83(6)
In ₃ -Co ₄	2.582(6)	Co ₃ -C ₃₄	1.76(5)
Co ₁ -C ₁₁	1.74(5)	C ₃₁ -O ₃₁	1.13(4)
Co ₁ -C ₁₂	1.76(5)	C ₃₂ -O ₃₂	1.18(4)
Co ₁ -C ₁₃	1.78(4)	C ₃₃ -O ₃₃	1.09(5)
C ₁₁ -O ₁₁	1.16(5)	C ₃₄ -O ₃₄	1.21(5)
C ₁₂ -O ₁₂	1.17(5)	Co ₄ -C ₄₃	1.79(5)
C ₁₃ -O ₁₃	1.17(4)	Co ₄ -C ₄₂	1.75(5)
		Co ₄ -C ₄₁	1.76(6)
		Co ₄ -C ₄₄	1.76(5)
		C ₄₃ -O ₄₃	1.13(5)
		C ₄₂ -O ₄₂	1.15(5)
		C ₄₁ -O ₄₁	1.19(6)
		C ₄₄ -O ₄₄	1.19(5)

TABLE 24
INTRAMOLECULAR NON-BONDED CONTACTS

Atom 1	Atom 2	Distance	Atom 1	Atom 2	Distance
In ₁	C ₂₂	2.93	C ₄₁	C ₄₃	2.59
In ₁	C ₂₃	2.92	C ₄₁	C ₄₄	2.65
In ₁	C ₂₄	2.90	C ₄₂	C ₄₃	3.07
In ₂	C ₃₂	2.95	C ₄₃	C ₄₄	3.06
In ₂	C ₃₃	3.00	C ₄₄	C ₄₂	2.99
In ₂	C ₃₄	2.97	C ₁₁	In ₂	3.00
In ₃	C ₄₃	2.99	C ₁₁	In ₃	3.10
In ₃	C ₄₂	2.93	C ₁₂	In ₂	3.15
In ₃	C ₄₄	2.97	C ₁₂	In ₃	3.13
C ₂₁	C ₂₂	2.76 (6)	C ₁₃	In ₁	3.07
C ₂₁	C ₂₃	2.59	C ₁₃	In ₂	3.14
C ₂₁	C ₂₄	2.63	C ₁₁	C ₁₂	2.75
C ₂₂	C ₂₃	3.02	C ₁₂	C ₁₃	2.71
C ₂₃	C ₂₄	2.96	C ₁₃	C ₁₂	2.71
C ₂₄	C ₂₂	3.07	O ₁₁	O ₃₄	3.90 (4)
C ₃₁	C ₃₂	2.70	O ₁₁	O ₄₄	3.30
C ₃₁	C ₃₃	2.66	O ₁₃	O ₃₃	3.69
C ₃₁	C ₃₄	2.68	O ₁₃	O ₃₂	3.26
C ₃₂	C ₃₃	3.05	O ₁₃	O ₂₃	2.06
C ₃₃	C ₃₄	3.18	O ₁₂	O ₄₁	3.15
C ₃₄	C ₃₂	2.92	O ₁₂	O ₂₂	3.28
C ₄₁	C ₄₂	2.65			

TABLE 25
INTERMOLECULAR CONTACTS

Atom 1	Atom 2	Vector to be applied to Atom 2	Distance (Å)
Br ₂	O ₃₁	$\bar{x}, \bar{y}+1, \bar{z}+1$	3.42
O ₁₂	O ₃₃	$x, \frac{1}{2}-y, \frac{1}{2}+z-1$	3.23
O ₁₂	O ₃₁	$\bar{x}, \frac{1}{2}+y-1, \frac{1}{2}-z$	3.23
O ₁₃	O ₄₂	$\frac{1}{2}+x-1, \frac{1}{2}-y, z$	3.19
O ₁₃	O ₄₁	$\frac{1}{2}+x-1, \frac{1}{2}-y, z$	3.24
O ₂₁	O ₃₃	$\bar{x}, \bar{y}, \bar{z}-1$	3.13
O ₂₂	O ₂₂	$\frac{1}{2}-x, y, \frac{1}{2}-z$	3.29
O ₂₃	O ₁₁	$\bar{x}, \frac{1}{2}+y-1, \frac{1}{2}-z$	3.09
O ₂₃	O ₄₄	$\bar{x}, \frac{1}{2}+y-1, \frac{1}{2}-z$	3.10
O ₂₄	O ₄₁	$x, \frac{1}{2}-y, \frac{1}{2}+z$	3.14
O ₂₄	O ₄₄	$x, \frac{1}{2}-y, \frac{1}{2}+z$	3.25
O ₁₁	O ₂₃	$\bar{x}, \frac{1}{2}+y, \frac{1}{2}-z$	3.09
O ₃₄	O ₃₃	$\bar{x}, \bar{y}+1, \bar{z}+1$	3.28
O ₃₄	O ₄₁	$\frac{1}{2}-x, \bar{y}+1, \frac{1}{2}-z$	3.17
O ₄₄	O ₂₃	$\bar{x}, \frac{1}{2}+y, \frac{1}{2}-z$	3.10
O ₄₄	O ₂₄	$x, \frac{1}{2}-y, \frac{1}{2}+z-1$	3.25

Mean error in O-O contacts is 0.04 Å.

TABLE 26

BOND ANGLES

Atoms	Angle(°)	Atoms	Angle(°)
Co ₁ -In ₁ -Co ₂	134.5 (2)	In ₁ -Co ₂ -C ₂₁	178 (2)
Br ₁ -In ₁ -Br ₃	98.3 (2)	In ₁ -Co ₂ -C ₂₂	83 (2)
Br ₁ -In ₁ -Co ₁	101.0 (2)	In ₁ -Co ₂ -C ₂₃	85 (1)
Br ₁ -In ₁ -Co ₂	106.6 (2)	In ₁ -Co ₂ -C ₂₄	83 (1)
Br ₃ -In ₁ -Co ₁	102.5 (2)	C ₂₁ -Co ₂ -C ₂₂	99 (2)
Br ₃ -In ₁ -Co ₂	108.4 (2)	C ₂₁ -Co ₂ -C ₂₃	94 (2)
		C ₂₁ -Co ₂ -C ₂₄	95 (2)
Co ₁ -In ₂ -Co ₃	129.0 (2)	C ₂₂ -Co ₂ -C ₂₃	118 (2)
Br ₁ -In ₂ -Br ₂	94.8 (2)	C ₂₃ -Co ₂ -C ₂₄	118 (2)
Br ₁ -In ₂ -Co ₁	102.1 (2)	C ₂₄ -Co ₂ -C ₂₂	120 (2)
Br ₁ -In ₂ -Co ₃	114.9 (2)		
Br ₂ -In ₂ -Co ₁	101.5 (2)	In ₂ -Co ₃ -C ₃₁	177 (1)
Br ₂ -In ₂ -Co ₃	108.8 (2)	In ₂ -Co ₃ -C ₃₂	84 (1)
		In ₂ -Co ₃ -C ₃₃	84 (1)
Co ₁ -In ₃ -Co ₄	132.6 (2)	In ₂ -Co ₃ -C ₃₄	84 (2)
Br ₂ -In ₃ -Br ₃	92.6 (2)	C ₃₁ -Co ₃ -C ₃₂	99 (2)
Br ₂ -In ₃ -Co ₁	102.2 (2)	C ₃₁ -Co ₃ -C ₃₃	93 (2)
Br ₂ -In ₃ -Co ₄	109.3 (2)	C ₃₁ -Co ₃ -C ₃₄	97 (2)
Br ₃ -In ₃ -Co ₁	102.6 (2)	C ₃₂ -Co ₃ -C ₃₃	118 (2)
Br ₃ -In ₃ -Co ₄	110.2 (2)	C ₃₃ -Co ₃ -C ₃₄	125 (2)
		C ₃₄ -Co ₃ -C ₃₂	114 (2)
In ₁ -Br ₁ -In ₂	75.0 (1)		
In ₂ -Br ₂ -In ₃	76.0 (1)		
In ₃ -Br ₃ -In ₁	74.5 (1)		

Table 26 cont'd.

Atoms	Angle	Atoms	Angle
In ₁ -Co ₁ -In ₂	79.9 (2)	In ₃ -Co ₄ -C ₄₁	178 (2)
In ₂ -Co ₁ -In ₃	79.9 (2)	In ₃ -Co ₄ -C ₄₂	83 (2)
In ₃ -Co ₁ -In ₁	79 (1)	In ₃ -Co ₄ -C ₄₃	84 (2)
In ₁ -Co ₁ -C ₁₁	162 (2)	In ₃ -Co ₄ -C ₄₄	84 (2)
In ₁ -Co ₁ -C ₁₂	91 (1)	C ₄₁ -Co ₄ -C ₄₂	98 (2)
In ₁ -Co ₁ -C ₁₃	88 (1)	C ₄₁ -Co ₄ -C ₄₃	94 (2)
In ₂ -Co ₁ -C ₁₁	84 (2)	C ₄₁ -Co ₄ -C ₄₄	97 (2)
In ₂ -Co ₁ -C ₁₂	168 (1)	C ₄₂ -Co ₄ -C ₄₃	120 (2)
In ₂ -Co ₁ -C ₁₃	88 (2)	C ₄₃ -Co ₄ -C ₄₄	119 (2)
In ₃ -Co ₁ -C ₁₁	89 (1)	C ₄₄ -Co ₄ -C ₄₂	117 (2)
In ₃ -Co ₁ -C ₁₂	90 (1)		
In ₃ -Co ₁ -C ₁₃	164 (1)		
C ₁₁ -Co ₁ -C ₁₂	103 (2)		
C ₁₂ -Co ₁ -C ₁₃	100 (2)		
C ₁₃ -Co ₁ -C ₁₁	101 (2)		
<u>Co-C=O Angles</u>			
Co ₁ -C ₁₁ -O ₁₁	178 (4)	Co ₃ -C ₃₁ -O ₃₁	176 (4)
Co ₁ -C ₁₂ -O ₁₂	178 (4)	Co ₃ -C ₃₂ -O ₃₂	172 (4)
Co ₁ -C ₁₃ -O ₁₃	175 (3)	Co ₃ -C ₃₃ -O ₃₃	173 (4)
Co ₂ -C ₂₁ -O ₂₁	178 (5)	Co ₃ -C ₃₄ -O ₃₄	175 (5)
Co ₂ -C ₂₂ -O ₂₂	173 (5)	Co ₄ -C ₄₁ -O ₄₁	175 (5)
Co ₂ -C ₂₃ -O ₂₃	179 (4)	Co ₄ -C ₄₂ -O ₄₂	180 (5)
Co ₂ -C ₂₄ -O ₂₄	174 (4)	Co ₄ -C ₄₃ -O ₄₃	172 (5)
		Co ₄ -C ₄₄ -O ₄₄	175 (5)

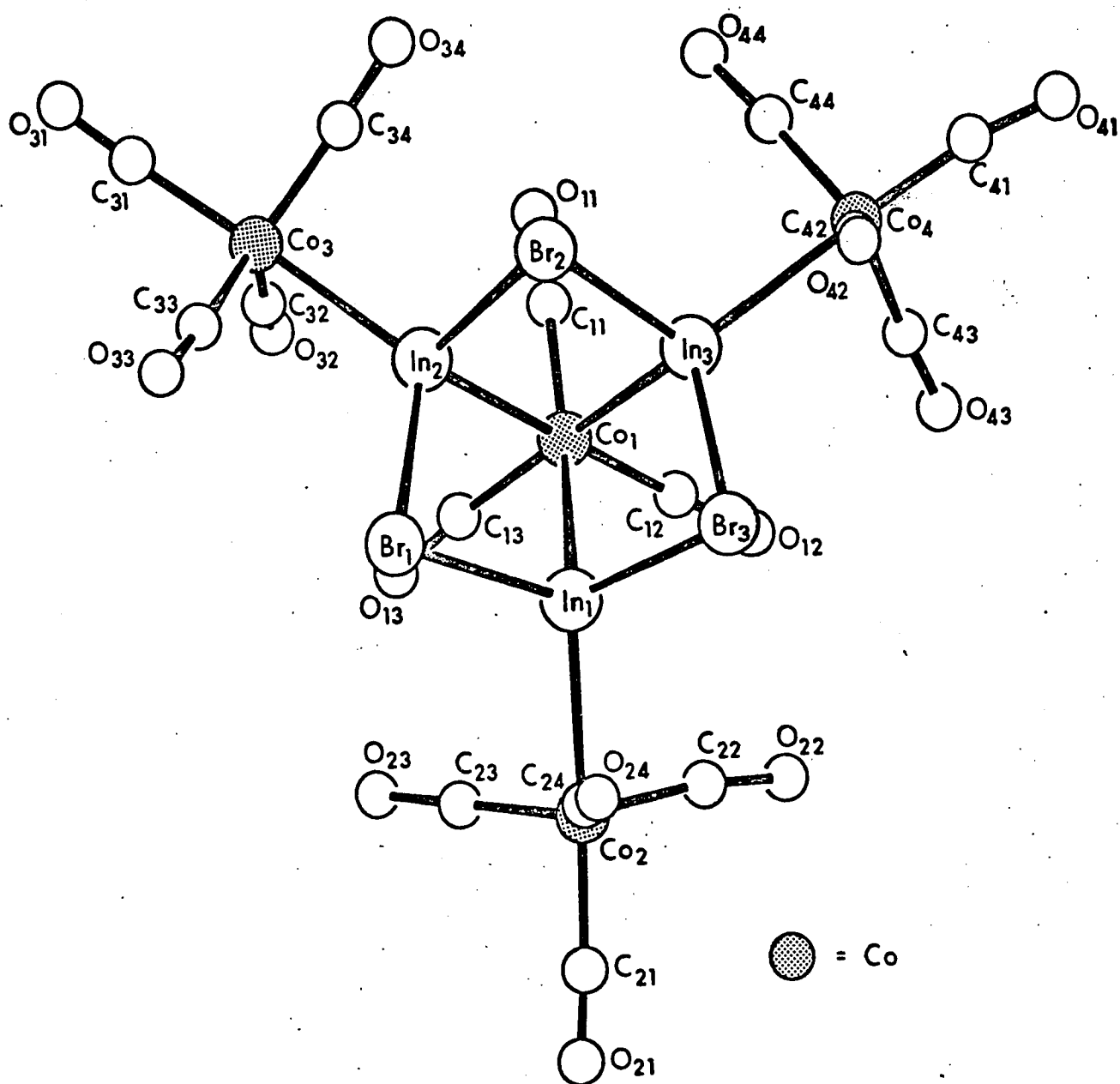


Fig. 19. Numbering scheme.

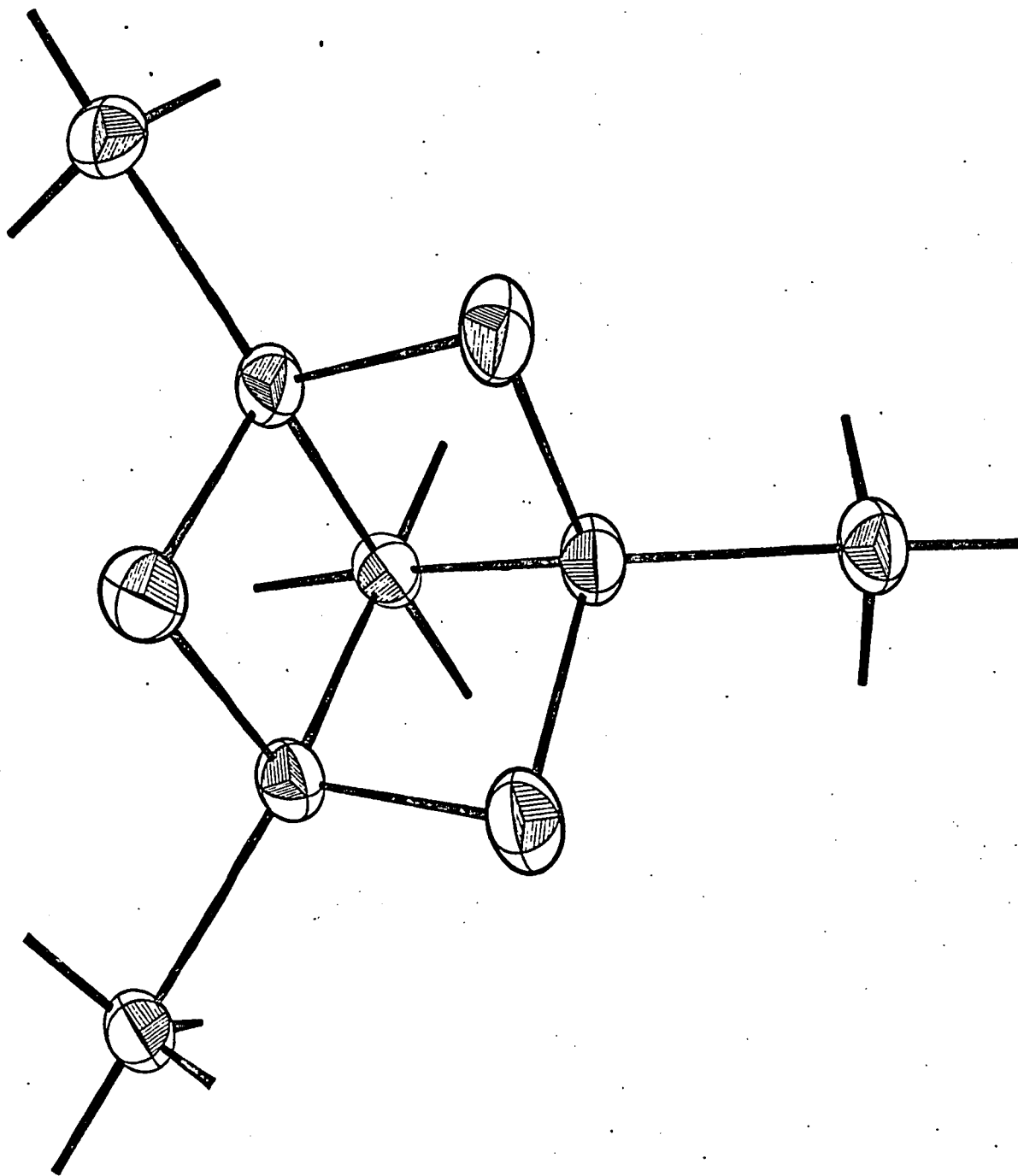


Fig. 20. Thermal ellipsoids for heavy atoms.

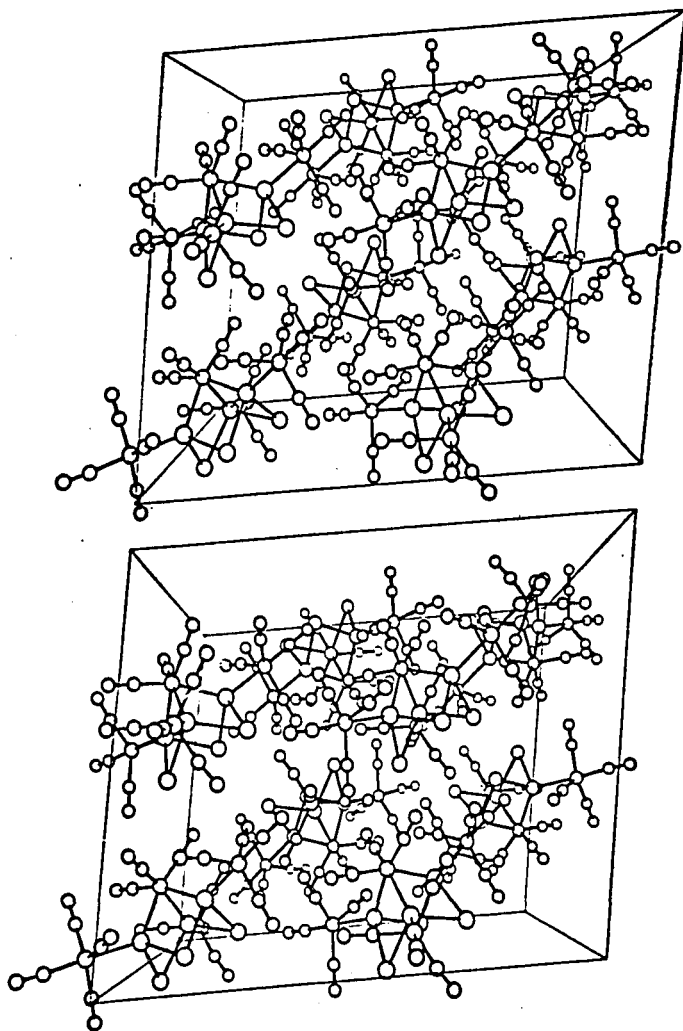


Fig. 21. Molecular packing

Discussion

The indium atoms are tetrahedral; each is bonded to two bromine atoms, a terminal cobalt tetracarbonyl and the triply bridging unique cobalt atom Co_1 . This cobalt atom is octahedral having three bonds to the indium atoms and three to carbonyl groups. The bromine atoms bridge pairs of indium atoms and lie on the opposite side of the indium plane, to the unique cobalt atom. The indium-indium distances are 3.346 \AA , 3.292 \AA , 3.356 \AA which are sufficiently greater than twice the indium covalent radius of 1.42 \AA (estimated from the indium-bromine bond in In_2Br_6 (92, 93)) to indicate the absence of any indium-indium bonding interaction. Each cobalt atom gains the krypton electron configuration i.e. cobalt has $27 e^-$ and thus requires $9 e^-$ in order to complete the third shell. The bridging cobalt receives $6 e^-$ from the carbonyl groups and three from the indium atoms, whereas the terminal cobalt receives $8 e^-$ from the carbonyls and $1 e^-$ from an indium atom. Each bromine atom contributes $3 e^-$ to the indium-bromine-indium bridges whereas the indium atoms contribute only $1 e^-$ to one of the two bridges in which it is involved. Each indium can now receive three electrons from these bridges and these with two electrons from two cobalt atoms give the indium atoms the xenon electron configuration.

The bond angles about the indium atoms are approximately 109° with two obvious exceptions: the bromine-indium-bromine and the cobalt-indium-cobalt angles are $\sim 94^\circ$ and $\sim 132^\circ$ respectively. These values suggest that the indium-bromine bonds have greater p character whereas the indium-cobalt bonds have greater s character, implying unequal mixing of these indium orbitals in forming hybrid orbitals. This is only possibly true since the requirements of the structure probably impose other restrictions upon the angles at the indium atoms. The trend, however, is in the right direction. The difference in sp character of the indium hybrids should also affect the bond lengths of the indium bonds (94): the bonds with greater s character will be shortened, those with greater p character i.e. those to the more electronegative element, will be longer. The average value of the indium-cobalt bonds is 2.58 \AA and there are two significant deviations from this value: $\text{In}_1\text{-Co}_2$ and $\text{In}_2\text{-Co}_1$ which are 2.532 \AA and 2.637 \AA respectively, corresponding to a deviation of 10σ . The average value is somewhat shorter than the sum of the covalent radii for the constituent atoms i.e. the covalent radius for indium (estimated from the indium-bromine bond in In_2Br_6 (92, 93)), is 1.42 \AA and

if that of cobalt is taken as 1.23 \AA (estimated from the cobalt-cobalt bond of 2.45 \AA in $\text{Co}_2(\text{CO})_4(\text{C}_2\text{H}_5\text{Bu}^t)_3$ which does not have carbonyl bridges (91)), then the expected indium-cobalt bond would be 2.65 \AA . A bond between these atoms has not been previously observed so that direct comparison cannot be drawn from the literature. The average value of the indium-bromine bonds is 2.727 \AA and once again there are only two significant deviations from this figure: the bonds $\text{In}_1\text{-Br}_1$ of 2.800 \AA and $\text{In}_2\text{-Br}_1$ of 2.696 \AA represent deviations of 12σ and 6σ respectively from the average value. It seems significant that the bonds that show deviations from the average values are associated with the same indium atoms: In_1 , In_2 , so that the distortion in the bromine and cobalt bonds are probably related, although there does not seem to be any reason to account for them. The average value of the indium-bromine bonds is considerably larger than the value for this bond observed in In_2Br_6 (92, 93) of 2.56 \AA . The lengthening of these bonds is most likely due to bromine-bromine interactions within one molecule, as the average value for this distance is 3.96 \AA which is close to twice the Van der Waals radius for bromine (3.90 \AA). The non-bonded distances between the bromine atoms and the

carbonyls on Co_1 (4.3 \AA to the carbon atoms and 4.7 \AA to the oxygen atoms) are much greater than the sum of the Van der Waals radii of the atoms involved (3.35 \AA), so clearly the positions of the bromine atoms are defined principally by the bond angle requirements of the indium atoms and the bromine-bromine interactions.

There are two orientations for the terminal cobalt tetracarbonyl groups attached to the indium atoms i.e. the $\text{Co}_2\text{-C}_{24}$ and $\text{Co}_4\text{-C}_{42}$ bonds are approximately parallel to the normal to the plane of the indium atoms (the angles between this normal and these bonds are 4.4° and 5.1° respectively), whereas the angle between the $\text{Co}_3\text{-C}_{33}$ bond and the indium plane normal is 42.5° . There are no short intramolecular contacts between any of the carbonyl atoms on the three terminal cobalt atoms and the carbonyls on Co_1 (the shortest contact, $\text{O}_{13}\text{-O}_{23}$ is 3.06 \AA and the Van der Waals contact is 2.8 \AA), hence the orientation of these groups about the indium-cobalt bonds must be defined by packing requirements of the molecule.

It is usually observed in molecules involving the bipyramidal groups $\text{Co}(\text{CO})_4$ and $\text{Mn}(\text{CO})_5$ (83) that the equatorial carbonyls are inclined toward the atom to which these groups are bonded, by about $5^\circ\text{-}7^\circ$.

This effect is observed in the present structure where the appropriate indium-cobalt-carbon angles range from 83° to 85° . The fact that there are nine of these angles in the present structure and the values observed are very consistent, suggests that intermolecular contacts are not responsible. Repulsion between the equatorial and the axial carbonyls and between the equatorial carbonyls and the indium atom are probably contributing to this bending. It appears from comparison of compounds in which bending is observed of comparable magnitude e.g. $\text{HMn}(\text{CO})_5$, (84); $\text{Co}(\text{SiCl}_3)(\text{CO})_4$, (90); $\text{HgCo}_8(\text{CO})_8$, (82) that the former effect is the more important, and in the present structure the average carbon-carbon contact is 2.85 \AA whereas the indium equatorial carbon distance is approximately 3 \AA , considerably shorter than the sum of the Van der Waals radii for these atoms (In: 2.55 (113), C: 1.7 \AA (3)^b). If the indium-carbon contact was the more important, then there is no reason why the equatorial-axial carbon-carbon contacts could not be reduced, as contacts less than 2.4 \AA have been observed in "overcrowded" situations e.g. in $\text{bipy}(\text{CO})_3\text{BrWGeBr}_3$ (85) dithiahexane $(\text{CO})_3\text{ClWSnCH}_3\text{Cl}$ (86), and $\text{bipy}(\text{CO})_3\text{CLMoSnCH}_3\text{Cl}_2$ (87). A further contributing factor to this effect has been postulated by Bennett and Mason (88), who have shown that bending of the

magnitude observed results in a decrease in repulsions between the non-bonding orbitals of the transition metal (Mn or Co). A consequence of this will be an increase in the overlap of the π bonding orbitals between the transition metal and the axial carbonyl resulting in a decrease in the metal-carbon bond lengths. In view of the errors in these bonds in the present structure, no significant difference could be observed in the cobalt-carbon bond lengths.

PART II

(C) The Crystal and Molecular Structure of
 Tetraethylammonium dibromobistettracarbonyl
 cobalt indate(III) $(\text{InBr}_2\text{Co}_2(\text{CO})_8)^- \text{Et}_4\text{N}^+$

Experimental

The crystals of this compound were provided by Dr. D. Patmore, who has described the preparation in (50). The crystals were yellow needles with approximately square cross-section and as signs of decomposition were noticed on exposure to air for 24 hours (the surfaces turned completely black), the study crystal was sealed in a nitrogen atmosphere in a Lindemann glass capillary. The unit cell and space group were determined from precession photographs; the errors in axial lengths were estimated by the method of Patterson and Love (64). The density was measured by flotation in a solution of 1,2-dibromo ethane and carbon tetrachloride.

Crystal DataSpace Group $P2_1/n$

$$a = 17.63 \pm .02 \text{ \AA}$$

$$b = 18.56 \pm .03 \text{ \AA}$$

$$c = 16.47 \pm .02 \text{ \AA}$$

$$\beta = 104.7 \pm 0.5^\circ$$

$$d_{\text{calc}} = 2.0 \text{ gm/cm}^3 \quad (z = 8, \text{ M.W.} = 746.4)$$

$$d_{\text{obs}} = 2.05 \text{ gm/cm}^3$$

Intensity data were collected on the Pailred linear diffractometer using crystal-monochromatised $\text{MoK}\alpha$ radiation, with the crystal rotating about the needle or [b] axis; the layers $k = 0$ to $k = 11$ were collected. Each reflection was scanned for 60 secs at the rate of $1^\circ/\text{min}$ and the background was counted each side of the peak, for a total of 80 secs. Reflections were rejected on the basis of two tests: (1) $I \leq 0$ and (2) $\sigma I/I > 0.5$ (see p. 28) leaving a total of 898 observed reflections out of 2542 reflections scanned. The crystal was checked for decomposition by recounting ten zero layer reflections after the collection of each layer, but no significant decrease was observed in these intensities. The data was not corrected for absorption as the linear absorption coefficient for $\text{MoK}\alpha$ radiation was 66.4 cm^{-1} and by approximating the crystal to a cylinder, the value for μR was 0.36. The Lorentz and Polarisation corrections were applied to the data and all equivalent reflections ($0k\ell$, $0k\bar{\ell}$) were averaged.

A notable feature of the data set was the surprisingly low $\sin\theta$ 'cut-off' along all axes. The maximum $\sin\theta$ value for observed reflections was 0.3, indicating that some atoms in the structure must have large thermal vibrations to reduce the high angle scattering so markedly. This has the unfortunate

consequence of severely reducing the amount of observed data, which could be serious in a structure of this complexity: with eight molecules in a unit cell containing four general positions, there will be two molecules in the asymmetric unit or a total of 60 atoms (excluding hydrogens). Cruickshank has given a formula (46) for calculating the coordinate standard deviation of atoms which clearly shows that the lack of high $\sin\theta$ data can seriously affect the accuracy to which atoms may be positioned. This formula is:

$$\sigma = \frac{R}{\bar{s}} \cdot \left[\frac{N}{8p} \right]^{1/2}$$

where R is the expected R factor;

\bar{s} is the root-mean-square reciprocal radius for the measured reflections, $(2\sin\theta/\lambda)_{\text{r.m.s.}}$.

p is the number of unique reflections less the number of parameters determined.

N is the number of atoms of the type for which σ is being determined that are required to give the same total scattering as does the asymmetric unit, calculated at \bar{s} .

For any atom of a given structure R , N , p will be constant thus σ is inversely proportional to \bar{s} . In this structure $\bar{s} = 0.54 \text{ \AA}^{-1}$, thus if $R = 0.10$, then for the carbon atoms $\sigma = 0.06 \text{ \AA}$ which will result in rather large errors in

bond lengths involving these atoms. A further result of the lack of high $\sin\theta$ data is that the best resolution to be expected ($0.715 d_{\min}^b$, $(106)^b$) is $\sim 0.9 \text{ \AA}$ which implies that difficulty may be experienced in locating the light atoms from the Fourier maps. As these factors should not seriously affect the heavy atoms, it was decided to continue with the structural determination as the desired result was further observation of the heavy metal bonding between the atoms concerned.

Another feature of the data set was the fact that in addition to the systematic absences due to the n glide $((h0\ell), h + \ell = 2n + 1)$, reflections of the type $((h0\ell), \ell = 2n + 1)$ were noticeably weaker than the $(\ell = 2n)$ reflections. This indicates that an approximate c glide relationship exists between some atoms in the unit cell. Molecules related by the general positions of $P2_1/n$ can not fulfil this condition, thus the near c glide relates the two molecules in the asymmetric unit.

Structure Solution

A three dimensional Patterson synthesis was calculated in order to locate the heavy atom positions. The maxima were sharpened to improve definition and reduce ripples (caused by abrupt series termination) by assuming the electron density to be constricted to

a point and each atom to be at rest, whence the scattering of each atom will be invariant with $\sin\theta$. After sharpening (see p. 86) the average structure amplitudes were calculated for ranges of $\sin\theta$ ($\Delta\sin\theta = 0.09$) and found to be constant to within 15%.

There were two Harker sections on the Patterson map; (a) a line at $(x = \frac{1}{2}, z = \frac{1}{2})$ which contained all vectors between atoms related by the n glide i.e. vectors of the general form $(\frac{1}{2}, \frac{1}{2} + 2y, \frac{1}{2})$ and (b) a plane which contained all vectors between atoms related by the screw axis i.e. vectors of the form $(\frac{1}{2} + 2x, \frac{1}{2}, \frac{1}{2} + 2z)$. The Harker line showed only one large peak (which was very broad) which most likely contained vectors of the expected type due to all the heavy atoms of one anion. Because of the pseudo symmetry between the two molecules in the asymmetric unit the Harker line peaks due to the second anion will coincide with those of the first anion. If the indium atoms are at (x, y, z) and $(x, \bar{y}, \frac{1}{2} + z)$, then they will give rise to vectors on the Harker line at the positions:

$$(x, y, z) - (\frac{1}{2} + x, \frac{1}{2} - y, \frac{1}{2} + z) = (\frac{1}{2}, \frac{1}{2} + 2y, \frac{1}{2})$$

$$\text{and } (x, \bar{y}, \frac{1}{2} + z) - (\frac{1}{2} + x, \frac{1}{2} + y, z) = (\frac{1}{2}, \frac{1}{2} - 2y, \frac{1}{2})$$

and because of the mirror plane at $y = \frac{1}{2}$ (symmetry of the Patterson space group $P2/m$), these vectors will coincide.

The Harker plane showed eleven large vectors two of which were clearly dominant and therefore were considered in the first instance to be indium-indium vectors. Subsequent analysis proved this solution to be false, however, as no cross-vectors could be found between the indium atoms deduced from these Harker vectors, which, therefore must be due to superposed light atom Harker vectors or cross-vectors. In view of the near certainty that the heavy atoms would be tetrahedrally arranged about the indium atom, the vector space within about 3 Å from the origin was searched in the hope of finding the two superposed images of the anions. These images should be clearly visible as the vectors concerned are cross-vectors from the bromine and cobalt atoms to the indium atom. All vectors close to the origin were plotted on a three dimensional model which, when completed, showed only a single tetrahedron (with its centrosymmetrically related image) orientated in such a way that a mirror symmetry element of the tetrahedron was perpendicular to the [b] axis. This then must be the orientation of both asymmetric anions in the unit cell. The identification of these intramolecular vectors can often lead to the positioning of the molecules in the unit cell from consideration of the Harker plane: two atoms at

$(x_1, y_1, z_1), (x_2, y_2, z_2)$ will give rise to vectors on the Harker plane at $((\frac{1}{2} - x, \frac{1}{2} + y, \frac{1}{2} - z) - (x, y, z))$ i.e. $(\frac{1}{2} - 2x_1, \frac{1}{2}, \frac{1}{2} - 2z_1), (\frac{1}{2} - 2x_2, \frac{1}{2}, \frac{1}{2} - 2z_2)$. The difference between the Harker vectors is $2(x_2 - x_1), 0, 2(z_2 - z_1)$ which is effectively a double scale projection of the intramolecular vector between the original atoms $(x_2 - x_1), (y_2 - y_1), (z_2 - z_1)$ onto the section $y = \frac{1}{2}$. As the arrangement of intramolecular vectors about the origin is tetrahedral, it follows that the double scale intramolecular vectors on the Harker plane will form a "projected" tetrahedron about the indium Harker vector. Thus the Harker plane can be searched to find pairs of vectors that bear the above relationship to each of the observed intramolecular vectors. The solution of the structure was attempted in this way and because of the fairly large number of peaks on the Harker section several reasonable models were found. An efficient method of checking the validity of any model is by the superposition procedure described in Appendix C and this was the method used to check possible models: if a superposition is done using one of the atoms of a possible model, and if this model is correct i.e. all cross-vectors between the atoms exist in the Patterson synthesis then peaks corresponding to atoms of

this model will remain after superposition. Tetrahedral models found from the Harker section analysis were tested in this manner but most were rejected as the original tetrahedral atoms did not remain after superposition and in the instances when they remained, the second tetrahedron was not visible. One model did produce a satisfactory result, however, and the two anions were then refined by full matrix least squares (33) from an R factor ($\sum ||F_o| - |F_c|| / \sum |F_o|$) of 0.50 to 0.32. Further refinement by least squares or Fourier synthesis methods was not possible, and this model was reluctantly discarded as a false solution. A systematic analysis of the eleven large Harker peaks was now undertaken: each vector considered was assumed to be a true Harker vector and all cross-vectors were generated between the atom positions deduced from these Harker vectors, in the hope that the heavy atoms would become apparent from the number of larger cross-vectors found from the Patterson synthesis. The result of this analysis showed that the seventh largest Harker peak did indeed have a larger number of cross-vectors than any other atom, although the (projected) tetrahedral pattern of Harker vectors expected on the basis of the intramolecular vectors could not be found. Despite the conflicting evidence, the atom derived from this Harker

vector was used in the superposition procedure, which showed rather unexpectedly two tetrahedra; this seemingly insignificant Harker vector was actually due to the approximate superposition of the Harker vectors of both indium atoms! The anions found from the superposition were then refined by full matrix least squares from an R factor of 0.45 to one of 0.22, at which stage a difference Fourier was calculated in order to position the light atoms. The arrangement of the carbonyl atoms indicated that the assignment of one bromine atom and one cobalt atom on the second anion should be reversed. This error could be clearly seen from the position of the light atom peaks, despite the fact that the actual geometry of the carbonyl peaks about the cobalt atoms showed rather unexpected distortions for this anion e.g. the plane of the equatorial carbonyl groups was not normal to the indium-cobalt bond for one cobalt atom, and often the Co-C-O bond was far from linear. These distortions are almost certainly due to the resolution problem which was expected in the positioning of the light atoms. The carbonyls of the first anion (In_1) did not show any marked distortion from the expected geometry thus these atoms were included in the refinement resulting

in a drop in R factor to 0.18. The difference Fourier synthesis calculated at this stage still showed the same distortions for the second anion carbonyl atoms, thus these atoms were included (at their observed positions) in the refinement and the R factor dropped to 0.15. A difference Fourier synthesis was now calculated to locate the two cations and to observe how well the scattering from the carbonyl atoms had been accounted for. A marked feature of this Fourier was the fact that all heavy atoms showed the characteristic features of uncorrected anisotropic motion i.e. four alternating negative-positive regions about the atom position (106)^a. However, the assumption of anisotropic thermal motion for the heavy atoms was not considered justifiable in view of the quantity of observed data (the number of degrees of freedom will be reduced by 50 which will result in greater errors in atomic coordinates). The cation peaks were badly resolved in this Fourier map, thus considerable difficulty was experienced when positioning these atoms. When both cations had been found with reasonable (but by no means ideal) geometry, they were included in the least squares refinement. All such refinements to this point had included the observed reflections with unit weights, but now it was felt that the inclusion of the unobserved

data, appropriately down weighted, might result in better placing of the light atoms i.e. the presence of unobserved reflections can be as significant as the presence of observed reflections (100); the number of data is greatly increased in the present situation thus lower errors in the positioning of the atoms should result (Cruickshanks' formula predicts $\sigma_c = 0.03$). The unobserved reflections were initially given the values and standard deviations recommended by Hamilton (100) i.e.

$I_u = I_{\min}/3$, $\sigma_u^2 = 4I_{\min}^2/45$ (I_{\min} was estimated from the local background for each reflection) and the observed

reflections were now weighted according to the function: $\sigma = (T + t^2_B + (kI)^2)^{1/2}$ (95) where k was assigned the arbitrary value of 0.03. The purpose of adding a fixed percentage of the intensity to $\sigma I (= (T + t^2_B)^{1/2})$ is to account for machine instability which can be critical when counting large intensities.

The full matrix least squares refinement proceeded slowly to an R factor of 0.12 when it was noticed that the geometry involving some of the light atoms was unreasonable. Thus the atoms at fault were shifted to more sensible positions (although little justification for this was observed in the difference Fourier synthesis) and the unobserved reflections were further down-weighted by 25%. The refinement was thus continued and when convergence was reached, the R factor for the observed reflections had dropped to 0.113, although most of the

"readjusted" atoms had regained their original positions. The overall R factor (including unobserved data) was 0.257 and the weighted R factors ($R_w = \Sigma w ||F_o| - |F_c||^2 / \Sigma w |F_o|^2$)^{1/2} including and excluding the unobserved reflections were 0.109 and 0.088 respectively. When absolute weights are used the criterion which should be achieved is that the quantity representing the standard deviation of a reflection of unit weight, $(\Sigma w ||F_o| - |F_c|| / (n-m))^{1/2}$ has the value unity; at convergence this value was 1.140 indicating that the weighting scheme was adequate to give meaningful least squares refinement.

Results

The final atomic coordinates and isotropic temperature factors are listed in Table 28, Fig. 22 shows the anion and cations with the numbering scheme used (the carbon atoms directly attached to the nitrogen atoms in the cations are labelled NCX); the packing in the unit cell is shown in the stereoscopic diagram Fig. 23. Bond lengths and angles are given in Table 29 and 30. The final structure factors are shown in Table 32 in which unobserved reflections are marked with an asterisk. This table shows that several reflections

TABLE 28

FINAL ATOMIC COORDINATES AND TEMPERATURE FACTORS (\AA^2)

Atom	x	y	z	B
In ₁	0.4755(3)	0.4604(3)	0.7324(3)	4.5(2)
Br ₁	0.5301(4)	0.4754(4)	0.8910(5)	6.5(2)
Br ₂	0.3563(5)	0.3794(4)	0.7202(5)	6.8(3)
Co ₁	0.4268(6)	0.5852(6)	0.6652(7)	6.3(3)
Co ₂	0.5805(7)	0.3812(7)	0.6882(8)	6.9(3)
In ₂	0.5017(3)	0.0721(3)	0.2339(3)	4.6(2)
Br ₁₁	0.5851(4)	0.0535(4)	0.3849(5)	6.7(2)
Br ₁₂	0.4382(7)	0.1942(5)	0.2448(5)	8.0(3)
Co ₁₁	0.5960(6)	0.0911(5)	0.1369(6)	4.9(3)
Co ₁₂	0.3921(9)	-0.0228(8)	0.2001(8)	5.8(3)
O ₂₁	0.538(3)	0.274(3)	0.785(3)	10(2)
C ₂₁	0.560(5)	0.331(6)	0.763(6)	14(3)
O ₂₂	0.684(4)	0.483(3)	0.780(4)	13(2)
C ₂₂	0.647(7)	0.438(7)	0.717(7)	17(4)
O ₂₃	0.703(6)	0.302(5)	0.638(6)	22(4)
C ₂₃	0.654(8)	0.303(7)	0.643(8)	20(6)
O ₂₄	0.482(4)	0.405(4)	0.531(5)	16(2)
C ₂₄	0.534(6)	0.403(5)	0.602(7)	12(3)
O ₁₁	0.388(3)	0.717(4)	0.600(4)	13(3)
C ₁₁	0.395(4)	0.664(5)	0.611(4)	5(2)

Table 28 cont'd.

Atom	x	y	z	B
O ₁₂	0.356(3)	0.595(3)	0.803(4)	11(2)
C ₁₂	0.378(5)	0.594(4)	0.741(6)	9(3)
O ₁₃	0.589(3)	0.612(2)	0.698(3)	7(2)
C ₁₃	0.524(5)	0.609(4)	0.696(4)	6(2)
O ₁₄	0.330(3)	0.492(3)	0.532(3)	11(2)
C ₁₄	0.379(3)	0.534(3)	0.575(3)	3(2)
O ₁₁₁	0.681(3)	0.130(3)	0.022(4)	8(2)
C ₁₁₁	0.659(4)	0.104(4)	0.078(5)	8(2)
O ₁₁₂	0.643(3)	0.221(3)	0.244(4)	12(2)
C ₁₁₂	0.629(3)	0.170(4)	0.207(4)	4(2)
O ₁₁₃	0.675(3)	-0.035(3)	0.209(3)	8(2)
C ₁₁₃	0.638(4)	0.020(4)	0.173(4)	6(2)
O ₁₁₄	0.455(2)	0.081(2)	0.010(3)	7(1)
C ₁₁₄	0.511(5)	0.092(4)	0.075(5)	9(2)
O ₁₂₁	0.394(4)	-0.001(3)	0.361(4)	12(2)
C ₁₂₁	0.369(10)	0.003(10)	0.294(13)	29(9)
O ₁₂₂	0.508(3)	-0.107(3)	0.161(3)	10(2)
C ₁₂₂	0.454(5)	-0.072(5)	0.180(4)	8(2)
O ₁₂₃	0.274(3)	-0.134(3)	0.169(3)	9(2)
C ₁₂₃	0.332(7)	-0.087(7)	0.198(7)	17(4)
O ₁₂₄	0.301(3)	0.077(3)	0.085(3)	7(1)
C ₁₂₄	0.344(4)	0.034(5)	0.140(5)	8(2)

Table 28 cont'd.

Atom	x	y	z	B
N ₁	0.352(4)	0.171(4)	0.510(4)	7(2)
NC ₁	0.421(6)	0.136(5)	0.515(5)	10(3)
NC ₂	0.292(5)	0.121(4)	0.496(4)	7(2)
NC ₃	0.347(7)	0.224(9)	0.588(10)	27(6)
NC ₄	0.367(7)	0.272(8)	0.456(9)	25(5)
C ₁	0.494(6)	0.175(6)	0.517(6)	15(4)
C ₂	0.206(4)	0.151(4)	0.501(4)	6(2)
C ₃	0.366(5)	0.163(5)	0.659(5)	11(3)
C ₄	0.301(5)	0.200(5)	0.385(6)	14(3)
N ₂	0.344(3)	0.325(3)	0.977(3)	3(1)
NC ₅	0.322(4)	0.248(4)	0.987(4)	7(2)
NC ₆	0.278(4)	0.366(4)	0.920(4)	7(2)
NC ₇	0.351(3)	0.352(3)	1.075(3)	4(2)
NC ₈	0.429(3)	0.335(3)	0.956(3)	3(2)
C ₅	0.318(3)	0.210(3)	0.892(3)	4(2)
C ₆	0.304(3)	0.448(3)	0.934(3)	3(1)
C ₇	0.268(4)	0.354(4)	1.090(4)	8(2)
C ₈	0.493(4)	0.291(4)	1.047(4)	8(2)

TABLE 29
INTRAMOLECULAR DISTANCES (Å)

In ₁ -Br ₁	2.561(9)	C ₁₁ -O ₁₁	1.02(12)
In ₁ -Br ₂	2.586(10)	C ₁₂ -O ₁₂	1.18(11)
In ₁ -Co ₁	2.638(12)	C ₁₃ -O ₁₃	1.16(10)
In ₁ -Co ₂	2.644(14)	C ₁₄ -O ₁₄	1.24(8)
In ₂ -Br ₁₁	2.576(9)	C ₂₁ -O ₂₁	1.28(12)
In ₂ -Br ₁₂	2.582(10)	C ₂₂ -O ₂₂	1.43(14)
In ₂ -Co ₁₁	2.637(12)	C ₂₃ -O ₂₃	0.91(18)
In ₂ -Co ₁₂	2.596(14)	C ₂₄ -O ₂₄	1.30(14)
		C ₁₁₁ -O ₁₁₁	1.16(10)
Co ₁ -C ₁₁	1.75(8)	C ₁₁₂ -O ₁₁₂	1.13(9)
Co ₁ -C ₁₂	1.71(9)	C ₁₁₃ -O ₁₁₃	1.27(9)
Co ₁ -C ₁₃	1.74(8)	C ₁₁₄ -O ₁₁₄	1.28(10)
Co ₁ -C ₁₄	1.80(5)	C ₁₂₁ -O ₁₂₁	1.09(22)
Co ₂ -C ₂₁	1.67(10)	C ₁₂₂ -O ₁₂₂	1.29(11)
Co ₂ -C ₂₂	1.46(13)	C ₁₂₃ -O ₁₂₃	1.36(14)
Co ₂ -C ₂₃	2.22(14)	C ₁₂₄ -O ₁₂₄	1.31(10)
Co ₂ -C ₂₄	1.50(12)		
Co ₁₁ -C ₁₁₁	1.69(8)		
Co ₁₁ -C ₁₁₂	1.87(7)		
Co ₁₁ -C ₁₁₃	1.58(8)		
Co ₁₁ -C ₁₁₄	1.60(9)		
Co ₁₂ -C ₁₂₁	1.74(21)		
Co ₁₂ -C ₁₂₂	1.54(9)		
Co ₁₂ -C ₁₂₃	1.61(13)		
Co ₁₂ -C ₁₂₄	1.58(8)		

Table 29 cont'd.

N_1-NC_1	1.39 (12)	N_2-NC_5	1.52 (9)
N_1-NC_2	1.40 (10)	N_2-NC_6	1.52 (9)
N_1-NC_3	1.66 (17)	N_2-NC_7	1.67 (7)
N_1-NC_4	2.14 (16)	N_2-NC_8	1.53 (8)
NC_1-C_1	2.52 (13)	NC_5-C_5	1.70 (8)
NC_2-C_2	1.66 (11)	NC_6-C_6	1.61 (9)
NC_3-C_3	1.61 (19)	NC_7-C_7	1.58 (10)
NC_4-C_4	2.00 (17)	NC_8-C_8	1.65 (9)

TABLE 30
BOND ANGLES

Atoms	Angle (°)	Atoms	Angle (°)
Br ₁ -In ₁ -Br ₂	103.5 (3)	In ₂ -Co ₁₁ -C ₁₁₃	89 (3)
Co ₁ -In ₁ -Co ₂	124.3 (4)	In ₂ -Co ₁₁ -C ₁₁₄	75 (3)
Br ₁ -In ₁ -Co ₁	109.2 (4)	In ₂ -Co ₁₂ -C ₁₂₁	89 (7)
Br ₁ -In ₁ -Co ₂	103.4 (4)	In ₂ -Co ₁₂ -C ₁₂₂	85 (3)
Br ₂ -In ₁ -Co ₁	108.0 (4)	In ₂ -Co ₁₂ -C ₁₂₃	171 (4)
Br ₂ -In ₁ -Co ₂	106.5 (4)	In ₂ -Co ₁₂ -C ₁₂₄	86 (3)
Br ₁₁ -In ₂ -Br ₁₂	102.1 (3)		
Co ₁₁ -In ₂ -Co ₁₂	122.6 (4)	Co ₁ -C ₁₁ -O ₁₁	161 (8)
Br ₁₁ -In ₂ -Co ₁₁	107.6 (3)	Co ₁ -C ₁₂ -O ₁₂	168 (8)
Br ₁₁ -In ₂ -Co ₁₂	108.7 (4)	Co ₁ -C ₁₃ -O ₁₃	161 (7)
Br ₁₂ -In ₂ -Co ₁₁	106.7 (3)	Co ₁ -C ₁₄ -O ₁₄	158 (5)
Br ₁₂ -In ₂ -Co ₁₂	107.4 (4)	Co ₂ -C ₂₁ -O ₂₁	125 (6)
		Co ₂ -C ₂₂ -O ₂₂	154 (10)
In ₁ -Co ₁ -C ₁₁	174 (3)	Co ₂ -C ₂₃ -O ₂₃	136 (13)
In ₁ -Co ₁ -C ₁₂	88 (3)	Co ₂ -C ₂₄ -O ₂₄	163 (9)
In ₁ -Co ₁ -C ₁₃	85 (3)	Co ₁₁ -C ₁₁₁ -O ₁₁₁	155 (7)
In ₁ -Co ₁ -C ₁₄	85 (2)	Co ₁₁ -C ₁₁₂ -O ₁₁₂	172 (6)
In ₁ -Co ₂ -C ₂₁	79 (3)	Co ₁₁ -C ₁₁₃ -O ₁₁₃	174 (6)
In ₁ -Co ₂ -C ₂₂	89 (5)	Co ₁₁ -C ₁₁₄ -O ₁₁₄	161 (7)
In ₁ -Co ₂ -C ₂₃	171 (4)	Co ₁₂ -C ₁₂₁ -O ₁₂₁	138 (16)
In ₁ -Co ₂ -C ₂₄	82 (4)	Co ₁₂ -C ₁₂₂ -O ₁₂₂	174 (7)
In ₂ -Co ₁₁ -C ₁₁₁	178 (3)	Co ₁₂ -C ₁₂₃ -O ₁₂₃	162 (10)
In ₂ -Co ₁₁ -C ₁₁₂	83 (2)	Co ₁₂ -C ₁₂₄ -O ₁₂₄	176 (7)

Table 30 cont'd.

Atoms	Angle (°)	Atoms	(Angle (°))
NC ₁ -N ₁ -NC ₂	110 (7)	NC ₅ -N ₂ -NC ₆	111 (5)
NC ₁ -N ₁ -NC ₃	119 (8)	NC ₅ -N ₂ -NC ₇	98 (4)
NC ₁ -N ₁ -NC ₄	104 (6)	NC ₅ -N ₂ -NC ₈	114 (4)
NC ₂ -N ₁ -NC ₃	109 (7)	NC ₆ -N ₂ -NC ₇	108 (4)
NC ₂ -N ₁ -NC ₄	134 (6)	NC ₆ -N ₂ -NC ₈	123 (5)
NC ₃ -N ₁ -NC ₄	80 (7)	NC ₇ -N ₂ -NC ₈	99 (4)
N ₁ -NC ₁ -C ₁	122 (8)	N ₂ -NC ₅ -C ₅	104 (5)
N ₁ -NC ₂ -C ₂	117 (6)	N ₂ -NC ₆ -C ₆	104 (5)
N ₁ -NC ₃ -C ₃	95 (9)	N ₂ -NC ₇ -C ₇	109 (5)
N ₁ -NC ₄ -C ₄	62 (5)	N ₂ -NC ₈ -C ₈	116 (5)

TABLE 31

PSEUDO c GLIDE RELATIONSHIP

<u>Molecule 1</u>				<u>Molecule 2</u>			
Atom	x	$\frac{1}{2}-y$	$\frac{1}{2}+z$	Atom	x	y	z
In ₁	0.48	0.04	0.23	In ₂	0.50	0.07	0.23
Br ₁	0.53	0.02	0.39	Br ₁₁	0.59	0.05	0.38
Br ₂	0.36	0.12	0.22	Br ₁₂	0.44	0.19	0.25
Co ₁	0.43	-0.09	0.17	Co ₁₂	0.39	-0.02	0.20
Co ₂	0.58	0.12	0.19	Co ₁₁	0.59	0.09	0.13
N ₁	0.35	0.33	0.01	N ₂	0.34	0.33	0.98
NC ₁	0.42	0.36	0.02	NC ₈	0.43	0.34	0.96
NC ₂	0.29	0.38	0.00	NC ₆	0.28	0.37	0.92
NC ₃	0.35	0.28	0.09	NC ₇	0.35	0.35	0.07
NC ₄	0.37	0.23	0.96	NC ₅	0.32	0.25	0.98
C ₁	0.49	0.32	0.02	C ₈	0.49	0.29	0.05
C ₂	0.21	0.35	0.00	C ₇	0.27	0.35	0.09
C ₃	0.37	0.34	0.16	C ₆	0.30	0.45	0.93
C ₄	0.30	0.30	0.89	C ₅	0.32	0.21	0.89

TABLE 32

[illegible]

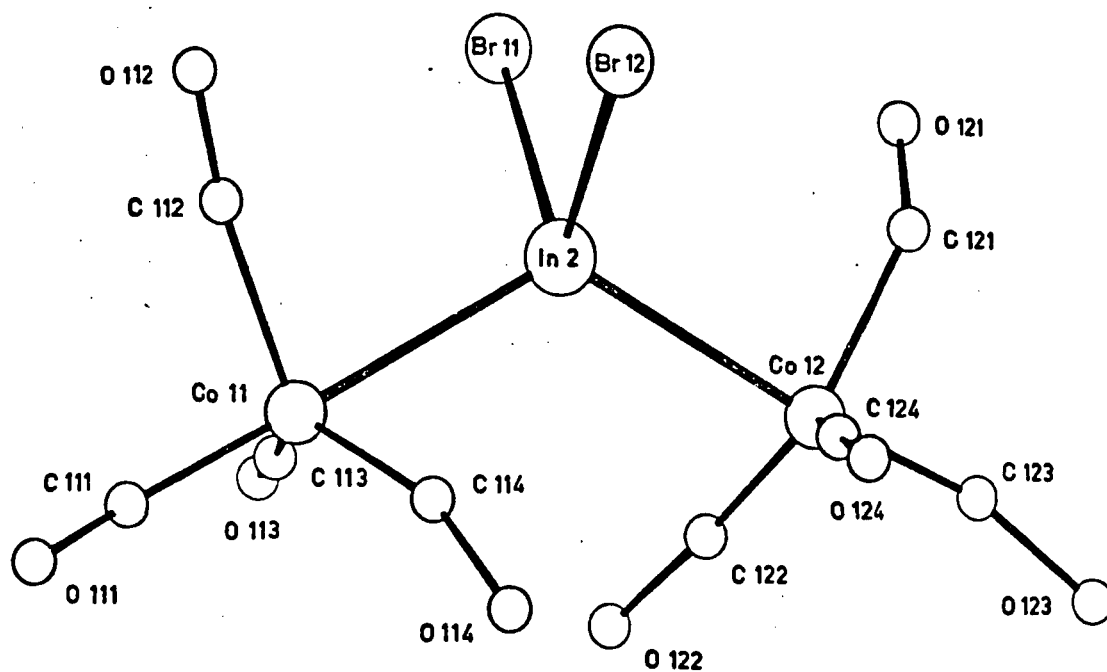
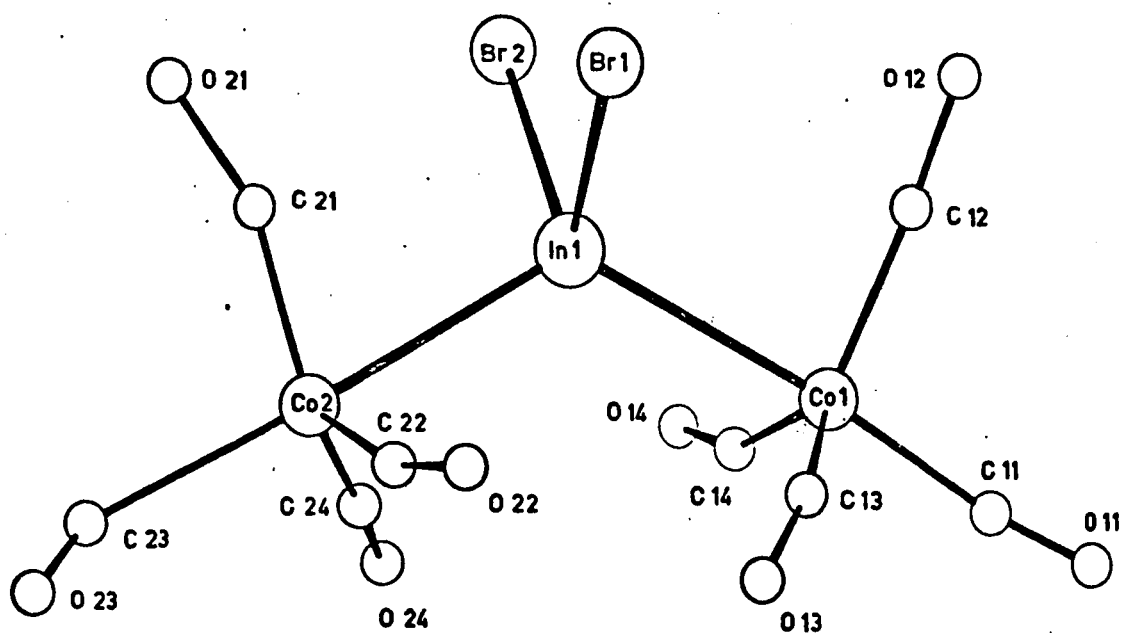
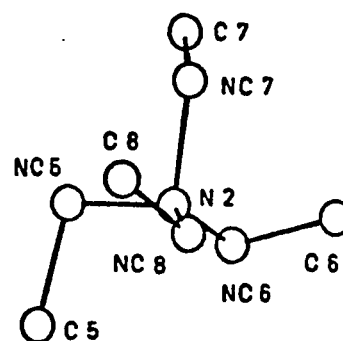
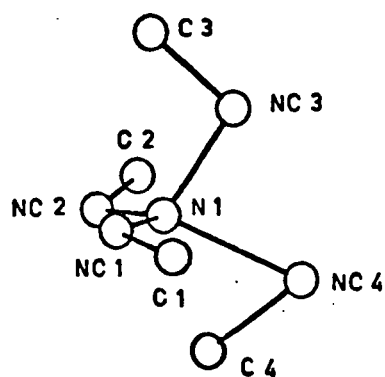


Fig. 22. Numbering scheme.



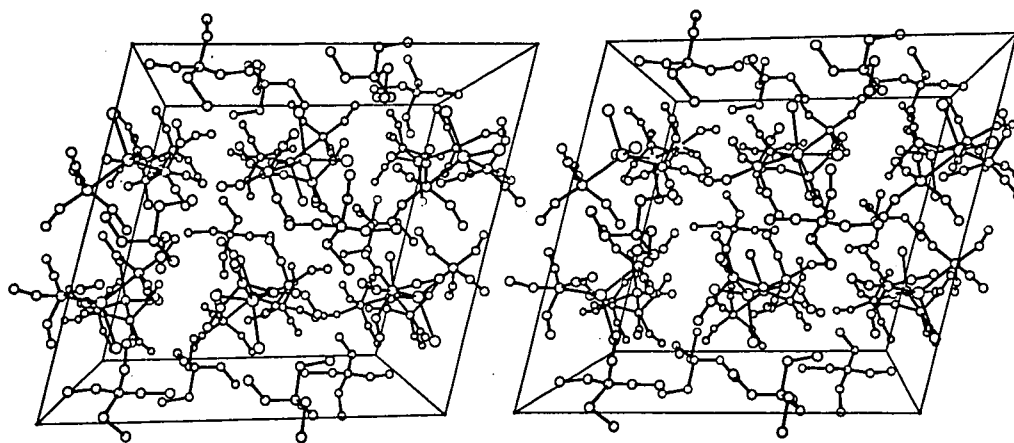


Fig. 23. Molecular packing.

have been classed as observed when they clearly calculate as unobserved; inspection of the $\sigma I/I$ values for these reflections indicate that they could have been rejected if a slightly lower limit had been taken at the initial data processing stage e.g. $\sigma I/I = 0.3$

Discussion

Molecular Geometry

The anion and cations are tetrahedral with indium and nitrogen atoms forming the centres of the tetrahedron; the anion tetrahedral angles are close to the expected value of 109° with the exception of the cobalt-indium-cobalt angles which are considerably greater at 124.2° , 122.5° . The bonding of the anion can be envisaged as three sigma bonds involving three singly occupied sp^3 hybrid orbitals of the indium atom, and one d^2sp^2 hybrid on each cobalt atom and a p orbital on one of the bromine atoms. The second bromine will then donate two electrons to the unoccupied sp^3 hybrid remaining on the indium and the electron deficiency of this bromine will be filled by charge transfer from the cation, which will have the usual NH_4^+ type bonding. This scheme localises the negative charge on one bromine atom whereas resonance no doubt occurs, the main contributors being those where the negative charge

resides on the bromine atoms because of their much greater electronegativities (Br, 2.96; In, 1.78; Co, 1.88 (89)). The negative charge will thus have little effect on the geometry by virtue of this charge dispersion. The distortion of the tetrahedral angles has been shown to be a consequence of the difference in electronegativity of the X, Y atoms in compounds of the type X_2MY_2 (102) i.e. if X is more electronegative than Y, then there will be an increase in p character of the sp^3 hybrid orbitals of M thus decreasing the X-M-X angle. Conversely the M-Y bond will contain more s character and the X-M-Y angle will be increased. Torkington (48) has deduced that for configuration of C_{2v} symmetry, the angles astride the two-fold axis (2α and 2β) are related by $\cot^2 \alpha + \cot^2 \beta = 1.0$. In the present compound, the cobalt-indium-cobalt angles of 124.3° and 122.6° imply bromine-indium-bromine angles of 99.4° and 100.2° , which are both somewhat smaller than the measured values of 103.5° and 102.1° ; the difference can probably be accounted for by steric repulsion between the carbonyl groups on the cobalt atoms. Although reasonable agreement with Torkington's theory has been observed in the present case, the molecules of the trihalides of the group III metals all show similar distortions

whereas the electronegativities of the X and Y atoms would be identical!

The average value obtained for the indium-cobalt bonds is $2.632(7) \text{ \AA}$ which is significantly greater than the value observed in $\text{In}_3\text{Br}_3\text{Co}_4(\text{CO})_{15}$ (see p.137). By the subtraction of the covalent radius of bromine (1.14 \AA) from the indium-bromine bond length in In_2Br_6 (92, 93), a value of 1.42 \AA is obtained for the covalent radius of indium. The covalent radius of cobalt can be reasonably estimated from known cobalt-cobalt bond lengths, some of which have been listed by Lewis (103); an appropriate value is 2.45 \AA (see p.138) which implies a covalent radius of 1.22 \AA for cobalt. Using this value the expected indium-cobalt bond length would be 2.64 \AA . This value is in good agreement with the value observed in the present structure, thus it is likely that the expected increase in the indium covalent radius due to the negative charge has been counteracted by the reduction in the In-Co bond length as a result of the change in hybridisation of the indium atom giving more s character to the hybrid orbital involved in bonding with the cobalt atoms. The average indium-bromine bond is $2.575(5) \text{ \AA}$ which is in reasonable agreement with the value observed in In_2Br_6 of 2.56 \AA .

Discussion of the geometry of the cations is severely handicapped by the large errors involved in positioning these atoms, although when weighted averages ($\sum w_i r_i / \sum w_i$) are taken of the equivalent bond lengths they do agree reasonably with those observed in other structures involving the same cation. The structure of $[\text{InCl}_5]^{2-} [\text{NEt}_4]^+_2$ has recently been published (104) and the average nitrogen-carbon and carbon-carbon bond lengths for the cations are: 1.53 \AA and 1.63 \AA respectively, and for the present compound the average values are: 1.57 \AA and 1.62 \AA . The errors in the individual bonds in both structures are rather large i.e. $\sim 0.1 \text{ \AA}$, which accounts for the marked deviation from the expected values of 1.48 \AA (40) and 1.54 \AA (40). The structure of $[\text{InCl}_5]^{2-} [\text{NEt}_4]^+_2$ clearly demonstrates the likelihood of disorder in the cation and this would contribute to the difficulty in placing the atoms of these groups; clearly the warning given by Lipscomb (105) as regards the triethylammonium cation viz: "... we do not recommend them as ordered positive ions in the studies of negative ions," applies equally to tetraethylammonium cations!

Molecular Packing

The heavy atoms of the two anions, and the two cations in the asymmetric unit are related by a pseudo

c glide. This relationship is demonstrated in Table 31 which lists the coordinates of molecule (1) after application of the c glide relationship, $(x, \frac{1}{2} - y, \frac{1}{2} + z)$, and compares these with the coordinates of molecule (2). This relationship between the molecules in the asymmetric unit is not rigidly maintained and this fact almost certainly contributed (along with the poor resolution inherent in the data set) to the difficulty experienced in locating the light atoms from the Fourier maps.

The ions pack in the unit cell in an electrostatically favourable manner; the shortest distances between opposite charges (assuming the charges to be centred on the indium and nitrogen atoms which may not be strictly true!) are between 5 \AA and 6.5 \AA , and between like charges: 7 \AA and 8 \AA . However, the electrostatic forces may not be the dominant packing forces as the charges on the ions would be fairly well screened by the atoms of these groups.

This crystal structure analysis demonstrates the importance of the close inspection of preliminary film data, and the manner in which this information should be interpreted in the light of the desired aims of the structural determination. The resolution of the Fourier maps can be determined as a function

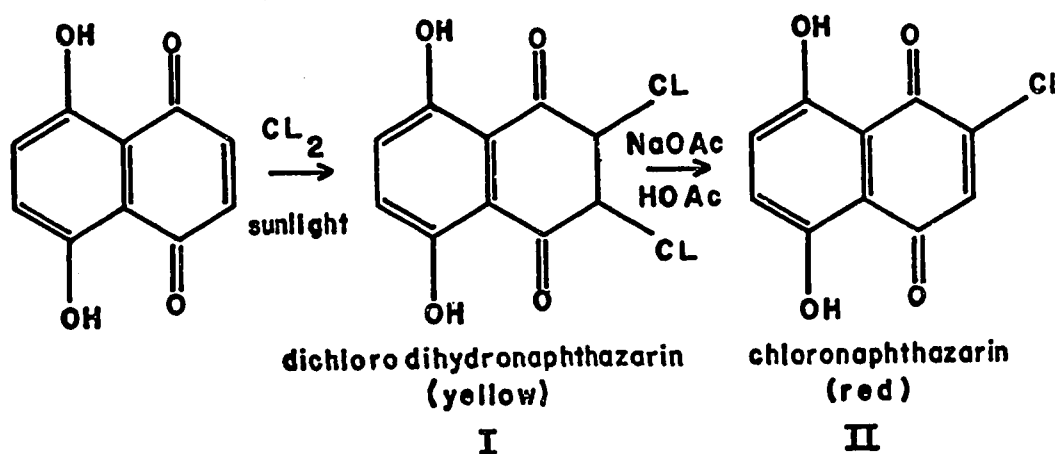
of the maximum observed $\sin\theta$ value i.e.

$r = 0.715\lambda / (2\sin\theta)(106)^b$ and if the number of parameters to be refined is large while the amount of available data is limited, as in the present structure, then the expected standard deviation in the atomic coordinates can be determined by the use of Cruickshank's formula (see p.144). If there is any doubt that the desired information will be obtained by a crystal structure determination, then these simple calculations will enable a more meaningful decision to be made.

PART III

- (A) The crystal and molecular structure of
2,5-dichloro 3,6-dihydroxy-p-benzoquinone
(chloranilic acid)

The preparation of chloronaphthazarin was undertaken as the first attempt to introduce asymmetry into the naphthazarin molecule. The use of chlorine as a substituent was a natural choice, as this atom can be used to phase the Fourier syntheses during the structure determination. Chloronaphthazarin is made from naphthazarin by the following scheme:



The preparation was carried out in the manner described by Bruce and Thomson (96) and after much recrystallisation, some small red plate-like crystals were obtained from ethanol. The analysis for chlorine

showed 29%; II requires 16% and I requires 27%, hence the crystals were assumed to be those of dichlorodihydronaphthazarin.

Experimental

A single crystal with approximate dimensions (.4 mm x .37 mm x .12 mm) was mounted about the [b] axis (contained within the plate) and rotation and Weissenberg films were taken for unit cell identification although the accurate cell dimensions quoted below were measured from precession films, the errors being estimated by the method of Patterson and Love (64). The density was measured by flotation in a solution of diiodomethane and chloroform.

Crystal data

Space Group $P2_1/n$

$$a = 7.589 \pm .005 \text{ \AA}$$

$$b = 5.537 \pm .003 \text{ \AA}$$

$$c = 8.703 \pm .006 \text{ \AA}$$

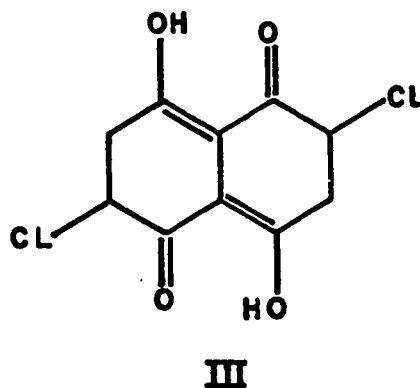
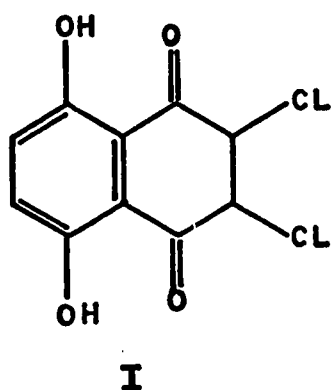
$$\beta = 104.0 \pm 0.5^\circ$$

$$d_{\text{calc}} = 2.4 \text{ gms/cm}^3 \text{ (} z = 2 \text{)}$$

$$d_{\text{obs}} = 2.01 \text{ gms/cm}^3$$

The bad agreement shown by the densities raised the first doubts as to the chemical composition of the molecule. Unfortunately too little sample was available to allow further chemical analysis or even the running

of an n.m.r. spectrum (which was attempted). The presence of two molecules in the unit cell in space group $P2_1/n$ implies that the molecules must lie on centres of symmetry which is of course impossible (excluding the possibility of disorder) for dichlorodihydronaphthazarin when formulated as I, but is possible if the molecule has the form shown below as III:



This would imply that naphthazarin had reacted in the form 1,5-dihydroxy, 4,8-naphthoquinone (naphthazarin has never been observed to react in this form!) to produce 2,3,6,7-tetrachloronaphthazarin and that partial removal of HCl had occurred. The chemistry involved, while not impossible, does not appear to be very likely and thus the space group was thoroughly checked, but this only confirmed that the assignment of $P2_1/n$ was in

fact correct. Since the solution of the structure would certainly decide the true nature of the molecule the determination was continued.

Intensity data were collected on the Pailred linear diffractometer using crystal monochromatised $\text{CuK}\alpha$ radiation and included the layers $k = 0$ to $k = 5$. The scan rate for each reflection was fixed at $1^\circ/\text{min}$ but the scan time (t_T) and the background counting time (t_B) varied with k i.e. for $k = 0$ $t_T = 2.8$ mins, $t_B = 2$ mins; for $k = 5$, $t_T = 6$ mins, $t_B = 6$ mins. The increase in the scan for the higher layers was necessary because of the broadening of the low $\sin\theta$ reflections which is a normal consequence of equi-inclination geometry. The background counting time was made approximately equal to the scan time to ensure favourable counting statistics. Data was rejected on the basis of two tests: (i) $I \leq 0$,

$$(ii) \quad \sigma I \geq 0.2$$

leaving a total of 508 reflections observed above background. In the above test, $I = T - tB$ and $\sigma I = (T + t^2 B)^{1/2}$, where T is the total count, B the total background and t is the ratio of counting times, t_T/t_B . The linear absorption coefficient for $\text{CuK}\alpha$ radiation is 67.4 cm^{-1} and the considerable variation in

path length through the flat plate, ($1.7 \leq uR \leq 5.4$) meant that a correction for absorption was necessary. Unfortunately a programme for calculating this correction was not available at this stage. Lorentz and Polarisation corrections were applied to the data and all equivalent reflections ($hk0$, $\bar{h}k0$) were averaged.

Structure Solution

A three dimensional Patterson synthesis was calculated in order to locate the chlorine atoms. The Patterson map has the same general form as those previously described for structures in space group $P2_1/n$ (e.g., see p. 87,146) i.e. there will be two Harker sections containing vectors of the general form $(\frac{1}{2} + 2x, \frac{1}{2}, \frac{1}{2} + 2z)$; $(\frac{1}{2}, \frac{1}{2} + 2y, \frac{1}{2})$. The Harker line contained one large vector which was assumed to be due to the chlorine atom and of the three large vectors observed on the Harker plane, the largest was assumed to be the chlorine Harker vector. The atomic coordinates were derived from these vectors and as the $(2x, 2y, 2z)$ vector (between chlorine atoms at (x, y, z) and $(\bar{x}, \bar{y}, \bar{z})$) was found in the expected position, these coordinates were used to calculate structure factors. The R factor $(\sum ||F_o| - |F_c|| / \sum |F_o|)$ for this calculation was 0.5 and the Fourier map phased by the chlorine atom

showed twelve peaks arranged in two concentric hexagons about the origin. This was the first clear indication that the molecule was not a derivative of naphthazarin but was in fact a fully substituted benzene derivative. A search was then made for such a compound containing approximately 30% chlorine. Chloroanilic acid (2,5-dichloro, 3,6-dihydroxy-p-benzoquinone), which contains 34% chlorine, was chosen as the most likely compound although the chlorine analysis is in error by 5%. Assuming this to be the true compound, the calculated density is now 1.97 gm/cm^3 which now agrees favourably with the observed density of 2.01 gm/cm^3 . The linear absorption coefficient is increased to 82.8 cm^{-1} and the range of μR is now: $2.1 \leq \mu R \leq 6.6$. All atoms were positioned from the heavy atom Fourier map and structure factors were calculated assuming individual isotropic temperature factors for each atom; the R factor for this calculation was 0.31. A Fourier synthesis, using the phased F_{obs} values as coefficients, showed the atoms to be positioned satisfactorily i.e. all atoms were observed to be on large peaks and no extraneous peaks were visible. All positional and thermal parameters were now refined by full matrix least squares to an R factor of 0.18. Although it was fully realised that the refinement of a

model, in which the atoms are allowed to vibrate with anisotropic motion, is not justified when systematic errors are present in the data, it was decided to continue the refinement in this manner to observe the effects of the absorption errors on the model. Up to this stage the observations were all given unit weights in the least squares procedure; for the anisotropic refinement, however, weights were calculated from the expression $(w)^{1/2} = 1/(1 + [(F_o - b)/a]^2)^{1/2}$ where a and b were given the values 5, 7.5 e^- respectively. Eight low $\sin\theta$ reflections clearly suffering from effects of secondary extinction (see p. 29) were removed from the data set. At the convergence of the anisotropic refinement the R factor was 0.087 and the observed and calculated structure factors were used, at this stage, to calculate a difference Fourier map through the plane of the molecule (using FORDAP (55)) in order to locate the hydrogen atom. This difference Fourier map is shown in Fig. 26 and the effect of uncorrected absorption is clearly visible. The large peaks on either side of the chlorine atom are the result of absorption errors (112). Although this effect is usually more marked for the heavy atom, the other regions of positive electron density about the carbon and oxygen atoms could well be

due to the systematic errors in the data arising from absorption. The peak close to O_2 , which could well be distorted by absorption errors, is no doubt due principally to the hydrogen atom. Since it was still not possible to correct for absorption, the hydrogen atom was placed on this peak and its positional and thermal parameters included in the least squares refinement. This refinement converged at an R factor of 0.084.

Results

Final atomic coordinates and temperature factors are listed in Table 33. Fig. 24 shows the molecular dimensions for the non-hydrogen atoms and also the thermal ellipsoids for these atoms; the root-mean-square amplitudes of vibration are listed in Table 34. Fig. 25 shows the crystal packing of the molecules. The hydrogen atom refined to a geometrically sensible position, the O_2 -H bond being 0.98 \AA and the Cl- O_2 -H angle being 116° . A statistical test can be applied to determine whether the drop in R factor, after refinement of the hydrogen atom, is due to a significant improvement of the model or merely a result of increasing the number of parameters in the least squares process.

This test is described below:

Hamilton's R factor test (20)

Weighted R factors R_w are used in this test and these are defined as $R_w = (\sum w ||F_o| - |F_c||^2 / \sum w |F_o|^2)^{1/2}$.

The relevant values of the conventional R factor

($R = \sum ||F_o| - |F_c|| / \sum |F_o|$) and R_w are listed below:

	<u>R</u>	<u>R_w</u>
R factors without the hydrogen atom	0.0873	0.1126
R factors with the hydrogen atom	0.0844	0.1076

The dimension of the hypothesis = 4

Number of degrees of freedom = 500 - 59 = 441

R factor ratio = 0.1126/0.1076 = 1.047

Pertinent values taken from the table at significance points in (20) are:

$$R_{4,411,0.05} = 1.011$$

$$R_{4,411,0.005} = 1.017$$

Since the R_w ratio does not exceed the value of

$R_{b,N_1,\alpha}$ even at $\alpha = 0.005$, the improvement in the model is significant.

Rigid body analysis

The thermal ellipsoid diagram (Fig.24) shows a rather unusual effect in that the major axes of most ellipsoids are aligned along the same direction (the only exception being O_2). This is not a physically meaningful result since it implies a molecular vibration in the direction of the C_3-O_2 bond and as the molecule is packed in hydrogen bonded chains involving both oxygen atoms (see Molecular Packing) this mode of vibration is unlikely. This effect is most probably a result of the absorption errors present in the data. The programme described in Appendix B was used to analyse the thermal motion parameters in terms of rigid body vibrations. In the absence of absorption errors in the data, the expected result would be a larger translational vibration in the direction C_2-CL i.e. perpendicular to the hydrogen bonds, than in the two directions normal to the C_2-CL bond. The libration should be small and in particular the in-plane libration should be smallest. The results of the rigid body thermal analysis are shown in Table 35 and the unrealistic nature of the temperature factors is obvious. The librations about the three axes appear reasonable, but the greatest translational vibration is

along the y axis which is the direction of the intermolecular hydrogen bond. Further, the agreement between U_{obs} and U_{calc} is not particularly good; $R(= \Sigma ||U_o| - |U_c|| / \Sigma |U_o|)$ is 9.3% (cf. 5% for naphthazarin, p. 39) indicating that the assumption that rigid body motion is the major mode of vibration is not a particularly good one.

TABLE 33

FINAL ATOMIC COORDINATES

Atom	x	y	z	B
CL	0.1669(2)	0.3593(3)	0.4418(2)	
C ₁	0.4801(7)	0.1953(12)	0.3912(7)	
C ₂	0.3506(7)	0.1695(11)	0.4705(7)	
C ₃	0.3600(7)	-0.0247(12)	0.5845(6)	
O ₁	0.2498(6)	-0.0614(10)	0.6613(5)	
O ₂	0.4731(6)	0.3701(8)	0.2844(5)	
H	0.567(11)	0.365(13)	0.224(9)	4.2(15)

ANISTROPIC TEMPERATURE FACTORS

Atom	U ₁₁	U ₂₂	U ₃₃	U ₁₂	U ₁₃	U ₂₃	equivalent isotropic B
CL	0.0270(9)	0.0515(14)	0.0397(10)	0.0141(6)	0.0160(6)	0.0049(7)	3.01
C ₁	0.025(3)	0.040(4)	0.032(3)	0.004(2)	0.011(2)	-0.006(3)	2.48
C ₂	0.023(3)	0.037(4)	0.032(3)	0.002(2)	0.012(2)	-0.003(3)	2.36
C ₃	0.020(3)	0.043(4)	0.028(3)	-0.001(2)	0.010(2)	-0.005(3)	2.34
O ₁	0.030(2)	0.052(3)	0.043(3)	0.044(2)	0.025(2)	0.002(2)	3.05
O ₂	0.054(2)	0.044(3)	0.042(2)	0.009(2)	0.021(2)	0.018(2)	2.98

TABLE 34ROOT-MEAN-SQUARE AMPLITUDES OF VIBRATION

Atom	minor axis	medium axis	major axis
CL	0.1297	0.1951	0.2435
C ₁	0.1396	0.1778	0.2079
C ₂	0.1365	0.1806	0.1959
C ₃	0.1289	0.1655	0.2119
O ₁	0.1145	0.2190	0.2343
O ₂	0.1393	0.1713	0.2542

TABLE 35
RIGID BODY VIBRATIONS

(a) <u>Translational Tensor</u>	\AA		
T_{11}	0.025(1) 0.160(4)		
T_{22}	0.034(2) 0.185(4)		
T_{33}	0.020(2) 0.141(9)		
T_{12}	-0.005(1)		
T_{13}	0.006(2)		
T_{23}	-0.002(2)		
<hr/>			
(b) <u>Librational Tensor</u>	($^{\circ}$)		
ω_{11}	0.0052(6) 4.1(2)		
ω_{22}	0.0032(4) 3.2(2)		
ω_{33}	0.0013(3) 2.0(1)		
ω_{12}	0.0007(3)		
ω_{13}	-0.0002(4)		
ω_{23}	0.0003(3)		
<hr/>			
(c) <u>Direction cosines of molecular axes referred to abc*</u>			
x	-0.7411	0.6490	-0.1720
y	-0.5714	-0.4752	0.6691
z	0.3477	0.5984	0.7219

The z axis is normal to the least squares plane, and the x axis passes through C_2

Table 35 cont'd.

Observed and Rigid Body U_{ij} s Referred to
Molecule axis (OBS/CALC)

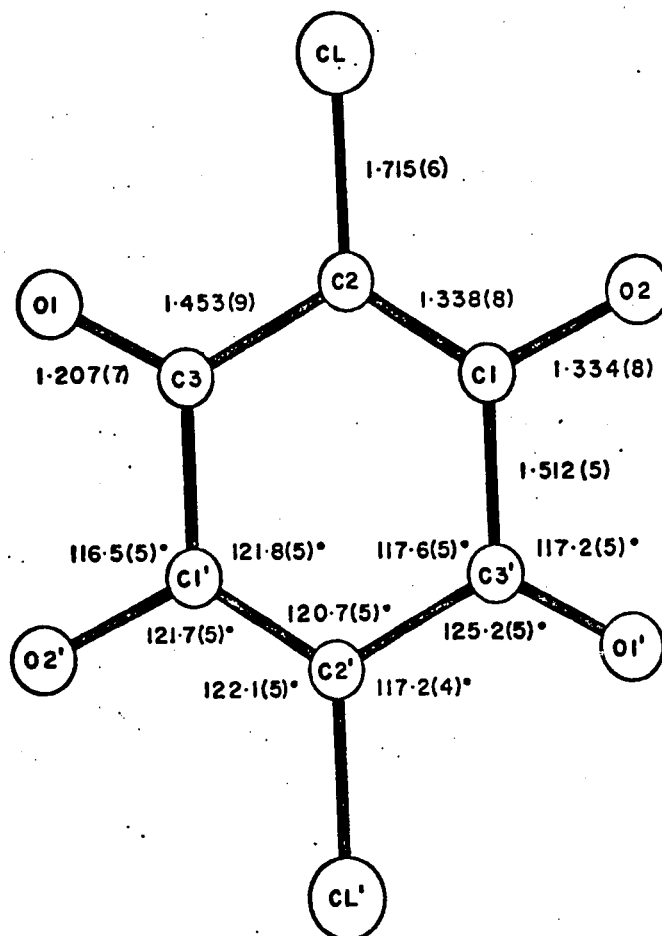
	U_{11}	U_{22}	U_{33}	U_{12}	U_{13}	U_{23}
CL	0.023	0.045	0.051	-0.005	0.009	-0.007
	0.025	0.047	0.051	-0.006	0.006	-0.005
C ₁	0.027	0.042	0.029	-0.006	0.005	-0.003
	0.027	0.035	0.030	-0.004	0.006	-0.002
C ₂	0.026	0.037	0.029	-0.005	0.005	-0.001
	0.025	0.037	0.026	-0.005	0.006	-0.002
C ₃	0.030	0.035	0.026	-0.009	0.008	-0.003
	0.027	0.035	0.028	-0.006	0.007	-0.002
O ₁	0.035	0.038	0.050	-0.010	0.005	-0.002
	0.032	0.036	0.049	-0.009	0.008	-0.003
O ₂	0.030	0.030	0.060	0.004	0.009	0.000
	0.032	0.037	0.059	-0.001	0.006	-0.002

TABLE 36
INTERMOLECULAR CONTACTS

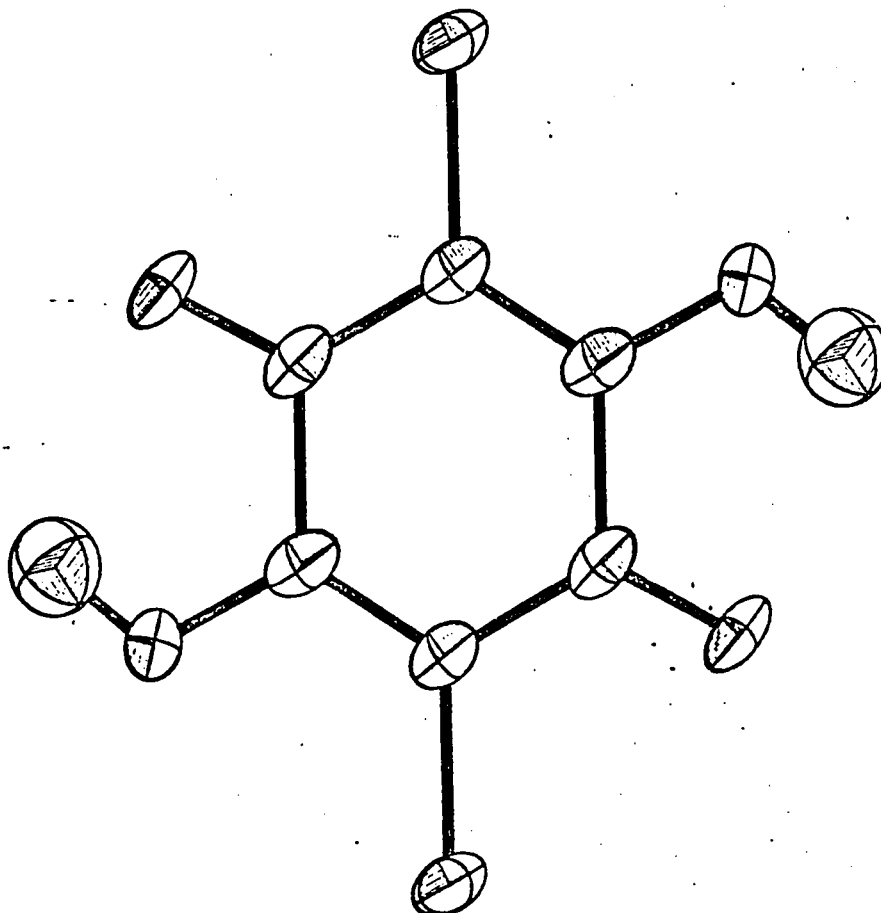
Atom 1	Atom 2	Vector to be applied to Atom 2	Distance (Å)
CL	CL'	$x-1, y+1, z$	3.33
CL	O ₁ '	$x-1, y, z$	3.49
CL	H	$\frac{1}{2}x-1, \frac{1}{2}y, \frac{1}{2}z$	3.02
CL	O ₁ '	$\frac{1}{2}x-1, \frac{1}{2}y, \frac{1}{2}z$	3.39
CL	O ₂ '	$\frac{1}{2}x-1, \frac{1}{2}y, \frac{1}{2}z-1$	3.46
CL	O ₂ '	$\frac{1}{2}x-1, \frac{1}{2}y-1, \frac{1}{2}z-1$	3.37
CL	H'	$\frac{1}{2}x-1, \frac{1}{2}y-1, \frac{1}{2}z-1$	3.39
CL	H'	$\frac{1}{2}x, \frac{1}{2}y, \frac{1}{2}z+1$	3.01
O ₁	O ₁ '	$\frac{1}{2}x-1, \frac{1}{2}y, \frac{1}{2}z$	3.17
O ₁	H	$\frac{1}{2}x-1, \frac{1}{2}y, \frac{1}{2}z$	1.94
O ₁	O ₂	$\frac{1}{2}x-1, \frac{1}{2}y, \frac{1}{2}z$	2.79

TABLE 37

M	L	FN	FC	M	L	FN	FC	M	L	FN	FC	M	L	FN	FC	M	L	FN	FC
0	2	171	168	0	2	171	168	0	2	171	168	0	2	171	168	0	2	171	168
0	4	10	-10	0	4	10	-10	0	4	10	-10	0	4	10	-10	0	4	10	-10
0	4	70	-73	0	4	70	-73	0	4	70	-73	0	4	70	-73	0	4	70	-73
0	4	71	-75	0	4	71	-75	0	4	71	-75	0	4	71	-75	0	4	71	-75
0	10	24	-24	0	10	24	-24	0	10	24	-24	0	10	24	-24	0	10	24	-24
1	1	111	105	1	1	111	105	1	1	111	105	1	1	111	105	1	1	111	105
1	1	234	-221	1	1	234	-221	1	1	234	-221	1	1	234	-221	1	1	234	-221
1	1	27	28	1	1	27	28	1	1	27	28	1	1	27	28	1	1	27	28
1	5	164	-152	1	5	164	-152	1	5	164	-152	1	5	164	-152	1	5	164	-152
1	5	217	222	1	5	217	222	1	5	217	222	1	5	217	222	1	5	217	222
1	7	45	-45	1	7	45	-45	1	7	45	-45	1	7	45	-45	1	7	45	-45
1	7	44	48	1	7	44	48	1	7	44	48	1	7	44	48	1	7	44	48
1	0	28	40	1	0	28	40	1	0	28	40	1	0	28	40	1	0	28	40
1	0	72	77	1	0	72	77	1	0	72	77	1	0	72	77	1	0	72	77
2	0	02	-03	2	0	02	-03	2	0	02	-03	2	0	02	-03	2	0	02	-03
2	2	16	-11	2	2	16	-11	2	2	16	-11	2	2	16	-11	2	2	16	-11
2	2	180	147	2	2	180	147	2	2	180	147	2	2	180	147	2	2	180	147
-2	4	120	-144	-2	4	120	-144	-2	4	120	-144	-2	4	120	-144	-2	4	120	-144
-2	4	17	12	-2	4	17	12	-2	4	17	12	-2	4	17	12	-2	4	17	12
-2	4	85	-02	-2	4	85	-02	-2	4	85	-02	-2	4	85	-02	-2	4	85	-02
-2	8	32	31	-2	8	32	31	-2	8	32	31	-2	8	32	31	-2	8	32	31
-2	8	60	72	-2	8	60	72	-2	8	60	72	-2	8	60	72	-2	8	60	72
-2	10	111	111	-2	10	111	111	-2	10	111	111	-2	10	111	111	-2	10	111	111
-3	1	24	31	-3	1	24	31	-3	1	24	31	-3	1	24	31	-3	1	24	31
-3	1	40	-47	-3	1	40	-47	-3	1	40	-47	-3	1	40	-47	-3	1	40	-47
-3	5	65	-50	-3	5	65	-50	-3	5	65	-50	-3	5	65	-50	-3	5	65	-50
-3	7	75	-72	-3	7	75	-72	-3	7	75	-72	-3	7	75	-72	-3	7	75	-72
-3	7	61	-70	-3	7	61	-70	-3	7	61	-70	-3	7	61	-70	-3	7	61	-70
-3	0	14	-17	-3	0	14	-17	-3	0	14	-17	-3	0	14	-17	-3	0	14	-17
-4	2	273	-248	-4	2	273	-248	-4	2	273	-248	-4	2	273	-248	-4	2	273	-248
-4	2	50	-44	-4	2	50	-44	-4	2	50	-44	-4	2	50	-44	-4	2	50	-44
-4	4	115	-102	-4	4	115	-102	-4	4	115	-102	-4	4	115	-102	-4	4	115	-102
-4	4	49	40	-4	4	49	40	-4	4	49	40	-4	4	49	40	-4	4	49	40
-4	6	145	144	-4	6	145	144	-4	6	145	144	-4	6	145	144	-4	6	145	144
-4	6	23	21	-4	6	23	21	-4	6	23	21	-4	6	23	21	-4	6	23	21
-4	1	17	-14	-4	1	17	-14	-4	1	17	-14	-4	1	17	-14	-4	1	17	-14
-4	1	48	-70	-4	1	48	-70	-4	1	48	-70	-4	1	48	-70	-4	1	48	-70
-4	3	29	24	-4	3	29	24	-4	3	29	24	-4	3	29	24	-4	3	29	24
-4	3	171	-144	-4	3	171	-144	-4	3	171	-144	-4	3	171	-144	-4	3	171	-144
-4	5	47	53	-4	5	47	53	-4	5	47	53	-4	5	47	53	-4	5	47	53
-4	5	26	-24	-4	5	26	-24	-4	5	26	-24	-4	5	26	-24	-4	5	26	-24
-4	7	96	-06	-4	7	96	-06	-4	7	96	-06	-4	7	96	-06	-4	7	96	-06
-4	0	23	21	-4	0	23	21	-4	0	23	21	-4	0	23	21	-4	0	23	21
-6	2	123	140	-6	2	123	140	-6	2	123	140	-6	2	123	140	-6	2	123	140
-6	2	56	47	-6	2	56	47	-6	2	56	47	-6	2	56	47	-6	2	56	47
-6	2	146	101	-6	2	146	101	-6	2	146	101	-6	2	146	101	-6	2	146	101
-6	4	19	17	-6	4	19	17	-6	4	19	17	-6	4	19	17	-6	4	19	17
-6	4	31	32	-6	4	31	32	-6	4	31	32	-6	4	31	32	-6	4	31	32
-6	6	117	-116	-6	6	117	-116	-6	6	117	-116	-6	6	117	-116	-6	6	117	-116
-6	6	124	-123	-6	6	124	-123	-6	6	124	-123	-6	6	124	-123	-6	6	124	-123
-7	1	61	-64	-7	1	61	-64	-7	1	61	-64	-7	1	61	-64	-7	1	61	-64
-7	1	108	114	-7	1	108	114	-7	1	108	114	-7	1	108	114	-7	1	108	114
-7	3	59	-64	-7	3	59	-64	-7	3	59	-64	-7	3	59	-64	-7	3	59	-64
-7	3	46	48	-7	3	46	48	-7	3	46	48	-7	3	46	48	-7	3	46	48
-7	5	71	47	-7	5	71	47	-7	5	71	47	-7	5	71	47	-7	5	71	47
-7	7	47	42	-7	7	47	42	-7	7	47	42	-7	7	47	42	-7	7	47	42
-8	0	21	17	-8	0	21	17	-8	0	21	17	-8	0	21	17	-8	0	21	17
-8	2	40	-60	-8	2	40	-60	-8	2	40	-60	-8	2	40	-60	-8	2	40	-60
-8	4	126	-119	-8	4	126	-119	-8	4	126	-119	-8	4	126	-119	-8	4	126	-119
F = 1																			
0	1	23	-20	0	1	23	-20	0	1	23	-20	0	1	23	-20	0	1	23	-20
0	2	207	318	0	2	207	318	0	2	207	318	0	2	207	318	0	2	207	318
0	2	102	06	0	2	102	06	0	2	102	06	0	2	102	06	0	2	102	06
0	4	123	125	0	4	123	125	0	4	123	125	0	4	123	125	0	4	123	125
0	4	33	31	0	4	33	31	0	4	33	31	0	4	33	31	0	4	33	31
0	4	96	02	0	4	96	02	0	4	96	02	0	4	96	02	0	4	96	02
0	7	48	-17	0	7	48	-17	0	7	48	-17	0	7	48	-17	0	7	48	-17
0	9	14	-17	0	9	14	-17	0	9	14	-17	0	9	14	-17	0	9	14	-17
1	0	07	-105	1	0	07	-105	1	0	07	-105	1	0	07	-105	1	0	07	-105
1	1	310	327	1	1	310	327	1	1	310	327	1	1	310	327	1	1	310	327
1	7	168	-186	1	7	168	-186	1	7	168	-186	1	7	168	-186	1	7	168	-186
-1	2	43	40	-1	2	43	40	-1	2	43	40	-1	2	43	40	-1	2	43	40
-1	2	70	80	-1	2	70	80	-1	2	70	80	-1	2	70	80	-1	2	70	80
-1	2	174	-103	-1	2	174	-103	-1	2	174	-103	-1	2	174	-103	-1	2	174	-103
-1	4	98	100	-1	4	98	100	-1	4	98	100	-1	4	98	100	-1	4	98	100
-1	4	21	-24	-1	4	21	-24	-1	4	21	-24	-1	4	21	-24	-1	4	21	-24
-1	4	74	77	-1	4	74	77	-1	4	74	77	-1	4	74	77	-1	4	74	77
-1	7	85	-80	-1	7	85	-80	-1	7	85	-80	-1	7	85	-80	-1	7	85	-80
-1	7	20	24	-1	7	20	24	-1	7	20	24	-1	7	20	24	-1	7	20	24
-1	8	24	28	-1	8	24	28	-1	8	24	28	-1	8	24	28	-1	8	24	28
-1	0	17	-20	-1	0	17	-20	-1	0	17	-20	-1	0	17	-20	-1	0	17	-20
-1	0	35	37	-1	0	35	37	-1	0	35	37	-1	0	35	37	-1	0	35	37
-1	10	32	24	-1	10	32	24	-1	10	32	24	-1	10	32	24	-1	10	32	24
-1	10	24	-21	-1	10	24	-21	-1	10	24	-21	-1	10	24	-21	-1	10	24	-21
-2	0	67	-70	-2	0	67	-70	-2	0	67	-70	-2	0	67	-70	-2	0	67	-70
-2	2	04	-80	-2	2	04	-80	-2	2	04	-80	-2	2	04	-80	-2	2	04	-80
-2	2	55	70	-2	2	55	70	-2	2	55	70	-2	2	55	70	-2	2	55	70
-2	2	46	-50	-2															



Molecular dimensions



Thermal ellipsoids
Fig. 24.

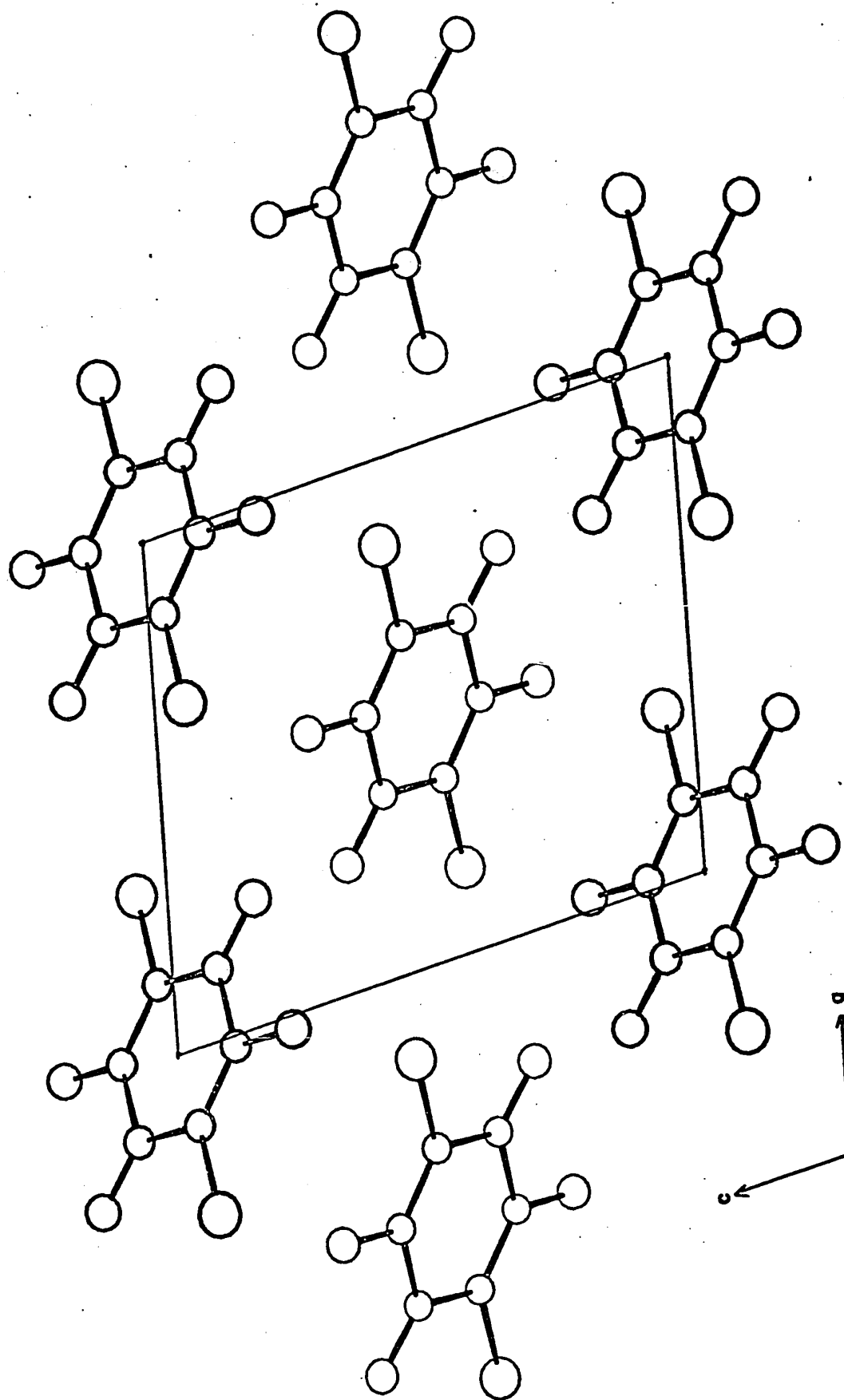


Fig. 25. Molecular packing. Projection onto [ac] plane.

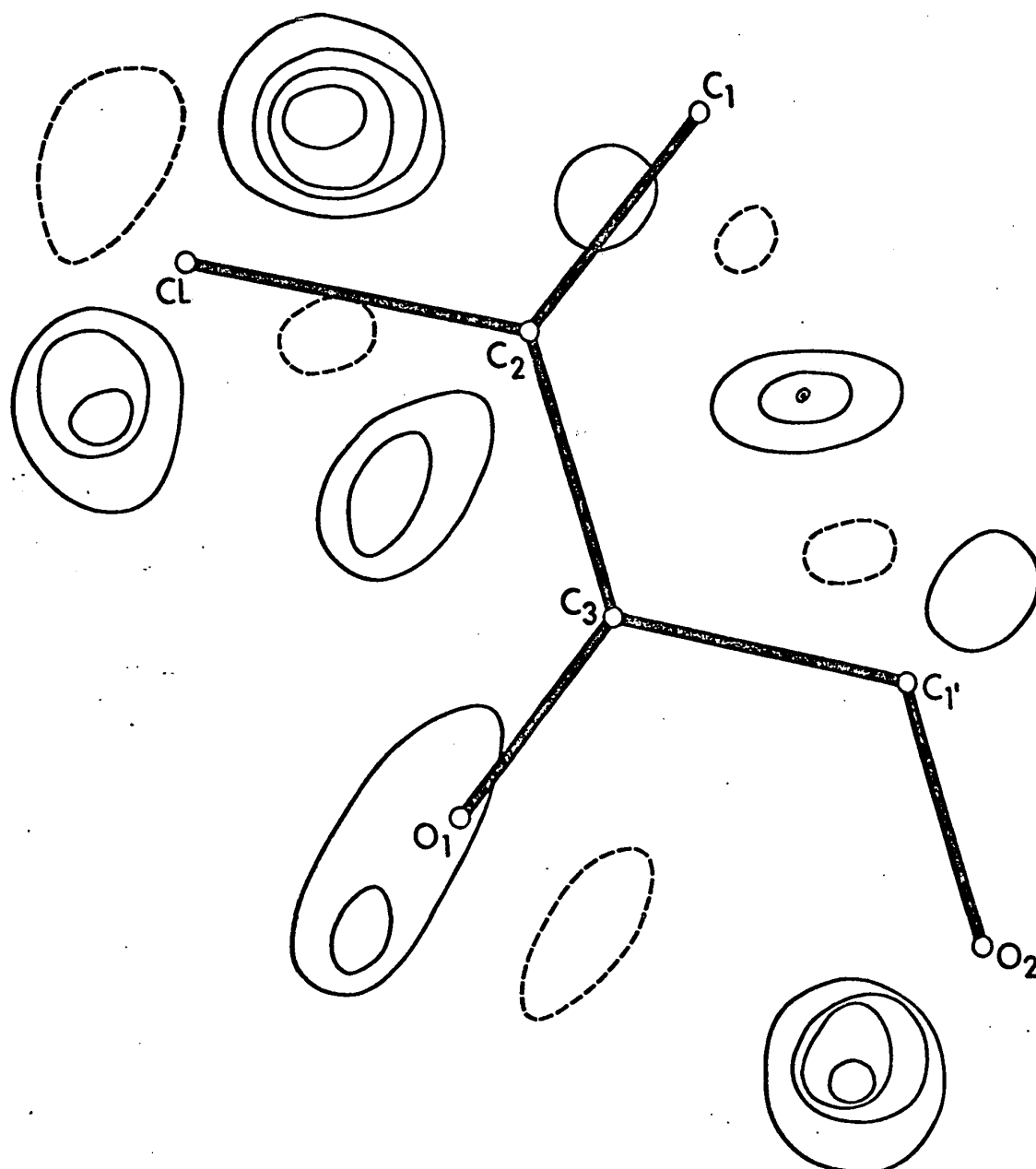


Fig. 26. Electron density before inclusion of hydrogen atoms.

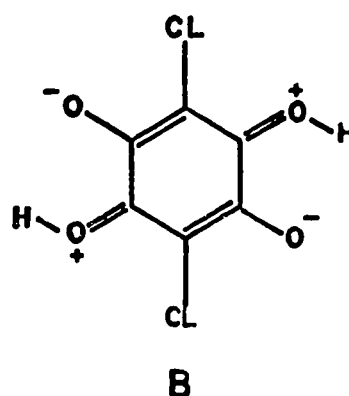
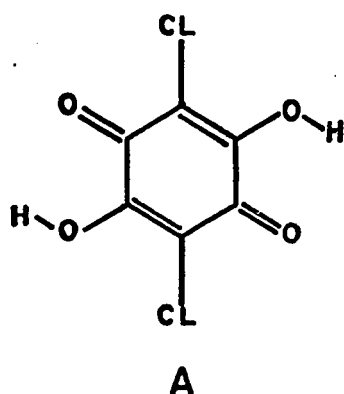
Discussion

Towards the end of the refinement, the crystal structure of chloranilic acid, in refined form, was published by Andersen (81). The unit cell chosen by him was $P2_1/a$ and on transforming the unit cell data of the present structure to this space group, good agreement is observed:

<u>Andersen $P2_1/a$</u>	<u>Present work transformed to $P2_1/a$</u>
$a = 10.025 \text{ \AA}$	$a = 10.069 \text{ \AA}$
$b = 5.544 \text{ \AA}$	$b = 5.537 \text{ \AA}$
$c = 7.566 \text{ \AA}$	$c = 7.589 \text{ \AA}$
$\beta = 122.9^\circ$	$\beta = 122.9^\circ$

Molecular Geometry

The bond length pattern clearly indicates that the molecule has the quinonoid form shown below in A.



Bond	This work	Andersens' model
C ₁ -C ₂	1.338 (8)	1.346 (6)
C ₁ -C ₃ '	1.512 (5)	1.501
C ₂ -C ₃	1.453 (9)	1.445 (6)
C ₁ -O ₂	1.334 (8)	1.322 (6)
C ₂ -CL	1.715 (6)	1.717 (6)
C ₃ -O ₁	1.207 (7)	1.222 (6)

Most bond lengths are within error of the expected values and agree well with Andersen's values (see above, and Table 19 p.107). The bond C₂-C₃ is the only exception: this bond differs from the expected value (1.495 Å) by 4.5σ and may be the result of contribution from the charged canonical shown in B above, although there is little evidence of this in the other bond lengths. Andersen has observed the same shortening of the C₂-C₃ bond and has explained it in this manner. An intramolecular hydrogen bond is formed in this molecule; the distance between the oxygen atoms O₁ and O₂ is 2.661 Å (c.f. 2.57 Å in Naphthazarin, p.72). The hydrogen atom is clearly asymmetric: the H.....O₁' distance is 2.26 Å compared to 0.98 Å for the O₂-H bond. The C₁-O₂-H angle is 116° and the O₁'-H.....O₂ angle is 104°.

Molecular Packing

The molecules are inclined at an angle of $\sim 54^\circ$ to the [b] axis and are stacked in parallel chains along this axis. The perpendicular distance between molecules is 3.28 \AA which is slightly less than the expected separation of 3.4 \AA and this suggests some form of intermolecular interaction through overlap of the aromatic π orbitals (70). The parallel chains are linked through hydrogen bonds involving O_1 of a molecule in one column and O_2 of a molecule in a neighbouring column (see the last two distances in Table 36). The bonds connect columns lying along the long diagonal as seen in the packing diagram, Fig. 25.

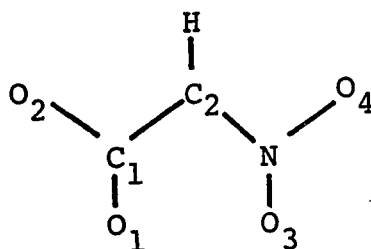
Although the molecular geometry has not been greatly affected by absorption errors (as demonstrated by Lingafelter (114)), the thermal vibration parameters are clearly erroneous. It is hoped to correct the data for absorption at a later date and thus remove these anomalies in the model.

PART III

(B) The refinement of dipotassium nitroacetate

The structure of dipotassium nitroacetate was determined in 1954 by Sutor, Llewellyn and Maslen (52) and each projection was refined by successive difference Fourier syntheses calculated with the aid of Robertson's strips. The space group was found to be $Pb2_1m$ with two molecules in the unit cell.

The structure consists of coplanar anions in the (001) plane at $z = 0$, and the potassium ions are also coplanar in (001) but at $z = 0.5$. The anion is nearly symmetrical and hence in the early stages of refinement, the true designation C_1 , N will not be apparent from projection difference synthesis.



The authors however attempted to determine the correct model on the basis of reliability factors. The two models were found to differ by 0.001 in R, hence they proceeded with the refinement to an overall R index of 0.126 with the supposed better model.

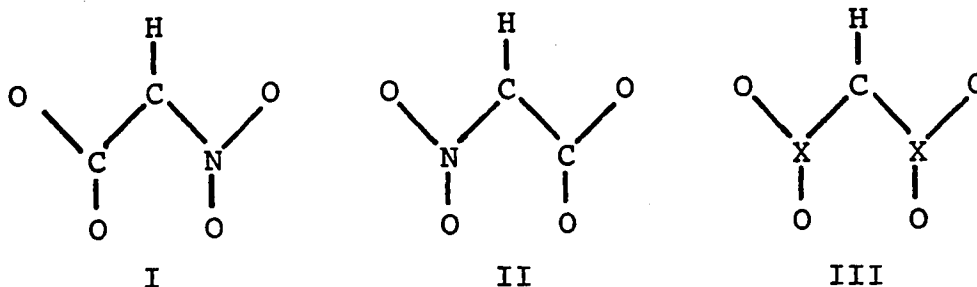
This difference, as noted in Structure Reports (29) is really insufficient evidence to distinguish between the two models and it was thought that further least squares refinement with individual temperature corrected scattering curves, and the possibility of anisotropic temperature factors would indicate which was the true model. The scattering factors used in the original determination were obtained assuming the shape of a unitary scattering curve (\hat{f}) and applying the appropriate atomic number multiplier for any particular atom.

$$\text{e.g. } f_N = Z_N \cdot \hat{f}$$

This is a fairly big assumption in view of the different shape of the scattering curve even for atoms of similar atomic number, also no consideration can be given to individual temperature factors with this system. The data used was that given by Sutor et al. in (52), the indefinite weak reflections being omitted leaving 309 reflections.

Refinement

Three models are possible for this structure:



where I is the model accepted by Sutor et al., II is the model with N and C reversed and III represents a disordered model, the atoms designated X having a scattering curve which is the average of the C and N scattering curves.

These three models were refined with isotropic temperature factors using the Oak Ridge full matrix least squares program ORFLS (33), until no further change in R factor was observed. It was then attempted to refine the models using anisotropic temperature parameters, but these were found to assume physically meaningless values for the light atoms, thus further refinement was carried out with only the potassium atoms anisotropic. The molecular dimensions were then calculated for each of the three models, but there were no significant differences (Fig.27). Hamilton's R factor test (20) was applied to test for a significant difference in the three reliability factors, and also to test whether the anisotropic thermal parameters for the potassium atoms were significant.

Results

The coordinates corresponding to model III are listed in Table 38, and the bond lengths and angles for all models are shown in Fig 27.

Hamilton's R Factor Test

The test is made on the basis of the weighted R factors R_w , as these are statistically more significant, and was thus applied to determine whether models I and II are significantly better than III. If the R factor ratio of the two models being tested is greater than the significance point pertinent to the situation, obtained from a table in (20), then the hypothesis under test (i.e. is one model better than the other) can be rejected at the specified significance level.

i.e. if $R > R_{b,n-m,\alpha}$

where R = ratio of weighted R factor,

b = dimensions of the hypothesis,

$n-m$ = no. of degrees of freedom

then the hypothesis can be rejected at the $100.\alpha\%$ significance level.

The conventional R factor, R , and the weighted R factor, R_w , for each situation are listed in Table 39.

These quantities are defined as:

$$R = \frac{\sum ||F_o| - |F_c||}{\sum |F_o|}$$

$$R_w = [\sum W ||F_o| - |F_c||^2 / \sum W |F_o|^2]^{1/2}$$

The following significance values relevant to the present situation were found by interpolation of the table in (20) using the relation:

$$R_{1,276,\alpha} = 1 + 0.43(R_{1,120,\alpha} - 1)$$

<u>100. α</u>		
.5%	$R_{1,276,.005}$	= 1.015
1%	$R_{1,276,.01}$	= 1.012
5%	$R_{1,276,.05}$	= 1.007
10%	$R_{1,276,.1}$	= 1.005
25%	$R_{1,276,.25}$	= 1.003
50%	$R_{1,276,.5}$	= 1.001

(I) All atoms isotropic

Number of parameters = 27

Number of degrees of freedom = 282

- (i) hypothesis: "That model I is significantly better than III"

R factor ratio = $.1259/.1253 = 1.005$

Thus the hypothesis can be rejected at, or slightly greater than the 10% level of significance.

- (ii) hypothesis: "That model II is significantly better than III"

R factor ratio = $.1273/.1253 = 1.016$

This hypothesis can be rejected at the 0.5 significance level.

(II) Potassium atoms anisotropic

Number of observations = 309

Number of parameters = 33

Number of degrees of freedom = 276

Two atoms are interchanged but a change in one implies a change in the other, hence the dimension of the hypothesis is 1.

(i) hypothesis: "That model I is significantly better than III"

R factor ratio = $.1218/.1211 = 1.006$

Thus the hypothesis can only be rejected at the 10% significance level.

(ii) hypothesis: "That model II is significantly better than III"

R factor ratio = $.1233/.1211 = 1.018$

This hypothesis can be rejected at a significance level $<0.5\%$.

(III) To test significance of anisotropy for model III

	<u>III(a)</u>	<u>III(b)</u>
Number of parameters refined	33	27
Dimension of hypothesis = $33 - 27$	= 6	
Number of degrees of freedom = $309 - 33$	= 276	

hypothesis: "That the isotropic refinement is more significant than anisotropic refinement"

$$R \text{ factor ratio} = .1253/.1211 = 1.035$$

$$R_{6,176,.005} = 1.034$$

Thus the hypothesis can be rejected at the 0.5% significance level.

(IV) To test the significance of including the hydrogen atom

The hydrogen atom was included in the refinement of model III(a) and the (x,y) parameters of the hydrogen atom were refined, with the positional (x,y) and temperature parameters of the other atoms. The R factors at the conclusion of this refinement were:

$$R = 0.1063$$

$$R_w = 0.1198$$

Dimension of the hypothesis = 2 (two new parameters were refined)

$$\text{Number of degrees of freedom} = 309 - 35 = 274$$

$$R \text{ factor ratio} = 0.1211/0.1198 = 1.010$$

$$R_{2,274,0.1} = 1.008$$

Thus the hypothesis can only be rejected at a 10% significance level.

TABLE 38

FINAL ATOMIC COORDINATES (FRACTIONAL) AND
ISOTROPIC TEMPERATURE FACTORS (\AA^2)

Atom	x	y	z	B
K ₁	0.0344(5)	0.579	0.5	
K ₂	0.3668(6)	0.276(1)	0.5	
X ₁	0.329(3)	0.648(3)	0.0	1.2(4)
X ₂	0.201(3)	0.921(4)	0.0	0.9(3)
C ₂	0.311(3)	0.829(4)	0.0	1.6(5)
O ₁	0.083(2)	0.843(3)	0.0	1.4(3)
O ₂	0.200(2)	0.094(3)	0.0	2.0(3)
O ₃	0.239(2)	0.527(3)	0.0	1.4(4)
O ₄	0.449(2)	0.599(4)	0.0	2.7(4)

ANISOTROPIC TEMPERATURE FACTORS (\AA^2)

Atom	U ₁₁	U ₂₂	U ₃₃	U ₁₂	U ₁₃	U ₂₃	equivalent isotropic B
K ₁	0.019(3)	0.000(3)	0.002(3)	-0.007(2)	0.0	0.0	1.1
K ₂	0.021(3)	0.018(3)	0.018(3)	0.003(3)	0.0	0.0	1.5

TABLE 39
R FACTORS FOR VARIOUS MODELS

	R	R _w
(a) <u>All atoms isotropic</u>		
Model I	0.1101	0.1259
Model II	0.1140	0.1273
Model III	0.1116	0.1253
(b) <u>Potassium atoms anisotropic</u>		
Model I	0.1061	0.1218
Model II	0.1094	0.1233
Model III	0.1068	0.1211
Model III + hydrogen	0.1063	0.1198

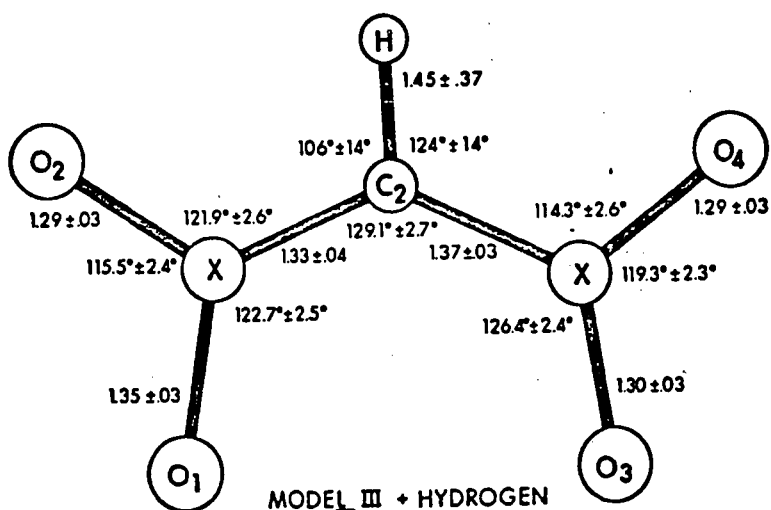
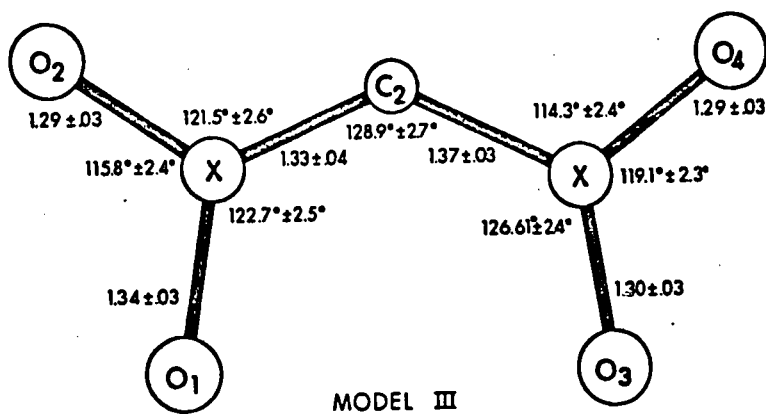
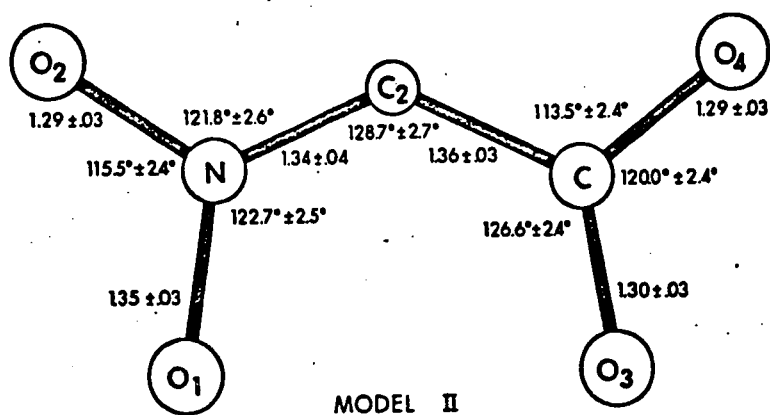
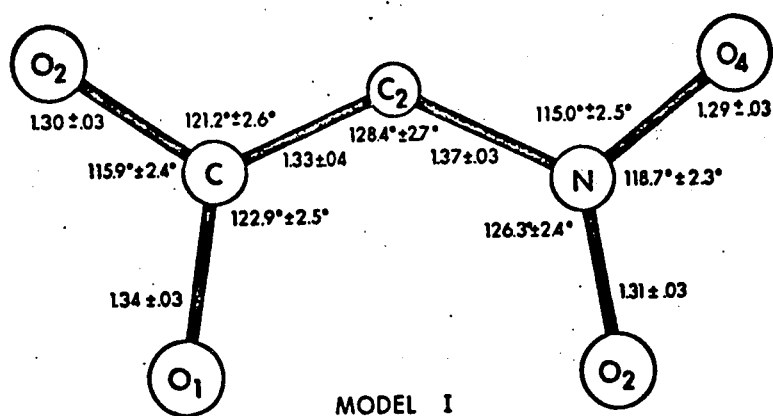


Fig. 27. Molecular dimensions.

Discussion

The criterion for rejection of hypotheses has been stated by Hamilton (65) as:

"Rejection at a significance level greater than 5% is not significant"

On the basis of the above tests then, it is obvious that model II has the least likelihood of being correct, whereas models I and III are virtually indistinguishable. The failure of the above tests to decide the better model of I and III must be taken as indicative of serious systematic errors within the data set. It would appear that the assumption of anisotropic temperature factors for the heavy atoms is significant, although with systematic errors in the data, it is more likely that the additional parameters will be used by the least squares process in an attempt to account for these errors and thus it would be meaningless to interpret physically the vibrational ellipsoids. The inclusion of the hydrogen atom in the refinement is obviously not meaningful, a conclusion that is supported by the fact that the C-H distance had refined to the unrealistic value of 1.4 \AA .

It is probable that if the original data had been scaled together by a more exact process e.g., by the method of Rae (26) or Hamilton (27), then a more significant difference in R factor would be observed between the three models.

PART III

(C) Refinement of 2,2',2''-triaminotriethylene

Ni(II) dithiocyanate ($\text{Ni tren}(\text{SCN})_2$)

The ligand 2,2',2''-triaminotriethylene is of interest chemically as it is potentially quadridentate but is sterically unable to form a square planar complex with a metal atom. Complexes of this ligand with Ni(II) have long been known (35, 36, 37) they are paramagnetic, and the coordination could thus be octahedral or tetrahedral. The latter type of coordination is most favourable energetically (as was supposed by Reihlen (24) and Asmussen (25)) but if the ligand field is sufficiently strong, nickel can accommodate two 3d electrons in "outer d" configuration enabling the complex to be octahedral. Crystal structure data has shown that this is the type of coordination in 2,2',2''-triaminotriethylene Ni(II) dithiocyanate; all four nitrogen atoms in the ligand are coordinated to the nickel atom and the two thiocyanate ions also occupy cis positions (Fig.28).

The crystal structure of 2,2',2''-triaminotriethylene Ni(II) dithiocyanate was determined independently by Rasmussen (53) in Denmark and by Hall and Woulfe (22, 23) in New Zealand. The crystal data are:

$a = 10.79 \overset{\circ}{\text{\AA}}$	4 molecules per unit cell
$b = 14.69 \overset{\circ}{\text{\AA}}$	in Space group $P2_1^2 2_1^2 2_1^2$
$c = 8.59 \overset{\circ}{\text{\AA}}$	

In neither case was a high degree of precision attained. This is not unexpected in the case of Woulfe's data; the study of projections is simply not a satisfactory procedure for molecules of this complexity. Rasmussens' data was three dimensional, and thus this criticism does not apply. Detailed study of his data however, revealed a very high proportion of unobserved reflections, and in particular, few reflections have been observed with high $\sin\theta$. Woulfe's projection data does not suffer in this way, and it is probable that Rasmussen did not take photographs of sufficiently long exposure. The two data sets, while each is somewhat deficient, are thus complementary, and it appeared likely that a more satisfactory structure might result if the two were combined.

Data scaling and refinement

It was thus proposed to scale the two data sets together using the method described by Rae (26) in which individual scale factors are given to each layer to be scaled, and the scale factors are then adjusted by least squares to put the layers on a common scale. In this instance the three projection data sets of Woulfe were considered individually, the three dimensional data set of Rasmussen was considered as a fourth set, and the four were then combined. The procedure is normally iterative in that common reflections which show bad correlation are excluded after each cycle. As these are not known

beforehand, all reflections are initially included and those showing worst agreement are then eliminated. On each cycle the criterion for inclusion is made more stringent, and the accepted "best" solution is in fact a compromise between: the inclusion of as many terms as possible on the one hand, and the basing of the scale constants on terms which are in good agreement, on the other. In this project the initial data comprised 707(hkℓ) data of Rasmussen and 139(0kℓ), 93(h0ℓ) and 153(hk0) data of Woulfe. Of these, 208 data were common to two or more data sets. After several cycles, scale constants were obtained such that ~60% of these common pairs passed the test that $0.8 < F_i/F_j < 1.25$, where F_i and F_j represent the scaled values of terms common to the i and j sets. The agreement index over all common terms, defined as:

$$C = \frac{\sum ||F_i| - |F_j||}{\frac{1}{2} \sum (|F_i| + |F_j|)}$$

was 0.15. The agreement obtained when scaling three dimensional film data is normally a little better than this, with C at about 0.10. The final combined data set contained 867 unique reflections.

The atom coordinates listed by Rasmussen were chosen as the starting model. These were refined by full matrix least squares (33) assuming isotropic temperature factors, to a reliability index of 0.127. The scattering factors

listed in the International tables (38) were used, with the real dispersion correction correction for the nickel atom being applied. Anisotropic temperature parameters were then assumed for the nickel and sulphur atoms and the reliability index at the convergence of refinement was 0.107.

Results

Final atom coordinates and temperature factors are listed in Tables 41 and 42. The bond lengths of the refined model are compared with those of the two individual determinations in Table 43. Bond angles are listed in Table 44 and Fig. 28 shows the vibrational ellipsoids and numbering scheme.

Hamiltons R factor test

The assumption of anisotropic motion will in itself result in a better agreement due to the increase in the number of variable parameters in the least squares process, and to test the validity of this decrease in R, Hamilton (20) has devised a significance test which utilises the ratio of the weighted R factors before and after the anisotropic motion is assumed. The weighted R factor, R_w , is defined as:

$$R_w = [\sum W(|F_o| - |F_c|)^2 / \sum W|F_o|^2]^{1/2}$$

TABLE 41
FINAL ATOMIC COORDINATES

Atom	x	y	z
Ni	0.1220 (3)	0.3333 (3)	0.8347 (4)
S ₁	0.0082 (7)	0.0209 (4)	0.7600 (9)
S ₂	-0.3081 (5)	0.3868 (5)	0.9310 (8)
C ₈	0.351 (2)	0.444 (2)	0.864 (3)
C ₇	0.255 (2)	0.497 (2)	0.947 (3)
C ₆	0.361 (2)	0.276 (2)	0.950 (3)
C ₅	0.295 (2)	0.296 (2)	1.101 (3)
C ₄	0.353 (2)	0.315 (2)	0.672 (3)
C ₃	0.268 (2)	0.363 (2)	0.548 (3)
C ₂	0.077 (2)	0.119 (2)	0.785 (3)
C ₁	-0.169 (2)	0.359 (2)	0.885 (2)
N ₆	0.317 (2)	0.348 (2)	0.856 (2)
N ₅	0.130 (2)	0.477 (1)	0.885 (2)
N ₄	0.158 (2)	0.304 (2)	1.076 (2)
N ₃	0.140 (2)	0.384 (2)	0.593 (2)
N ₂	0.112 (2)	0.191 (2)	0.791 (3)
N ₁	-0.065 (2)	0.348 (2)	0.858 (2)

TABLE 42
TEMPERATURE FACTORS (\AA^2)

(a) <u>Anisotropic Atoms</u>							
Atoms	U_{11}	U_{22}	U_{33}	U_{12}	U_{13}	U_{23}	equivalent isotropic B
Ni	0.012(1)	0.021(2)	0.020(2)	0.002(2)	-0.001(2)	+0.005(2)	1.38
S ₁	0.051(4)	0.027(4)	0.045(4)	-0.009(4)	-0.030(4)	0.014(4)	3.23
S ₂	0.019(3)	0.035(4)	0.045(4)	0.014(3)	0.009(3)	0.016(4)	2.59
(b) <u>Isotropic Atoms</u>							
Atom	B	Atom	B				
C ₈	1.9(4)	C ₁	1.3(4)				
C ₇	2.4(4)	N ₆	1.7(3)				
C ₆	2.1(4)	N ₅	2.5(4)				
C ₅	2.6(5)	N ₄	2.4(4)				
C ₄	1.9(4)	N ₃	2.3(4)				
C ₃	2.3(4)	N ₂	3.2(4)				
C ₂	2.0(4)	N ₁	2.3(4)				

TABLE 43
SUMMARY OF BOND LENGTHS

Rasmussen's data	Woulfe's data	Combined data	expected values and references
-CH₂-N₆			
1.53	1.54	1.58 (3)	C ₆ -N ₆
1.68	1.36	1.49 (3)	C ₈ -N ₆ 1.47... (40)
1.45	1.51	1.47 (3)	C ₄ -N ₆
range: 0.23	0.18	0.11	
-N=C= in SCN			
1.16	1.16	1.17 (3)	N ₁ -C ₁ 1.17... (51)
1.22	1.16	1.12 (3)	N ₂ -C ₂
range: 0.06	0.0	0.04	
-CH₂-NH₂			
1.48	1.32	1.48 (3)	C ₅ -N ₄
1.53	1.44	1.45 (3)	C ₃ -N ₃ 1.47... (40)
1.49	1.43	1.50 (3)	C ₇ -N ₅
range: 0.05	0.12	0.05	
-H₂C-CH₂-			
1.66	1.32	1.47 (3)	C ₇ -C ₈
1.57	1.31	1.51 (3)	C ₅ -C ₆ 1.54... (40)
1.55	1.50	1.58 (3)	C ₃ -C ₄
range: 0.12	0.19	0.12	

Table 43 cont'd.

Rasmussen's data	Woulfe's data	Combined data	expected values and references	
<hr/>				
S=C				
1.63	1.64	1.64 (3)	S ₂ -C ₂	
1.61	1.61	1.61 (2)	S ₁ -C ₁	1.61... (39)
range: 0.02	0.03	0.03		
Ni-NH ₂ -				
2.20	2.13	2.16 (2)	Ni-N ₄	
2.17	2.21	2.16 (2)	Ni-N ₅	2.13... (28)
2.24	2.09	2.10 (2)	Ni-N ₃	
range: 0.07	0.12	0.05		
Ni-N ₆				
2.13	2.10	2.11 (2)	Ni-N ₆	2.10... (28)
Ni-N=				
2.10	2.06	2.13 (2)	Ni-N ₂	
2.02	2.02	2.03 (2)	Ni-N ₁	2.07... (39)
range: 0.08	0.04	0.10		

TABLE 44

BOND ANGLES

Atoms	Angle (°)	Atoms	Angle (°)
N ₄ -Ni-N ₅	89.8 (8)	Ni-N ₆ -C ₈	110 (1)
N ₄ -Ni-N ₂	89.0 (8)	Ni-N ₆ -C ₄	105 (1)
N ₄ -Ni-N ₁	95.4 (8)	Ni-N ₂ -C ₂	162 (2)
N ₄ -Ni-N ₆	82.9 (7)	N ₂ -C ₂ -S ₂	171 (2)
N ₅ -Ni-N ₃	93.3 (6)	Ni-N ₁ -C ₁	169 (2)
N ₅ -Ni-N ₆	82.2 (8)	N ₁ -C ₁ -S ₁	177 (2)
N ₅ -Ni-N ₁	87.8 (9)	Ni-N ₄ -C ₅	109 (2)
N ₂ -Ni-N ₃	86.1 (8)	N ₄ -C ₅ -C ₆	111 (2)
N ₂ -Ni-N ₆	98.6 (8)	C ₅ -C ₆ -N ₆	108 (2)
N ₁ -Ni-N ₃	100.5 (8)	Ni-N ₅ -C ₇	107 (2)
N ₆ -Ni-N ₃	82.1 (7)	N ₅ -C ₇ -C ₈	112 (2)
C ₆ -N ₆ -C ₈	114 (2)	C ₇ -C ₈ -N ₆	115 (2)
C ₆ -N ₆ -C ₄	108 (2)	Ni-N ₃ -C ₃	112 (1)
C ₈ -N ₆ -C ₄	117 (2)	N ₃ -C ₃ -C ₄	108 (2)
Ni-N ₆ -C ₆	102 (1)	C ₃ -C ₄ -N ₆	108 (2)

TABLE 45

216

M	K	FO	FC	M	K	FO	FC	M	K	FO	FC	M	K	FO	FC	M	K	FO	FC	M	K	FO	FC	M	K	FO	FC	M	K	FO	FC
0	2	511	444	10	4	167	115	11	0	165	44	13	6	107	134	3	2	589	520	9	2	263	241	5	6	193	165	5	6	193	165
0	2	511	444	10	5	121	94	11	1	222	242	13	7	275	291	3	3	212	122	9	3	168	237	6	1	231	245	6	1	231	245
0	4	768	799	10	6	111	106	11	2	232	197	13	8	281	297	3	4	324	318	10	0	328	342	6	2	160	177	6	2	160	177
0	6	1516	1763	10	8	415	406	11	4	221	223	13	10	380	396	3	6	400	394	10	1	336	349	6	4	192	205	6	4	192	205
0	8	210	100	10	10	335	252	11	6	170	222	13	12	451	542	3	8	490	484	10	2	170	181	6	6	295	268	6	6	295	268
0	10	8	78	11	1	177	177	12	1	199	221	13	14	561	562	4	10	590	584	10	4	251	261	6	8	292	270	6	8	292	270
0	12	183	153	11	3	121	94	12	3	149	215	13	16	671	782	4	12	620	614	10	6	251	261	6	10	148	163	6	10	148	163
0	14	160	150	11	5	268	264	12	5	166	157	13	18	781	892	4	14	710	704	10	8	251	261	6	12	149	164	6	12	149	164
0	16	115	117	11	7	121	94	12	7	179	123	13	20	891	1002	4	16	820	814	10	10	251	261	6	14	150	165	6	14	150	165
0	18	112	122	11	9	268	264	12	9	166	157	13	22	1001	1112	4	18	850	844	10	12	251	261	6	16	151	166	6	16	151	166
0	20	1791	973	11	11	268	264	12	11	166	157	13	24	1121	1232	4	20	880	874	10	14	251	261	6	18	152	167	6	18	152	167
1	2	862	732	11	13	268	264	12	13	166	157	13	26	1241	1352	4	22	910	904	10	16	251	261	6	20	153	168	6	20	153	168
1	4	905	907	11	15	268	264	12	15	166	157	13	28	1361	1472	4	24	940	934	10	18	251	261	6	22	154	169	6	22	154	169
1	6	952	957	12	1	194	184	13	1	167	120	14	1	167	120	5	2	579	509	11	5	229	246	9	1	122	129	9	1	122	129
1	8	720	724	12	3	194	184	13	3	167	120	14	3	167	120	5	4	599	529	12	0	83	111	9	3	180	146	9	3	180	146
1	10	874	944	12	5	194	184	13	5	167	120	14	5	167	120	5	6	619	549	12	2	83	111	9	5	181	147	9	5	181	147
1	12	937	944	12	7	194	184	13	7	167	120	14	7	167	120	5	8	639	569	12	4	83	111	9	7	182	148	9	7	182	148
1	14	1000	1004	12	9	194	184	13	9	167	120	14	9	167	120	5	10	659	589	12	6	83	111	9	9	183	149	9	9	183	149
1	16	1063	1067	12	11	194	184	13	11	167	120	14	11	167	120	5	12	679	609	12	8	83	111	9	11	184	150	9	11	184	150
1	18	1126	1130	12	13	194	184	13	13	167	120	14	13	167	120	5	14	699	629	12	10	83	111	9	13	185	151	9	13	185	151
1	20	1189	1193	12	15	194	184	13	15	167	120	14	15	167	120	5	16	719	649	12	12	83	111	9	15	186	152	9	15	186	152
1	22	1252	1256	12	17	194	184	13	17	167	120	14	17	167	120	5	18	739	669	12	14	83	111	9	17	187	153	9	17	187	153
1	24	1315	1319	12	19	194	184	13	19	167	120	14	19	167	120	5	20	759	689	12	16	83	111	9	19	188	154	9	19	188	154
1	26	1378	1382	12	21	194	184	13	21	167	120	14	21	167	120	5	22	779	709	12	18	83	111	9	21	189	155	9	21	189	155
1	28	1441	1445	12	23	194	184	13	23	167	120	14	23	167	120	5	24	799	729	12	20	83	111	9	23	190	156	9	23	190	156
1	30	1504	1508	12	25	194	184	13	25	167	120	14	25	167	120	5	26	819	749	12	22	83	111	9	25	191	157	9	25	191	157
1	32	1567	1571	12	27	194	184	13	27	167	120	14	27	167	120	5	28	839	769	12	24	83	111	9	27	192	158	9	27	192	158
1	34	1630	1634	12	29	194	184	13	29	167	120	14	29	167	120	5	30	859	789	12	26	83	111	9	29	193	159	9	29	193	159
1	36	1693	1697	12	31	194	184	13	31	167	120	14	31	167	120	5	32	879	809	12	28	83	111	9	31	194	160	9	31	194	160
1	38	1756	1760	12	33	194	184	13	33	167	120	14	33	167	120	5	34	899	829	12	30	83	111	9	33	195	161	9	33	195	161
1	40	1819	1823	12	35	194	184	13	35	167	120	14	35	167	120	5	36	919	849	12	32	83	111	9	35	196	162	9	35	196	162
1	42	1882	1886	12	37	194	184	13	37	167	120	14	37	167	120	5	38	939	869	12	34	83	111	9	37	197	163	9	37	197	163
1	44	1945	1949	12	39	194	184	13	39	167	120	14	39	167	120	5	40	959	889	12	36	83	111	9	39	198	164	9	39	198	164
1	46	2008	2012	12	41	194	184	13	41	167	120	14	41	167	120	5	42	979	909	12	38	83	111	9	41	199	165	9	41	199	165
1	48	2071	2075	12	43	194	184	13	43	167	120	14	43	167	120	5	44	999	929	12	40	83	111	9	43	200	166	9	43	200	166
1	50	2134	2138	12	45	194	184	13	45	167	120	14	45	167	120	5	46	1019	949	12	42	83	111	9	45	201	167	9	45	201	167
1	52	2197	2201	12	47	194	184	13	47	167	120	14	47	167	120	5	48	1039	969	12	44	83	111	9	47	202	168	9	47	202	168
1	54	2260	2264	12	49	194	184	13	49	167	120	14	49	167	120	5	50	1059	989	12	46	83	111	9	49	203	169	9	49	203	169
1	56	2323	2327	12	51	194	184	13	51	167	120	14	51	167	120	5	52	1079	1009	12	48	83	111	9	51	204	170	9	51	204	170
1	58	2386	2390	12	53	194	184	13	53	167	120	14	53	167	120	5	54	1099	1029	12	50	83	111	9	53	205	171	9	53	205	171
1	60	2449	2453	12	55	194	184	13	55	167	120	14	55	167	120	5	56	1119	1049	12	52	83	111	9	55	206	172	9	55	206	172
1	62	2512	2516	12	57	194	184	13	57	167	120	14	57	167	120	5	58	1139	1069	12	54	83	111	9	57	207	173	9	57	207	173
1	64	2575	2579	12	59	194	184	13	59	167	120	14	59	167	120	5	60	1159	1089	12	56	83	111	9	59	208	174	9	59	208	174
1	66	2638	2642	12	61	194	184	13	61	167	120	14	61	167	120	5	62	1179	1109	12	58	83	111	9	61	209	175	9	61	209	175
1	68	2701	2705	12	63	194	184	13	63	167	120	14	63	167	120	5	64	1199	1129	12	60	83	111	9	63	210	176	9	63	210	176
1	70	2764	2768	12	65	194	184	13	65	167	120	14	65	167	120	5	66	1219	1149	12	62	83	111	9	65	211	177	9	65	211	177
1	72	2827	2831	12	67	194	184	13	67	167	120	14	67	167	120	5	68	1239	1169	12	64	83	111	9	67	212	178	9	67	212	178
1	74	2890	2894	12	69	194	184	13	69	167	120	14	69	167	120	5	70	1259	1189	12	66	83	111	9	69	213	179	9	69	213	179
1	76	2953	2957	12	71	194	184	13	71	167	120	14	71	167	120	5	72	1279	1209	12	68	83	111	9	71	214	180	9	71	214	180
1	78	3016	3020	12	73	194	184	13	73	167	120	14	73	167	120	5	74	1299	1229	12	70	83	111	9	73	215	181	9	73	215	181
1	80	3079	3083	12																											

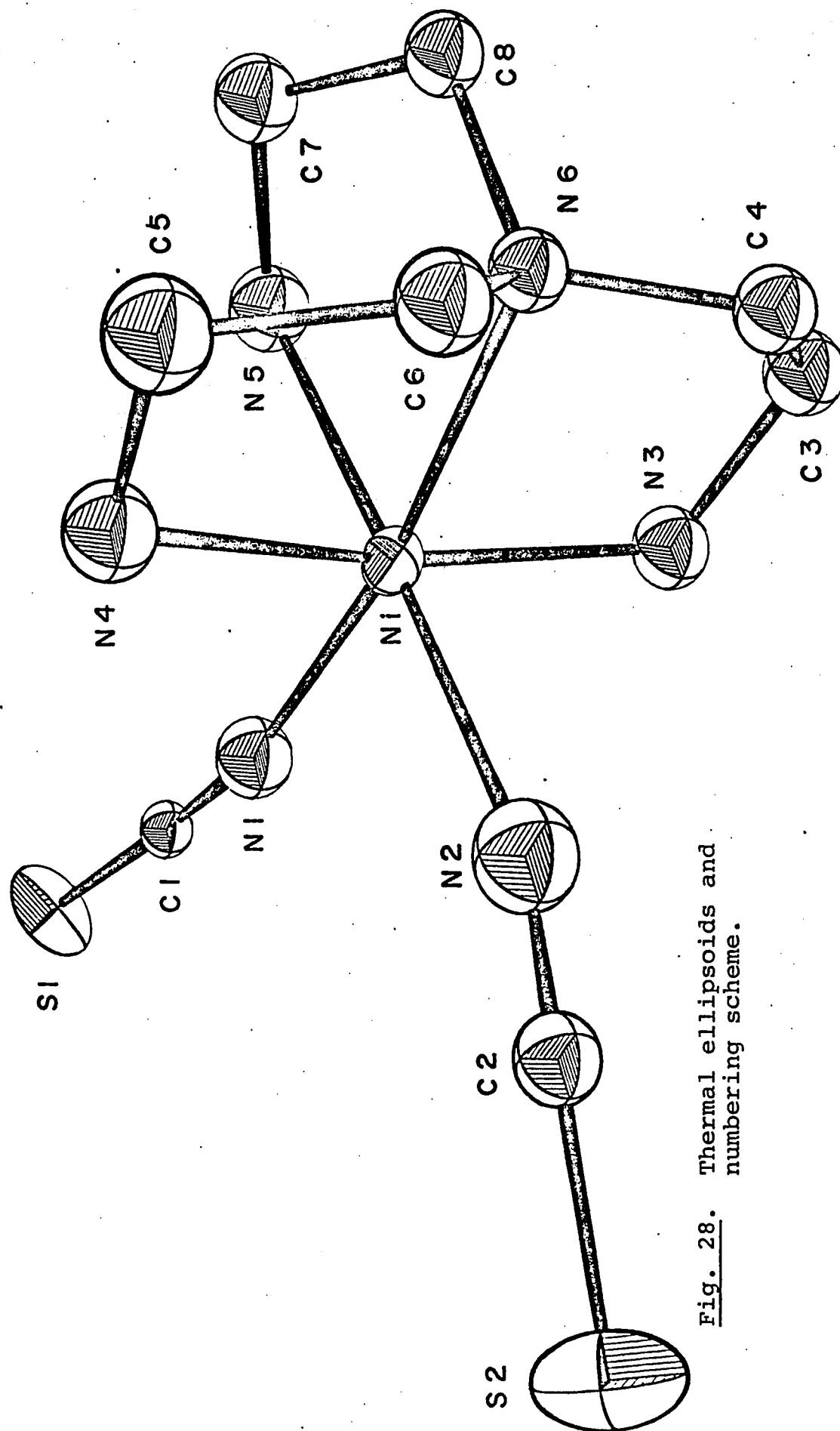


Fig. 28. Thermal ellipsoids and numbering scheme.

Weighted R factor for isotropic model = 0.1420

Weighted R factor for anisotropic model = 0.1386

R factor ratio = 1.025

The hypothesis under test is: "That the nickel and sulphur atoms have isotropic thermal motion"

Dimension of hypothesis = 15 (=difference in the
no. of parameters
refined)

No. of degrees of freedom = 783

A pertinent value of $R_{b,N,\alpha}$ obtained by interpolation of the table given by Hamilton is:

$$R_{15,783,0.005} = 1.005$$

As the observed R_w ratio is greater than this, the hypothesis may be rejected at the 0.5% significance level. It was thought that neither the quality nor the quantity of data would justify anisotropic refinement for the light atoms, and the refinement was considered complete at this stage.

Discussion

On the basis of Hamilton's hypothesis rejection criterion (see p.206), the assumption of anisotropic motion for the nickel and sulphur atoms seems valid, although it must be remembered that the test assumes that systematic errors in the data are absent; an

assumption that may not be valid in view of method of data collection employed.

The overall description of the molecule and the structure has of course not altered in any way, but the measured bond lengths are in many cases significantly different to those previously reported. With one exception, viz N_6-C_6 , the lengths of the chemically equivalent bonds are in reasonable agreement, and are within error of the commonly accepted values. It is unlikely that N_6-C_6 is genuinely long, and it thus seems probable that the derived errors are in fact underestimated. This in turn would suggest some systematic errors in the data which is hardly surprising.

Despite this, the result of combining the data sets has been to produce a more extensive and better balanced set of data which is now capable of describing the molecule more precisely than either of the original sets alone.

PART III(D) Preliminary investigation of 2-methyl 5,8-dihydroxy
1,4-naphthoquinone (Methyl naphthazarin)Experimental

Methyl naphthazarin was prepared by a Friedel-Crafts reaction between methyl-hydroquinone and maleic anhydride; dark red prisms being readily obtained on recrystallisation from glacial acetic acid. The density was measured by flotation in an aqueous solution of zinc bromide.

Crystal data:

$$a = 7.42 \text{ \AA}$$

$$b = 8.48 \text{ \AA}$$

$$c = 16.67 \text{ \AA}$$

$$\alpha = 88^\circ$$

$$\beta = 107^\circ$$

$$\gamma = 114^\circ$$

$$d_{\text{calc}} = 1.49 \text{ gm/cm}^3 \quad (z = 4, \text{ M.W.} = 204)$$

$$d_{\text{obs}} = 1.51 \text{ gm/cm}^3$$

Intensity data were collected on the Pailred linear diffractometer using crystal-monochromatised $\text{CuK}\alpha$ radiation, with the crystal rotating about the [a] axis; the layers $h = 0$ to $h = 5$ were recorded. All reflections were scanned at the rate of $1^\circ/\text{m}$ for 4 to 6 mins; the

scan width being gradually increased for the higher layers because of the broadening of the peak profile as μ was increased. The total background counting time was made approximately equal to the total scan time to ensure favourable counting statistics, and reflections were rejected from the data set on the basis of two tests: (a) $I \leq 0$, and (b) $\sigma I/I > 0.5$. (see p. 28) leaving a total of 1801 unique above background reflections out of the 2487 reflections scanned. Lorentz and Polarisation corrections were applied to the data, and all equivalent reflections were averaged assuming Friedel's Law.

The implication of having four molecules in the unit cell are as follows: if the space group is $P1$, there will be four molecules in the asymmetric unit and if the space group is $P\bar{1}$, there will be two molecules in the asymmetric unit, or 4 molecules on centres of symmetry, where the stacking will have to be disordered as the molecule itself is not centrosymmetric.

When a molecule is planar, the molecular plane will generally coincide with a crystallographic plane and as the phase change between scattered rays from the atoms in the plane will be zero, the resultant reflection from this plane will have a large intensity. The (200) reflection had the largest intensity of the data set

(approximately twice as large as the next biggest reflection) and the value of the unitary structure factor, which compares the amplitude of a reflection with that of the reflection (000), for which all atoms scatter in phase i.e.

$U_{hkl} = F_{hkl} / (F_{000} \cdot \exp(-B \cdot \sin^2 \theta / \lambda^2))$ (100)^b, was 0.52 indicating that a substantial number of atoms scatter in phase for reflection (200). Thus the molecular plane obviously lies close to (200) i.e. is perpendicular to the [a] axis, and the two asymmetric molecules are separated by 1/2 in the [a] direction. The phase of reflections cannot be determined experimentally, but if the space group is centrosymmetric (see next section) i.e. $P\bar{1}$ in the present case, the choice is limited to the signs + or -, and depending on which value is given to (200), the molecular planes will be close to the planes $x = 0, 1/2$ or $x = 1/4, 3/4$. Considering only the trigonometrical part of the structure factor expression for $P\bar{1}$ i.e. $F = \cos 2\pi(hx + ky + lz)$:

when $x = 0, 1/2$ and when $x = 1/4, 3/4$

$F_{200} = \cos 2\pi 2.1/2$	$F_{200} = \cos 2\pi 2.1/4$
$= \cos 2\pi$	$= \cos \pi$
$= +1$	$= -1$

Structure Solution

There is no way of distinguishing between $P1$ and $P\bar{1}$ (when strong anomalous scatterers are not present in the structure) from the diffraction pattern as this is always centrosymmetric regardless of the space group; statistical methods however can often be used to indicate the presence of a centre of symmetry. Normalised structure factors (E values defined by the formula $E_{hkl}^2 = |F_{hkl}^2| / \epsilon \cdot \sum_i^N f_i^2$ where ϵ is a term to account for systematic absences in the data (32)) were calculated as the distribution of these values is primarily dependent on the presence or absence of a centre of symmetry in the space group, and the distribution obtained is shown below and compared with the theoretical values:

	This structure	Centrosymmetric	Non-centrosymmetric
$\langle E \rangle$	0.698	0.798	0.886
$\langle E ^2 \rangle$	1.037	1.000	1.000
$\langle E ^2 - 1 \rangle$	1.264	0.968	0.736
$ E > 3$	2.3%	0.3%	0.01%
$ E > 2$	6.5%	5.0%	1.8%
$ E > 1$	21.8%	32.0%	37.0%

Although the agreement with either of the theoretical distributions is not good, the deviations all favour the centrosymmetric space group $P\bar{1}$, thus it was decided to attempt the solution by statistical methods using the sigma II relationship of Karle (32). Sets of reflections satisfying the Sayre relationship (107) $sE_h \sim sE_k \cdot sE_{h-k}$ (where s means "the sign of", and the subscripts refer to index triples, hkl) were calculated by a program written by F. Ahmed (SAP3 (49)), and after assigning three origin fixing signs ($\bar{1}67$), $E = +4.947$; (256), $E = +4.429$; (265), $E = +4.357$) and four symbols (A, B, C, D), 260 reflections were given signs by the manual application of the Sayre relationship. Symbols were assigned to reflections with large E values, the symbol A being given to reflection (200). Signs were only accepted if the probability of the sign being positive ($P_+ \sim 0.5 + 0.5 \tanh[(\sigma_3/\sigma_2^{1.5}) \cdot |E_h \cdot E_k \cdot E_{h-k}|]$) where $\sigma_3 = \sum_i n_i^3$, $\sigma_2 = \sum_i n_i^2$, $n_i = f_i / \sum_j f_j$ (1019) was greater than 0.97 for positive signs and less than 0.03 for negative signs. During this process there were many indications that the signs of the symbols A and C were positive e.g., if the signs of three terms satisfying Sayre's equation have been determined independently as $sE_h = A$, $sE_k = -$, $sE_{h-k} = -$, then clearly

the sign of A must be +. These indications were not accepted at the present stage and all phases were left in symbol form during the assignment of signs except those that had already been absolutely determined as + e.g., the origin signs. A computer programme was now written to apply the sigma II relationship

$sE_h \sim s_k E_k E_{h-k}$ after the four symbols had been assigned absolute values + or -. The most consistent

set of signs was obtained when A and C were positive. Thus three Fourier maps were calculated with the signed

E values as coefficients (E maps) in which the two remaining symbols B and D were given one of the 2^2-1 combinations of + and -.

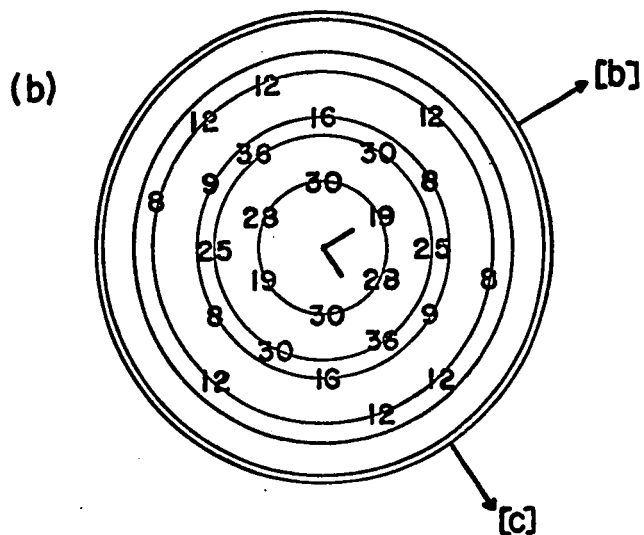
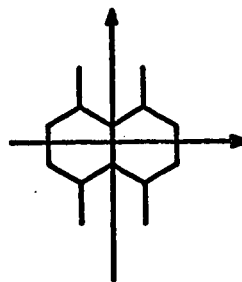
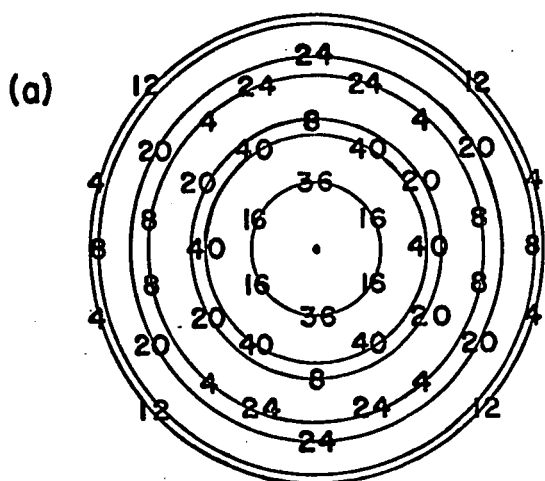
If B and D were both given positive signs, then all phases would be positive resulting in a large peak at the origin and as this molecule clearly cannot have an atom on the origin,

this possibility was not accepted, hence the total number of possible sign combinations was 2^2-1 and not 2^2 .

Unfortunately none of the E maps showed recognisable features of the molecule so the remaining 12 E maps in which the symbols A and C were allowed to have negative signs were calculated (the total number of sign combinations when four symbols are used is 2^4), and reflections which gave probabilities in the range 0.03-0.97 were rejected.

The three dimensional Patterson had been calculated by this stage thus the probable orientations of the two asymmetric molecules were known (see later), but even with this knowledge no acceptable model could be found in these maps. E maps effectively represent the probability of finding an atom at any location in the unit cell, and the most promising maps showed rows of peaks in a "close packing" arrangement, located on the sections $x = 0$, $1/2$ or $x = 1/4$, $3/4$, depending on whether the reflection (200) had a positive or negative phase. This array of peaks gives little information about the locality of the molecules in these planes when the molecule in question is so regular in its atomic arrangement. It seems likely that the failure of this method of solution was due to the fact that the arrangement of atoms within the unit cell is highly ordered and not random, the latter situation being the assumption upon which the method is founded (107).

As mentioned previously, the three dimensional Patterson map was calculated primarily to determine the orientations of the two molecules in the asymmetric unit from the intramolecular vectors about the origin. The absence of a Harker section in the Patterson space group $P\bar{1}$ implies that the positioning of the molecules in the unit cell, even with the knowledge of the molecular



Vectors on arbitrary scale.
Origin peaks removed from
all diagrams.

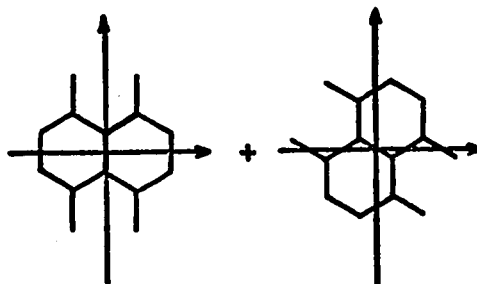
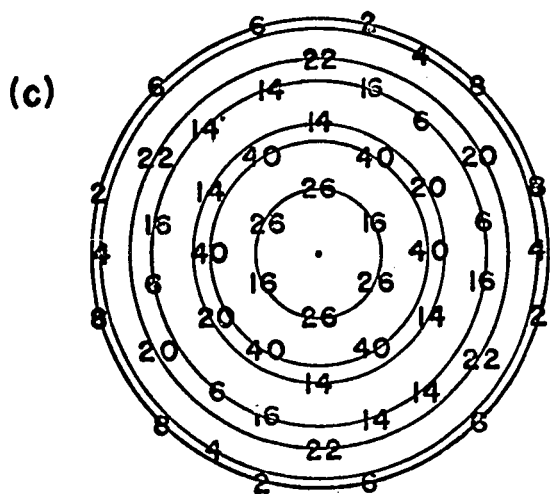


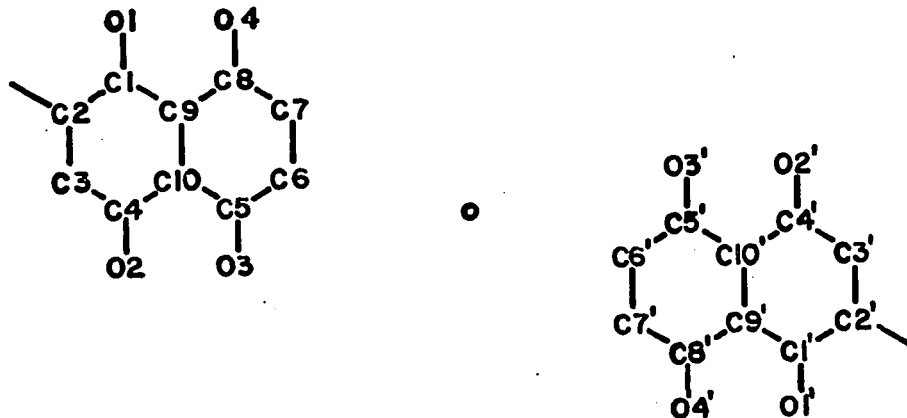
Fig. 29. Intramolecular vectors.

orientations, could prove exceedingly difficult if not impossible for an all light atom molecule of this type. The Patterson synthesis was sharpened in the normal manner (see p. 86) with application of an artificial temperature factor to reduce ripples about the origin peak due to series termination errors (109) which may well obscure intramolecular vectors if not suppressed.

In general the Patterson synthesis showed concentrations of peaks only on the sections $x = 0, 1/2$. Assuming the carbon-carbon, carbon-oxygen, oxygen-oxygen vectors to have peak heights in the ratio 36:48:64 i.e. 2:3:4, and all bonds to be equal in length, the expected intramolecular vectors for a single molecule are shown in Fig. 29 (the methyl carbon atom has been ignored in (a) and (c)).

Fig 29(b) shows the pattern observed in the [bc] plane which suggests that the two molecules are oriented at $\sim 60^\circ$ to each other i.e. if a copy of Fig 29(a) is rotated 60° and superimposed on (a) and the coinciding vectors are averaged, the pattern shown in (c) results which closely resembles the observed vector pattern shown in (b). Thus the orientation relationship between the two asymmetric molecules is established and the orientations with respect to the unit cell axes are determined: the C_9-C_{10} bonds (see Fig. 29) of the molecules make angles of 60° and 120° with the [b] axis.

The symbolic addition procedure provided strong indications that the phase of (200) was positive, which implies that the four molecules in the unit cell are situated close to $x = 0, 1/2$. When two planar molecules are themselves coplanar, and are further related by a centre of symmetry, the pattern of vectors between these molecules can be readily predicted. These vectors will form a "close-packed" array on the section $x = 0$, and will be centred around one dominant vector which is the superposition of the fourteen parallel vectors of the type C_1-C_5' , C_2-C_6' , C_3-C_7' etc (see below)



This vector will be effectively a centre-centre vector i.e. it represents the hypothetical vector between the centres of the C_9-C_{10} bonds of the two centrosymmetrically related molecules, thus if this vector is identified and placed with its midpoint on a centre of symmetry, the ends of the vector should correspond to the centres of the two related molecules. Furthermore, this vector will lie

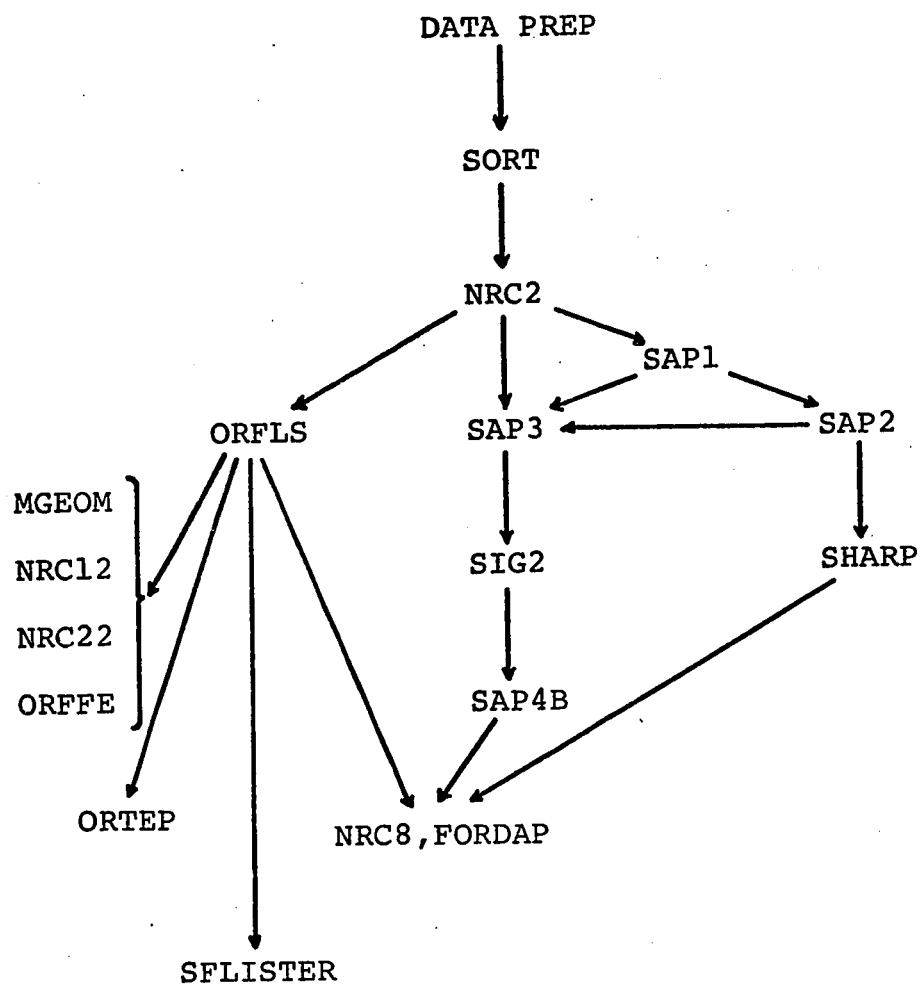
at the centre of the C_9-C_{10} bond of the double scale molecule formed by the pattern of $(2x, 2y, 2z)$ vectors, and although these vectors may not be prominent they should definitely be present on the section $x = 0$. All the above arguments apply equally to the molecules situated at $x = 1/2$ and thus the pattern of vectors on $x = 0$ will be exceedingly complicated as a result of the relative orientation of the asymmetric molecules (60°) which implies that the two sets of vectors will approximately superpose! As the molecules must lie well clear of the centres of symmetry (no atom can be within $1/2$ the Van der Waals radius for that atom) the dominant "centre-centre" vectors will probably lie close to the position $(0, 1/2, 1/2)$. The Patterson map showed several large peaks in this region and all were considered as "centre-centre" vectors but no model could be found which gave an R factor agreement of less than 0.60 and none of these models could be refined using Fourier methods to improve the agreement by more than ~ 0.02 .

Vectors between the two independent molecules in the asymmetric unit will occur on section $x = 1/2$ and when the vectors near $(1/2, 0, 0)$ were plotted to scale, an image of a single molecule was observed. This means that the two molecules must lie approximately over each other, but are displaced by one half a bond length.

Unfortunately this does not help to position the molecules in the unit cell, but now the relationship between the asymmetric molecules is fairly well established and it seemed that the most promising approach might be one in which one molecule was systematically moved over the unit cell and the other was constrained to have the fixed relationship to the first as regards orientation and positioning, and at each change structure factors could be calculated. Any drop in R factor would be an indication of the positions of molecules within the unit cell and hopefully conventional methods of refinement could be used from this point. Before this method was fully employed, it was decided that too much time had been spent on this problem, since the results had already been anticipated from the n.m.r. spectrum published by Moore and Shueur (34) and they could not be directly related to naphthazarin. Thus this structure solution was abandoned for this thesis, although it is hoped to continue with this work at a later date.

APPENDIX A

Programme system

TABLE 46

All computations were performed on the IBM 7040 computer up to mid 1968 when this computer was changed for an IBM 360/67 computer which was used thereafter.

DATA PREP

The main purpose of this program is to convert intensities, I , measured with equi-inclination geometry to structure factors, F , by the application of the Lorentz and Polarisation corrections. The Pailred linear diffractometer employs crystal-monochromatised radiation, thus the incident beam will be partially polarised and a different polarisation correction must be made for this data, as opposed to data measured by film techniques. A completely general expression was therefore used to apply these corrections (110 and 111).

$$(LP)^{-1} = (1 + q) \cdot \sin T / [(1 + q) / \cos^2 v - q \cdot \sin^2 v - (1 - \cos^2 v) (1 + \cos T)^2]$$

where $q = \cos^2 2\alpha$, α being the Bragg angle of the monochromatic beam which will be zero for film data;

T = azimuthal angle of the diffracted beam ($= 2\theta$)

v = equi-inclination angle ($= -\mu$)

F values are now obtained from the formula

$$F_o = (I \cdot (LP)^{-1})^{1/2}$$

Data obtained from the diffractometer is indexed in terms of machine axes which may or may not correspond to the crystallographic axes. The simple transformation to Miller indices is also accomplished by the programme when such transformation is necessary.

SORT

Use of the Fourier summation program NRC8 requires that data be previously sorted in a manner dependent upon the sections being calculated. SORT accepts punched card data from DATA PREP and writes a magnetic tape containing sorted data suitable for input to NRC2. The availability of a computer with large core storage is a necessary criterion for the use of this programme. SORT was written by Dr. M. Elder.

NRC2

This programme is one of a series of crystallographic programmes written by F. Ahmed (49) and was used in this laboratory to prepare a magnetic tape containing the sorted (hkl) data and all information relevant to each reflection viz: F_o , $\sin^2\theta(s^2)$, interpolated scattering factors (f_s), multiplicity (m), parity and observed-unobserved status. Also included on the output tape is information relevant to the unit cell and space group of the structure being determined. This tape could

therefore be used as input to any of the programmes in Ahmed's program system. All programmes in Table 46 that are prefixed NRC or SAP belong to this system.

SAP1

This programme uses intensity statistics to calculate the scale factor required to put the data on the absolute scale and also the overall temperature factor, by the method of Wilson (57). The data is split up into ranges of $\sin^2\theta$ and for each range the average values of $m. @. \sum f_s^2$, $m.F_O$, $\sin^2\theta$ are calculated. The symbol @ is a factor to account for systematic absences in the data. A linear least squares procedure is then applied to obtain the coefficients A_0 and A_1 for the line:

$$\ln(<m. @. \sum f_s^2>/<m.F_O>) = A_0 + A_1.<\sin^2\theta>$$

The scale factor, K , and the overall temperature factor, B , are then obtained from the equations:

$$K = \exp(A_0/2), B = A_1.\lambda^2/2.$$

SAP2

The function of this programme is to calculate E values (see p. 223) and also to calculate the point-atom-at-rest sharpening function M_s from the relation:

$$M_s = [\sum f_O^2 / \sum f_s^2] . [K^2 . \exp(2Bs^2)]$$

For large values of $\sin\theta$ i.e. in the range $S_m^2 < S^2 \leq 1/\lambda^2$, where S_m is a value set by the user, the sharpening function is given as $M_s = M_s + a(S^2 - S_m^2)\lambda^2$. The coefficient, a , is negative hence the second term will sharply reduce the value of M_s which will have the effect of reducing ripples around the origin peak in the Patterson summation (Point-atom sharpening enhances series termination errors unless this is done). The M_s curve is punched on cards to be used as input to SHARP.

SHARP

This program simply interpolates the M_s curve calculated by SAP2 and by reading the NRC2 output tape, creates a new tape which now contains the coefficients F_o , F_o^2 , and the sharpened F_o^2 value, F_s^2 . Unit cell data are transferred from the NRC2 output tape to the new data tape which can then be used as input to the Fourier summation program NRC8 whence a Patterson summation can be calculated.

SAP3

All reflections satisfying the Sayre relationship $E_h \sim sE_k \cdot sE_{h-k}$ are found by this programme and are listed in the form of printed output as pairs of reflections E_k , E_{h-k} for decreasing magnitude of the

reflection E_h . The probability of sE_h being positive is also calculated as this only depends on the absolute magnitudes of the E values concerned (see p. 224).

Reflections signed by the Sayre relation (in terms of symbols and/or absolute signs) are then punched on cards which are used as input to SIG2. SAP3 also prepares a magnetic tape containing the same information as the printed output.

SIG2

If signs are still in symbol form, they can be assigned absolute values in this programme, and when all reflections have absolute signs (+ or -), the sigma II relationship of Karle (32) i.e. $sE_h \sim \sum_k sE_k \cdot sE_{h-k}$, is applied using all signed E values. The output tape of SAP3 is read for this purpose and the probability of sE_h being positive is calculated using the formula given in (32):

$$P_+ \sim 0.5 + 0.5 \tanh[\sigma_3/\sigma_2^{1.5} |E_h| \cdot \sum_k E_k E_{h-k}].$$

Reflections with probabilities in the range 0.03-0.97 are excluded from the input and the procedure is repeated. An output tape is created containing the signed reflections. This program was written by the author.

SAP4B

The only function of this programme in the present system is to sort the signed E values which are read from the output tape of SIG2. The NRC2 output tape is also read, and relevant data from these two input tapes are combined on a further tape which can be used as input to the Fourier summation programme NRC8. The latter programme can then be used to calculate an "E map".

ORFLS (33)

All least squares refinements were carried out using this programme. Refinement of atomic parameters in this way involves minimisation of the quantity $w[|F_o| - |F_c|]^2$, where w is a weighting factor and the summation is taken over all observations. Since the structure factor F_c is not a linear function of the atomic parameters, the least squares procedure is linearised by means of a truncated Taylor series i.e. second and higher powers are neglected. In this way a series of "normal" equations are obtained which are linear in terms of the parameter shifts Δx . These equations have the general form:

$$\sum_r [a_n^2 \Delta x_n + \sum_m a_n a_m \Delta x_m] = \sum_r w(F_o - F_c)$$

where the summation \sum_r is over all observations, \sum_m is summed over all parameters except x_n , and $a_i = \partial F_c / \partial x_i$.

If there are n parameters, there will be n of these equations and these can therefore be solved for the parameter shifts Δx_i . Iterations of this procedure will normally result in convergence (providing the initial model does approximate to the true model), at which stage the parameter shifts will be less than the standard deviation in the parameter.

The programme ORFLS utilises the full matrix of the coefficients of the parameter shifts Δx_i ; inversion of this matrix followed by multiplication by the observation matrix, yields the parameter shifts Δx_i . The standard errors in each parameter are calculated from the diagonal elements of the inverse matrix, $\sigma_i = (C_{ii} \cdot \sum_r (F_o - F_c)^2 / (r-m))^{1/2}$, where σ_i is the standard deviation in the i th parameter, C_{ii} is the diagonal element of the inverse matrix. The weights, w , are calculated internally, and for this work the expression used was $w^{1/2} = [1 / (1 + (F_o - b)^2 / a^2)]^{1/2}$. The NRC2 output tape is used as input to ORFLS and an output tape of the same form is created. The extensive modifications required to "fit" this program into the present system were done by Dr. M. Elder.

NRC8

This is the Fourier summation programme used throughout this work for general Fourier calculations. A magnetic tape output of any Fourier summation is written if required and in the case of Patterson syntheses, this tape could be used as input to the Patterson superposition programme (see Appendix C). The Fourier calculation requires the factorisation of the Fourier expression for any space group.

FORDAP(55)

This programme is a more flexible Fourier summation programme; the Fourier expression need not be factorised, and the data need not be sorted for use in this programme, (with some loss of speed in computation). A further very useful feature of this programme is the ability to calculate Fourier sections through a general plane. FORDAP was not available for extensive use in this thesis and was therefore only used to calculate the general sections through planar molecules which are shown in the text.

MGEOM, NRC12, ORFFE, NRC22

These programmes are for calculating the geometry of the final model, and differ in respect to input and ease of operation. MGEOM is simply a card input programme for which each individual angle must be specified and the bonds making this angle are computed as well as the value of this angle. NRC12 reads the structure factor output tape from ORFLS and computes all bonds and angles within specified limits. ORFFE (115) is a comprehensive results programme computing bond lengths and angles as well as analysing thermal parameters. The input to ORFFE is written on a special tape by ORFLS and individual functions are read from cards. ORFFE and MGEOM compute bond length errors taking into account the fact that in oblique coordinate systems, the individual coordinates of any one atom may not be statistically independent. In ORFFE the variance-covariance matrix is read from the input tape whereas MGEOM computes the variances internally. NRC22 computes a least squares plane and calculates errors in the deviations from this plane, enabling the χ^2 test to be used to test the planarity by statistical methods.

S. F. LISTER

This programme was used to list structure factors for all structures in this thesis. Dr. M. Elder wrote this programme.

ORTEP (66)

All full page diagrams in this thesis were computed by ORTEP and plotted on the Calcomp plotter; an off line device in the computing centre. For most structures, ORTEP was also used to calculate intermolecular contacts, use being made of the "sphere of contact" facility of the program.

APPENDIX B

Analysis of Rigid Body Thermal Motion

Symbols used (the coordinate system is referred to molecular axes)

- T_{ij} : elements of a symmetric tensor giving the mean square amplitude of rigid body transitional motion.
- ω_{ij} : elements of a symmetric tensor giving the mean-square amplitude of rigid body librational motion
- \mathbf{l} : a unit vector with direction cosines $(l_1 l_2 l_3)$
- \mathbf{r} : the positional vector of an atom (x, y, z)
- β_{ij}, U_{ij} : elements of symmetric tensors describing the ellipsoids of vibration for any atom.
- n : the total number of rigid body parameters to be varied (=12)
- \bar{u}^2 : the mean-square amplitude of vibration of an atom.
- \mathbf{x}_i : the rigid body parameters T_{ij}, ω_{ij} considered together for simplicity in the least-squares procedure.

The mean-square amplitude of vibration of an atom in the direction of the unit vector \underline{l} is:

$$\bar{u}^2 = \sum_{ij} \sum_{\ell} U_{ij}^{\ell} \ell_i \ell_j \quad \underline{1}$$

Molecular libration will result in movement of an atom, r , in the direction defined by \underline{l} when the libration axis coincides with the vector $(\underline{l} \times \underline{r})$ and furthermore, the component of movement due to the libration ω along \underline{l} will be given by $(\underline{l} \times \underline{r}) \omega$. Thus the mean-square amplitude of vibration of the atom in the direction \underline{l} due to molecular libration is:

$$\bar{u}_L^2 = \sum_{ij} \sum_{\omega} \omega_{ij} (\underline{l} \times \underline{r})_i (\underline{l} \times \underline{r})_j$$

Similarly the translational contribution to the motion of the atom, r , (in the direction \underline{l}) due to molecular vibration is:

$$\bar{u}_T^2 = \sum_{ij} \sum_{\ell} T_{ij}^{\ell} \ell_i \ell_j$$

Assuming that the motion of any atom is due entirely to rigid body translations and librations, \bar{u}^2 can also be given by the sum of the contributions from translational vibrations of the centre of mass, and from rigid body librations, i.e.

$$\bar{u}^2 = \bar{u}_T^2 + \bar{u}_L^2 = \sum_{ij} \sum_{\ell} (T_{ij}^{\ell} \ell_i \ell_j + \omega_{ij} (\underline{l} \times \underline{r})_i (\underline{l} \times \underline{r})_j) \quad \underline{2}$$

Comparison of equations 1 and 2 yields the equation

$$\sum_{ij} \sum_{ij} U_{ij} l_i l_j = \sum_{ij} \sum_{ij} (T_{ij} l_i l_j + \omega_{ij} (l \times r)_i (l \times r)_j)$$

By expanding the cross products on the right hand side e.g. $(l \times r)_2 = l_1 z - l_3 x$ and equating coefficients in $l_i l_j$, it is possible to derive expressions for the U_{ij} s in terms of T_{ij} and ω_{ij} , which, in the simple case of a planar molecule with the z axis parallel to the molecular normal, reduce to the equations shown below:

$$\begin{aligned} U_{11} &= T_{11} + y^2 \omega_{33} \\ U_{22} &= T_{22} + x^2 \omega_{33} \\ U_{33} &= T_{33} + y^2 \omega_{11} + x^2 \omega_{22} - 2xy \omega_{12} \\ U_{12} &= T_{12} - xy \omega_{33} \\ U_{13} &= T_{13} - y^2 \omega_{13} + xy \omega_{23} \\ U_{23} &= T_{23} - x^2 \omega_{23} + xy \omega_{13} \end{aligned} \quad \underline{3}$$

Thus if the T and ω tensors are known, the U_{ij} values which are the thermal motion parameters for each atom, due entirely to rigid body vibrations, can be calculated. The T and ω tensors can best be evaluated by a least squares procedure where the term $\sum_n (U_n^C - U_n^O)^2$ is minimised with respect to the n rigid body parameters (T_{ij} and ω_{ij}). The ith "normal" equation is:

$$\sum_n (U_n^C - U_n^O) \cdot \frac{\partial U_n^C}{\partial x_i} = 0$$

$$\text{i.e. } \sum_n U_n^C \cdot \frac{\partial U_n^C}{\partial x_i} = \sum_n U_n^O \cdot \frac{\partial U_n^C}{\partial x_i}$$

and since any linear equation $y = f(x)$ can be expressed in the form $y = \sum_j \frac{\partial f}{\partial x_j} \cdot x_j$, the normal equations can be written:

$$\sum_j \left[\sum_n U_n^C \cdot \frac{\partial U_n^C}{\partial x_j} \right] \cdot x_j = \sum_n U_n^O \cdot \frac{\partial U_n^C}{\partial x_i}$$

Twelve equations result which reduce to three sets of four in the simpler case of a planar molecule, and these can be readily solved for the parameters, x_j , which are the required rigid-body parameters, T_{ij} and ω_{ij} , i.e. the above equation can be written in matrix notation as $(A) \cdot (x) = (B)$, thus the equation $(x) = (A)^{-1} \cdot (B)$ yields the solution of the parameter matrix. These values can now be used in equations 3 to calculate the rigid body U_{ij} values, which can then be compared with the observed values. Good agreement indicates that the atomic vibrations are principally determined by the rigid body motion of the molecule. The ω_{ij} values can be used to correct bond lengths, as previously described in the structural determination of

Naphthazarin (see p. 38), by using the formula given by Busing and Levy (61)

$$S = S_0 + \omega_{ii} \cdot S_0 \cdot \sin^2 \psi / 2 \quad .$$

where S_0 is the uncorrected bond length and ψ is the angle between this bond and the axis, i . For independent oscillations about more than one principal axis, the corrections are additive.

Transformations to molecular axes

The above analysis requires that a molecular coordinate system be used, thus the refined anisotropic parameters, β_{ij} , and the atomic coordinates which refer to crystallographic axes must be transformed.

Transformations to an orthogonal set of axes, abc^* , is first required and these are then rotated (and translated if necessary) so as to coincide with the molecular axes. The method of Rollet and Davies (108) which was used to transform the β_{ij} values to the orthogonal coordinate axes, abc^* , is described below.

The (hkl) indices referred to crystallographic axes can be transformed to the orthogonal axes, abc^* , by the following transformation (for the monoclinic case):

$$\begin{pmatrix} h_o \\ k_o \\ l_o \end{pmatrix} = \begin{pmatrix} \sin\beta^* & 0 & 0 \\ 0 & 1 & 0 \\ \cos\beta^* & 0 & 1 \end{pmatrix} \cdot \begin{pmatrix} h \\ k \\ l \end{pmatrix}$$

and the anisotropic temperature factor in terms of β_{ij} is:

$$h^2\beta_{11} + k^2\beta_{22} + l^2\beta_{33} + 2hk\beta_{12} + 2hl\beta_{13} + 2kl\beta_{23} \quad \underline{4}$$

If the parameters in this expression are now referred to the orthogonal axes then the β_{ij} values become β'_{ij} and equation 4 becomes:

$$\begin{aligned} & h^2\sin^2\beta^*\beta'_{11} + k^2\beta'_{22} + 2h\cos\beta^*\beta'_{33} + h^2\cos^2\beta^*\beta'_{33} \\ & + 2hk\sin\beta^*\beta'_{12} + 2hl\sin\beta^*\beta'_{13} + 2h^2\sin\beta^*\cos\beta^*\beta'_{13} \\ & + 2kl\beta'_{23} + 2hk\cos\beta^*\beta'_{23} \end{aligned} \quad \underline{5}$$

Equation coefficients of (hkl) in 4 and 5, the β'_{ij} terms are obtained:

$$\beta'_{11} = \frac{\beta_{11}}{\sin^2\beta^*} + \frac{\cos^2\beta^*}{\sin^2\beta^*} \cdot \beta_{33} - \frac{2\cos\beta^*}{\sin^2\beta^*} \cdot \beta_{13}$$

$$\beta'_{22} = \beta_{22}$$

$$\beta'_{33} = \beta_{33}$$

$$\beta'_{12} = \frac{\beta_{12}}{\sin\beta^*} - \frac{\cos\beta^*}{\sin\beta^*} \cdot \beta_{23}$$

$$\beta'_{13} = \frac{\beta_{13}}{\sin\beta^*} - \frac{\cos\beta^*}{\sin\beta^*} \cdot \beta_{33}$$

$$\beta'_{33} = \beta_{33}$$

and these values can then be transformed to U_{ij} values using the relationship $U_{ij} = \beta'_{ij} / (2\pi^2 a_i^* \cdot a_j^*)$ where $a_1^* = [a^*]$, $a_2^* = [b^*]$, $a_3^* = [c^*]$ (67).

The atomic coordinates (xyz) are transformed to the orthogonal coordinate system by the transformation:

$$\begin{pmatrix} x_o \\ y_o \\ z_o \end{pmatrix} = \begin{pmatrix} a & 0 & c \cos\beta \\ 0 & b & 0 \\ 0 & 0 & c \sin\beta \end{pmatrix} \cdot \begin{pmatrix} x \\ y \\ z \end{pmatrix}$$

The rotation matrix that transforms the orthogonal coordinates and U_{ij} values to the molecular axes can now be set up. The normal to the molecular plane coincides with the molecular z axis, and the equation of this plane ($l_3x + m_3y + n_3z = d$) directly yields the direction cosines of the z axis with respect to abc^* . The x molecular axis can be defined as passing through any atom of the molecule, and the direction cosines of this axis with respect to abc^* can be calculated, i.e. if the crystallographic origin coincides with the molecular origin then the required direction cosines

are: $l_1 = x_0/r$, $m_1 = y_0/r$, $n_1 = z_0/r$ where
 $r = (x_0^2 + y_0^2 + z_0^2)^{1/2}$. To ensure that a right handed
 system of axes is chosen, the y molecular axis is
 defined by taking the cross product ($z \times x$):

$$\begin{vmatrix} 1 & 1 & 1 \\ l_3 & m_3 & n_3 \\ l_1 & m_1 & n_1 \end{vmatrix} = (m_3 n_1 - n_3 m_1) - (l_3 n_1 - n_3 l_1) \\ + (l_3 m_1 - m_3 l_1)$$

If the cofactors of the determinant are called p,q,r
 then the required direction cosines relating the y
 axis to abc* are: $l_2 = p/s$, $m_2 = q/s$, $n_2 = r/s$
 where $s = (p^2 + q^2 + r^2)^{1/2}$. The rotation matrix is
 given by

$$(R) = \begin{pmatrix} l_1 & m_1 & n_1 \\ l_2 & m_2 & n_2 \\ l_3 & m_3 & n_3 \end{pmatrix}$$

and the transformation of the orthogonal atomic
 coordinates and the U_{ij} tensor to molecular axes is
 accomplished by the following matrix equations:

$$(x) = (R) \cdot (x_0)$$

$$(U_{ij}) = (R) \cdot (U_{ij}) \cdot (R)^{\sim}$$

APPENDIX C

Patterson Superposition

The Patterson function, $P(u, v, w)$, of any structure consists of a large number of images of the three dimensional atomic structure. If there are N atoms in the structure there will be $N-1$ unique vectors from any given atom to all other atoms and these vectors represent the atomic structure as seen from the atom N . If one of these complete vector sets i.e. the atomic positions as seen from atom N , can be sorted out from the general Patterson map, the atomic positions will be obtained.

Frequently, the structure will contain a small number of dominant atoms whose vectors can be readily identified from their peak heights and these atoms can then be used to phase the coefficients in a Fourier summation from which the positions of the lighter atoms can usually be found. In some cases, however, the dominant atoms are present in too large a number to allow ready identification of their vectors, or are insufficient to phase all the atoms by the normal heavy atom procedure, and in these situations the method of Patterson superposition can often yield the positions of all or most of the atoms in the structure. There are

two methods by which Patterson superposition can be carried out: *Vector superposition* and *Atomic superposition*, and both will be described briefly below.

The basic criterion of either method is that a set of consistent vectors be correctly identified as arising from one or more atoms e.g. in the centrosymmetric space group $P2_1/c$, it may be possible to identify the vectors $(2x, 2y, 2z)$, $(2x, \frac{1}{2}, \frac{1}{2} + 2z)$, $(0, \frac{1}{2} - 2y, \frac{1}{2})$ such that they are self-consistent and will therefore give rise to the atomic position (x, y, z) , and similarly in the non-centrosymmetric space group $P2_12_12_1$ a self-consistent set of Harker vectors may be identified $(\frac{1}{2} + 2x, 2y, \frac{1}{2})$, $(\frac{1}{2}, \frac{1}{2} + 2y, 2z)$, $(2x, \frac{1}{2}, \frac{1}{2} + 2z)$, yielding the atomic position (x, y, z) . The *vector superposition* consists of translating a copy of the Patterson $P_2(u, v, w)$ so that one of the above vectors e.g. $(2x, 2y, 2z)$ coincides with the origin of the original Patterson $P_1(u, v, w)$. Because of the multiple image nature of $P(u, v, w)$, a molecular image of $P_2(u, v, w)$ should now coincide with an image of $P_1(u, v, w)$, whereas those vectors that belong to other images will not in principal coincide. If, however, the vector chosen for superposition is actually a double vector due to the accidental superposing of two genuine vectors, then a double image will result

from a single superposition and the procedure will generally have to be repeated to obtain a unique solution. When analytical procedures are used it is usual to take a minimum function when recording the result of a superposition i.e. the minimum value of two coinciding vectors is taken. The disadvantage of this method is that the position of the origin of the unit cell will change with each superposition e.g. in the above example where the vector $(2x, 2y, 2z)$ is used for superposition, the origin will be located at (x, y, z) and in order to locate the true origin of the unit cell the superposition must be carried out using extended Patterson maps so that all symmetry related molecules can be recognised. The true origin can then be found from the positions of the symmetry elements. This difficulty is obviated in the method of *atomic superposition* where the origins of the two copies of the Patterson i.e. $P_1(u, v, w)$, $P_2(u, v, w)$ are translated to an atomic position as well as to positions related by space group symmetry (47); a minimum function is taken on each translation as before. That this process is in fact analogous to *vector superposition* can be readily seen when both methods are employed on a structure in a centrosymmetric space group: the atomic positions (x, y, z) , $(\bar{x}, \bar{y}, \bar{z})$ will be among those to which the origins of

$P_1(u,v,w)$ and $P_2(u,v,w)$ respectively will be translated, and the distance between the two origins will be equal to the vector $(2x, 2y, 2z)$ as it would be in the case of vector superposition using the vector $(2x, 2y, 2z)$. The origin of the resulting map, after atom superposition is used, will always be at the origin of the unit cell and if all the symmetry related positions are employed, this map will have true space group symmetry.

The computer programme listed below translates the Patterson map and takes a minimum function when more than one translation has been accomplished. Only the asymmetric unit of the Patterson map is used, and the subroutine ASYM ensures that the computed section of the Patterson map is not exceeded by applying the appropriate symmetry operations when a point required for superposition lies outside the asymmetric unit. This is the only space group dependent part of the program, and modification for any Patterson space group is readily accomplished. A three dimensional linear interpolation is used when the superposition coordinates do not lie exactly on calculated grid points of the Patterson map.

References

1. S.W. Peterson and H.A. Levy: J. Chem. Phys. (1952), 20, 704.
2. A.I. Vogel: "Quantitative Inorganic Chemistry" Longmans (1960), p. 7.
3. L. Pauling: "The nature of the chemical bond", Cornell University Press (1960), a: p.479, b: p.260.
4. K. Zahn and P. Ochwat: Ann. (1928), 81, 462.
5. M-L. Josien, N. Fuson, J-M. Lebas, T.M. Gregory: J. Chem. Phys. (1953), 21, 331.
6. D. Hadzi and N. Sheppard: Trans. Fara. Soc., (1953), 21, 331.
7. C. Pascard-Billy: Acta Cryst. (1962), 15, 519.
8. C. Pascard-Billy: Comptes Rendus Acad. Sci. Paris (1961) 1350.
9. C. Pascard-Billy: Bull. Soc. Chim. France, (1962) 2282.
10. C. Pascard-Billy: Bull. Soc. Chim. France, (1962) 2299
11. C. Pascard-Billy: Bull. Soc. Chim. France, (1962) 2293
12. C. Billy: Comptes Rendus Acad. Sci. Paris (1955) 240, 887.
13. C. Billy: Comptes Rendus Acad. Sci. Paris (1958) 247, 1019.
14. O. Borgen: Acta Chem. Scand., (1956) 10, 867.

15. H. Watase, K. Osaki, I. Nitta: Bull. Chem. Soc. Japan, (1957) 30, 532.
16. P. Srivastava: Zeit. Krist., (1958), 111, 77.
17. P. Srivastava: Indian J. Phys. (1959), 33, 123
18. G.A. Golder and G.S. Zhdanov: Doklady Akad. Nauk. USSR (1958), 118, 6, 1131.
19. J. Palacios and R. Salvia: Anales. Soc. espan. fis. Quim. (1932), 32, 49.
20. W.C. Hamilton: Acta Cryst. (1965), 18, 508.
21. P. Srivastava: Indian J. Phys. (1961), 35, 640.
22. D. Hall and M.D. Woulfe: Proc. Chem. Soc. (1958), 346.
23. M.D. Woulfe: M.Sc. Thesis University of Auckland, New Zealand. 1958.
24. H. Reihlen: Annalen (1927), 448, 314.
25. R.W. Asmussen: Magnetokemiske Undersogelser over unorganiske Komplex forbindelser, Copenhagen (1944), 222.
26. D. Rae: Acta Cryst. (1965), 19, 683.
27. W.C. Hamilton, J.S. Rollet and Sparks: Acta Crystl (1965), 18, 129.
- 28.
29. Structure Reports: (1954), 18, 657.
30. W.A.G. Graham and D. Patmore: Inorg. Chem. (1966) 5, 1586.
31. P.G. Simpson, R.D. Dobrott and W.N. Lipscomb: Acta Cryst. (1965), 18, 169.

32. I. Karle and J. Karle: Acta Cryst. (1966), 21, 849.
33. W.R. Busing and H.A. Levy: "ORFLS" A Fortran crystallographic least-squares programme. Oak Ridge report ORNL-TM-305 (1962).
34. R.E. Moore and P.J. Shueur: J. Org. Chem. (1966), 31, 3272.
35. F.G. Mann and W.J. Pope: Proc. Roy. Soc. (1925), A109, 444 .
36. F.G. Mann and W.J. Pope: Chem. and Ind. (1925), 44, 834.
37. F.G. Mann and W.J. Pope: J. Chem. Soc. (1926), 482.
38. International Tables for X-ray crystallography Vol III.
39. E.K. Iukhno and M.A. Porai-Koshits: Krystallografia (1957), 2, 239.
40. L.E. Sutton: Interatomic distances supplement No. 18 The Chemical Society.
41. J.R. Dyer: "Applications of absorption spectroscopy of Organic compounds", Prentice Hall N.J. (1965), p. 36.
42. W.A.G. Graham and D. Patmore: Inorg. Chem. (1966), 5, 1405.
43. M. Renninger: Zeit. Phys. (1937), 106, 141.
44. H.L. Yakel and I. Fankuchen: Acta Cryst. (1962), 15, 1188.
45. W.H. Zachariasen: Acta Cryst. (1965), 18, 705.
46. D.W.J. Cruickshank: Acta Cryst. (1960), 13, 774.

47. J. Kraut: Acta Cryst. (1961), 14, 1146.
48. P. Torkington: J. Chem. Phys. (1951), 19, 528.
49. F. Ahmed: NRC crystallographic programmes for the IBM/360 system, N.R.C. Ottawa.
50. D. Patmore: Ph.D. Thesis, University of Alberta 1968.
51. S. Baggio and L.N. Becka: Chem. Comm (1967), 506.
52. D.J. Sutor, F.J. Llewellyn, H.S. Maslen: Acta Cryst. (1954), 7, 145.
53. S.E. Rasmussen: Acta Chem. Scand. (1959), 13, 2009.
54. R. Mason: "Advances in structure research by diffraction methods" Interscience, J. Wiley and Sons,
55. A. Zalkin: "Fordap", a general Fourier programme. University of California.
56. D.W.J. Cruickshank: Acta Cryst. (1949), 2, 65.
57. A.J.C. Wilson: Nature (1942), 150, 152.
58. D.C. Phillips: Acta Cryst. (1956), 9, 237.
59. G.R. Robertson: Nature (1961), 191, 593.
60. D.W.J. Cruickshank: Acta Cryst. (1956), 9, 757.
61. W.R. Busing and H.A. Levy: Acta Cryst. (1964), 17, 142.
62. E.G. Cox, D.W.J. Cruickshank, J.A.S. Smith: Proc. Roy. Soc. (1958) A247, 1
63. D.W.J. Cruickshank: Acta Cryst. (1956), 9, 754.
64. A.L. Patterson and W.E. Love: Amer. Minn. (1960), 45, 325.

65. W.C. Hamilton: "Statistics in Physical Science"
(1964) The Ronald press Co. N.Y, p. 48.
66. C.K. Johnson: "ORTEP". A Fortran thermal-ellipsoid
plot program for crystal structure illustrations.
Oak Ridge report ORNL 3794 (1965).
67. D.W.J. Cruickshank: Acta Cryst. (1965), 19, 153.
68. M. Mack: Norelco Reporter (1965), 12, 41.
69. J.M. Robertson: "organic Crystals and molecules"
(1953) Cornell University press N.Y, p. 182.
70. C.K. Prout and S.C. Wallwork: Acta Cryst. (1966),
21, 449.
71. H. Matsuda, K. Osaki and I. Nitta: Bull. Chem.
Soc. Japan (1958), 31, 611.
72. D. Hall and C. Nobbs: Acta Cryst. (1966), 21, 927.
73. M. Bailey and C.J. Brown: Acta Cryst. (1967), 22, 392.
74. M. Ehrenberg: Acta Cryst. (1967), 22, 482.
75. J. Gaultier and C. Hauw: Acta Cryst. (1966), 21, 694.
76. M. Breton-Lacombe: Acta Cryst. (1967), 23, 1031.
77. M. Breton-Lacombe: Acta Cryst. (1967), 23, 1024.
78. H. Klug: Acta Cryst. (1965), 19, 983.
79. G. Pimentel and A. McClellan: "The hydrogen bond",
Freeman and Co. (1960), p. 172.
80. E.K. Andersen: Acta Cryst. (1967), 22, 191.
81. E.K. Andersen: Acta Cryst. (1967), 22, 188.

82. G.M. Sheldrick and R.N.F. Simpson: J. Chem. Soc. (1968), A5, 1005.
83. L.F. Dahl and R.E. Rundle: Acta Cryst. (1967), 16, 419.
84. S.J. LaPlaca, W.C. Hamilton and J.A. Ibers: Inorg. Chem. (1964), 3, 1491.
85. M.E. Cradwick and D. Hall: Private communication.
86. M. Elder and D. Hall: Inorg. Chem. in press.
87. M. Elder and D. Hall: Inorg. Chem. in press.
88. M.J. Bennett and R. Mason: Nature (1965), 205, 760.
89. F.A. Cotton and G. Wilkinson: "Advanced inorganic chemistry" Interscience, J. Wiley (1966), p. 108.
90. W.T. Robinson and J.A. Ibers: Inorg. Chem. (1967), 6, 1208
91. O.S. Mills and G. Robinson: Proc. Chem. Soc. (1964) 187 as quoted by Lewis (103).
92. V. Shomaker and D.P. Stevenson: J. Am. Chem. Soc. (1942), 64, 2514.
93. H. Brode: Ann. Physik. (1940), 37, 344.
94. M.A. Bush and P.W. Woodward: J. Chem. Soc. (A) (1967), 1833.
95. B.G. deBoor, A. Zalkin and D.H. Templeton: Inorg. Chem. (1968), 7, 2288.
96. D.B. Bruce and R.H. Thomson: J. Chem. Soc. (1955), 1089.
97. K. Nakamoto, M. Margoshes and R. Rundle: J. Am. Chem. Soc. (195), 77, 6480.

98. M. Sunderalingam and L.H. Jensen: Acta Cryst.
(1965), 18, 1053.
99. L.L. Meritt and C. Quare: Acta Cryst. (1954), 7, 650.
100. W.C. Hamilton: Acta Cryst. (1955), 8, 185.
101. G.H. Stout and L.H. Jensen: "X-ray structure determination"
MacMillan and Co. (1960), a: p. 410, b: p. 317, c: p.322.
102. H.A. Bent: Chem. Rev. (1961), 61, 275.
103. J. Lewis: Pure and Applied Chem. (1965), 10, 11.
104. D.S. Brown, F.W.B. Einstein and D.G. Tuck:
Inorg. Chem. (1969), 8, 14.
105. C.H. Schwalke and W.N. Lipscomb: J. Am. Chem. Soc.
(1969), 91, 194.
106. M.J. Buerger: "Crystal Structure Analysis"
J. Wiley and Sons (1960), a: p. 608, b: p. 596.
107. D. Sayre: Acta Cryst. (1952), 5, 60.
108. J.S. Rollet and D.R. Davies: Acta Cryst. (1955),
8, 125.
109. R.A. Jacobson, J.A. Wunderlich and W.N. Lipscomb:
Acta Cryst. (1961), 14, 598.
110. E.J.W. Whittacker: Acta Cryst. (1953), 6, 222.
111. W.L. Bond: Acta Cryst. (1959), 12, 375.
112. F.J. Jellinek: Acta Cryst. (1958), 11, 677.
113. A. Bondi: J. Phys. Chem. (1964), 68, 441.
114. R.C. Srivastava and E.C. Lingafelter: Acta Cryst.
(1966), 20, 918

115. W.R. Busing and H.A. Levy: ORFEE. A Fortran
crystallographic function and error program.
Oak Ridge report ORNL-TM-306 (1964).
116. F. Bonati and G. Wilkinson: J. Chem. Soc. (1964). 179.